UNIVERSITY OF SHEFFIELD
Department of Civil and Structural Engineering

ROBUSTNESS OF FLEXIBLE ENDPLATE CONNECTIONS UNDER FIRE CONDITIONS

By Ying HU

Supervisors:

Professor Ian Burgess
Dr. Buick Davison
Professor Roger Plank

A thesis submitted to the Department of Civil and Structural Engineering in partial fulfilment of the requirements for the degree of Doctor of Philosophy

October 2009

ABSTRACT

Worldwide interest in how to prevent the progressive collapse for tall and large buildings under exceptional loading conditions was heightened by the collapse of the twin towers at the World Trade. The performance of steel-framed structures subjected to fire loading is heavily reliant on the interaction between structural members such as columns, slabs and beams. The implicit assumption in fire engineering design is that bolted connections are able to maintain the structural integrity for a large and tall building under fire conditions. Unfortunately, evidence from the collapse of the World Trade Centre towers and full scale fire tests at the BRE Cardington Laboratory indicates that connections may be particularly vulnerable during both heating and cooling. Hence, this PhD research is focused on structural performance of simple steel connections under fire conditions, particularly the interaction mechanism between non-ductile and ductile components in a connection and connection failure mechanism in a steel-framed structure subjected to fire loading.

The research involved experimental testing of simple steel connections and components (structural 8.8 bolts) at elevated temperatures. High temperature tests on structural bolts demonstrated two modes of failure at elevated temperatures: bolt breakage and thread stripping. In order to prevent the thread stripping in a connection, the manufacturing process of bolts and nuts has been investigated and the 'over-tapping' of nut threads to accommodate the (zinc) coating layer for corrosion resistance has been indentified as a primary reason resulting in this premature failure between bolts and nuts. Experimental tests on endplate connections revealed the ductility of these connections to decrease at high temperatures, which might hinder the development of catenary actions in fire if plastic hinges are attempted to be formed within the connection zones. Component-based modelling and finite element simulation have been utilized for investigation of the performance of these connections.

An improved component-based model has been developed which includes non-ductile (brittle) components (bolts and welds) into a connection model with a reasonable assumption of their failure displacements, based on experimental tests. This model also features vertical components for consideration of shear response of these connections in fire. The component-based connection model has been used in a sub-frame structure and a parametric study demonstrates that a connection may fail due to a lack of rotational capacity (failure of bolts or welds) in a structure exposed to a fire. Therefore, partial depth endplate connections are recommended to be fire-protected to prevent the failure of these brittle components. Alternatively, ensuring the strength of brittle components (bolts and welds) is higher than that of other components in each bolt row is necessary to achieve the ductile failure mechanism of simple connections. Based on the experimental tests, component-based connection modelling and finite element simulation, recommendations to improve the robustness of simple steel connections in fire have been presented.

TABLE OF CONTENTS

LIST OF FIGURES

LIST OF TABLES

LIST OF NOTATIONS

a	Effective throat thickness of a fillet weld
a_f	The weld thickness between the beam flange and the endplate
b_{eff}	The effective length given by Eq. 6.8
b_{fc}	The width of the column flange
A_b	The nominal area of the bolt shank
A_s	The net area of the bolt threaded part
B_u	The ultimate load for a bolt
c	The load width calculated by using a dispersion angle of 45^o in the end-plate
c_d	The wave speed of the material
d	The depth of the test specimen
d_b	The nominal diameter of a bolt.
d_{wc}	The clear depth of the column web
e_2	The end distance
E	Modulus of elasticity at ambient temperature
E_b	Young's modulus of the bolt material
E_s	Young's modulus of steel
$E_{s,\theta}$	Young's modulus of steel at elevated temperatures
$\boldsymbol{E_I}$	The internal energy in a system
$\boldsymbol{E_{KE}}$	The kinetic energy
$\boldsymbol{E_{total}}$	The total energy in a system
$\boldsymbol{E_W}$	The work applied by the external force
f_u	The nominal ultimate tensile strength of the weaker of the two parts joined
f_y	Yield strength of steel
$f_{y,\theta}$	Yield strength of steel at elevated temperatures
F	The applied force or the corresponding level of shear force for a bolt (Equ. 6.18)
F_{Rd}	Design resistance
$F_{b,Rd}$	Bearing resistance for a component

$F_{v,Rd}$	The bolt shearing strength (Equ. 6.18)
$F_{w,Rd}$	Design resistance of a weld
$F_{w,fract}$	The weld fracture resistance
$F_{T,fail}$	The ultimate T-stub resistance
I_b	The second moment area of a beam
k	Initial stiffness (for a component) or a shear correction factor (Equ. 6.20)
k_b	=8 for frames with the bracing system or =25 for other frames
$k_{y,\theta}$	Reduction factors for yield strength f_y
$k_{E,\theta}$	Reduction factors for Young's modulus Es
K_b	The bolt elastic stiffness
K_i	The initial stiffness for a component
$K_{v,b}$	The bolt shearing stiffness
l	Length of steel at $20^o C$
l_y	The yielded length of the web
L	The span of a specimen
L_b	The span of a beam
L_s	The length of bolt shank
L_{tg}	The bolt threaded length included in the grip
L^e	The element length
$M_{j,Rd}$	The design moment resistance of a connection
$M_{pl,Rd}$	The design plastic moment resistance of the connecting members
$M_{b,pl,Rd}$	The design plastic moment resistance of a beam
$M_{c,pl,Rd}$	The design plastic moment resistance of a column
n	A parameter defining the curve sharpness for curve fitting
n_{th}	The number of threads per unit length of a bolt
$R_{f,v,b}$	The strength reduction factor for bolt in shear (20°C, $R_{f,v,b} = 0.58$)
$S_{j,ini}$	The initial rotational stiffness of a joint
t_{fb}	The thickness of the beam flange in compression
t_{fc}	The thickness of the column flange
t_p	The thickness of the endplate
t_{wc}	The thickness of the column web
t	Time
T	Temperature

T_0	Cohesive strength
u	The distance between the beam flange and the edge of the endplate
v	Poisson's ratio
α_T	Coefficient of thermal expansion
β	A steel correction factor
β_w	The appropriate correlation factor (taken from Table 4.1 in EC3-1.8)
γ_{M2}	A partial safety factor
χ	The slenderness parameter
Ψ	A curve fitting parameter
Φ	A curve fitting parameter
Ω	A curve fitting parameter
Γ_o	Cohesive energy
θ_a	Steel temperature
Θ_g	The gas (fire) temperature
δ_0	The critical separation
δ_b	The elongation for a bolt component
$\delta_{b.fract}$	The fracture displacement for a weld
δ_u	The ultimate displacement of a column web component
δ_w	The elongation for a weld component
δ_T	The deformation for a T-stub component
σ_{true}	True stress
σ_{nom}	Nominal stress
ε_{true}	True strain
ε_{nom}	Nominal strain
$\varepsilon_{pl,\,true}$	Plastic true strain
$\varepsilon_{u.b}$	The ultimate strain of bolt material
Δ	The relative bolt deflection
Δl	Temperature induced elongation
Δt_{stable}	The stability limit
Δ_{total}	The total deformation for one bolt row
$\overline{\Delta}$	The normalized deformation

ACKNOWLEDGEMENTS

About four years ago, I was interviewed by my current supervisors; Prof. Burgess, Dr Davison and Prof. Plank for this EPSRC-funded project. I was very pleased to be offered a PhD research student position and I have appreciated the chance to conduct research in structural fire engineering. I am very grateful to them for taking me as one of their PhD students under their joint supervision. Without their support, encouragement and excellent communication skills this project would not have been completed successfully. The financial support of EPSRC for this project is gratefully acknowledged.

Grateful acknowledgment should be given to Dr Brian Kirby, Dr John Dowling from Corus and Mr Mark Tiddy from Cooper and Turner for their valuable suggestions and comments on my research work on structural bolts and connections at elevated temperatures. As a cooperative partner in this jointed project, Prof. Y.C. Wang at the University of Manchester is acknowledged for his altruistic and valuable support and suggestions of my PhD research work.

I would also like to thank a number of previous PhD research students for their assistance. They are Dr Florian Block, Dr Marwan Sarraj, Dr Spyros Spyrou and Dr Khalifa Saif Al-Jabri. In addition, the friendly communication and help from my colleagues (two research associates) in this joint project should be acknowledged; they are Dr. H.X.Yu at the University of Tsinghua and Dr. X.H. Dai at the University of Leeds.

My special thanks go to Shane Smith, Chris Todd, Paul Blackbourn, Glenn Brawn, Jonathan Wood and Dick Smith at the University of Sheffield for their help, comments and continued commitment of time and resources in the development of experimental tests of simple steel connections at elevated temperatures.

The continued encouragement and support of my family members and friends will always be remembered.

DECLARATION

Except where specific reference has been made to the work of others, this thesis is the result of my own work. No part of it has been submitted to any other university for a degree, diploma, or other qualification.

Ying Hu

CHAPTER 1

INTRODUCTION

1.1 Introduction

Steel building construction offers many benefits to structural engineers, such as lower cost, lighter weight, low maintenance and fast construction. As a consequence, portal frames, steel structures and steel-concrete composite structures are widely used for high-rise and office buildings in many places around the world. However, there are two problematic issues closely associated with a steel-framed structure: corrosion and fire. As far as fire is concerned, steel is a non-combustible material, but the mechanical properties of structural steel are affected by temperatures. One of the most important factors to describe the fire performance of a structure is *fire resistance*, which is defined as the time during which structural elements can withstand the standard provisions of a fire test (Gehri, 1985). Previous research (Sanad et al., 2000) has demonstrated that composite floor beam systems can have a significantly greater fire resistance than suggested by conventional tests on isolated elements, largely owing to the interaction between the beams and floor slabs in the fire compartment, and the restraint afforded by the surrounding structures. Nevertheless, the full-scale fire tests at Cardington (British Steel, 1999) and the evidence from the pancake-like collapse of the World Trade Centre buildings (FEMA, 2002) indicates that steel joints might be vulnerable structural components in a structure under fire conditions, which contradicts the previously held assumption of steel joints being capable of retaining their structural integrity in fire engineering design. This is the research background to launch this connection robustness project under fire conditions which was jointly conducted by the University of Sheffield and the University of Manchester.

1.2 Fundamental Structural Concepts

Before discussing the research background of this robustness project in more detail, it is necessary to clarify the definitions for a number of terminologies being used in the following research discussion - progressive collapse, tying force, robustness, ductility and structural integrity.

The basic requirement for tall and large buildings is to provide a safe environment for people within them, and also ensure their escape to safety under extreme man-made or naturally-occurring events (IStructE, 2002). Hence, a structural requirement for these buildings is to prevent progressive collapse under exceptional loading conditions (fire or explosion). The term *progressive collapse* (or disproportionate collapse) refers to a failure mechanism for a structure characterized by a distinct disproportion in size between a triggering event (or local failure) and the resulting widespread collapse (Starossek, 2007). Steel-framed structures are required to possess sufficient material strength, ductility and energy absorption capacity for the structural members (including steel connections) to resist their failure under fire or explosive conditions. The term *ductility* is the ability of a structural component or structural system to withstand large deformations (Starossek and Haberland, 2008). For metal materials, ductility is a mechanical property to describe the extent to which materials can be deformed plastically without fracture, which may be quantified as a ratio of an engineering strain at fracture over that at the elastic limit. For connections, ductility usually means rotational capacities of bolted connections whilst sustaining moment, but may also mean extension of a connection if this connection is only subjected to pure tensile loading (Owens and Moore, 1992), which may similarly be defined as a ratio between a rotation or displacement at failure (fracture of a connection) and an elastic rotation or displacement attained at the elastic limit. This concept (ductility) has a large influence on preventing the development of a (progressive) collapse mechanism of a structure and how to increase its structural integrity under exceptional loading conditions, which is also closely connected to the energy absorption capacities of the structural system and structural components.

In the preceding paragraph, the term *structural integrity* has been first mentioned in the statement of description of ductility of structural components. It may be defined

as insensitivity of a structure to accidental circumstances (Starossek and Haberland, 2008); the structure is capable of absorbing local failures without widespread collapse. The term *robustness* is more or less equivalent to the definition of structural integrity in this PhD dissertation and sometimes these two terminologies have been utilized interchangeably. In order to maintain the structural integrity, prescriptive design rules have been recommended in British codes. BS 5950: Part 1 (BSI, 2000) stipulates that all structural members (beams or columns) in a building should be effectively tied together at each principal floor level. Each column should be effectively held in position by means of horizontal ties in two directions approximately at right angles at each principal floor level supported by that column, and all horizontal ties, and all other horizontal members (connections and beams), should be capable of resisting a factored tensile load of not less than 75 kN (BSI, 2000). This approach (*tying force approach*) is intended to tie a steel frame horizontally and vertically to increase its structural continuity and create a structure with a high level of robustness (Hu et al., 2008). The *tying force* is the action which is generated within steel beams or columns and passed through steel connections. However, *tying resistance* refers to the ability of connections to resist the tying forces. More details of this aspect will be discussed in the following chapters.

1.3 Review of Collapse Related Events

In the UK, consideration of structural integrity as a design issue was initiated by the partial collapse of Ronan Point in 1968. The Ronan Point apartment building was constructed using the Larsen-Neilsen system developed in Denmark: pre-fabricated walls, floors and stairways and then assembling these concrete components, lifted into position by crane and held together by structural bolts. When an explosion occurred on the 18th floor of the new building, blowing out the sections of the outer walls, this modern construction method proved to have a major fault, which permitted a domino style collapse of wall and floor sections from the top of the building to the ground. This (partial) collapse mechanism of Ronan Point arose from a lack of positive attachment between principal elements in the structure (Owens and Moore, 1992), and the connections in this structure were unable to maintain structural integrity under the explosive loading conditions.

On June 23rd of 1990, a fire occurred in a partly completed fourteen storey at the Broadgate development in London (SCI, 1991). The connections were reported to have fractured bolts and end-plate failure due to this accidental fire, which exhibited that fire performance of brittle components (bolts) may be a severe concern in a connection for a steel-framed structure. Subsequently, a series of full-scale fire tests were conducted at the BRE Cardington Laboratory in 1996. This research work involved six large scale fire tests (restrained beam, plane frame, first corner, second corner, large compartment and simulated office) and extensive numerical modelling, funded by British Steel plc (Corus), ECSC, BRE, The Department of Environment Transport and Regions, TNO building and CTICM (British Steel, 1999). In the restrained beam test, partial depth end-plate connections were observed to fracture in the vicinity of the fillet welds, as shown in Fig.1.1 (a). In a subsequent plane frame test, shear failure of structural bolts was reported for the fin-plate connections in Fig.1.1 (b). In a large compartment test, a number of end-plate connections were discovered with end-plate fracture adjacent to the welds (Fig.1.1 (a)). Failure mechanisms of simple steel connections are related to fillet welds and structural bolts, and they are classified as brittle components in the research work of Kuhlmann, *et al.* (1998), due to the very small deformations which occurs before the fracture loads.

(a)

(b)

Figure 1.1: Failure of simple connections in the full-scale fire tests (a) end-plate connections (b) fin-plate connections

This PhD research is intended to discover the interaction mechanism between the brittle (non-ductile) components and ductile components in a connection and its effects on the connection failure mechanism in a steel-framed structure when subjected to fire loading.

1.4 Thesis Layout

This PhD research aims to increase understanding of the fire performance of steel connections in a steel-framed structure and reveal the failure mechanisms of these connections under fire conditions.

Chapter Two reviews the fundamental concepts in structural fire engineering and summarises the research literature on the development of the fire performance of steel connections. This chapter also introduces the component-based approach for modelling steel connections in fire conditions, because development of a component-based connection model is an important research topic in this robustness project.

Chapter Three presents the research methodology adopted, including experimental testing, finite element simulation, and development of component-based connection models.

The fire performance of steel connections is heavily dependent on the behaviour of their components e.g. bolts, welds or end-plates. Therefore, Chapter four presents the research findings of an experimental study of the performance of structural bolts in fire.

Chapter five reports details of an experimental study of partial-depth end-plate connections in fire and investigates the mechanism of connection failure (caused by end-plate fracture at elevated temperatures) using the component-based approach.

Chapter six and Chapter seven utilize two different research strategies: component-based modelling and finite element simulation, to investigate the performance of steel connections at high temperatures. Chapter eight is a further extension of these two chapters and is a parametric study of connection performance within a sub-frame structure.

Chapter nine draws together the knowledge on robustness of simple steel connections in fire and explains how to maintain the structural integrity for tall and large buildings under exceptional loading conditions. The final chapter presents the main conclusions of this PhD research work and recommends the potential research areas for further research.

CHAPTER 2

LITERATURE REVIEW

2.1 Introduction

The traditional approach of ensuring the strength and stability of a steel framed structure under fire conditions is to cover all the exposed areas of steel members with a protective material. Although this approach has proved adequate, it is extremely conservative and expensive in cost of construction. To reduce costs, structural fire design may be conducted which aims to match the mechanical resistance of a steel frame in fire to the loads it is required to maintain during fire exposure. Fire Safe Design (SCI, 2000) contains recommendations for fire protection of principal structural elements such as beams, columns and floors, but little guidance on steel connections. This is because beam-to-column connections are traditionally assumed to have sufficient fire resistance due to their slower rate of heating and thus cooler temperatures as a result of the large concentration of thermal mass in the connection zone than the members to which they are attached (Block, et al. , 2006). The full-scale fire tests at the BRE Cardington Laboratory (British Steel, 1999) and recent experimental tests (Yu et al., 2009 and Hu et al., 2008) have demonstrated that the performance of beam-to-column connections under fire conditions may be more vulnerable than previously assumed. The failure mechanism of steel connections is heavily dependent on connection types and geometry, material performance and resistance of individual components such as bolts and end-plates. Under fire conditions, prevention of progressive collapse of a steel framed structure requires the connections to be a robust structural component, which are capable of forming the plastic hinges and intended to develop catenary actions in a structural system. In providing fire protection to critical structural components, it is essential to have a basic knowledge of fire and its effect on the structural performance of a steel framed building.

2.2 Fire and Fire Development

A flaming fire involves the chemical oxidation of a fuel (e.g. wood) in which heat, light and energy are released with associated flame, usually generating carbon dioxide and water. During this exothermic reaction, substances commonly change to a more stable chemical form. Depending on the specific chemical and physical change taking place within the fuel, the flame may or may not be visible to the naked eye. For example, burning hydrogen or alcohol is usually invisible although tremendous heat is given off during the combustion reaction.

The visible flame has little mass, consisting of luminous gases associated with emission of energy (photons) during the oxidation process. The colour of the flame is dependent upon the energy level of the photons emitted. Lower energy levels produce colours toward the red end of the light spectrum while higher energy levels produce colours toward the blue end of the spectrum. For example, when burning organic matter (e.g. wood), incandescent solid particles produce the familiar red-orange glow of fire, whereas the complete combustion of gas has a dim blue flame due to the emission of single-wavelength radiation from burning substances.

In structural fire engineering, a *standard fire* (or standard fire curve) is the simplest approach to represent a fire by pre-determining some arbitrary temperature-time relationships, which are independent of ventilation and boundary conditions of a building. The primary aim of using a standard fire in tests on structural members is to determine the fire resistance for which an element can survive without violating any of the specified performance criteria (Al-Jabri, 1999). However, it should be realized that the standard fire cannot represent a real natural fire owing to differences in heating rate, fire intensity and duration, which can result in different structural performance.

Unlike the standard fire curve, the real temperature-time response in a compartment fire is a function of the compartment size, the type of compartment together with the available combustible material and air supply available for combustion, which is often referred to as a *natural fire* or *real fire* (Purkiss, 2007). The development of

real fires consists of two distinct phases: pre-flashover and post-flashover, as illustrated in Figure 2.1 (Leston-Jones, 1997). In the pre-flashover stage, the growth of a fire starts with the ignition of combustible material. In the ignition, the fuel must approach a sufficiently high temperature with enough supply of oxygen; then the combustion reactions take place and are restricted to small areas of the compartment. The ignition temperature (flash point) for most common materials is found to be a temperature of approximately 300°C. In this stage, active fire protection measures may be used against fire spread, such as installed fire detection devices and fire extinguishers in the building, which may play an important role for fire protection.

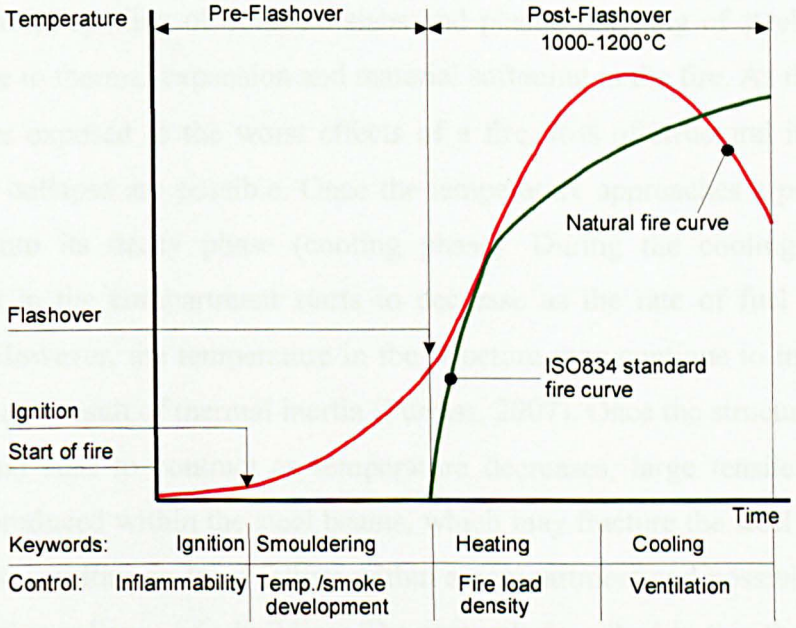

Figure 2.1: The development of a real fire and ISO 834 Standard fire curve (Leston-Jones, 1997)

Between the ignition and flashover (a transition from a growing fire to a fully developed fire) is the growth period of a natural fire. At this stage, the development of the fire involves the spreading from the ignition source and then becomes well established locally, as long as sufficient fuel and oxygen are available. Ventilation conditions in a room can play a significant part in controlling the rate of growth; if a door is opened or windows break, the fire growth may change dramatically (Leston-Jones, 1997). Flashover is the transition from a localised fire to combustion of all exposed combustible surfaces in a room, and the fire spreads to all the available fuel within a compartment. Once a fire reaches the flashover point fire fighters have no control in putting the fire out in the region where the fire initiated, and their concern

becomes stopping the fire from spreading to the adjacent floors or buildings until the fires dies out (Buchanan, 2001). It should be recognized that active fire protection approaches do not play an important role beyond the flashover and passive fire protection measures, including fire protection of essential structural members and means of escape from a building, are essential design issues.

During the *post-flashover* phase, the rate of temperature rise in the compartment is extremely high as the rate of heat release within the compartment reaches a peak. In the heating regime, maximum temperatures within this fire compartment may exceed 1000°C. For (unprotected) structural elements exposed to fire, damage may occur through thermal spalling of concrete slabs and plastic buckling of steel beams and columns due to thermal expansion and material softening in the fire. As the structural elements are exposed to the worst effects of a fire, loss of structural integrity and progressive collapse are possible. Once the temperature approaches a peak, the fire continues into its decay phase (cooling phase). During the cooling phase, the temperature in the compartment starts to decrease as the rate of fuel combustion decreases. However, the temperature in the structure may continue to increase for a short while as a result of thermal inertia (Purkiss, 2007). Once the structural elements (steel beams) start to contract as temperature decreases, large tensile contraction forces are produced within the steel beams, which may fracture the steel connections at both ends, resulting in local failure within a compartment and possibly leading to the progressive collapse of a building. The research described in this thesis is aimed toward developing a simple and economic approach to predict connection performance during the heating and cooling phases of a natural fire.

2.3 Fire Curves

Historically, *standard fire curves* were developed for standard fire furnace tests of structural elements and building materials. This is the simplest approach to represent a fire through the pre-determined temperature-time relationships, which are independent of ventilation and boundary conditions. Standard fire curves have some disadvantages and limitations in representing the real fire performance in a building, including (Bailey, 2006):

a) Standard fire curves do not represent the natural fire performance. The differences in the heating rate, fire load and duration between the standard and real fires can cause different structural behaviour.

b) Standard fires do not always represent the most severe fire conditions. Structural members designed to withstand standard fires may fail to survive in real fires.

The European standard of BS EN 1991-1-2 (2002), describes the standard fire curve as follows:

$$\Theta_g = 20 + 345\log_{10}(8t + 1) \quad (2.1)$$

Θ_g is the gas temperature in the fire compartment (°C)

t is the time (min)

This standard also presents a parametric temperature-time relationship in the annex for a compartment fire, as follows:

$$\Theta_g = 20 + 1325(1 - 0.324e^{-0.2t^*} - 0.204e^{-1.7t^*} - 0.472e^{-19t^*}) \quad (2.2)$$

Θ_g is the gas temperature in the fire compartment (°C)

$t^* = t \cdot \Gamma$ (min)

t is time (min) and Γ is a factor closely related to ventilation conditions, vertical openings and boundary conditions of a fire compartment.

However, this temperature-time curve is valid for fire compartments up to 500 m^2 of floor area, without openings in the roof and for a maximum compartment height of 4 m. It is also assumed that the fire load of the compartment is completely burnt out. The advantage of applying the parametric fire curves for structural member design is to take the compartment size, fire load, vertical openings, ventilation conditions and boundary conditions into account which is a realistic presentation of fire performance in a building fire compartment. More details of formulations for parametric fire curves have been well documented in the standard of BS EN 1991-1-2: Annex A (2002).

2.4 Physical Properties of Steel Materials at Elevated Temperatures

All materials lose their strength and stiffness at elevated temperatures and it is the purpose of fire resistant design that the reduced resistance of structural members exceeds the applied loading effects at the fire limit state (Lawson and Newman, 1996). For structural steel members, the coefficient of thermal expansion, specific heat and thermal conductivity are also important for describing the fire performance of a structure under fire conditions.

2.4.1 Physical properties of structural steel

Although structural steel is non-combustible, it softens when exposed to fire and it begins to lose its strength at temperatures above 300°C. Conventionally, steel is assumed to retain half its strength at 550 °C, which is often referred to as the 'failure temperature'. However, in reality structural steel displays higher strength retention at this temperature. The performance of steel in fire is influenced by the rate of heating, as the deformation component, arising from creep at high temperatures above 450 °C, cannot be neglected for structural member performance under fire conditions. Therefore experimental studies have to concentrate on the practical heating rates of between 5 °C/min for well insulated sections and 20 °C/min for unprotected or lightly insulated sections. These heating rates are related to a limiting temperature of 600°C under the assumption of the limiting temperature is reached after 30 and 120 minutes respectively with a linear heating rate. Lawson and Newman (1996) believe small-scale tensile tests using heating rates in this range would be representative of the performance of structural members in fire.

The physical properties of a material are generally expressed in terms of stress – strain characteristics. Two basic test methods are commonly used for determining these stress – strain relationships for structural steel at elevated temperatures. *Isothermal* or steady-state tests are conducted by heating up unloaded test specimens to a certain temperature and then performing a tensile test. The stress-strain curve is recorded for the given temperature. In order to establish a family of stress - strain relationships for structural steel at elevated temperatures, a series of isothermal tests must be carried out at different temperatures. *Anisothermal* or transient tests are the

case in which the specimen is subject to a constant load and increasing temperatures. The reference heating rate is generally taken as 10 °C/min (i.e. 600°C rise in 60 minutes). Since the test is carried out under a constant load, a temperature- strain relationship is recorded during the tests. Stress strain curves may be derived from a number of curves at different stresses. Kirby and Preston (1988) used these two methods to determine the physical properties for S275 and S355 steels over a temperature range of 20 °C to 900 °C. They found that the transient – state tests indicate lower strength than steady state tests, but may be considered to be more realistic for structural application. The stress-strain characteristics, established from these tests, have been adopted in BS 5950: Part 8 and later in EC3: Part 1-2 and a typical set of curves for a range of temperatures is shown in Figure 2.2.

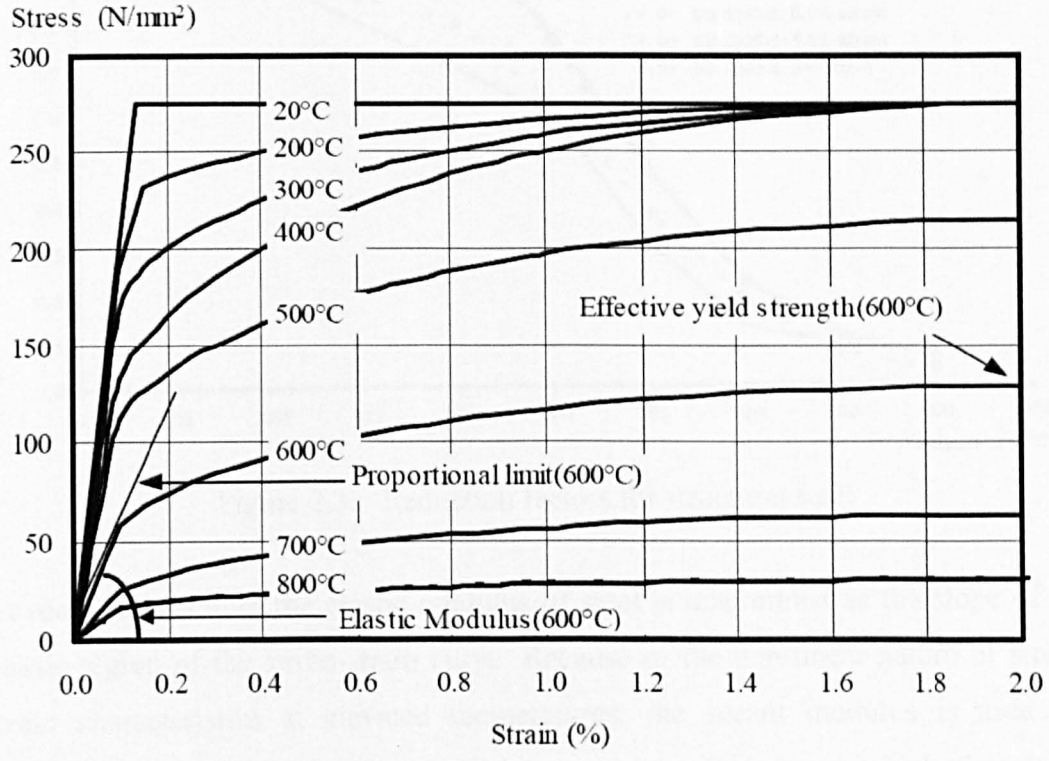

Figure 2.2: Stress-strain characteristics for S275 steel at elevated temperatures (Al-Jabri, 1999)

British standards adopt the concept of a "Strength Retention Factor" to represent the degradation of material strength at elevated temperatures; while in EC3: Part 1-2, the factor is termed as "Strength Reduction Factor". This factor indicates the residual strength of the steel at a particular temperature relative to the basic yield strength at room temperature. The strength reduction factors for structural steel according to BS

5950: Part 8 and EC3: Part 1.2 are presented in Figure 2.3. There are three different strain limits in BS 5950: Part 8 for application to different types of structural members. The lower strain limit of 0.5% is used for columns and reflects the influence of instability of these members under fire conditions. The strain value of 1.5% is used for universal beams with protection materials remaining intact in a fire and the higher strain limit of 2% is used for composite beams. In the standard of EC3: part 1.2, 2% strain is used throughout this code with modification for different types of members.

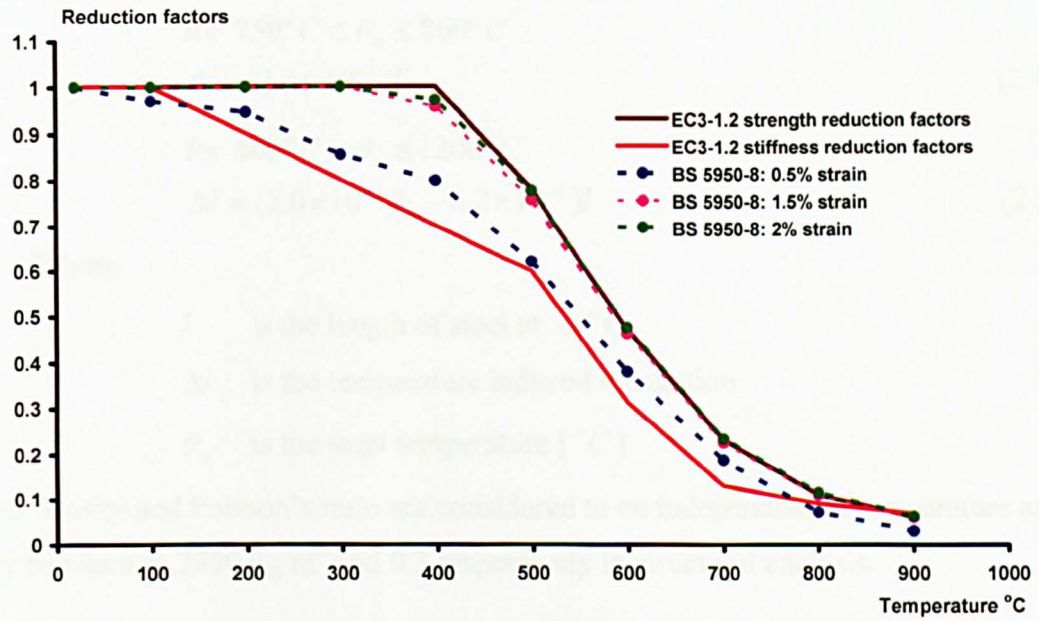

Figure 2.3: Reduction factors for structural steel

At room temperature the elastic modulus of steel is determined as the slope of the elastic region of the stress-strain curve. Because of the non-linear nature of stress-strain characteristics at elevated temperatures, the secant modulus is used for structural steel. However, this depends on the proof strain at which the elastic modulus is measured. The reduction of the elastic modulus of steel with increasing temperatures in BS 5950: Part 8 and EC3: Part 1.2, are very similar. Fig. 2.3 shows the stiffness reduction factor of EC3-1.2.

Steel expands when heated up and this expansion is a function of temperature represented as the coefficient of thermal expansion, α_T. This coefficient increases slightly with temperature. At room temperature α_T is taken as $12 \times 10^{-6}/^{o}C$, and $14 \times$

$10^{-6}/^{o}C$ is taken for the temperature range of 200 °C to 600 °C. These expansion coefficients are recommended in BS 5950: Part 8. At around 730 °C, steel undergoes a phase change and there is a marked change in the expansion properties as energy is absorbed and the material adopts a denser structure (Lawson and Newman, 1996). In the standard of EC3: Part 1.2, the total elongation (extension), Δl , of steel is expressed by the following tri-linear relationships including temperatures beyond the point of phase change:

$$\text{for } 20^{o}C \le \theta_a < 750^{o}C$$
$$\Delta l = (1.2\times10^{-5}\theta_a + 0.4\times10^{-8}\theta_a^2 - 2.416\times10^{-4})l \quad (2.3)$$

$$\text{for } 750^{o}C \le \theta_a \le 860^{o}C$$
$$\Delta l = (1.1\times10^{-2})l \quad (2.4)$$

$$\text{for } 860^{o}C < \theta_a \le 1200^{o}C$$
$$\Delta l = (2.0\times10^{-5}\theta_a - 6.2\times10^{-3})l \quad (2.5)$$

Where:

l is the length of steel at $20^{o}C$

Δl is the temperature induced elongation

θ_a is the steel temperature $[^{o}C]$

Steel density and Poisson's ratio are considered to be independent of temperature and may be taken as 7850 kg/m^3 and 0.3 respectively in structural analysis.

2.4.2 Bolts and welds at elevated temperatures

Bolts and welds are structural components with great importance when connecting different structural elements (beams and columns). Grade 4.6 and 8.8 bolts, specified to BS 3692 or BS 4190, are two major types of bolts used for building construction. Grade 4.6 bolts are forged from mild steel (low carbon steel), whereas grade 8.8 bolts are manufactured from micro-alloy steel which is quenched and tempered to obtain their high strength (Lawson and Newman, 1996). In general, the actual strength of structural bolts is higher than the nominal ultimate strength marked on the products, and the strength retention of these bolts is at least equivalent to the strength of the parent steel at elevated temperatures, but there is a more marked loss of strength between 600 °C and 700 °C. The normal partial safety factor of 1.25 for room temperature bolt design is set to 1.0 under fire conditions. Therefore, the actual

strength retention of bolts might be higher than the adjacent steel members in fire conditions. In order to determine the deterioration of bolts in fire a series of tests was carried out by Kirby (1995) on Grade 8.8 bolts. The author also conducted another series of tests on the same grade bolts because of new bolt standards published recently. The author's investigation on 8.8 bolts will be comparatively discussed with Kirby's tests in Chapter 4. The strength retention factors of bolts, recommended in the standards, are presented in Figure 2.4.

Little data has been found related to the behaviour of welds at elevated temperatures. Lawson and Newman (1996) mentioned that the strength of welds decreases markedly in the temperature range of 200 °C to 400 °C, but then becomes stabilized close to the reduced strength of the parent steel. The strength retention factors are shown in Figure 2.4.

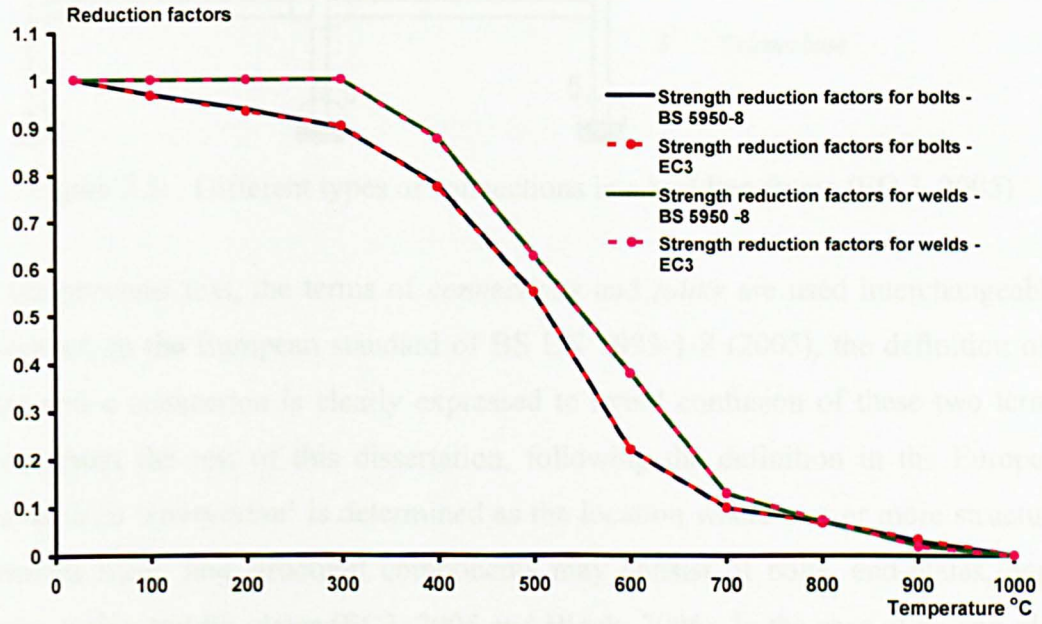

Figure 2.4: Strength reduction factors for bolts and welds

2.5 Connections and Joints

A steel frame structure is a complex assembly of many individual steel elements, consisting of universal beams and columns joined by means of *connections (joints)* to form a working unit. Beam-to-column connections are one of the structural elements which are found to be of great significance in retaining the structural

integrity and contributing to overall building stability at both ambient and elevated temperatures. Although early steel connections were fabricated using rivets, present beam-to-column connections are fabricated using high strength bolts and fillet welds. According to the location, the *joints* (*connections*) between the principal structural members may be classified as: beam-to-beam connections, beam-to-column connections, column splices, beam splices and column bases (EC3, 2005), as shown in Figure 2.5.

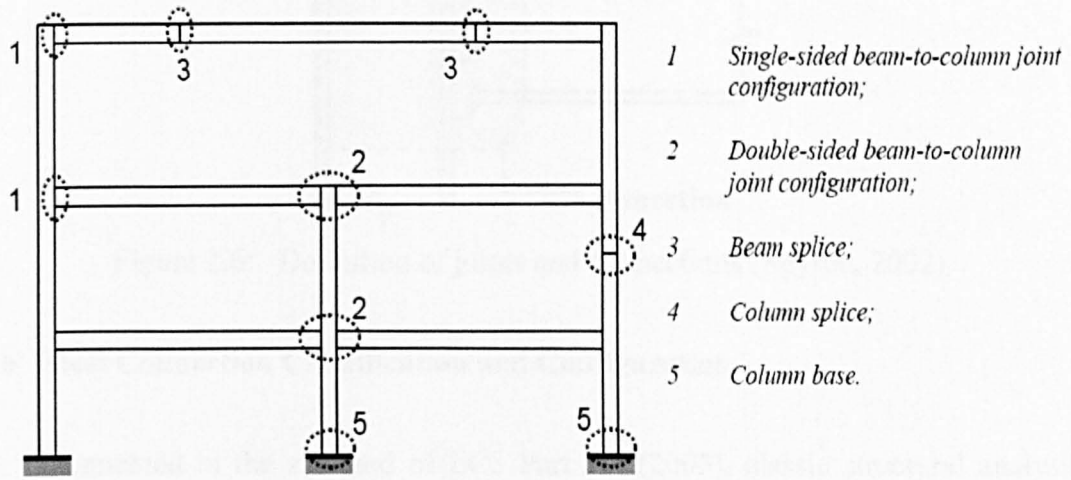

Figure 2.5: Different types of connections in a building frame (EC 3, 2005)

In the previous text, the terms of *connections* and *joints* are used interchangeably. However, in the European standard of BS EN 1993-1-8 (2005), the definition of a joint and a connection is clearly expressed to avoid confusion of these two terms. Throughout the rest of this dissertation, following the definition in the European standards, a '*connection*' is determined as the location where two or more structural elements meet; and structural components may consist of bolts, end-plates, angle cleats, welds and fin plates (EC3, 2005 and Block, 2006). In the case of an end-plate connection, the connection is comprised of the bolts, the welds, the end-plate and the column flange. A *joint* is defined as the whole region at which two or more members are interconnected. For example, a beam-to-column joint can include up to four connections, two major – axis connections attached to the column flanges and two minor – axis connections attached to the column web (Block, 2006), as shown in Fig. 2.6. In the conventional structural analysis of a steel-framed building, beam-to-column connections are assumed to perform with full moment resistance (moment connections) or without any moment resistance (pin connections). This theoretical

assumption has simplified connection design, but has also been questioned by experimental investigations on various connection types. This is because, in the experimental investigation, even the pin connections have some capacity to resist end beam moments (Sarraj, 2007).

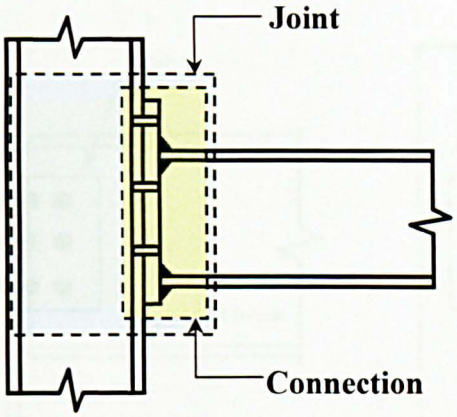

Figure 2.6: Definition of joints and connections (Spyrou, 2002)

2.6 Steel Connection Classification and Configuration

As documented in the standard of EC3 Part 1.8 (2005), classic structural analysis assumes the beam-to-column connections behave as *pinned* or as *fully fixed* (full moment resistance or rigid), which significantly simplifies the analysis and design procedures. However, the actual performance of steel connections is always located between these two extremes.

2.6.1 Simple and moment connections

In the design procedure, *simple connections* must carry shear forces transmitted from beams to columns, but their resistances to bending moments are not required for connection design. Since simple steel connections offer a significant degree of simplicity and standardisation, they are invariably cheaper to fabricate than moment connections, which is an important driving force for these connections to be utilized in the building construction. In the documentation of Joints in Steel Construction – Simple Connections (SCI, 2002), three simple connections have been outlined for detailed connection design, and they are partial depth end-plates (flexible end-plates), fin plates and double web angle cleats. Therefore, all these simple

connections are involved in the robustness project for investigation of their performance in fire. Moreover, simple steel connections also include top- and seat-angle connections, single web angle steel connections and top- and seat – angle with double web-angle connections, as shown in Figure 2.7, but these connections are not commonly used in UK steel construction.

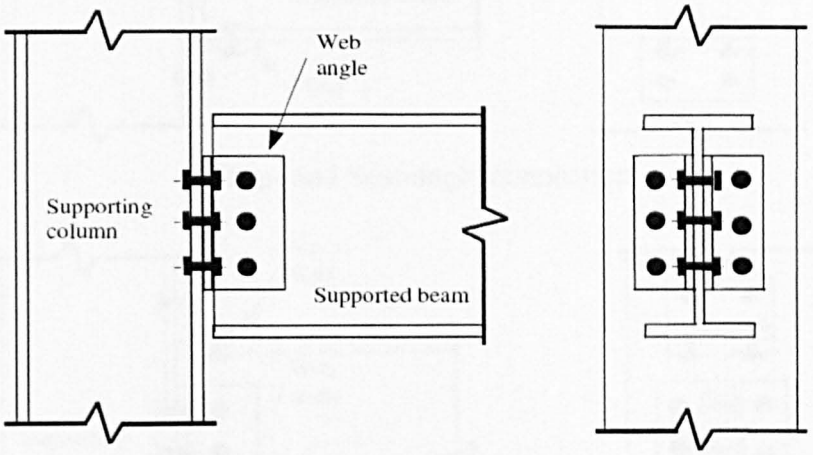

(a) Double web angle steel connection

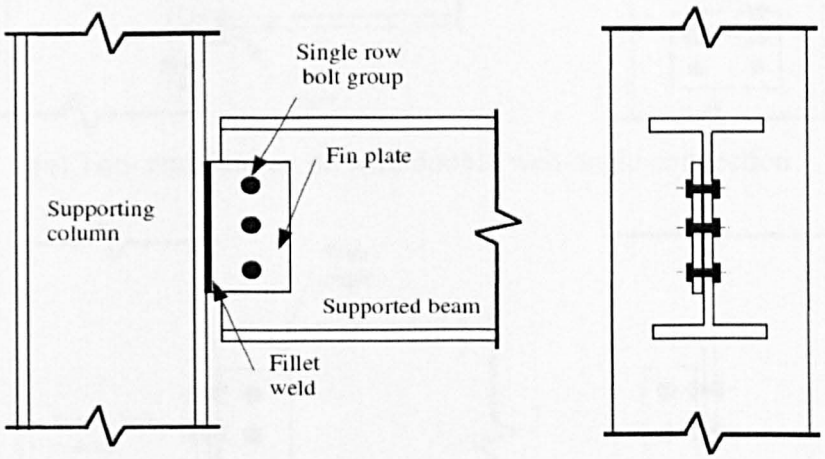

(b) Fin plate steel connection

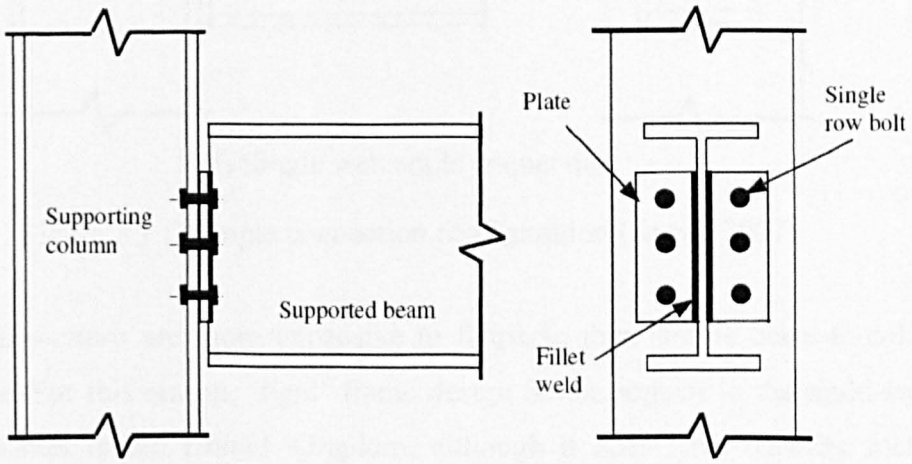

(c) Header plate steel connection

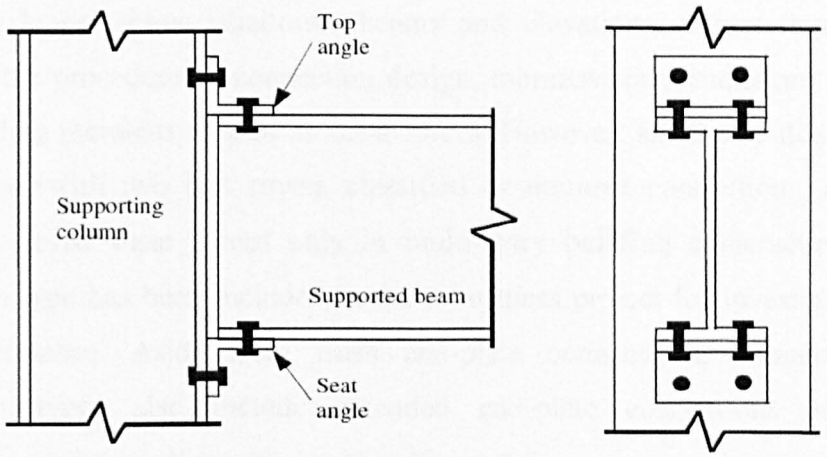

(d) Top- and Seat-angle connection

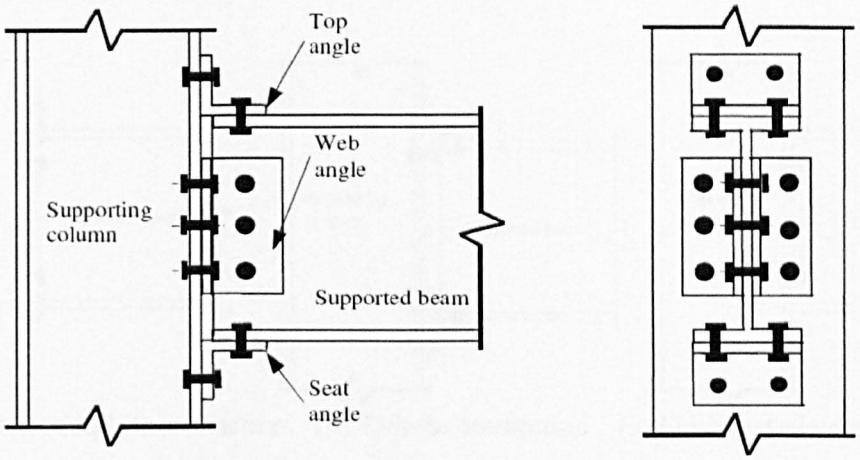

(e) Top- and Seat-angle with double web-angle connection

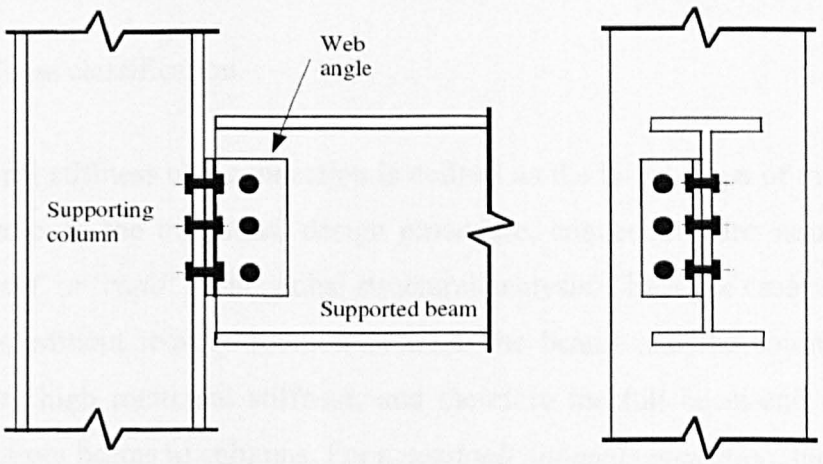

(f) Single web angle connection

Figure 2.7: Simple connection configuration (Sarraj, 2007)

Moment connections are more expensive to fabricate than simple beam-to-column connections. For this reason, 'rigid' frame design is not popular in the multi-storey building market in the United Kingdom, although it does have benefits such as

permitting longer spans, shallower beams and elevations without bracing (SCI, 1995). In the procedure of connection design, moment connections are required to resist bending moments as well as shear forces. However, small-size flush end-plate connections (with two bolt rows), classified as moment connections, are usually utilized to resist shear forces only in multi-story building construction. So this connection type has been included in the robustness project for investigation of its fire performance. Aside from flush end-plate connections, moment resisting connection types also include extended end-plate connections and T-Stub connections, and they all are displayed in Figure 2.8.

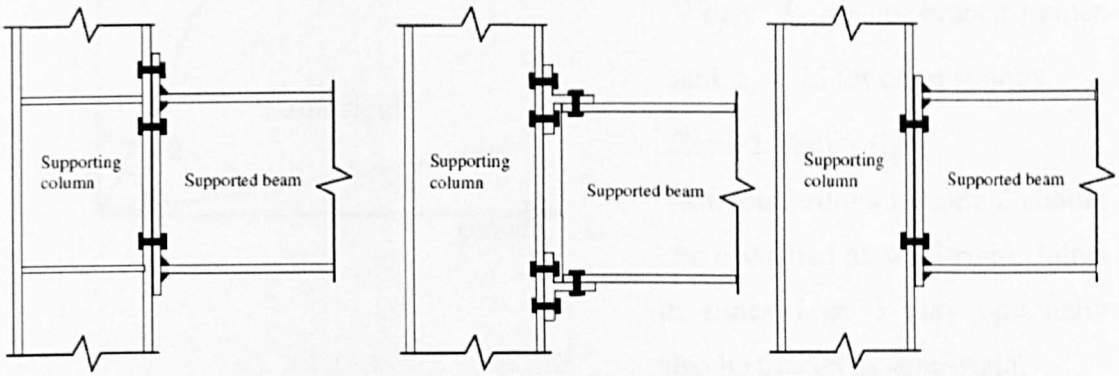

(a) Extended end-plate connection (b) T-Stubs connection (c) Flush end-plate connection

Figure 2.8: Moment connections (Sarraj, 2007)

2.6.2 Stiffness classification

The rotational stiffness of a connection is defined as the initial slope of the moment-rotation curve. In the traditional design procedure, connections are assumed to be either '*pinned*' or '*rigid*' in the global structural analysis. The *Rigid* case refers to the connections without relative rotation between the beams and the columns, which possess very high rotational stiffness, and therefore the full beam-end moment is transferred from beams to columns. For a *nominally pinned connection*, the rotational stiffness is assumed to be zero in the analysis, and therefore no moments can be transferred between the structural members at the theoretical level. However, pinned connections are able to transfer shear and horizontal loading effects to the steel columns and may possess the higher level of rotational ductility for analysis purposes. Over the last eighty years of investigation on steel connections, it has been shown that the real performance of steel connections is neither rigid, nor pinned. The

majority of steel connections used in building construction are *semi-rigid.* In this case, these connections allow some relative rotation between the beams and columns, and beam-end moments, dependent on the connection stiffness, are transferred within the structures. For simplification in design, the European standard of BS EN 1993-1-8 (2005) specifies the boundaries between connections which are assumed to behave as pinned or rigid, as shown in Figure 2.9.

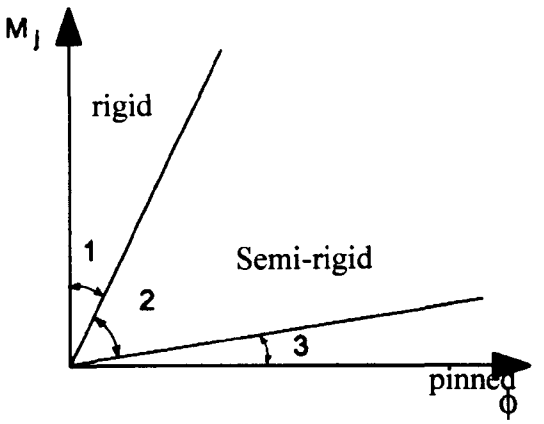

Zone 1: rigid, if $S_{j,ini} \geq k_b EI_b / L_b$

Where $k_b = 8$ for braced frames and $k_b = 25$ for other frames

Zone 2: semi - rigid

All connections in zone 2 should be classified as semi-rigid. Joints in zones 1 or 3 may optionally also be treated as semi-rigid.

Zone 3: nominally pinned, if $S_{j,ini} \leq 0.5EI_b / L_b$

Where I_b is the second moment of area of a beam and L_b is the span of a beam.

Figure 2.9: Stiffness classification of joints in EC3-1.8 (EC3, 2005)

2.6.3 Strength classification

The European standard of BS EN 1993-1-8 (EC3, 2005) recommends that a steel connection may be classified as full-strength, nominally pinned or partial strength by comparing its design moment resistance $M_{j,Rd}$ with the design moment resistances of the connected members $M_{pl,Rd}$. If the moment resistance of the connection is equal to or larger than the plastic moments of the connected members ($M_{j,Rd} \geq M_{Pl,Rd}$), then the connection is regarded as *full strength.* A *nominally pinned connection* means the bending resistance of the connection is not greater than 0.25 times the design moment resistance required for a full-strength connection ($M_{j,Rd} \leq 0.25M_{Pl,Rd}$). As a *partial strength connection,* it must not satisfy the criteria for a full strength

connection or a nominally pinned connection, and the bending moment resistance must be allocated between these two boundaries ($0.25M_{Pl,Rd} \angle M_{j,Rd} \angle M_{Pl,Rd}$). The plastic moment resistance of the connected member is commonly regarded as the plastic moment of the connected beam $M_{b,pl,Rd}$, but might be the plastic moment of the connected column $M_{c,pl,Rd}$ as well. This detail has been well documented in the connection standard and the strength classification of the connections has also been illustrated in Figure 2.10, as follows.

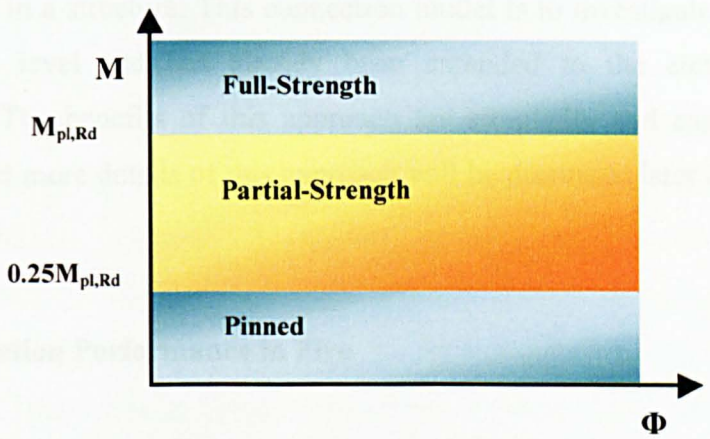

Figure 2.10: Classification of connections by strength (Spyrou, 2002)

2.6.4 Rotation capacity classification

In Joints in Steel Construction – Moment Connections (SCI, 1995), the ductility of a connection has been referred to as rotational capacity, representing the ability of the connection to rotate whilst maintaining its plastic moment resistance over a sufficient rotation range (Gomes *et al.*, 1998). In applying plastic analysis in structural design, plastic hinges may form in the simple steel connections and not in the adjacent members. Therefore, sufficient rotational capacity of a connection is required to enable the development of the assumed plastic mechanism in the mid-span of the adjacent members. This connection is therefore categorised as *ductile* (Class 1 connections), in accordance with the research work of Jaspart (1996, 1997 and 1998). The lower bound of the ductility classification is Class 3, indicating brittle failure or instability limits the rotation capacity or moment resistance and full redistribution of the internal forces is not allowed in the joint. It is worth pointing out that brittle performance of the connections in this class may be caused by the failure of brittle connection components; and therefore moment resistance and ductility are limited.

Class 2 connections are allocated between the ductile and the brittle performance, called 'semi-ductile'; however, the boundaries between these classes are not clearly determined in Jaspart's research (Block, 2007). In EC3 – Part 1.8, the rotational capacity or ductility of connections is treated in a very approximate way (Block, 2007) through a component-based approach. A number of researchers in Europe and UK (Simoes da Silva and Coelho, 2001; Spyrou, 2004a and 2004b; Beg et al., 2004 and Coelho et al., 2004) have already conducted some research work on the component-based connection model in order to predict the performance of steel connections in a structure. This connection model is to investigate a connection in a macro-scale level and has already been extended to the elevated temperature conditions. The benefits of this approach are simplicity and ease without loss of accuracy and more details of this approach will be discussed later in this chapter and in Chapter 6.

2.7 Connection Performance in Fire

Beam-to-column connections represent one of the most important components in a real structure for which reliable assessment and simulation are required (Sulong, 2005). The earliest experimental investigations on the performance of beam-to-column connections under fire conditions are rather limited in number, due to the high cost of the fire tests, limitations on the size of furnace used and difficulties in recording the deformation of steel connections. The current design procedures for bolted steel connections are based on moment-rotation relationships through isolated connection tests in fire and therefore fail to account for the actual interactions that take place in a real structure. Nevertheless, the results from the fire tests carried out on isolated connections provide very important fundamental data on the behaviour of bean-to-column connections.

The first experimental fire tests on steel connections were carried out by Kruppa (1976) at CTICM in France with connection types ranging from "flexible" to "rigid". The primary purpose of these tests was to look into the performance of high-strength bolts under fire conditions and the experimental results demonstrate that the failure of bolts was inevitable.

By contrast, two elevated-temperature connection tests carried out by British Steel (1982) indicated that bolts and their connected components experienced considerable deformation under fire conditions and there was no failure of brittle components (bolts and welds) for these two moment connections subjected to fire loading.

The first tests to investigate the structural continuity afforded by beam-to-column connections at elevated temperatures were carried out by Lawson (1990). The aim of this experimental programme was to develop a design approach for steel beams taking the rotational restraint provided by the connections into consideration. In this experimental programme, composite and non-composite connections were tested under fire conditions. These tests demonstrated the strength of these connections in fire and showed that up to two-thirds of their ambient temperature design moment capacity could be sustained in fire conditions. It was also shown that the rotation of the connections in all tests exceeded 6° (104.7 mrads) and the premature failure in structural bolts did not take place. Sulong (2005) believes that this may be a proof of the inherent robustness of connections in fire. Lawson also indicated the composite action in fire may contribute to an enhanced moment capacity of steel connections. Although the test results afforded insufficient experimental data to describe the moment-rotation characteristics of the connections, they did provide some essential information for connection modelling.

Eleven experimental tests were conducted by Leston-Jones et al. (1997) to establish the moment-rotation relationships for flush end-plate connections at elevated temperatures. The experimental results demonstrated that both the stiffness and moment capacity of the connections decreased with increasing temperature with a significant reduction in capacity for temperatures in the range of 500 – 600 °C. Al-Jabri (1999) developed a series of elevated-temperature connection tests as an extension of the previous investigation. This research work investigated the influence of parameters such as member size, end-plate type and thickness and composite slab characteristics on the connection response in fire. A family of moment-rotation-temperature curves was established for each connection. In these tests, it was also reported that the structural bolts in the connections failed due to the premature failure of nut threads stripping off at elevated temperatures.

As documented in the book of *steel and composite structures: behaviour and design for fire safety* (Wang, 2002), Allam et al. (2002), in collaboration with the research staff at the University of Manchester (Liu et al., 2002), carried out some experiments on restrained beams to investigate the effects of translational and rotational restraint to the performance of steel beams under fire conditions. This study highlights the effect of the axial horizontal restraints under fire conditions. In these experiments, large axial compressive forces were recorded in the early stages of a furnace fire, but after the vertical beam deformations increased, the compressive forces changed to tensile (or catenary forces) and increased the failure temperature of the beam considerably compared with an un-restrained beam (Block, 2006). Allam and his co-researchers (2002) also indicate that the tensile axial force at large deflection can lead to integrity failure and consequent fire spread, if sufficient strength and ductility are not secured for key elements such as connections and beams. In this experimental programme, since columns and connections were fire-protected, no failure of connections was reported in these tests.

More recently, Spyrou et al. (2004a and 2004b) and Block (2006) reported the results of an experimental investigation of the performance of the tension and compression zones of steel connections at elevated temperatures. In Spyrou's study, bolt premature failure due to threads stripping occurred in testing the T-stub elements. Both researchers developed analytical models for the tension zone and compression zone components at both ambient and elevated temperatures. This formed an important theoretical base for the development of component-based models in fire. Sarraj (2007) developed an empirical mathematical model for shear components in steel connections in fire.

A series of full-scale fire tests were conducted on an eight-story composite building at the BRE Cardington Laboratories in Bedfordshire between 1995 and 1996. In 2003, the seventh fire test at Cardington has been carried out by Wald (2006), and focused the research efforts on temperature distribution and damage mechanisms of beam-to-column connections under a natural fire. These connections were exposed to fire without protective materials, and then rupture of partial depth of end-plate connections along welds and fracture of bolts in the fin plate connections were

reported in this fire test. Local buckling of the beam bottom flange, shear buckling of beam webs and plastic deformation of the column flange were also found in these full-scale fire tests. All these failure mechanisms indicate considerable axial forces were developed within the steel beams and that robustness of steel connections against the failure in fire is much more important for maintaining structural integrity of a steel frame structure under fire conditions.

The experimental results from the preceding fire tests supplied very important and fundamental information about connection performance in fire. As mentioned earlier, inaccurate idealised fire conditions (standard fires) do not always represent the most severe fire conditions. Hence, it is demonstrated that the actual connection behaviour in a steel-framed structure is much more complicated than in the isolated connection tests, when subjected to fire loading (Sulong, 2005).

2.8 Component-based Approaches

In the last twenty years, finite element simulation has been popular to predict the connection response at both ambient and elevated temperatures. In comparison with experimental testing, this approach is cost-effective and reliable for capturing the connection behaviour in fire. As an alternative, the component-based approach has been introduced in the European standard of EC3 – part 1.8, which can be employed for simulating the performance of beam-to-column connections. This new approach is very simple without loss of accuracy in prediction, and more economical and efficient in comparison with the finite element simulation, which is therefore suitable for use as a tool for robustness connection design.

The component-based method offers an attractive solution for connection modelling due to its versatility and efficiency (Sulong, 2005). The original concept of this approach is to regard any connection as a mechanical (or spring) model consisting of a group of extensional springs to represent the performance of the connection. Nonlinearity of the connection response is accounted for through adoption of inelastic constitutive laws (nonlinear load and displacement relationships) for the

deformable components. The development of the component-based method is reviewed in the following sections.

2.8.1 Development of the component method

Wales and Rossow (1983) applied the component-based approach to describe the coupled moment-axial force performance in bolted connections. Their research concentrated on double web angle connections, and the connection was simplified as an assembly of two rigid bars and nonlinear distribution spring elements, which simulates the angle segments. Tri-linear load and displacement relationships were determined as the constitutive laws for these springs. Good agreements with experimental results were obtained.

Tschemmernegg and Humer (1988) studied end-plate connections through using three nonlinear springs, including a "load introduction spring", a "shear spring" and a "connection spring". These springs are adopted for determination of the deformation performance of the beam flanges, panel zone and connection components. Satisfactory connection response was obtained when calibrated against experimental data.

Madas (1993) extended the research work of Wales and Rossow (1983) on connection modelling, and applied the component-based method to different types of connections including both bare steel and composite connections. The connection types included flexible end-plate, double web angle and top and seat angle connections.

Shi and his co-researchers (1996) investigated the moment-rotation response of end-plate connections by means of T-Stub components. In the analysis of deformation, the connection was divided into three zones: tension, compression and shear zone. The end-plate response was assumed to be the assembled behaviour of a number of T-shape elements, each corresponding to a single bolt row. Based on the classical beam theory, the relation between deformation and tension force has been determined for each T-shape element. The deformation relationship for compression

and shear was based on an assumption of the components in these two zones yielding at a certain load level. The authors determined the connection maximum moment-resistance and deformation, according to the following properties:

1. Fracture of bolts in the tension zone
2. Yielding of column flange, end-plate, column web and beam web in tension
3. Buckling or yielding of column web and beam flange in compression
4. Yielding of column web due to shear force
5. Rupture of welds

Through using displacement control, the connection moment was obtained for a given rotation.

Pucinotti (2001) focused his research efforts on the moment-rotational performance of top-and-seat and web angle connections for an extension of EC3 Annex J. The analysis takes the web angle and material hardening into consideration and the maximum resistance of the weakest component in the connection governed the connection overall capacity and ductility. At present, the effect of axial forces in the connection is not accounted for in the connection design procedure (EC3-1-8, 2003).

As mentioned previously, the component-based approach is efficient and versatile as a design approach for analyzing the performance of connections. Recent investigation proves that the connection response under bending and axial force can be represented by means of the component method. But a further need in this approach is to develop component-based models accounting for all possible loading conditions at both ambient and elevated temperatures. Therefore, the component-based method has been applied to the elevated temperature conditions by using the component models of ambient-temperature in combination with high-temperature material properties.

Leston-Jones (1997) created a spring model for high temperatures with four basic components: column flange in bending, bolts in tension, end-plate in bending and column web in compression. This spring model is for a flush end-plate connection with two bolt rows. The force and displacement curves of these components were

determined in a tri-linear fashion and the model was verified against the elevated-temperature tests by the researcher.

Al-Jabri (1999, 2005) extended the research work of Leston-Jones to partial depth end-plate connections through applying the component-based approach to connection modelling of high temperature experimental tests. Good agreements were achieved between his spring model and the experiments.

Important progress in the component method, documented in Spyrou (2002) and Spyrou et al. (2004a and 2004b), is clarification of the T-Stub component behaviour at ambient and elevated temperatures. As mentioned above, the T-Stub component is used to represent the behaviour of two bolt rows or a single bolt row in the tension zone (Zoetemeijer, 1974). As a T-stub assembly, there are three possible collapse mechanisms leading to the component failure, as shown in Figure 2.11:

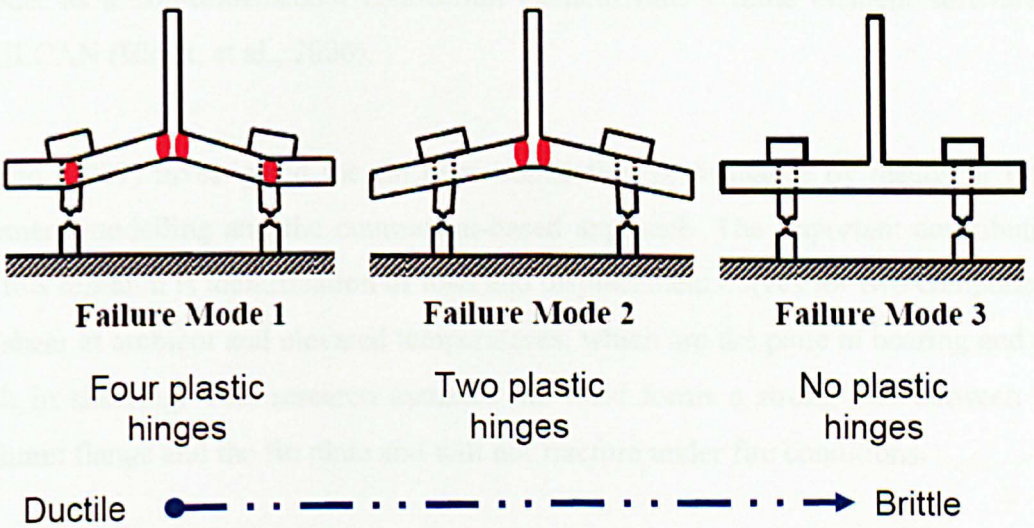

Figure 2.11: Failure mechanisms of T-Stub components

a) In the first mode of failure, the flange of the T-stub is very thin and the bolts are relatively strong in the assembly. Four plastic hinges (complete yielding of the T-Stub flange) are formed within the T-Stub flange.
b) In the second failure mode case, only two plastic hinges are formed at the flange-to-web connection, and then followed by yielding and fracture of the bolts.

c) In the final mode of failure, no plastic hinges are formed within the T-stub flange and failure is due to fracture of the bolts.

The authors developed the analytical models, based on classical beam theories, to describe the above three failure mechanisms and these models will be reviewed in Chapter 6. The advantage of these analytical models is the inclusion of prying effects and compatibility of bolts' and end-plates' deformation into the analysis. Unfortunately, weld failure is not considered for the T-Stub components at ambient and elevated temperatures.

Block (2006) carried on the research of Spyrou (2002), focusing on the behaviour of components in the compression zone. The most important contribution from this researcher is presentation of a simplified analytical model for the force-displacement behaviour of the compression zone with inclusion of the effects of axial loads in the column. Block also successfully programmed the component-based connection model as a non-dimensional connection element into a finite element software – VULCAN (Block, et al., 2006).

Sarraj (2007) investigated the fin plate connection performance by means of finite element modelling and the component-based approach. The important contribution of this research is identification of load and displacement curves for two components in shear at ambient and elevated temperatures, which are the plate in bearing and the bolt in shearing. This research assumes the weld forms a strong link between the column flange and the fin plate and will not fracture under fire conditions.

2.8.2 The standard procedure of the component-based approach

Current design codes (EC3-1-8, 2003) adopt the component-based approach for prediction of the rotational behaviour of steel beam-to-column connections. The fundamental idea of this approach is to model a connection as an assembly of extensional springs and rigid bars (Weynard *et al.*, 1995). Therefore, the connection is divided into three different zones: tension, compression and shear, adopting the concept of Shi et al. (1996). Within each zone, the simple elemental parts (springs or components) are able to make a contribution to the overall response of the

connection. From a theoretical point of view, this methodology can be applied to any joint configuration and loading conditions provided that the basic components are properly characterized (Coelho, 2004). As illustrated in the example shown in Figure 2.12, an extended end-plate connection under pure bending moment is categorized into three major zones (tension, shear and compression) and then each zone is divided into the relevant components. Sulong (2005) notes that, when a connection is subjected to combined effects of axial forces and bending moments, the concept of tension and compression zone is no longer applicable. Furthermore, the connection in a steel frame may be subjected to a non-monotonic loading history in fire, and then the components in the tension zone might be subjected to compressive loading effects. Therefore, all possible components in every single bolt-row must be taken into consideration for an accurate representation of the connection response.

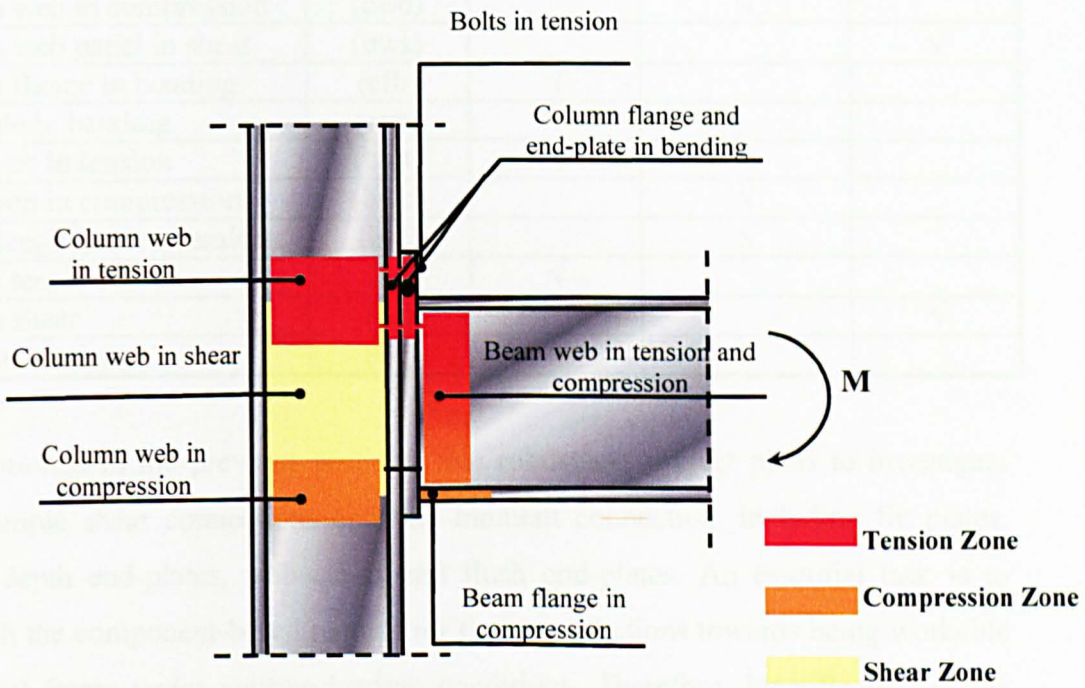

Figure 2.12: Three zones and their components within a steel connection (Spyrou, 2002)

Application of the component-based approach needs the following three basic steps:

1. Identification of the active components within a connection
2. Evaluation of the stiffness and resistance characteristics for each individual component

3. Assembly of all the active joint components into a mechanical/spring model for evaluation of the connection response

The first step of the component approach is the identification of the components contributing to the connection flexibility or limiting the connection resistance towards establishing connection response. As an example, for an extended end-plate connection subjected to pure bending, the European standard of EC3-1-8 presents the active components summarized in Table 2.1.

Table 2.1: Active components for extended end-plate connections

Components	Index	Tension zone	Compression zone	Shear zone
Column web in tension	(cwt)	√		
Column web in compression	(cwc)		√	
Column web panel in shear	(cws)			√
Column flange in bending	(cfb)	√		
End-plate in bending	(epb)	√		
Beam web in tension	(bwt)	√		
Beam web in compression	(bwc)		√	
Beam flange in compression	(bfc)		√	
Bolts in tension	(bt)	√		
Bolts in shear	(bs)			√
Welds in tension	(wt)	√		

As mentioned in the previous sections, this robustness project plans to investigate three simple shear connections and one moment connection, including fin plates, partial depth end-plates, web cleats and flush end-plates. An essential task is to establish the component-based models for these connections towards being workable in a steel frame under various loading conditions. Therefore, identification of the active components for these connections is the first step of establishing the connection performance.

a) Fin plate connection

Based on previous studies on fin plate connections (Astaneh, 1989 and Astaneh-Asl et al., 1993), Sarraj and Sulong (2007, 2005) respectively reported the six potential failure modes for this type of connection: yielding of the gross area of

the plate, bearing failure of bolt holes, fracture of net section of plate, facture of edge distance of plate, bolt fracture and welds fracture. In line with simple connection design, the first two patterns of failure (plate yielding and bearing failure of bolt holes) are regarded as ductile failure modes owing to yielding of steel material. Since the rest of the patterns for failure involve fracture of steel material, they are commonly regarded as brittle failure modes. Therefore, based on these failure mechanisms, the potential active components for fin plate connections are:

1) Bolts in shear
2) Beam web in bearing
3) Plate in bearing
4) Welds in shear/tension
5) Column web in compression

b) Double angle web cleats

Double angle web cleats are more flexible than end-plate connections. Yu et al. (2008) developed a 'web cleat' component for describing the non-linear load and displacement response of web angles under tensile loading. However, Sulong (2005) identified seven active components for these connections:

1) Bolts in tension
2) Bolts in shear
3) Column flange in bending
4) Beam web in bearing
5) Web angle in bearing
6) Web angle in bending
7) Web angle in tension

c) End-plate connections

End-plate connections comprise flexible and flush end-plate connections. For flush end-plate connections, Block (2006) assumed that no weld failure occurs in this type of connection and the active components are as follows:

1) End-plate in bending
2) Column flange in bending
3) Column web in compression
4) Bolts in tension

However, the Block's component-based model did not consider the possible active components in the direction of shear (e.g. bolts in shear) and beam web behaviour. These components might be critical in fire. For the flexible end-plate connections, more details of its component-based model are documented in Chapter 6.

Identification of the load and displacement constitutive laws for active components is the most important stage for development of component-based models. Based on the force and displacement constitutive laws and modes of failure, the components are categorized into three different classes: components with high ductility, components with limited ductility and components with brittle failure (Kuhlmann, et al. 1998). The individual load and displacement relationship may be elastic-plastic (bi-linear), multi-linear or nonlinear for each active component, as shown in Figure 2.13 (Block, 2006). In the standard of EC3-1-8, each component is characterised by an initial stiffness k and a design resistance F_{Rd}, which follows the elastic-perfectly plastic model. However, for higher accuracy in the approximation, the more complex force-displacement models can be employed, which are derived from experimental results or finite element simulation. Accounting for the effects of high temperature, the standard of EC 3-1-2 specifies the reduction factors for stiffness and strength of different steel materials (i.e. S275 steel, bolts and welds). Therefore, the component-based method can be extended to the elevated temperature situation by employing high temperature material properties.

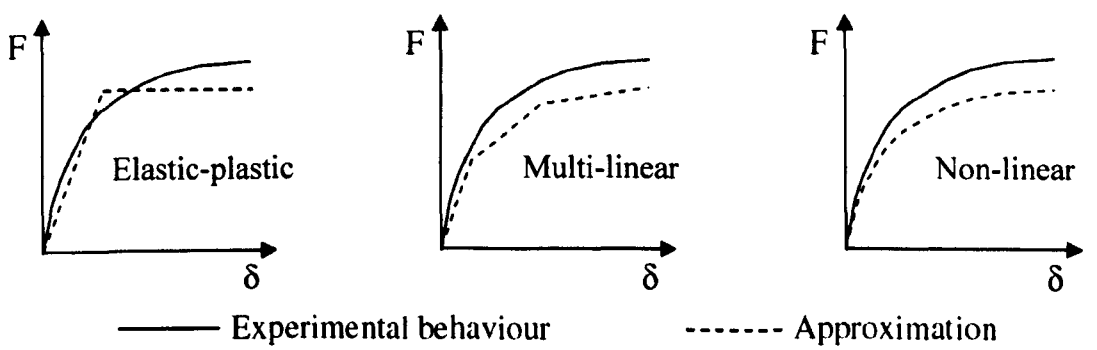

Figure 2.13: Component approximations and experimental behaviour (Block, 2006)

The final stage in the development of component-based models is assembly of the components and evaluation of the connection response. The component model consists of two rigid bars, representing the column centreline and the beam end. These rigid bars are connected by a series of nonlinear springs at each bolt-row, which simulate the various components in the connections. Figure 2.14 shows an illustration of a simplified component model for the case of an idealised flush end-plate connection.

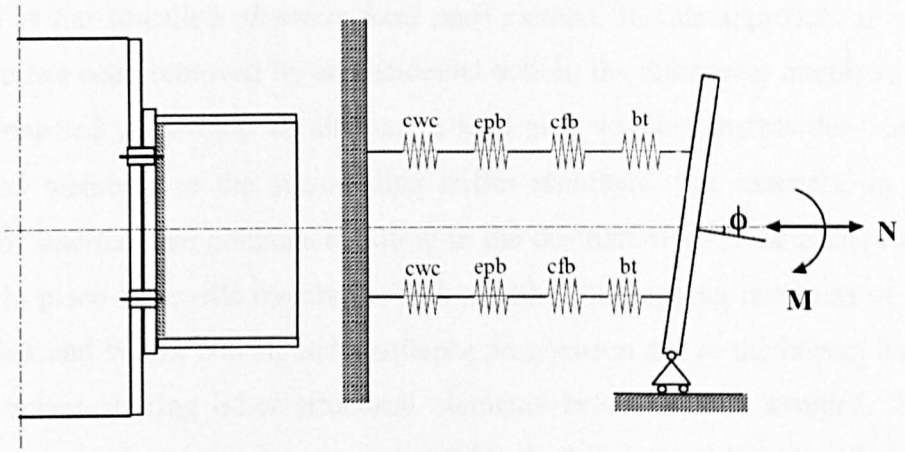

Figure 2.14: A simplified component-based model for flush end-plate connections (Sulong, 2005)

2.9 Introduction to Robustness (Structural Integrity)

The partial collapse of Ronan Point in 1968 arose from a lack of positive attachment between principal elements in a structure. As a result of this event, the problem of progressive collapse received more widespread attention and a minimum *Robustness* to resist accidental loading has been specified in structural design in the United Kingdom. Following the pancake-like collapse of the World Trade Centre Towers in 2001, research on progressive collapse has intensified recently.

The term *Robustness* is defined as the ability of a structure to withstand events like fire, explosions, impact or the consequences of human error, without being damaged to an extent disproportionate to the original cause (EC1-1-7, 2006). In light of this definition, *Robustness* is a property of the structure alone and independent of the loading (Starossek and Wolff, 2005a and 2005b). Recent research completed at Imperial College suggests factors such as (a) energy absorption capacity, (b) ductility

and (c) redundancy (or alternate load paths), need to be taken into consideration carefully, as indicators of structural robustness (Izzuddin, et al. 2008).

Concerning the design of buildings, Starossek and Wolff (2005a and 2005b) explain a number of design strategies for prevention of the progressive collapse in tall and large buildings. The first strategy is tying the major structural elements in a steel frame horizontally and vertically to increase its structural continuity and create a structure with a high level of robustness, named as *tying force approach.* The other strategy is the so-called *alternate load path method.* In this approach, if part of a structure has been removed by an accidental action, the remaining members are still well connected to develop an alternative load path which transfers the load of the collapsed members to the surrounding stiffer members. For example, in case of failure of intermediate columns resulting in the destruction of floor slabs, the debris is held in place by tensile membrane action within the sagging remnants of the slab (Starossek and Wolff, 2005a) and a collapse progression due to the impact loading of falling debris striking other structural elements below is thus avoided. *Enabling catenary action* is a requirement expected for steel beams subjected to fire loading. This action requires sufficient ductility in structural members (steel beams) and most importantly steel connections. As a consequence of this, the beams are able to act as cables hanging from the surrounding cold structure in a compartment fire. In case of local failure arising from fire, the ductility in structural members and connections allows for the utilization of plastic reserves and the dissipation of kinetic energy (Starossek and Wolff, 2005b).

2.10 Conclusions

This chapter clearly identified the differences between the real fire performance in a building and the standard fire (curve) assumed in furnace tests. As a result of this, standard fire curves cannot represent the natural fire performance (Bailey, 2006). The behaviour of structural members in a natural fire condition is therefore different from the structural response of these members in a furnace. A beam-to-column connection is always to act as an essential structural component in a structure, and it is evident that the elevated temperature behaviour of the connection is more complex than in the ambient cases. Failure with brittle components in some of the connections

has also been found in the full scale fire tests and standard furnace tests, causing attention for further investigation in Chapter 4. Previous researchers placed lots of efforts on the development of curve-fitting models and finite element simulation to represent the connection performance under fire conditions. The curve fitting model was used to present the moment-rotational response of the connection and the finite element simulation is computationally expensive in comparison with the component-based approach, and hence not suitable for robustness connection design. The efficient and versatile component-based approach has been outlined in this chapter for connection modelling at ambient and elevated temperatures. The details of development of the component-based model will be seen in a later chapter (Chapter 6) for flexible end-plate connections.

CHAPTER 3

RESEARCH METHODOLOGY

3.1 Introduction

In the previous chapter, basic theoretical aspects of the Component-based Approach have been explained together with a detailed review of the connection performance under fire conditions. However, understanding any aspect of the behaviour of a steel structure often starts from observations of the behaviour of physical models, either from carefully planned and executed experiments or uncontrolled accidents (Wang, 2002). These observations from accidental fires in steel structures can produce some qualitative speculations of the possible behaviour of steel structures under fire attack, but more precise and quantitative understanding can only be obtained from carefully planned and conducted experimental studies.

3.2 General Testing Procedure

Mechanical loading and thermal loading may be two independent load processes. In a fire event, the mechanical loading and fire event may take place simultaneously (totally or partially), or the mechanical loading takes place either before the fire events starts or after the fire event has reached its maximum temperature, as shown in Fig. 3.1 (Simoes da Silva et al., 2001). To date, numerous fire tests have been carried out on different types of structures and two types of testing methods may commonly be used for a loaded structure under fire conditions: (1) transient state testing; and (2) steady state testing. In the transient state testing, loads are applied to the structure first. These loads are then held constant and the structure is exposed to fire attack. The test is terminated when one of the specified failure criteria is reached. In the steady state testing, the temperature in the structure is raised to the pre-determined level and held constant. Loads are then applied to the structure until

structural failure. Wang (2002) believes if the structural behaviour is independent of the heating rate or the loading history, these two testing methods should produce the same results. Since the fire tests are commonly carried out using one of these two methods and the actual behaviour of steel is also dependent on the heating rate and the loading history, it is very difficult to make an assessment of the difference between these two testing methods. However, the transient state testing procedure is more like simulating the real behaviour of a steel-framed structure subjected to a fire attack and yet the steady state testing is commonly used in standard fire tests.

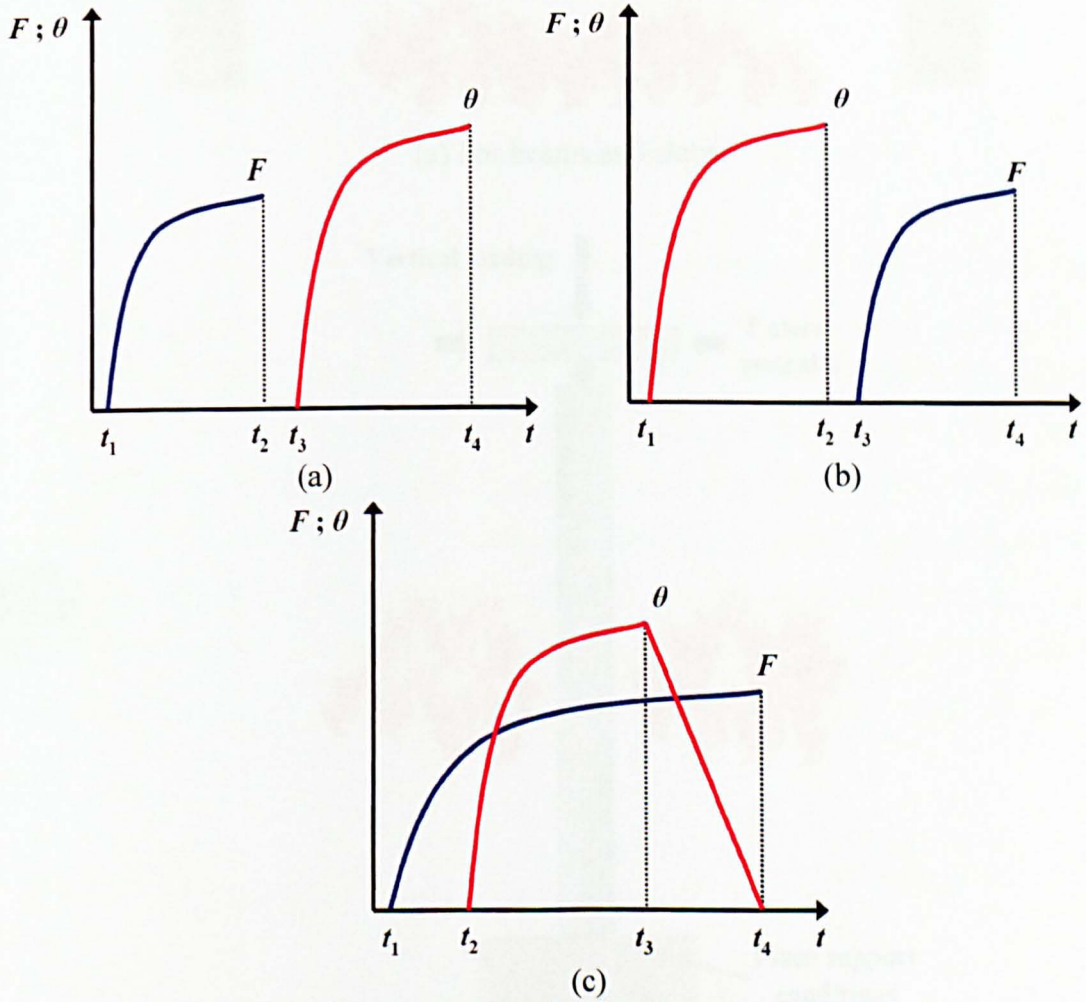

Figure 3.1: Variation of thermo-mechanical loading with time: (a) anisothermal; (b) isothermal (c) transient (Simoes da Silva et al., 2001)

3.3 Standard Fire Resistance Tests

The standard fire resistance test is usually carried out to make an assessment of a fire resistance rating to a construction element to enable it to meet the regulatory requirements for fire resistance. This test is carried out according to a specified

standard. In the United Kingdom, it was the British Standard BS 476, Part 20 (BSI, 1987a), but now the international standard ISO 834 has been adopted for fire testing, replacing the British Standard BS 476. For this reason, the standard fire exposure is also referred to as the ISO fire (Wang, 2002).

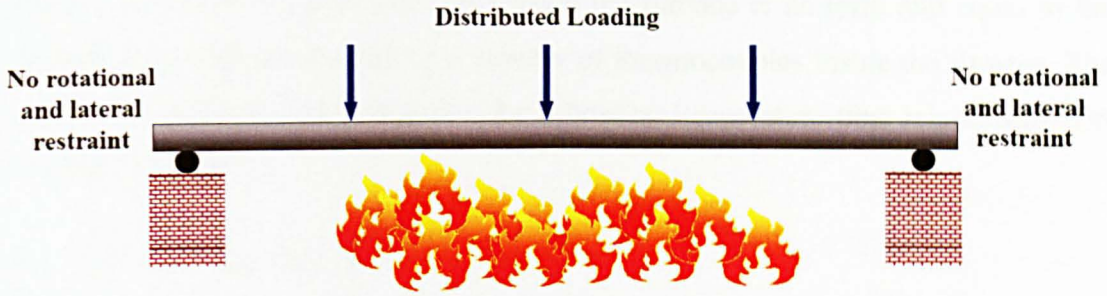

(a) For beams and slabs

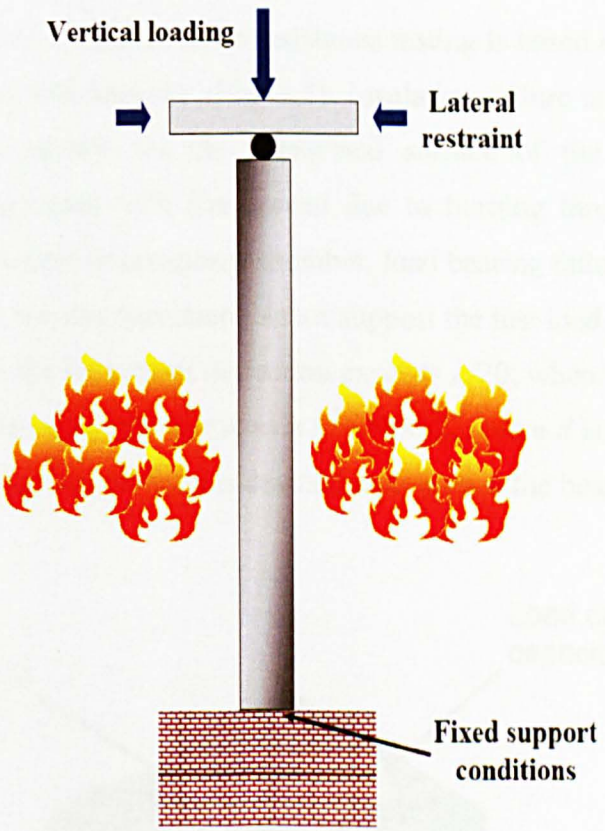

(b) For columns

Figure 3.2: Typical arrangements of structural elements in standard fire resistance tests (a) for beams and slabs (b) for columns (Wang, 2002)

The standard fire test is carried out in a furnace, either gas or oil fired and the testing furnace is either a horizontal one, suitable for testing beams and slabs, or a vertical

one, used for testing columns and wall panels, as illustrated in Fig. 3.2. Traditionally, beams and slabs are heated from underneath, while columns are heated on all four sides. Wall panels are usually heated from one side only. Depending on the type, number, size and locations of burners in the furnace, a non-uniform temperature distribution may exist in the furnace. However, in testing a specimen, it is assumed that the combustion gas temperature inside the furnace is uniform and equal to the average temperature recorded by a number of thermocouples inside the furnace. The average temperature rise is based on the following temperature-time relationship (BS EN 1991-1-2, 2002):

$$\Theta_g = 20 + 345\log_{10}(8t + 1)$$

Where Θ_g is the gas (fire) temperature and t is the fire exposure time.

The assessment of failure in standard fire resistance testing is based on three criteria: load bearing, insulation and integrity (Fig. 3.3). Insulation failure is concerned with excessive temperature growth on the unexposed surface of the test specimen. Integrity failure is associated with fire spread due to burning through of the test specimen. For a loaded steel or composite member, load bearing failure is considered to have occurred when the test specimen cannot support the test load. However, for a horizontal specimen, if the maximum deflection exceeds $L/20$, where L is the span of the specimen or the rate of deflection exceeds $L^2/(9000d)$, where d is the depth of the test specimen, the horizontal specimen is deemed to approach the bearing failure.

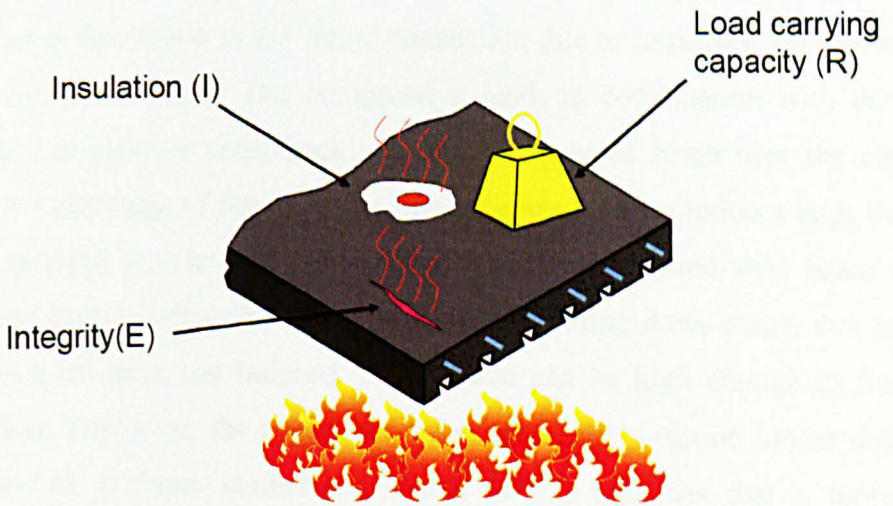

Figure 3.3: The usual fire resistance criteria

3.4 Fire Tests for Robustness of Steel Connections in Fire

As documented in Chapter 2, a number of experimental studies have been carried out to evaluate the performance of steel or composite-steel connections at both ambient and elevated temperatures. Since steel connections are usually designed to be pin-joints to resist vertical shear forces only, but they actually have some bending moment resistance in a steel-framed structure, previous connection studies aimed to establish the moment-rotation relationships of steel connections under fire conditions. The researchers Leston-Jones (1997) and Al-Jabri (1999) carried out a series of fire tests on isolated steel and composite connections, and produced a large volume of experimental data for the moment-rotational response of these connections in fire. In the much earlier SCI connection tests, it was found that temperatures in the connection region were much lower than that of the connected elements under fire conditions. Failure of the connection was due to plastic deformations of the plates, and bolts were not the weakest link of the connection. These isolated fire tests provide some valuable information to establish the basic understanding of the connection performance in fire.

However, experiences from full-scale fire tests at Cardington and the real fires at the World Trade Centre cast doubt on the suitability of using the performance of isolated connections to represent frame connections under fire conditions. The main difference between an isolated connection and a frame connection is the presence of an axial load in the frame connection. During the early stage of a fire, a compressive axial load is developed in the frame connection due to restrained thermal expansion of the connected beam. The compressive load, in combination with the bending moment, can produce local buckling in the connected beam near the connection. During the late stage of fire exposure, the connected beam produces large deflections and an inclined tensile force is developed within the heated steel beam (catenary action has been produced). Finally, during the cooling down stage, due to thermal contraction of steel, the induced tensile force can be high enough to fracture the connection. Therefore, the moment-rotation relationship can no longer describe the behaviour of a frame connection. Wang (2002) indicates that a more faithful representation of the steel connection behaviour should include the variable axial

load. A more simple and reliable method of representing the connection behaviour is the component-based approach, which has been documented in Eurocode 3 - Part 1.8. Using the component approach opens the possibility of including the axial load in a frame connection in the analysis.

3.4.1 Sub-frame fire tests in Manchester

In this robustness project, fire tests were conducted at Manchester and represented the actual connection behaviour in a complete steel structure. A series of experimental tests have been conducted on loaded beam-and-column "rugby-post" assemblies, with different types of connections, in order to investigate the interaction of connection and structural behaviour. Due to the high cost of the furnace tests, no replicate tests were carried out in this programme. Each tested specimen consists of two identical columns and one steel beam with the required connection types: fin plate, flexible end-plate, flush end-plate, web cleat and extended end-plate. The universal beam section UB 178 x 102 x 19 was used for all the sub-frame tests and the steel was S275. Two types of column sections were used in the programme. The first was a S355 universal column UC 254x254x73 for test No. 1 to 5 and the second was a S275 universal column UC 152x152x23 for test No. 6 to 10. In accordance with EC3 – 1.8, M20 Grade 8.8 bolts and nuts were used for most of the tested specimens. However, in order to prevent premature failure in moment connections (extended end-plates), M20 Grade 10.9 bolts and nuts were used for test 5 and 10 to fasten the beams and columns. All these specimen details and the related connection component dimensions are summarised and presented in Table 3.1.

The sub-frame fire tests were carried out in the furnace of the Fire Testing Laboratory of the University of Manchester. The furnace is a rectangular-shaped box with internal dimensions of 3000mm x 1600mm x 900mm. The furnace is gas-fired with two gas burners and an exhaust, as shown in Fig. 3.4. In order to achieve the uniform temperature distribution during the testing, the burner system is fully computer-controlled to follow the standard ISO 834 fire curve to raise the furnace temperatures. A moveable interior wall inside the furnace separates the internal space and redistributes the heat from two burners into the furnace.

Table 3.1: Summary of load and specimen details

Test No.	Column Section	Beam Section	Connection Type	Component dimension	Applied load per jack (kN) / Load ratio
1	UC 254x254x73	UB 178x102x19	Fin plate (LC)	150x130x10 (mm)	40 (0.5)
2	UC 254x254x73	UB 178x102x19	Flexible end-plate (LC)	150x130x8 (mm)	40 (0.5)
3	UC 254x254x73	UB 178x102x19	Flush end-plate (LC)	150x200x8 (mm)	40 (0.5)
4	UC 254x254x73	UB 178x102x19	Web cleat (LC)	90x150x10 (depth: 130)	40 (0.5)
5	UC 254x254x73	UB 178x102x19	Extended end-plate (LC)	150x250x8 (mm)	40 (0.5)
6	UC 152x152x23	UB 178x102x19	Fin plate (SC)	150x130x10 (mm)	40 (0.5)
7	UC 152x152x23	UB 178x102x19	Flexible end-plate (SC)	150x130x8 (mm)	40 (0.5)
8	UC 152x152x23	UB 178x102x19	Flush end-plate (SC)	150x200x8 (mm)	40 (0.5)
9	UC 152x152x23	UB 178x102x19	Web cleat (SC)	90x150x10 (depth: 130)	40 (0.5)
10	UC 152x152x23	UB 178x102x19	Extended end-plate (SC)	150x250x8 (mm)	40 (0.5)

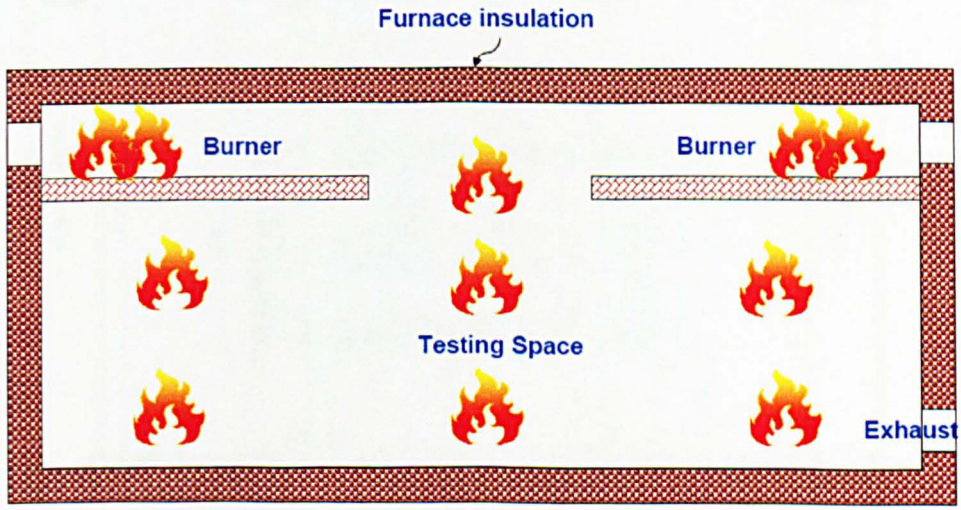

Figure 3.4: The arrangement of the furnace

The test arrangement (a complete 'Rugby-Post' frame) is illustrated in Fig. 3.5. The steel beam was mainly unprotected except for the top flange, which was protected with a 15 mm thick ceramic fibre blanket. In order to prevent lateral torsional buckling, a steel truss system was fixed on the top flange, wrapped with a fibre blanket as well, as shown in Fig 3.6. Two identical columns were unprotected during the testing, the lateral movements of which were restrained at both top and bottom by a bracket bolted to the reaction frame of the whole experimental system (Fig. 3.7). Elongation of steel columns in the vertical direction was allowed because of no restraint in this direction. Two vertical point loads were applied to the steel beam through using two independent hydraulic jacks, which are fixed on the reaction frame of the whole experimental system. Two insulated and wrapped steel bars were used to connect these jacks and steel beams in order to prevent heat escaping out of the furnace to damage the loading system. During the fire testing, a load ratio of 0.5 was adopted for all the sub-frame tests. Since all the experimental tests adopted the load-controlled testing procedure, the point load from each hydraulic jack was maintained as 40 kN during the testing. (The load ratio of 0.5 is a practical design value used for fire safety design and the applied fire load is approximately 0.5 times the ultimate load resistance of a steel beam at ambient temperature.)

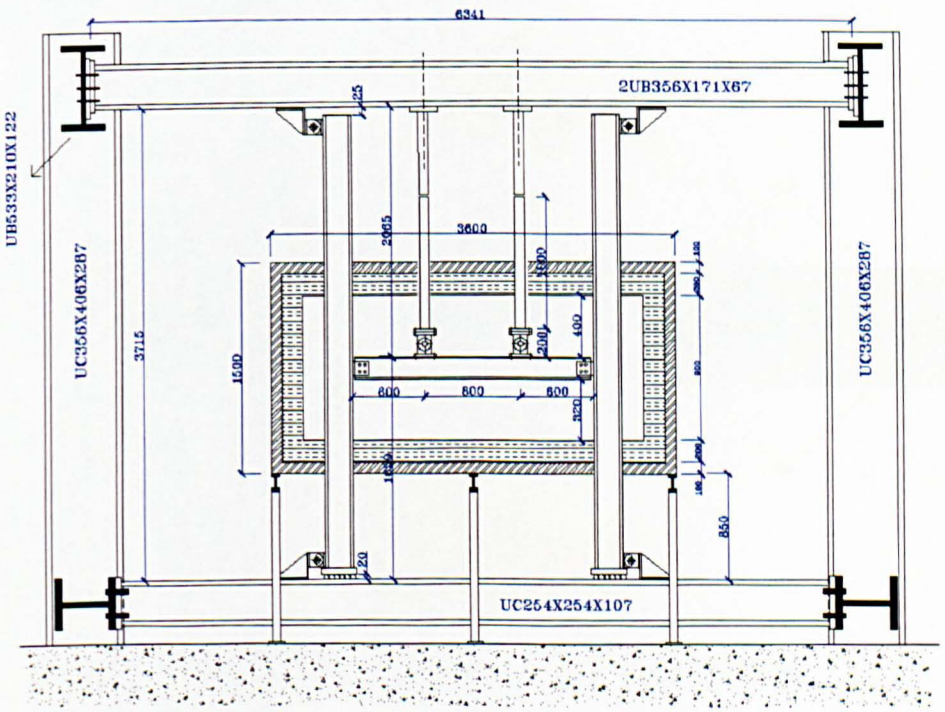

(a) Sketch view

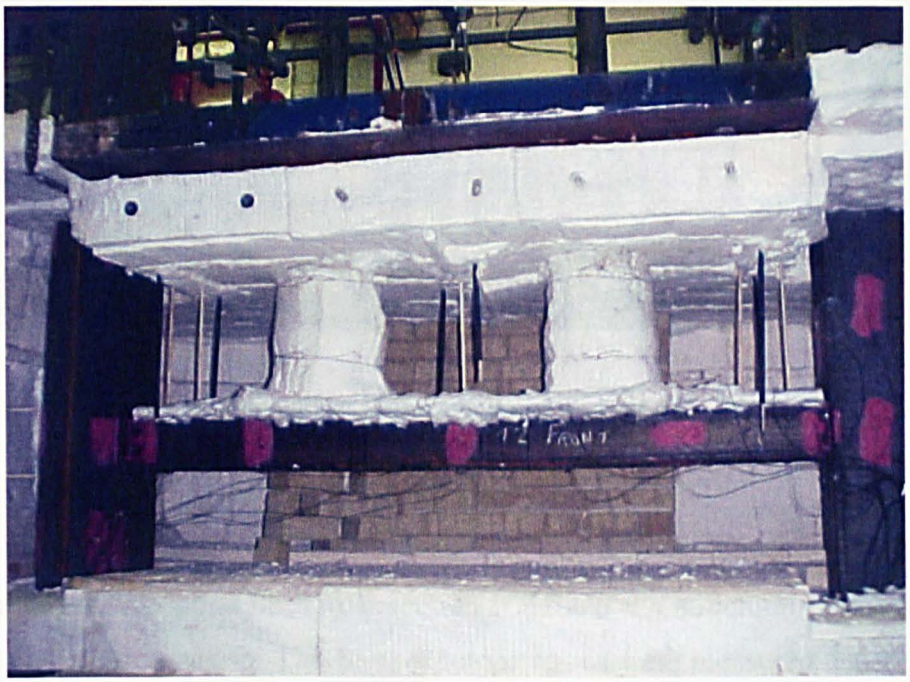

(b) Real test arrangement

Figure 3.5: Test setup for sub-frame tests (a) Sketch view (b) Real test arrangement

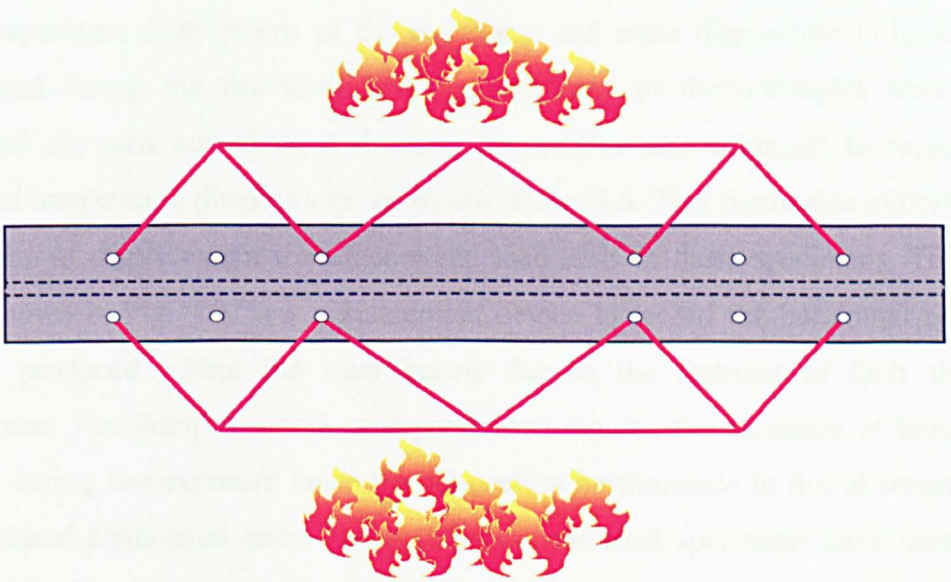

Figure 3.6: Plan sketch of lateral restraint

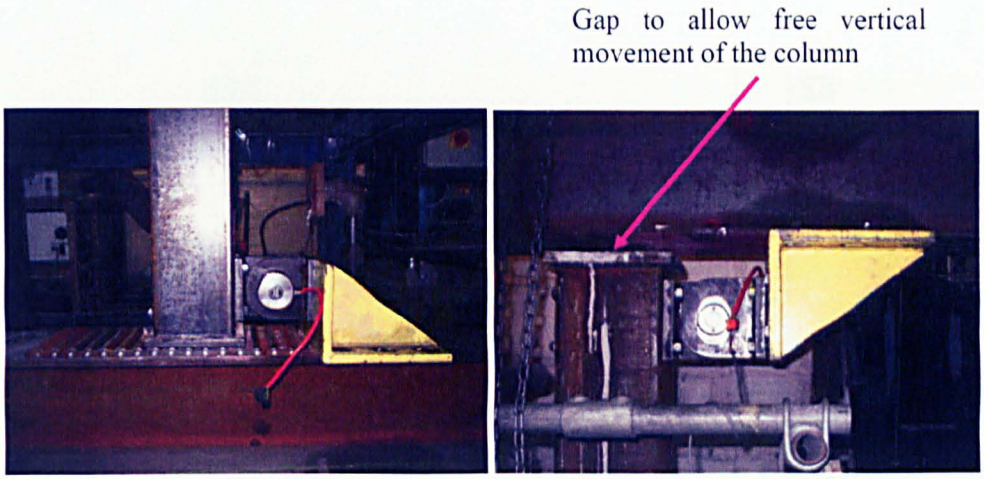

(a) Bottom end (b) Top end

Figure 3.7: Restraints between column ends and reaction frame (a) Bottom end (b) Top end

The objective of these experimental tests was to provide experimental information on temperature distributions in the connection zone and the structural members under the standard fire condition. The furnace temperatures were measured and controlled by a computing system monitoring six thermocouples, placed on the bottom of the furnace. Due to high temperatures in the furnace, no strain gauge was placed on these tested specimens as normal strain gauges are easy to be damaged under fire conditions and high temperature strain gauges are too expensive and unable to provide reliable strain-related information at very high temperatures. Therefore, only the temperature distributions of the specimens and some displacements have been measured during the fire testing. A large number of thermocouples have been installed on each test element (beams, connections and columns) to record the detailed temperature distributions, as shown in Fig. 3.8. This figure also indicates the locations of displacement transducers and load cells in these specimens. The load cell, shown in Fig. 3.9, is a measurement device to record the horizontal reaction forces produced within the steel beams due to the restraint of their thermal expansion. According to previous experimental results, the existence of horizontal forces during fire exposure made the connection performance in fire different from the isolated connection tests. The details of these steel specimens have been well documented in the paper to be published by the Manchester fire group (Wang, et al., 2009).

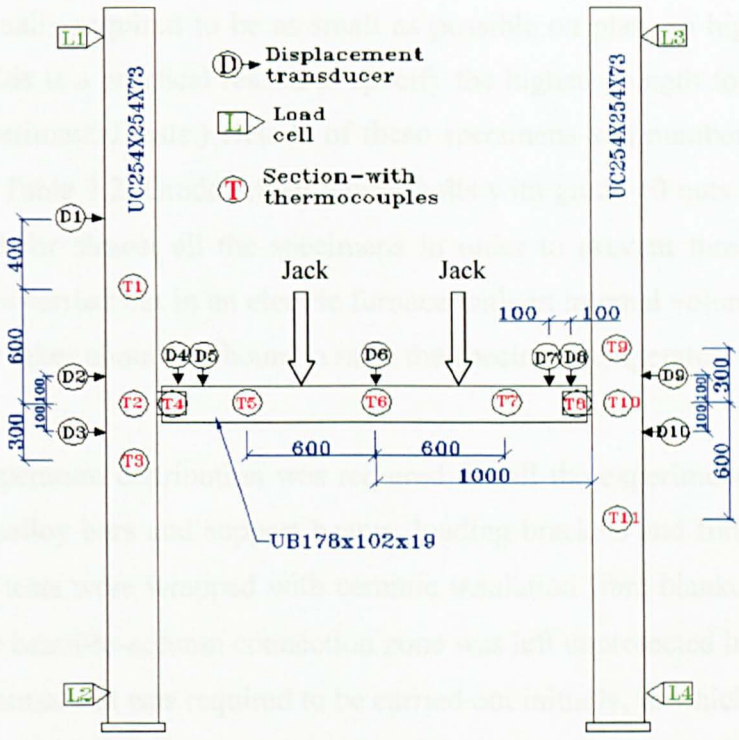

Figure 3.8: Measurement device arrangement on a typical specimen

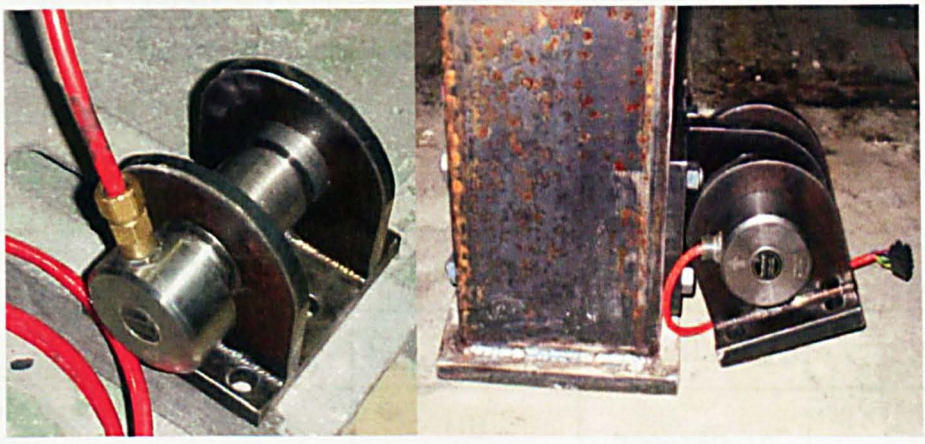

Figure 3.9: Arrangement of load cell

3.4.2 Isolated fire tests in Sheffield

A series of approximately sixty isothermal experiments have been carried out at the University of Sheffield to investigate the behaviour and failure of typical beam-to-column connections at constant elevated temperatures. The tested connections are full size specimens in accordance with practical designs. These specimens adopted a S355 universal column of UC 254x254x89 as the column section and a S275

universal beam of UB 305x165x40 as the beam section. (In common practice, the columns are usually required to be as small as possible on plan, so higher strength steel is used. This is a practical reason to specify the higher strength for the column sections in experimental tests.) Details of these specimens and number of tests are summarized in Table 3.2. Grade 8.8 structural bolts with grade 10 nuts (zinc plated) have been used for almost all the specimens in order to prevent thread stripping. These tests were carried out in an electric furnace with an internal volume of 1.0 m^3, which normally takes about two hours to raise the specimen temperature to 700 °C.

A uniform temperature distribution was required for all the experimental tests. The supporting Macalloy bars and support beams, loading brackets and furnace bars for the connection tests were wrapped with ceramic insulation fibre blankets under fire conditions. The beam-to-column connection zone was left unprotected in testing, and an unloaded thermal test was required to be carried out initially, in which twenty-five thermocouples were installed on the specimen to monitor the temperature distribution in this zone (Yu et al., 2009a). According to the experimental results, an almost uniform temperature distribution has been observed in this connection zone, and the differences in temperature between these thermocouples was less than 5° C at a stable furnace temperature of 700° C.

Table 3.2: Summary of specimen details

Connection Type	Column Section	Beam Section	Connection Fittings	Number of Tests
Fin plate connections	UC 254x254x89	UB 305x165x40	200x100x10	10
Flexible end-plate connections	UC 254x254x89	UB 305x165x40	200x150x10	12
Web cleat connections	UC 254x254x89	UB 305x165x40	90x90x8 (150x90x10)	14
Flush end-plate connections	UC 254x254x89	UB 305x165x40	323.4x200x10	18

The connection specimens were loaded with inclined tensile forces during the testing, as shown in Fig. 3.10 (a). Such an inclined force was able to produce both shear and tensile force components to a tested specimen, and moment arising due to

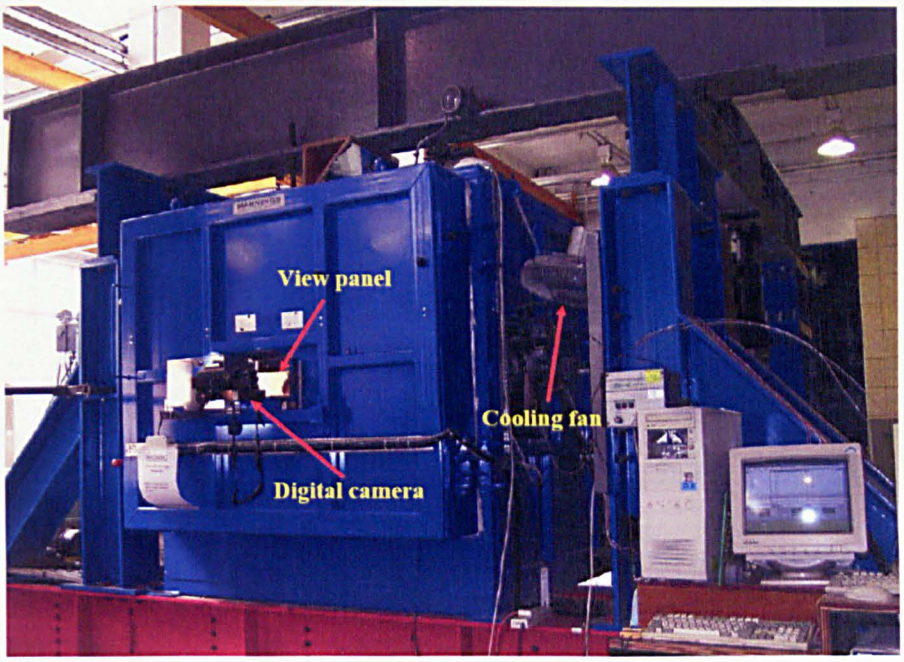

(b) Electrical furnace

Figure 3.10: Test up for isothermal connection tests (a) Sketch view (b) Electrical furnace

The essential requirement in this connection test programme was to obtain the resistances of steel connections against the inclined tying force at both normal and high temperatures. For ambient temperature testing, measurement of the forces may be achieved by using strain-gauges attached on the loading system (three Macalloy bars). So the inclined tensile force in testing can be directly recorded by the strain gauge placed on the furnace bar. In earlier unloaded thermal tests (Yu et al., 2009a), the furnace was heated up to 700 °C and the temperature was retained for two hours. Although the furnace bar was well insulated using a ceramic fibre blanket, the temperature for the furnace bar still increased to 120 °C. Nevertheless, the rest of the Macalloy bars stayed cool if a cooling fan was provided. Since the strain gauges would be damaged at high temperatures, the inclined applied force to a connection in the furnace bar could not be recorded straightforwardly. In order to obtain this force, strain gauges were fixed to the link and jack bars and the applied tensile force was then calculated by resolving the system of forces. Any change in inclination of these three bars was recorded using three angular transducers and a digital camera (Fig. 3.11).

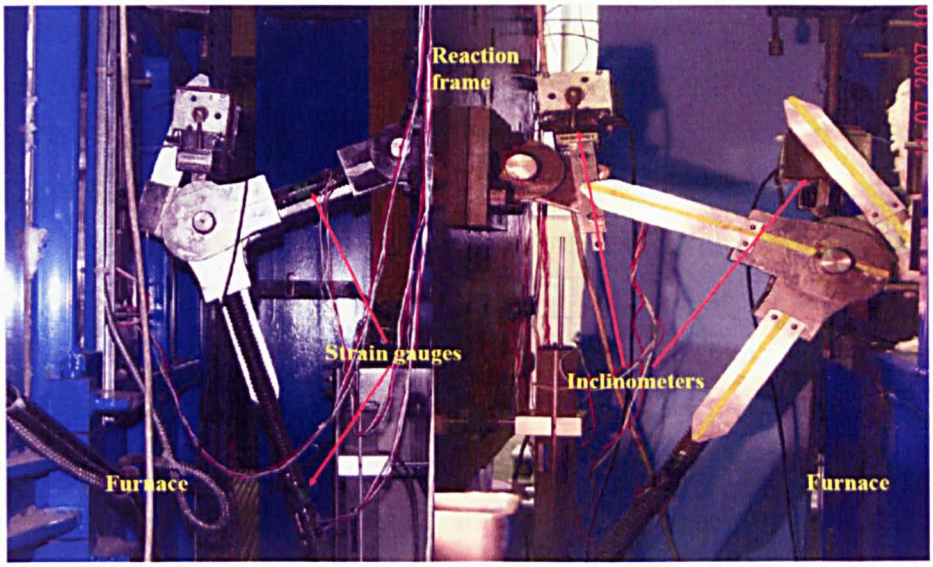

Figure 3.11: Arrangement of loading system

3.5 Image Acquisition and Processing Technique

One of the substantial objectives for isolated connection tests is to investigate the failure mechanism and ductility of each connection under fire conditions, because the ductility of a connection is closely associated with how this connection failed in a fire condition. More details of this aspect will be discussed in Chapter 5. For beam-to-column connections, ductility conventionally means rotational capacities of these connections whilst sustaining moment, but may also mean extension of a connection if this connection is only subjected to pure tensile loading (Owens and Moore, 1992). This robustness project is intended to identify the rotational capacities of the connections and their mechanisms of failure, possibly available under fire conditions.

An image acquisition and processing technique has been described for experimental tests of T-stubs at high temperatures by Spyrou and Davison (2001). The accuracy of the image processing software proved to be adequate for the experimental tests when used with the image acquisition taken from a high-resolution digital camera. This technique is usually used for direct and non-contacting measurements of deformations of specimens, and especially for use in connection with furnaces (high temperatures) or within a hostile environment. For the image capturing feature, some small targets (ceramic rods or drills) were embedded into the specimens before conducting the experiments. In the experimental tests of Spyrou and Davison (2001),

0.5 mm drills were used for the specimen as the image targets during the testing, as shown in Fig. 3.12. The distance between these targets in testing was recorded by the digital camera. Apart from the displacement (distance) readings at high temperatures, this approach also records the behaviour of the specimen as soon as the load is applied. It is possible to recognize the failure mechanism of the specimen through careful observation of a recorded test. Due to this advantage, this technique was adopted for these isolated connection tests under fire conditions. The targets for the image processing, made of ceramic rods (Fig. 3.12), were embedded into steel specimens before testing. The digital camera was fixed on the main door of the furnace to record the movements and deformations of the steel specimen through a 200mm x 100mm view panel (Fig. 3.10). The recorded digital photos were processed by image processing software to obtain the rotations and displacements of the steel connections.

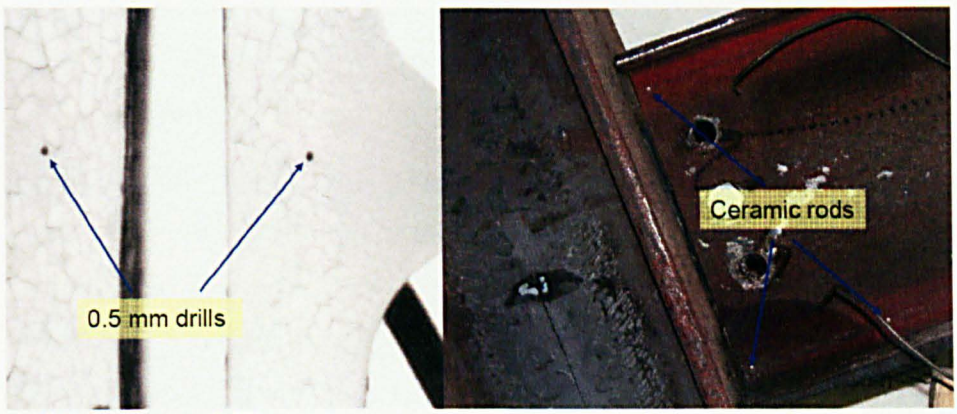

(a) 0.5 mm drills (b) ceramic rods

Figure 3.12: Targets for image processing

3.6 Conclusions

This chapter has explained the experimental arrangement for the tests carried out at the University of Sheffield and University of Manchester. In order to investigate the robustness of steel connections under fire conditions, the sub-frame tests, carried out at Manchester, mainly focused on observing the behaviour of a connection in a steel frame and exploring the influence of variable axial loads due to the restraint of thermal expansion of a steel beam to the connection under fire conditions. The research efforts at Sheffield concentrated on studying the deformation ability

(ductility) of a steel specimen in an isothermal situation, and identifying the possible contribution from each potential connection component to the rotational capacity of this connection when subjected to an inclined tying force. However, carrying out experimental tests under fire conditions is always expensive and time consuming in terms of the specimen preparation and hence the number of tests is limited due to the cost. As the testing furnaces are restricted in size, it is generally impossible to conduct large-scale sub-frame tests and isolated connection tests. Finite element simulation may be used to extend the understanding produced from experimental tests through parametric studies, as discussed in Chapters 7 and 8. The component-based approach has already been introduced in Chapter 2 and the simplified model (a component-based model) is very helpful in understanding and predicting the connection behaviour at both normal and high temperatures. More details of application of this component-based approach are discussed in Chapter 6 for flexible end-plate connections.

CHAPTER 4

INVESTIGATION ON BOLTS

4.1 Introduction

Bolted connections are widely used in steel structures as they enable prefabricated beams and columns to be erected quickly on site without the complication and expense of on-site welding. High-strength class 8.8 structural bolts are commonly available and are recommended for all main structural bolted connections. These bolts are generally intended for applications in ambient temperature environments; however they may achieve high temperatures under accidental fire conditions (Kirby, 1995). From observations in isolated connection tests and fire damaged buildings, some failure mechanisms of bolted connections are due to damage of bolts in shear and/or tension in fire conditions. This is possibly caused by the limited available deformation (or ductility) for these bolts. Moreover, a "brittle" failure of bolts could adversely affect the rotation capacity of joints, and possibly the behavior of a complete steel structure, unless the necessary ductility is provided through plate deformation capacity.

Before the research of Kirby (1995), little was known about the strength characteristics of 8.8 bolts in fire, yet the behavior of these components is extremely important in maintaining the structural integrity of a steel-framed building structure. As a result of this gap in knowledge, Kirby carried out a series of tests on property of grade 8.8 20 mm diameter bolts manufactured to an old British Standard (BS 4190: 1967). As an alternative, British Standard BS 3692: 1967 was also in use for non-preloaded bolts for many years in the UK. With the introduction of BS EN standards, the old British Standards for bolts have been declared obsolete. However, the introduction of European standards has not yet been fully accepted by the UK construction industry, and bolts are still ordered to the familiar British Standards.

Therefore, BS 3692 and BS 4190 were revised and re-published in 2001. These new British Standards specify mechanical properties of steel in line with BS EN ISO 898-1 (1999), and the new BS 4190: 2001 covers the full range of bolt grades from 4.6 to 10.9 for non-preloaded bolts. As a consequence of this, the new British Standard (BS 4190: 2001) and new European Standards (BS EN ISO 4014/4017:2001) have been recommended for ordering non-preloaded structural bolts in the National Structural Steelwork Specification for Building Construction 5th Ed (BCSA, 2007). A thorough understanding of the performance of these 'new' bolts at both ambient and elevated temperatures is of great importance in studies of connection behavior. This programme of research was launched to investigate the performance of structural 8.8 bolts to the new British Standard BS 4190 (2001) and the European Standard BS EN ISO 4014 (2001) at ambient and elevated temperatures.

4.2 Literature Review

4.2.1 Manufacturing process

Property class 8.8 structural bolts are normally manufactured using a cold forging process, which involves working a bolt metal below its recrystallization temperature, usually around room temperature or near room temperature. This initial process, also called heading, is used to produce a near bolt shape work billet for the thread rolling process. A cold-forming process is applied to the bottom of the work billet (the side without the head) in order to make the threads by rolling the work billet through two dies. The thread rolling process is usually chosen instead of machining (cutting threads) because thread rolling provides higher production rates, more effective material usage, stronger threads due to work hardening and finally better fatigue resistance because of the work billet experiencing compressive stresses during the rolling process. Alternatively, a hot forging process may be employed during the process of manufacturing bolts, which as the name suggests involves working a bolt metal above its recrystallization temperature. The main advantage of hot forging is that the strain-hardening effects are negated through the recrystallizaiton process as the metal is deformed. The final quench and temper heat treatment after thread rolling (quenching bolts from a temperature of 850 °C – 900 °C and subsequently tempering between 450 °C and 600 °C) normally provides structural bolts with the

required mechanical properties. Structural 8.8 bolts can be used in the self color (black) condition or can be provided with a coated finish such as zinc plating or hot dip galvanizing for oxidation prevention. But the choice of process route is dependent on various manufacturers and is controlled by the chemical composition of the feedstock, the size range and the demand for a particular bolt (Kirby, 1995).

In the current construction industry, M20 nuts are usually supplied with a black appearance or with a bright finish. The black nuts are normally manufactured through the hot forged process from steel bar, followed by the quenching and tempering heat treatment. The bright finished nuts are usually produced by cold forging steel bar with the finalized process of galvanizing or zinc plating.

4.2.2 Previous bolt tests

Godley and Needham (1983) conducted a series of tensile and shear tests on Grade 8.8 bolts, which have been compared with the tests of HSFG bolts at ambient temperatures. It was noted that grade 8.8 bolts with grade 8 nuts have a higher probability of thread stripping with the consequent loss of ductility. According to the results of this series of tests, grade 8.8 bolts combined with grade 10 nuts behaved in a similar manner at failure to HSFG bolts (Godley and Needham, 1983), which were not significantly weaker in direct tension than the same class HSFG bolts. These experimental results indicated two classic failure mechanisms for structural bolts under pure tension; tensile bolt breakage and thread stripping. In 1994, a group of tensile bolt tests was completed in the Materials Research Laboratory, Australia. The failure mechanism of thread stripping was identified as a three-stage process: threads elastically deformed, threads plastically deformed and threads sheared off (Mouritz, 1994). It was also noted that most of the threads were stripping off nuts rather than the bolts.

In order to provide data for designing at the fire limit state, Kirby (1995) investigated the performance of high strength grade 8.8 bolts at elevated temperatures and conducted a large series of tests at the Swinden Laboratories, Rotherham. In these tests, a marked loss in ultimate strength of the structural bolts took place in the

temperature range of 300°C to 700°C under pure tension or double shear loading conditions. The tests in tension showed the problems of premature failure of bolt assemblies at both ambient and elevated temperatures, which are caused by nut threads stripping off. To prevent the premature failure, Kirby highlighted the importance of the degree of fit between the threads of bolts and nuts (the tolerance class between these two components). The failure mechanism of bolts and nuts may be dependent on the tolerance class between the threads of these two components to some extent. Furthermore, the Strength Grade of nuts employed in combination with bolts is another factor affecting the failure mechanism of these bolt assembles, which was already noted by Barber (2003) and in the tests of Godley and Needham (1983).

However, a number of comments on tolerance class need to be borne in mind in the context of this review. First of all, before the publication of new bolt standards, bolts were usually ordered to either BS 4190:1967 or BS 3692: 1967; the difference between these two standards is that the requirement for the Tolerance Class of Grade 8.8 bolts is not the same. To BS 3692:1967 the tolerance class is 6H/6g, but to BS 4190: 1967 it is 7H/8g. In the comparative tests of Godley and Needham (1983), 8.8 structural bolts were ordered to BS 3692: 1967. In the high temperature tests of Kirby (1995), the mechanical properties of 8.8 bolts met the requirements of BS 3692:1967 but the dimensional tolerances of these components are in line with common practice and given in BS 4190: 1967. This possibly implies the tolerance class between bolts and nuts was 7H/8g in the Kirby's tests, a bit looser than that in the earlier bolt tests by Godley and Needham (1983). After publication of new bolt standards, the European Standards (BS EN ISO 4014 / 4017) accepts the value of 6H/6g as the Tolerance Class for bolts and nuts, while the British Standard (BS 4190: 2001) continues to adopt the Tolerance Class 7H/8g. The old bolt standards have now been declared obsolete, and are superseded by BS 4190: 2001 and BS EN ISO 4014 / 4017. Therefore, a knowledge gap on bolts specified to these new standards needs to be covered. The focus of this research is on this point, and on attempting to understand the behaviour of Grade 8.8 bolts specified to different standards at normal and elevated temperatures.

4.3 The Objectives of Bolt Tests

In this test programme, M20 grade 8.8 structural bolts were ordered to both British Standards (BS 4190) and European Standards (BS EN ISO 4014), partly-threaded and 100 mm long. These bolts were supplied from two manufacturers and the nuts were supplied according to the nut standards of BS 4190: 2001 and BS EN ISO 4032: 2001. Table 4.1 presents two types of nuts: bright-finish nuts of Property Class 8 and black nuts (self colour) of Property Class 10. In this research work, the assemblies of bolts and nuts were divided into four groups as illustrated in Table 4.1:

Table 4.1: Details of bolt assemblies in the experiments

BOLT SETS	BOLT STANDARDS	NUT STANDARDS	TOLERANCE CLASS
Group C	Grade 8.8 (BS 4190, Br*)	Grade 8 (BS 4190, Br*)	7H/8g
Group A	Grade 8.8 (BS 4190, Br*)	Grade 10 (BS 4190, Ba*)	7H/8g
Group D	Grade 8.8 (ISO 4014, Ba*)	Grade 8 (ISO 4032, Br*)	6H/6g
Group B	Grade 8.8 (ISO 4014, Ba*)	Grade 10 (ISO 4032, Ba*)	6H/6g

Br* = Bright finish (zinc plated) , Ba* = Black finish

As mentioned already, the tolerance class for bolts and nuts determines the degree of fit between these two components. Theoretically, a closer fit of the threads can assist in achieving a better performance of these two components in practice. Kirby (1995) therefore believed the premature failure due to thread stripping, which may be controlled by the degree of fit between bolt and nut threads. As a consequence, the first objective in this study was to identify an approach which would eliminate the premature failure due to thread stripping at elevated temperatures. The second was to observe the performance of bolts ordered to BS 4190 and to BS EN ISO 4014 in tension at both ambient and elevated temperatures.

4.4 Test Arrangement

A test rig used for all the bolts was designed to fit a compression/tension testing machine, as shown in Figure 4.1. The coupling system was made by Durehete alloy

and unprotected in testing. Seven thermal couples have been utilized for reporting temperature variation of the bolts and also within the furnace. The loading hydraulic jacks were fire-protected during the testing and displacements were recorded by measuring the movements of the jack system.

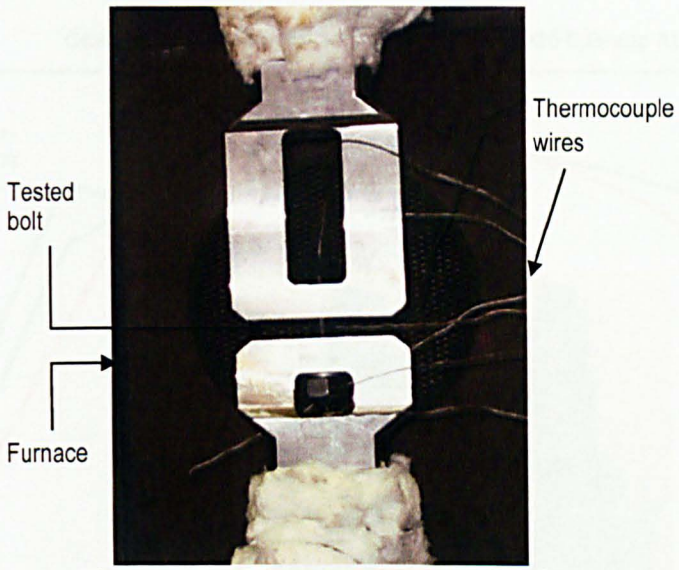

Figure 4.1: The arrangement of bolt tests

Since all the tests were carried out under displacement control, a nominal strain rate of between 0.001 and 0.003 mm/min was adopted in both the elastic and post-elastic regions, which is in keeping with the recommendation by Kirby (1995). In this series of tests, each bolt assembly was heated to the desired temperature, maintained for a period of 15 min for stabilization to establish a uniform temperature distribution, and then the tensile load was applied under displacement control. Kirby (1995) noted that a prolonged "soaking" period and a slow heating rate had little influence on the ultimate capacities of bolt assemblies. Therefore, a lower heating rate of 2-2.5°C /min was adopted throughout this investigation. After a couple of pilot bolt tests to check the equipment and experimental procedures, a total of 42 tests were completed at both ambient and elevated temperatures.

4.5 Test Results at Ambient Temperature

Figures 4.2 to 4.5 display a typical set of failed specimens with the corresponding load-deformation curves for each tested group. From these figures, it is clearly found that the bolts with Property Class 10 nuts failed by bolt breakage, and for the bolts

with Property Class 8 nuts, the failure mechanism was thread stripping of the nuts. According to these experimental results, the Tolerance Class (the degree of fit) did not appear to influence the final failure mode of the bolt assemblies and the property class of nuts seems to govern the failure mechanism between bolts and nuts.

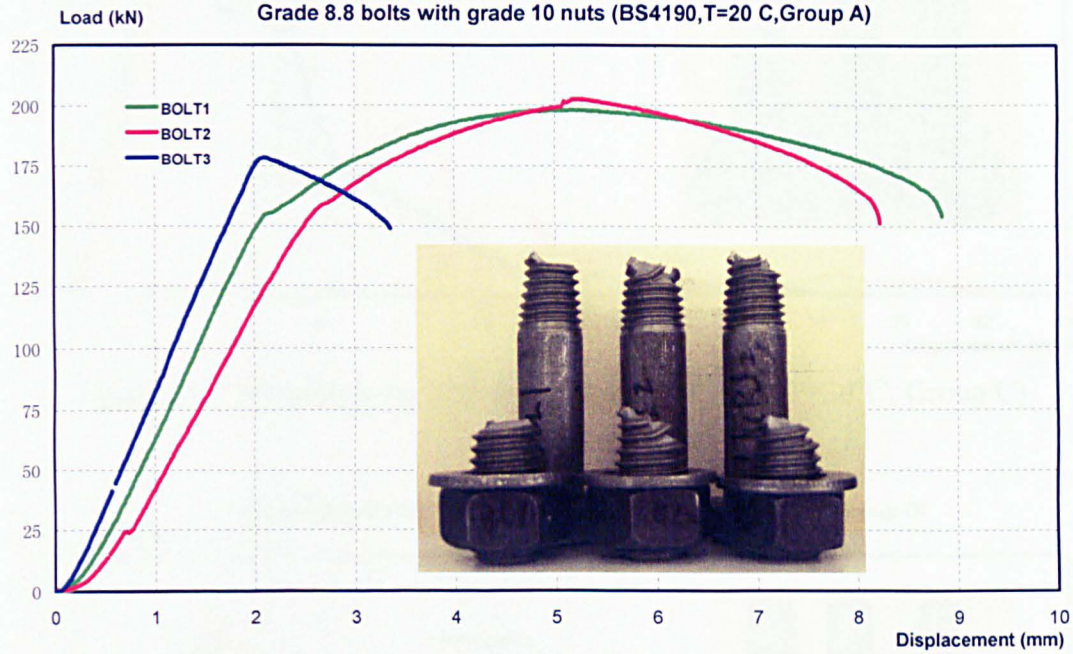

Figure 4.2: BS 4190 bolts with Property Class 10 nuts (T=20°C, Group A)

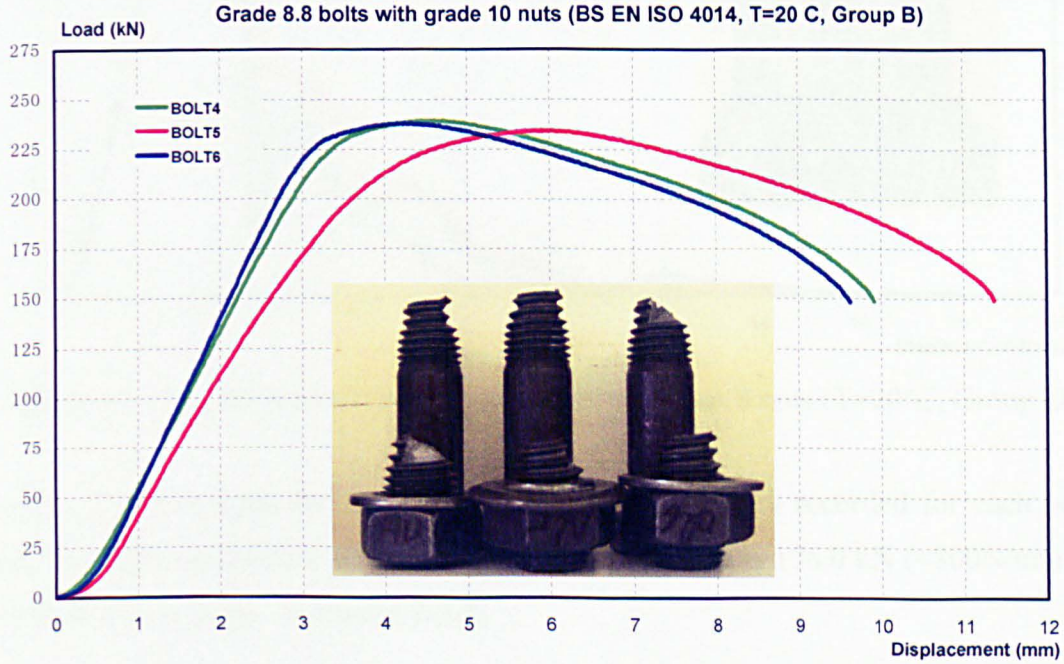

Figure 4.3: BS EN ISO 4014 bolts with Property Class 10 nuts (T=20°C, Group B)

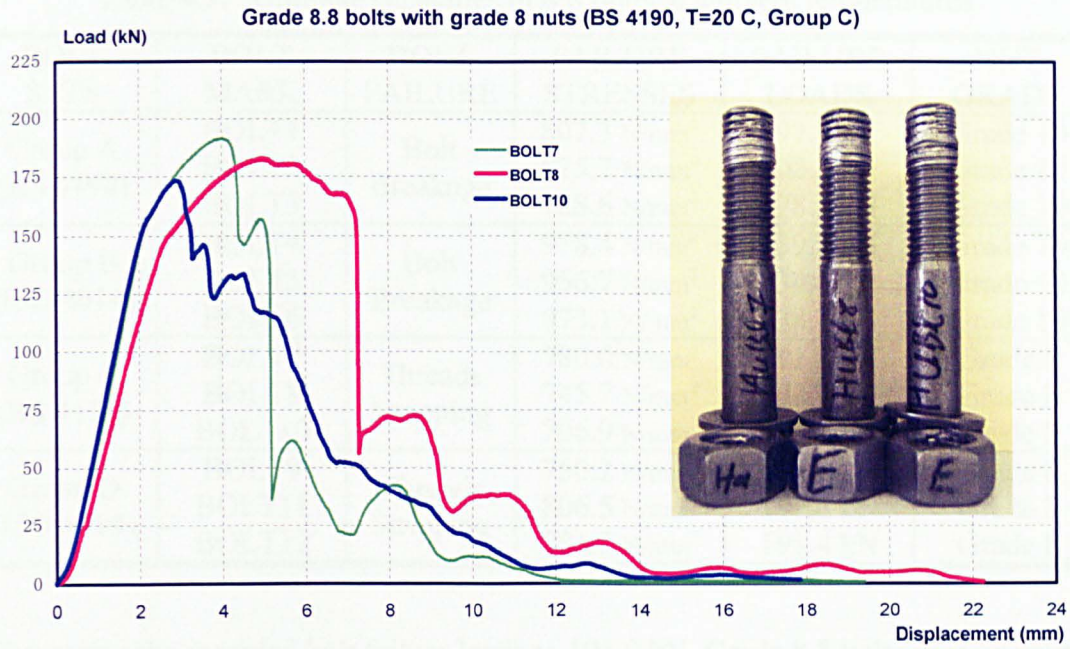

Figure 4.4: BS 4190 bolts with Property Class 8 nuts (T=20°C, Group C)

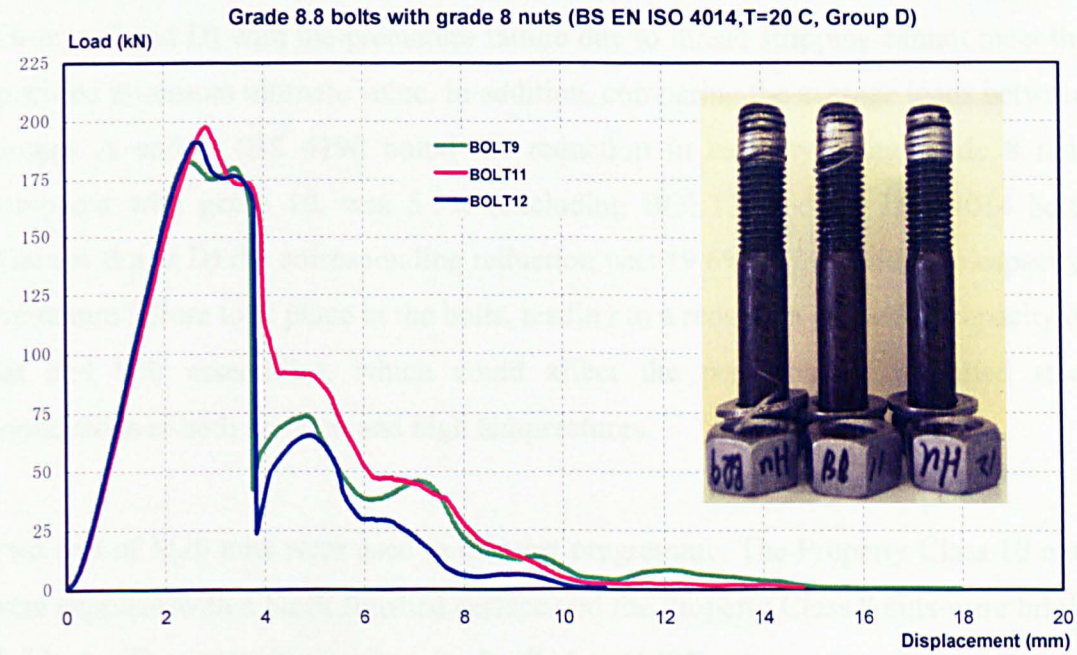

Figure 4.5: BS EN ISO 4014 bolts with Property Class 8 nuts (T=20°C, Group D)

Table 4.2 summarises the maximum failure load capacities recorded for each bolt test. The minimum ultimate load capacity in pure tension is 196.0 kN (=800N/mm^2 x 245mm^2) for a single standard 8.8 bolt.

Table 4.2: Ultimate capacities of 8.8 bolts at ambient temperatures

BOLT SETS	BOLT MARK	BOLT FAILURE	FAILURE STRESSES	FAILURE LOADS	NUT GRADE
Group A (BS 4190)	BOLT1	Bolt Breakage	807.3 N/mm^2	197.8 kN	Grade 10
	BOLT2		825.7 N/mm^2	202.3 kN	Grade 10
	BOLT3		728.6 N/mm^2	178.5 kN	Grade 10
Group B (ISO 4014)	BOLT4	Bolt Breakage	978.4 N/mm^2	239.7 kN	Grade 10
	BOLT5		956.7 N/mm^2	234.4 kN	Grade 10
	BOLT6		973.1 N/mm^2	238.4 kN	Grade 10
Group C (BS 4190)	BOLT7	Threads Stripping	780.0 N/mm^2	191.1 kN	Grade 8
	BOLT8		745.7 N/mm^2	182.7 kN	Grade 8
	BOLT10		706.9 N/mm^2	173.2 kN	Grade 8
Group D (ISO 4014)	BOLT9	Threads Stripping	750.2 N/mm^2	183.8 kN	Grade 8
	BOLT11		806.5 N/mm^2	197.6 kN	Grade 8
	BOLT12		781.2 N/mm^2	191.4 kN	Grade 8

Comparing the recorded bolt failure loads to 196.0 kN, Grade 8.8 bolts with Property Class 10 nuts (Groups A and B) can guarantee the minimum ultimate tensile value specified previously, except for one questionable bolt, BOLT3. However, the bolts (Groups C and D) with the premature failure due to thread stripping cannot meet the specified minimum ultimate value. In addition, comparing the average loads between Groups A and C (BS 4190 bolts) the reduction in capacity using grade 8 nuts compared with grade 10, was 5.5% (excluding BOLT3) and for ISO 4014 bolts (Groups B and D) the corresponding reduction was 19.6% in their ultimate capacity. Premature failure took place in the bolts, leading to a reduction of the full capacity of nut and bolt assemblies, which could affect the performance of bolted steel connections at both ambient and high temperatures.

Two sets of M20 nuts were used in this test programme. The Property Class 10 nuts were supplied with a black finished surface and the Property Class 8 nuts were bright finished (Zinc plated or galvanized). Kirby (1995) states that the process of manufacturing for black nuts involves hot forging from steel bar, quenching from 870°C and tempering back at around 540°C. By contrast, the bright finished nuts are produced by cold forging steel bar. In Kirby's test programme, the bolts with black nuts always failed by bolt breakage. In contrast, the failure of the same bolt assemblies using the bright nuts occurred entirely by thread-stripping. Therefore, the test results and failure modes of bolts suggest that the black nuts may have a slightly higher hardness value and proof load than bright finished nuts. Kirby also believes

that the threads of the bright nuts are slightly weaker than those of the black finished nuts, which is caused by the threads of bright finished nuts commonly being 'over-tapped' in order to accommodate the additional thickness of surface protective coatings. Similarly, in the bolt test programme reported here, the bolts in combination with the black nuts failed by ductile necking in the threaded portion; the bolts using the bright nuts failed by thread-stripping. From this discussion, it can be concluded that the failure patterns of bolt assemblies can be controlled by the type of nuts which are used.

Grade 8.8 bolts are manufactured by either hot or cold forging of steel, followed by a quenching and tempering process to develop the required mechanical properties. The processing method for bolts and nuts varies between manufacturers in the market, and is controlled by the chemical composition of the feedstock, the size range and the demand for a particular bolt, all of which are a function of producing a competitively priced product (Kirby, 1995). At ambient temperature, the bolts are made to meet the specifications of national or international standards, but the performance of bolts both during and after a fire will vary depending on how they have been manufactured. Therefore, it is important for the high temperature bolt tests to focus on the performance of two different types of bolts: BS 4190 bolts and ISO 4014 bolts, the former having a looser fit than the latter.

4.6 Test Results at Elevated Temperatures

The test programme at high temperatures employed the Grade 8.8 bolts with Property Class 10 nuts in order to prevent thread-stripping. A total of 36 bolt tests were carried out in the temperature range from 20 °C to 600 °C; two bolt sets were involved:

- Group A: Grade 8.8 bolts with Grade 10 nuts (BS 4190) – loose tolerance
- Group B: Grade 8.8 bolts with Grade 10 nuts (BS EN ISO 4014) – tight tolerance

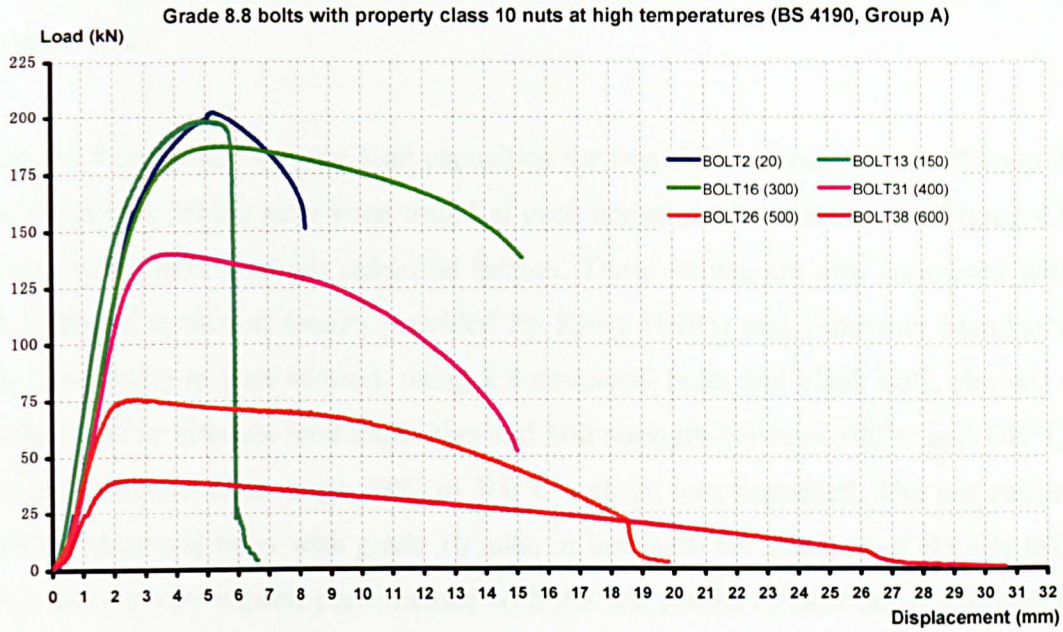

Figure 4.6: BS 4190 bolts with property class 10 nuts (T=20°C-600°C, Group A)

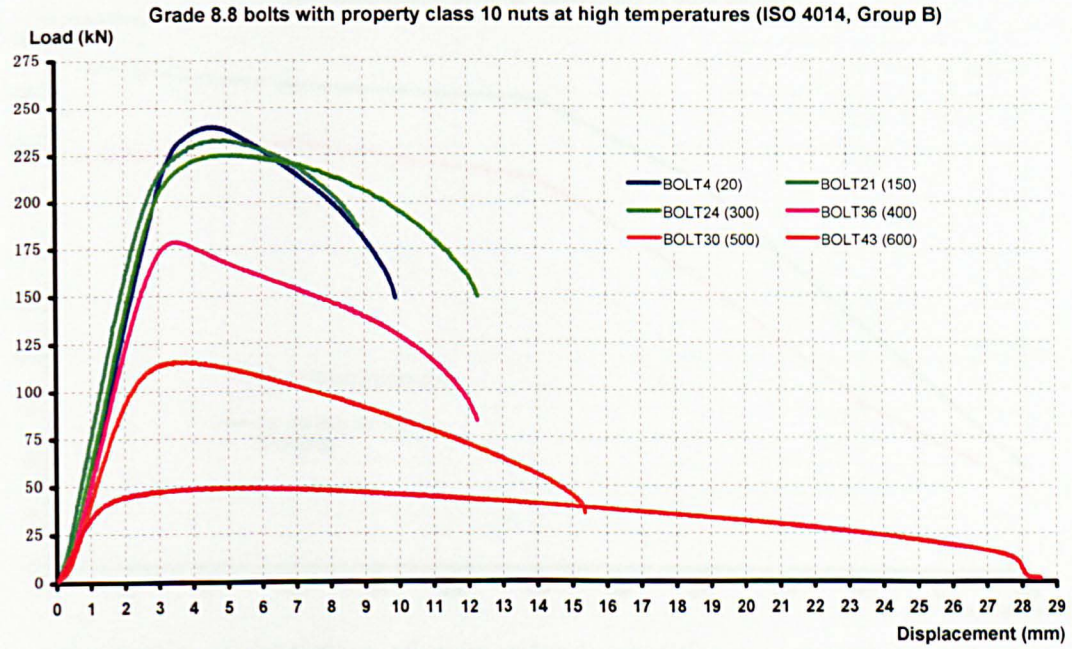

Figure 4.7: ISO 4014 bolts with property class 10 nuts (T=20°C-600°C, Group B)

Figures 4.6 and 4.7 present the typical load-displacement performance of bolts at different temperatures. In this high-temperature test programme, thirty-four structural bolts with grade 10 nuts (self-colour) failed by bolt breakage across the threaded part at all temperatures, and only two bolt assemblies (BOLT18 and BOLT19) failed by thread stripping at the temperature of 150°C. From these two figures, it is evident that the ultimate tensile load capacities decreased for each bolt

as the furnace temperatures increased, and the bolt elongation increased with temperature.

Figure 4.8 compares average load capacities for two different bolt groups (Group A and Group B), which have been tested at each constant temperature, and Figure 4.9 demonstrates their strength reduction factors. These values are also compared with the different reduction factors provided by Kirby (1995) and European Standards. The test results in pure tension, using 8.8 structural bolts and black nuts, showed a marked loss in ultimate load capacities and bolt strength between 300°C and 600°C, and in the temperature range 20°C to 300°C a slight loss happened. The test results indicate structural bolts with grade 10 nuts, in line with the standard of BS EN ISO 4014, have a very similar performance with the test results of Bolt Set A assembled with Nut Set A in Kirby's test programme.

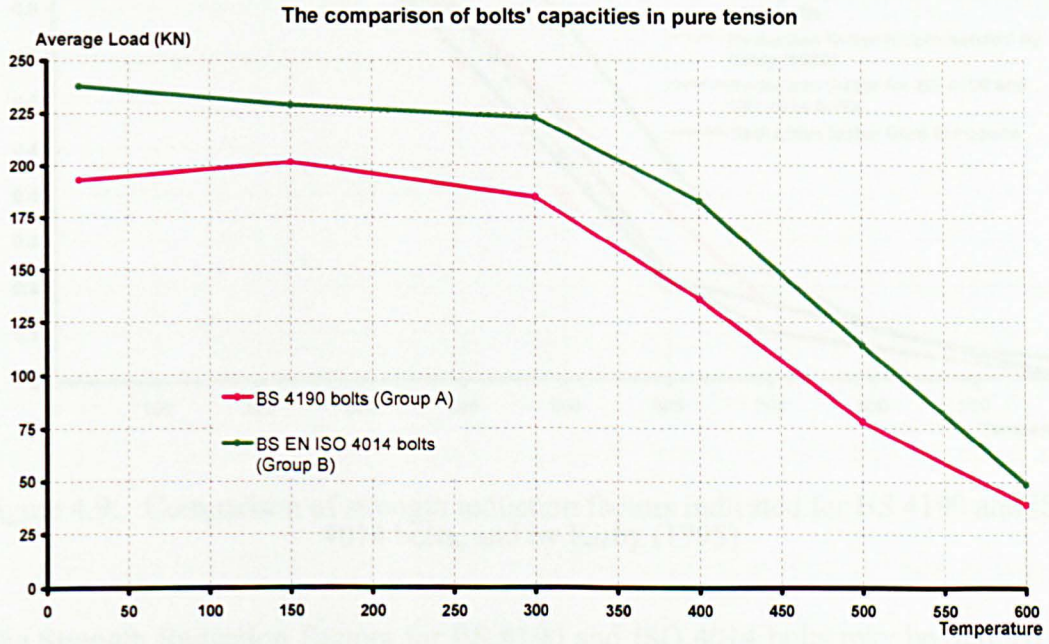

Figure 4.8: Comparison of average load capacities at various temperatures

For grade 8.8 bolts acting in either shear or tension, the strength reduction factor, presented by Kirby (1995), to describe the ultimate capacity at the fire limit state is defined by a tri-linear relationship as:

$$SRF = 1.0 \quad (T \leq 300\,^{\circ}C)$$
$$= 1 - 0.2128 \quad (T - 300) \times 10^{-2} (300\,^{\circ}C < T \leq 680\,^{\circ}C)$$
$$= 0.17 - 0.5312 \quad (T - 680) \times 10^{-3} (680\,^{\circ}C < T \leq 1000\,^{\circ}C)$$

where T = temperature.

The mechanical properties for Kirby's Grade 8.8 bolts meet the requirements of BS 3692 design rules. However, the bolts used in the reported test programme are specified to either BS 4190 or BS EN ISO 4014 standards. According to the test results, it would be appropriate to amend the Kirby's reduction factors to take into account the possible loss in bolt strength from 20 to 300°C and the slight change in reduction gradient for bolts between 300 and 600°C. For temperatures above 600°C it is reasonable to assume that the reduction curve for bolt strength is similar to Kirby's.

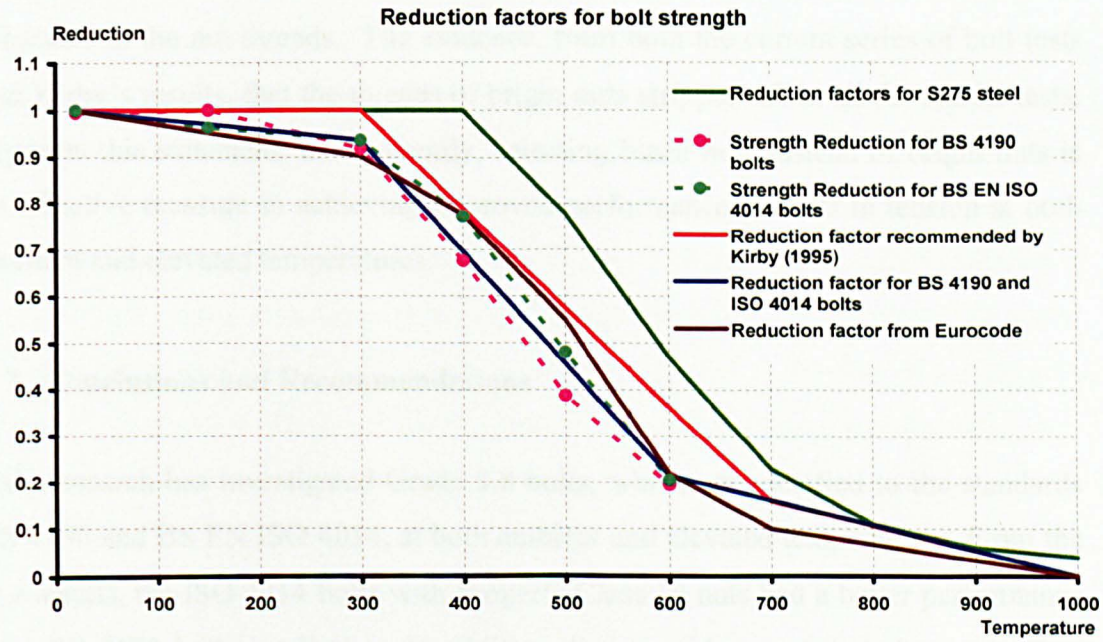

Figure 4.9: Comparison of strength reduction factors indicated for BS 4190 and ISO 4014 bolts, and by Kirby (1995)

The Strength Reduction Factors for BS 4190 and ISO 4014 bolts may be defined by an amended tri-linear relationship (Figure 4.9):

$$SRF = 1 - (0.2275\,T - 4.55) \times 10^{-3} \quad (20\,^{\circ}C \le T \le 300\,^{\circ}C)$$
$$= 0.9363 - 0.24\,(T - 300) \times 10^{-2} \quad (300\,^{\circ}C < T \le 600\,^{\circ}C)$$
$$= 0.5407\,(1 - T/1000) \quad (600\,^{\circ}C < T \le 1000\,^{\circ}C)$$

where T = temperature.

Structural bolts tested in pure tension usually experience the problem of premature failure by thread-stripping at both normal and high temperatures. Kirby (1995)

suggests that this type of failure mechanism may be controlled by improving the interaction of the threads between the nut and bolt. In order to achieve the full capacity of the bolts in tension, it is therefore recommended that bolts with the tolerance class given in BS EN ISO 4014 (6H/6g) be used, preferably together with nuts supplied to the higher strength Grade 10, specified in BS EN ISO 4032 (Barber, 2003). Moreover, it seems that the final process in manufacturing the bright finish nuts is usually galvanizing or zinc plating. In order to accommodate this anti-corrosive coating layer, the nut threads are commonly 'over-tapped' by 0.4mm in thickness (Wallace, 2009a and 2009b). The protective coatings such as zinc are relatively soft compared to steel, and zinc melts at 420°C. In consequence, this process results both in a reduction of cross-sectional area and a reduction in the tolerance in the nut threads. The evidence, from both the current series of bolt tests and Kirby's results, that the threads of bright nuts stripped off in all the tensile tests, supports this statement. Consequently, selecting black nuts instead of bright nuts is an effective measure in achieving improved performance of bolts in tension at both ambient and elevated temperatures.

4.7 Conclusions and Recommendations

This research has investigated Grade 8.8 bolts, which are specified to the standards BS 4190 and BS EN ISO 4014, at both ambient and elevated temperatures. From the test results, the ISO 4014 bolts with Property Class 10 nuts had a better performance than BS 4190 bolts in all tests. In addition, their avoidance of thread stripping has been illustrated at both ambient and elevated temperatures in this study. Finally, the amended reduction factors for BS 4190 and ISO 4014 bolts may be used to predict the strength reduction for bolts in a temperature-varying environment.

In this study, the bolts have been tested in pure tension at both ambient and elevated temperatures. Further research efforts are required to test BS 4190 and ISO 4014 bolts for performance in shear, especially under elevated-temperature conditions.

CHAPTER 5

INVESTIGATION ON END-PLATE CONNECTIONS

5.1 Introduction

Steel-framed structures must be constructed to secure life safety and property protection under fire conditions. This is because the load-carrying capacities of steel structures degrade rapidly in a real fire due to the reduction in both stiffness and strength of the material. The traditional approach of ensuring the material strength and load properties of structural members during a fire is to cover all the exposed areas of steel with a protective material. Although this approach has proved adequate, it is extremely conservative (Izzuddin and Moore, 2002). A number of researchers (Al-Jabri, et al. 2007; Robinson and Latham, 1986) suggest that it is more rational to design the structure to withstand fire without full protection of structural members rather than designing the structure at ambient temperature and then applying fire protection i.e. by covering the principal structural members with a predetermined thickness of an insulating material. As a consequence, many experimental tests have been conducted on different structural elements in order to understand their performance in fire.

As demonstrated by a number of research studies (Sanad et al., 2000), a steel and steel-composite structure can have a significantly greater fire resistance than is suggested by conventional tests on isolated components. Burgess (2007) explains that this is largely due to the interaction between the beams and floor slabs in the fire compartment, and the restraint provided by the surrounding structure. When a structure is exposed to fire, all structural members heat up but the rate of temperature rise in each member is different. Steel connections in steel-framed structures tend to

heat up more slowly than other structural members due to the additional mass concentration (bolts, plates, angles, etc.) in this location (Al-Jabri et al., 2007). The full-scale fire tests at Cardington (British Steel, 1999) showed the temperatures at joints of between 62% and 88% of that in the beam lower flange temperature at mid-span. In consequence, steel beam-to-column connections are assumed to have sufficient fire resistance in fire engineering design due to their cooler temperatures and lower heating rates. However, evidence from the collapse of the WTC twin tower buildings indicates that the progressive collapse might have been triggered by the failure of steel connections (Nethercot, 2007 and FEMA, 2002b). From full-scale fire tests, it has been found that steel connections may be the weakest components in fire conditions (SCI, 2000 and Newman et al., 2004). In research on the performance of large substructures in fire, non-linear three-dimensional analysis shows that the axial forces generated in the beams are seen to reach very high values (Allam et al., 2002). Typically these forces can vary from compression in the early stages of a fire, when thermal expansion is restrained by the surrounding structure, to tension in the later stages due to the heated members hanging essentially in catenary. Consequently, the connections at the ends of these members are subjected in turn to these axial forces whilst also undergoing large rotations.

In the traditional design of steel-framed structures, the behaviour of steel beam-to-column connections is assumed to be either rigid or pinned. However, the actual connection behaviour exhibits characteristics over a wide spectrum between these two limits; connections regarded as pinned generally possess some rotational stiffness while rigid connections display some flexibility (Nethercot, 2000). In addition, Al-Jabri et al. (2007) reports that steel connections, assumed as pinned at ambient temperatures, may provide considerable levels of both strength and stiffness at elevated temperatures. Furthermore, fire performance of steel connections may have a significant influence on the survival time of structural members and the internal force redistribution in a steel-framed structure under fire conditions. Therefore, for consideration of structural integrity (robustness) of steel-framed structures, this may require the beam-to-column connections to be more flexible or ductile under fire conditions than at ambient temperature. A ductile steel connection

may help steel-framed structures to develop catenary actions under fire conditions (Hu et al., 2008).

5.2 Structural Integrity of Steel Structures

In the UK, concern over robustness issues dates back to 1968 and the partial collapse of Ronan Point. This accident alerted the construction industry to the problem of progressive collapse arising from a lack of positive attachment between the principal structural elements in a structure (Owens and Moore, 1992). Current structural design codes are based on limit state principles and there is an implied expectation that the designed structure will be robust and able to resist natural and man-made hazards. This means that a structure should possess an ability to withstand some localized damage without the structure being damaged to an extent disproportionate to the original cause. Such a structure is *collapse resistant* or possesses *robustness or structural integrity*. To ensure a minimum level of structural robustness to resist accidental loading, one approach is to tie all the principal structural elements of a structure together. This means that the beam-to-column connections of a steel structure must be capable of carrying a horizontal *tying force* in order to prevent progressive collapse in the event of accidental damage. In 1987 a joint SCI/BCSA connection group was established to produce a series of publications which would standardise detailed design methods for commonly used steel connections. To ensure a minimum level of structural robustness, Owens and Moore (1992) carried out a series of tests to investigate the ability of simple steel connections to resist tying forces in a structure. This test programme involved 11 tests for web cleat steel connections and 10 tests for flexible end-plate beam-to-column connections. It is noted in their research that they regarded the tying forces applied to these steel connections as horizontal tie effects, as indicated by BS 5950-1 (2000) and building regulations. The experimental results demonstrate that a good level of inherent robustness was ensured by these bolted connections for a steel-framed building, and this conclusion was also confirmed by Byfield and Paramasivam (2007) in their research on gas explosions.

The progressive collapse of the World Trade Centre Towers on September 11th 2001 sharpened the research focus onto how to achieve robustness of steel-framed

structures under exceptional loading conditions (fire or explosion). The role of catenary actions in steel-framed buildings has been discussed by Byfield and Paramasivam (2007) in a case study in which one column was removed due to impact loading. The analytical results indicate that industry standard beam-column connections possess insufficient ductility to accommodate the large floor displacements that occur during catenary action. Furthermore, a post-September 11^{th} report (IStructE, 2002) states that it is insufficient merely to tie structural elements together; and tying alone does not inherently provide a ductile structure or one with good energy absorption capability. Recent research completed at Imperial College indicates factors, such as (a) energy absorption capacity, (b) ductility and (c) redundancy (alternate load paths), need to be taken into account carefully, as indicators of structural robustness for steel structural design (Izzuddin, et al. , 2008). The provision of redundancy should limit the effects of the localized failure by ensuring the availability of alternative load paths, whilst the provision of adequate ductility should ensure that damaged elements absorb energy without failure (Nethercot, 2007). Two main approaches have been recommended for structural robustness. The first strategy, as already discussed, is tying steel frame elements horizontally and vertically to increase its structural continuity and create a structure with a high level of robustness, named the *tying force approach.* In current practice, the connections are required to possess tensile strength is at least equal to the design shear force (the minimum tying strength was 75 kN for steel connections), and most industry standard steel connections have no difficulty meeting this requirement. The other strategy is the co-called *alternate load path method.* In this approach, if part of a structure has been removed by an accidental action (for example, a column is removed), the remaining members are still well connected to develop an alternative load path which transfers the load of the collapsed members to the surrounding stiffer members. The action may also need sufficient ductility from the beam-column connections to develop so-called catenary actions in the damaged zone.

During a compartment fire, the connections may experience a very complicated internal force variation as temperatures increase, and very large rotations develop due to catenary actions. By definition, in catenary action the beams act as a cable, due to softening of the steel in fire and the large reduction in flexural stiffness,

hanging from the surrounding cold structure. This feature has been observed in experimental fire tests performed by Allam et al. (2002), as shown in Fig. 5.1 and the full scale fire tests in Cardington (British Steel, 1999). The deformation of the steel beams may be very large in a fire situation, and utilization of catenary actions is believed to be able to enhance the fire resistance of structural steel beams, if sufficient strength and ductility are assured in the design of key elements such as beams and connections (Allam et al. 2002). As stipulated in the standards, the *tying forces*, are applied in a structure in both horizontal and vertical directions to help to achieve a good level of robustness. For catenary actions to develop, large beam deflections and significant connection rotations are required for structural beams and bolted connections. Byfield and Paramasivam (2007) and Hu et al. (2008) note that the tying force generated within a steel beam is no longer horizontal, as the design approach and building regulations assume, but inclined. This *inclined tying force* is representative of the forces arising due to catenary actions.

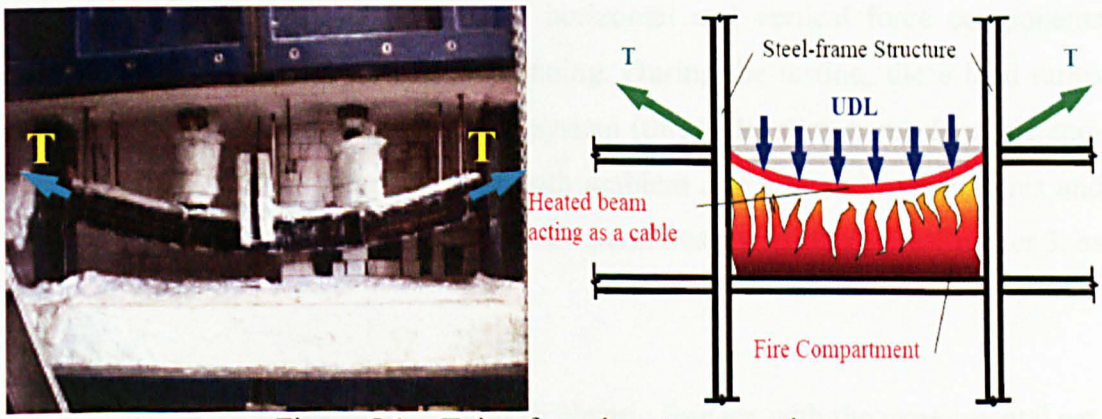

Figure 5.1: Tying force in catenary action

Under fire conditions, beam-to-column connections may receive a resultant force of shear, tension and moment during catenary actions and reduction in material strength due to high temperature will eventually result in reduced resistances in tying the principal structural elements from the connections. In the Green Book: Joints in Steel Construction – Moment Connections, the *ductility* is defined as the rotation capacity of a connection. Byfield and Paramasivam (2007) already found that catenary actions to be capable of preventing progressive collapse may not be fully developed if insufficient ductility and strength are afforded by the beam-to-column connections. As a consequence of this concern, investigation of the ductility and strength of beam-

to-column connections is extremely valuable for the robustness of steel-framed structures in fire. The research group at the University of Sheffield developed a series of experimental tests for investigating the ductility and strength of steel connections at elevated temperatures, including three commonly used simple connections and one moment connection. This chapter reports on the experiments conducted on flexible end-plate connections and details of the other connections (web cleats, fin plates and flush end-plates) may be found in Yu *et al.* (2009a, 2009b and 2009c).

5.3 Test Program on End-plate Connections in Fire

5.3.1 Test arrangement and instrumentation

In this series of fire tests, the loading arrangement (mechanism) for these specimens has already been discussed in Chapter 3. The initial loading angles (α): 35°, 45° and 55° only determined the load ratios of horizontal and vertical force components applied to these connections at the beginning. During the testing, these load ratios varied due to movements of the loading system (three Macalloy bars). Flexible end-plate (Fep) connections were tested at both ambient and elevated temperatures and the test schedule, test numbers and target temperatures are explained in Chapter 3, as shown in Table 3.3.

The connection tests were conducted in an electric furnace with the experimental set-up illustrated in Fig. 3.10. The details of testing arrangement have been documented in Chapter 3 and the essential requirement in this series of tests is to report the resistances of steel connections against inclined tying forces at both normal and high temperatures and their rotational capacities during the testing. The rotation of the steel connections was recorded by a non-contacting measuring technique (called image-acquisition technique), developed by Spyrou and Davison (2001) for high temperature experimental testing.

5.3.2 Fabrication and assembly

Steel sections (beams and columns) were supplied by Corus and fabricated by Billington Structures Ltd. The holes in the end-plates were punched according to current UK practice. Normal engineering procedures and standard tolerances were adopted during fabrication and no special effort was taken. All the specimens were assembled in the test rig and standard grade 8.8 M20 bolts were used for all tests.

5.3.3 Specimen details

In this series of connection tests, a 254UC89 was used for the column and a 305x165UB40 for the beam. The thickness for the end-plate was 10 mm and all the bolts were used in 22 mm clearance holes. The steel used was nominally S275 for universal beams and the column was S355. The design details and sizes of the specimens have been included in Fig. 5.2 and the numbers of ①-⑥ show the location of thermocouples used in testing. α is the initial or ending angle of external loading.

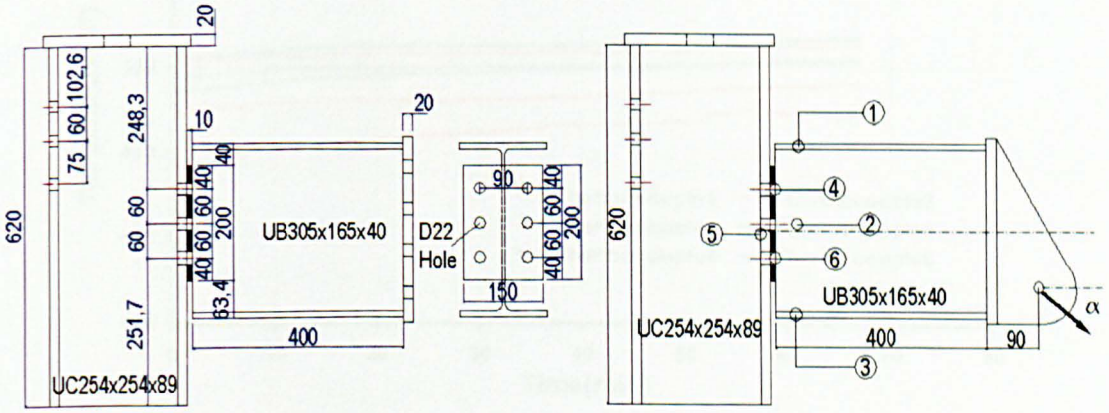

Figure 5.2: Design details for flexible end-plates

5.4 Experimental Observations

5.4.1 Temperature distribution

The main objective of this study was to investigate the resistance and ductility (rotational capacity) of flexible end-plate connections against the resultant force of shear, tension and moment at predetermined temperatures. Therefore, the testing procedure included heating a specimen up to the predetermined temperature and then applying the load through the loading jack. The column and beam in the furnace

were wrapped with a 20 mm thick ceramic fibre blanket and only the connection zone, including the end-plate, column flange, bolts and beam web, was exposed to heat throughout the testing. Six thermocouples were used to record the temperatures during the loading process. These were located at beam bottom and top flanges, beam web, top and bottom bolts and column flange (shown in Fig. 5.2). Fig. 5.3 demonstrates the typical temperature distribution in the connection zone against time for each predetermined temperature. Although there was a small discrepancy between these temperature curves in the connection zone, the difference in temperature distribution was less than 2% and did not have a considerable influence on the connection performance at elevated temperatures. Each tested connection can be assumed to be at a uniform temperature distribution in the subsequent finite element analyses and for the component-based approach.

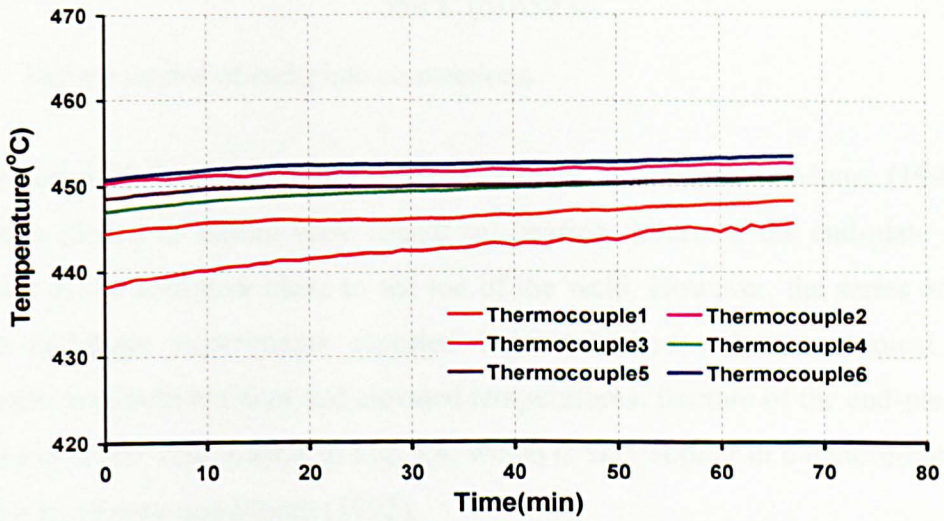

(a) Temperature distribution in the connection zone at 450 °C

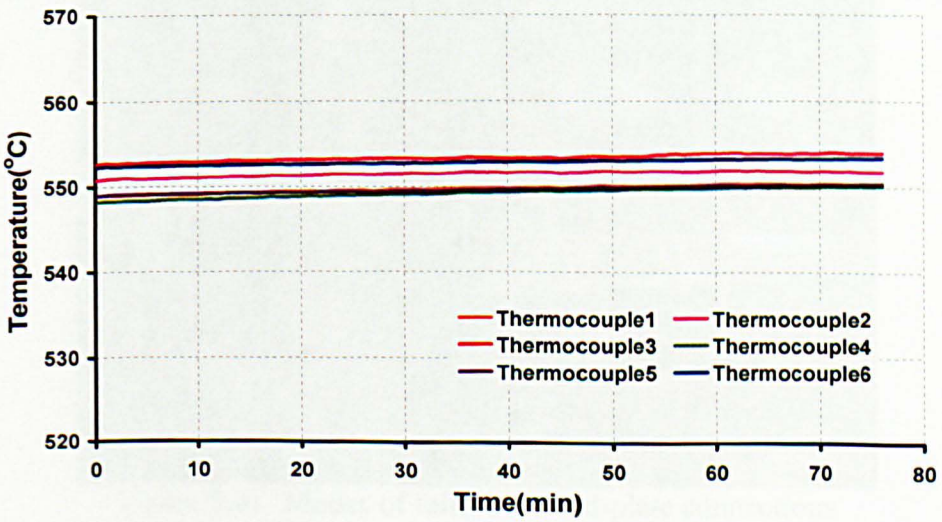

(b) Temperature distribution in the connection zone at 550 °C

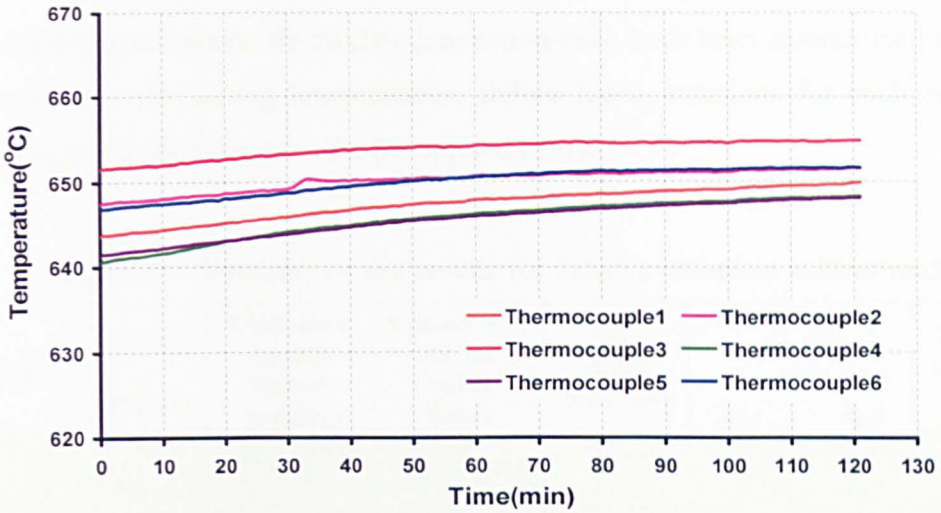

(c) Temperature distribution in the connection zone at 650 °C

Figure 5.3: Typical temperature distribution in the connection zone (a) 450°C (b) 550°C (c) 650°C

5.4.2 Failure modes of end-plate connections

In the series of flexible end-plate tests performed by Owens and Moore (1992), two different modes of failure were found: (a) bearing failure of the end-plate and (b) fracture of the end-plate close to the toe of the weld. However, the series of partial depth end-plate experiments reported here exhibited only one typical failure mechanism at both ambient and elevated temperatures: fracture of the end-plate close to the toe of the weld, shown in Fig. 5.4, which is very similar to the afore-mentioned finding by Owens and Moore (1992).

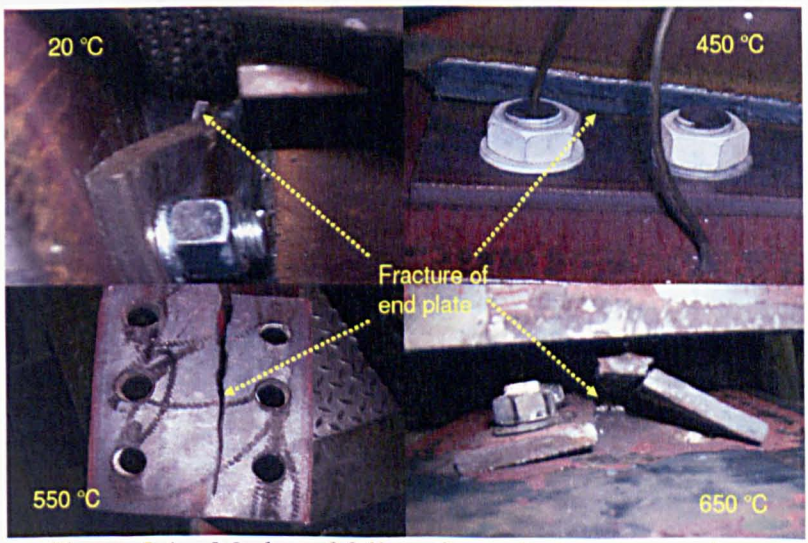

Figure 5.4: Modes of failure for end-plate connections

5.4.3 Test Results

The experimental results for twelve connection tests have been summarised in Table 5.1. including the testing temperatures, failure loads, rotations for each end-plate connection and the variation of α for applied loads.

Table 5.1: Summary of test results for flexible end-plate connections

Test no.	Ending α (degree)	Connection rotation (degree, {*mrads*})	Contact with column before failure	Max failure load (kN)	Tying capacity estimated by using EC3 (kN)		Minimum tying force (kN)
					$k_{y,\theta}$	$k_{p,\theta}$	
Fep35 - 20	43.49	8.6, {*150.1*}	yes	192.00	254.13	254.13	75.00
Fep35-450	38.71	4.2, { *73.3* }	no	90.36	226.18	99.11	75.00
Fep35-550	40.17	3.9, { *68.1* }	no	68.51	158.83	68.62	75.00
Fep35-650	39.62	3.6, { *62.8* }	no	32.55	88.95	33.04	75.00
Fep45 - 20	51.08	8.8, {*153.6*}	yes	150.00	254.13	254.13	75.00
Fep45-450	48.56	3.5, { *61.1* }	no	64.50	226.18	99.11	75.00
Fep45-550	47.86	3.2, { *55.9* }	no	44.10	158.83	68.62	75.00
Fep45-650	48.59	3.8, { *66.3* }	no	28.45	88.95	33.04	75.00
Fep55 - 20	56.10	11.2,{*195.5*}	yes	179.30	254.13	254.13	75.00
Fep55-450	55.90	4.8, { *83.8* }	no	55.56	226.18	99.11	75.00
Fep55-550	55.51	3.9, { *68.1* }	no	36.31	158.83	68.62	75.00
Fep55-650	55.67	4.5, { *78.5* }	no	22.09	88.95	33.04	75.00

As this research project is concerned with the ductility and resistance of simple connections, plots of variation of the load-rotation characteristics are shown in Fig. 5.5 (a) (b) (c). The connections tested at both ambient and elevated temperatures demonstrated a non-linear response. It is very obvious that the resistance and ductility (as measured by rotation capacity) of steel connections are both decreased at high temperatures. The reduced rotation capacity of simple steel connections at high temperatures is due to the rupture of the end-plates occurring before the beam flange contacts with the column flange, which occurs at ambient temperatures as evidenced by the kink in the curve at about 6^{o} (104.7 mrads) rotation.

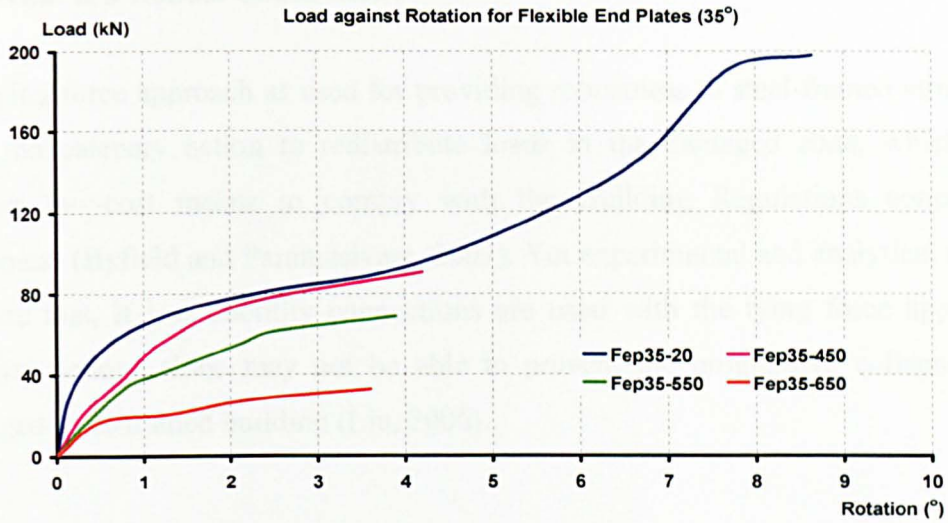

(a)

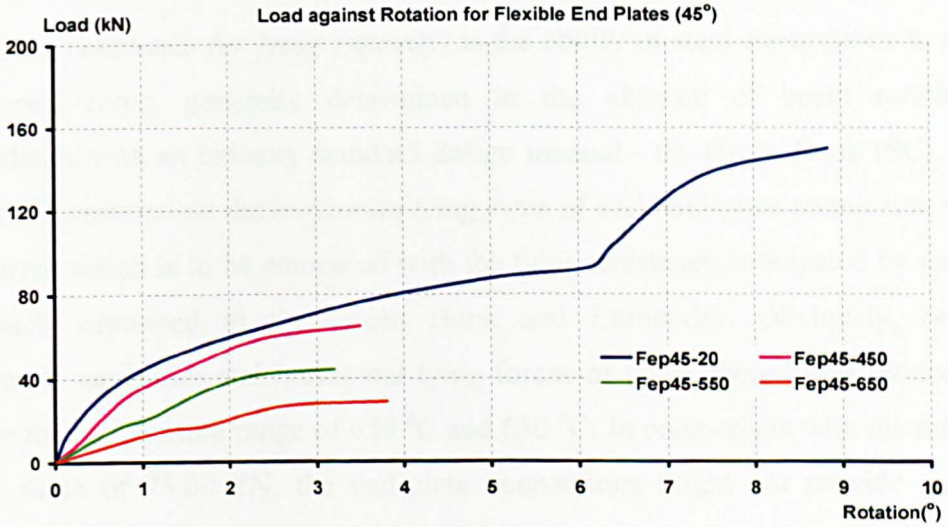

(b)

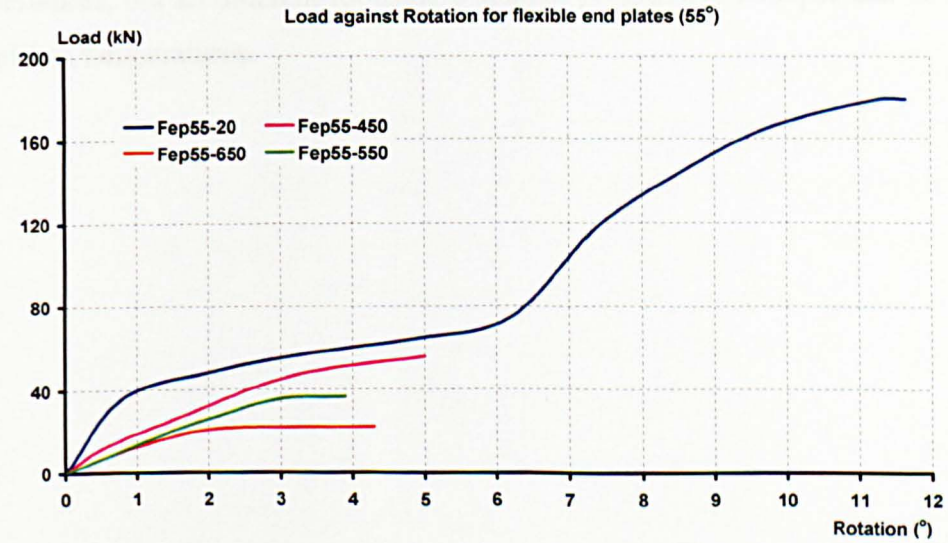

(c)

Figure 5.5: Test results for flexible end-plate connections (a) 35° (b) 45° (c) 55°

5.5 What is a Robust Connection?

The tying force approach as used for providing robustness to steel-framed structures relies on catenary action to redistribute loads in the damaged zone, which is a popular low-cost means to comply with the Building Regulations concerning robustness (Byfield and Paramasivam, 2007). Yet experimental and analytical results indicate that, if low ductility connections are used with the tying force approach, catenary actions alone may not be able to prevent the progressive collapse of a damaged steel-framed building (Liu, 2006).

5.5.1 Tying resistance

The *tying resistance (or tying capacity)* is the ability of steel connections to resist a horizontal force, generally determined in the absence of beam rotations in accordance with an industry standard design manual - the Green Book (SCI, 2002). Table 5.2 summarises the *horizontal tying force* of each end-plate connection when it fractured, which is to be compared with the tying resistance anticipated by using the approach stipulated in the Green Book and Eurocodes. Obviously, both the maximum capacities and horizontal tying forces of these connections reduced very fast in the temperature range of 450 °C and 650 °C. In comparison with the minimum tying force of 75.00 kN, the end-plate connections might not provide sufficient connection resistance to satisfy the minimum robustness requirement at elevated temperatures; but an inherent robustness against progressive collapse can be assured at ambient temperatures.

Table 5.2: Summary of tying capacities of flexible end-plate connections

Test no.	Maximum failure load [kN]	Horizontal tying force in the tests [kN]	Tying capacity estimated by using Green book [kN]		Tying capacity estimated by using EC3 [kN]		Minimum tying force [kN]
			$k_{y,\theta}$	$k_{p,\theta}$	$k_{y,\theta}$	$k_{p,\theta}$	
Fep35 - 20	192.00	139.33	249.28	249.28	254.13	254.13	75.00
Fep35-450	90.36	70.51	221.86	97.22	226.18	99.11	75.00
Fep35-550	68.51	52.35	155.80	67.31	158.83	68.62	75.00
Fep35-650	32.55	25.07	87.25	32.41	88.95	33.04	75.00
Fep45 - 20	150.00	94.21	249.28	249.28	254.13	254.13	75.00
Fep45-450	64.50	42.72	221.86	97.22	226.18	99.11	75.00
Fep45-550	44.10	29.58	155.80	67.31	158.83	68.62	75.00
Fep45-650	28.45	18.73	87.25	32.41	88.95	33.04	75.00
Fep55 - 20	179.30	100.00	249.28	249.28	254.13	254.13	75.00
Fep55-450	55.56	31.15	221.86	97.22	226.18	99.11	75.00
Fep55-550	36.31	20.57	155.80	67.31	158.83	68.62	75.00
Fep55-650	22.09	12.46	87.25	32.41	88.95	33.04	75.00

The tying capacities determined by using the Eurocodes are likely to overestimate the connection resistances to horizontal tying forces at both ambient and elevated temperatures. The factors of $k_{y,\theta}$ and $k_{p,\theta}$ were introduced in estimation of tying capacities at elevated temperatures in Table 5.2: $k_{y,\theta}$ standing for the reduction factors for effective yield strength and $k_{p,\theta}$ representing the factors for proportional limit. In Table 5.2, it is obvious that the tying capacities, calculated by using $k_{y,\theta}$ reduction factors, are higher than the connection resistances obtained in experiments, probably because the calculation of tying capacity in accordance with Eurocodes and the Green Book assumes zero beam rotation in the connection zone.

5.5.2 Ductility

The rotation capacity (ductility) of end-plate connections is mainly produced by deformation in the plates, column flanges and bolts. Deformation of column flange and end-plate was estimated by using the equivalent T-stubs method as presented by Spyrou (2002). In Spyrou's research, a total of 45 T-stubs were tested at elevated temperatures and then a simplified analytical model of the tension zone was developed and compared well with the experimental results. Figure 5.6 shows the failure of T-stubs in one of three modes (Spyrou, 2002), observed from the tests: complete yielding of the T-stub flange followed by yielding and fracture of bolts (mode 1), formation of two plastic hinges near the web followed by yielding and fracture of bolts (mode 2), and bolt fracture with the flanges remaining elastic (mode 3). The deformation of T-stubs which failed in a ductile manner (failure mode 1) was

considerably higher than that in other failure modes. In partial depth end-plate connections, plastic hinges are expected to form at four critical sections near the two toes of the fillet welds and at the two edges of the bolt holes (mode 1 failure). This mode of failure gives the end-plate connections with the maximum deformation under the loading conditions.

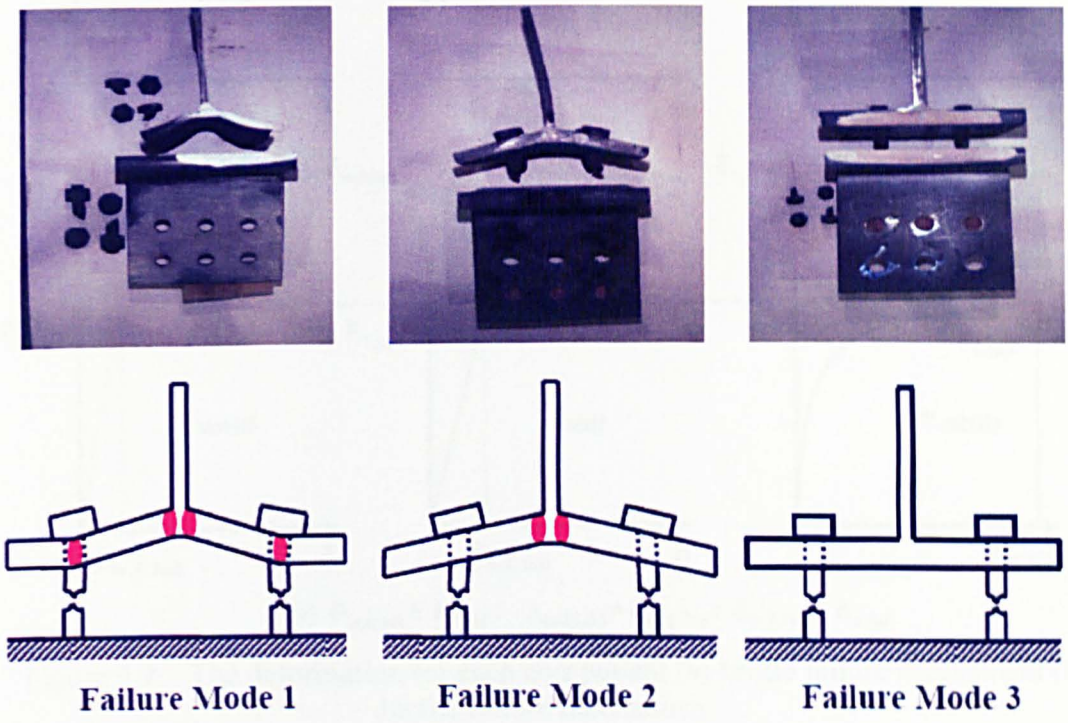

Figure 5.6: Failure mechanism of T-stubs at elevated temperatures

Current design practice (EC3, 2005) adopts the component-based approach for investigation of the behaviour of beam-to-column connections, which interprets a connection as a set of spring-like components. Each component is characterized by a pre-determined nonlinear load-and-displacement response. Kuhlmann et al. (1998) identified these components in terms of their deformation capacities and modes of failure. Bolts and welds are classified as brittle components due to their small deformations with increasing load. They also indicate that the deformation capacity of a connection is bound by the deformation capacity of its single components. As a result of this, in analyzing the ductility of a connection, the responses of brittle components can only be ignored if these components can be guaranteed to be the strongest components. Whilst this is often the case at ambient temperatures, under

fire conditions the rapid loss of strength in bolts and welds can lead to a different, less ductile failure mode for a connection.

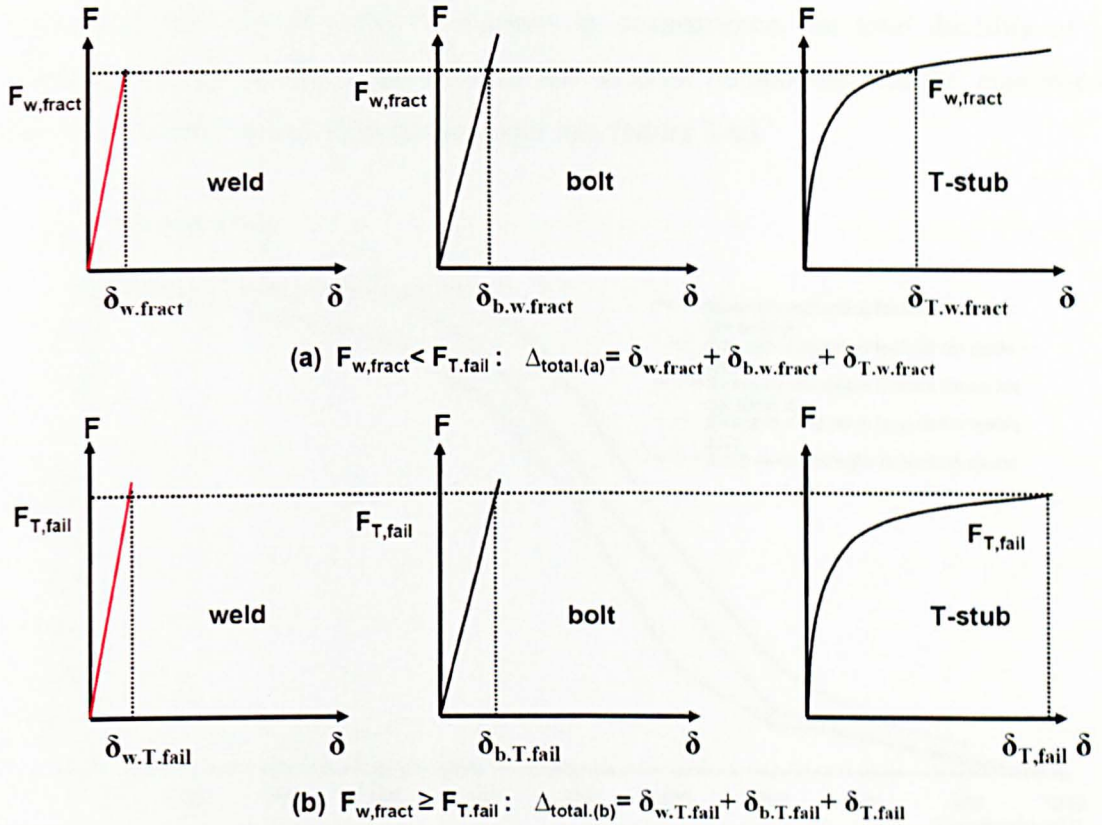

Figure 5.7: The deformation for each component (a) brittle failure mechanism (b) ductile failure mechanism

As demonstrated in Figure 5.7, each bolt row of an end-plate connection is simplified as a three-spring system including components for bolts, welds and T-stubs. The total deformation (Δ_{total}) for each bolt row is a summation of the elongation of each component involved ($\Delta_{total} = \delta_w + \delta_b + \delta_T$). This figure also shows that the ultimate resistance of brittle components exerts an influence on the total deformation of each bolt row, and will consequently affect the rotational capacity of an end-plate connection. The ultimate resistance of a T-stub may be assumed to remain unchanged in a flexible end-plate connection (the header plate of these tested connections usually being regarded as three parallel T-stub elements), and the bolts are usually assumed be the strongest in the three-spring system. If the weld is the weakest component in each bolt row ($F_{w.fract} < F_{T.fail}$), the failure load of a connection is limited by the fracture of the welds, and meanwhile the ductile component (T-Stub) may not be fully elongated or deformed before these

connections fracturing. If the weld is stronger than the T-stub element ($F_{w,fract} \geq F_{T,fail}$), each bolt row may approach the maximum elongation and the connection may fail in a ductile manner. In consequence, the total ductility of a connection relies on the failure load of the weakest component and the maximum extension of the ductile components under this failure load.

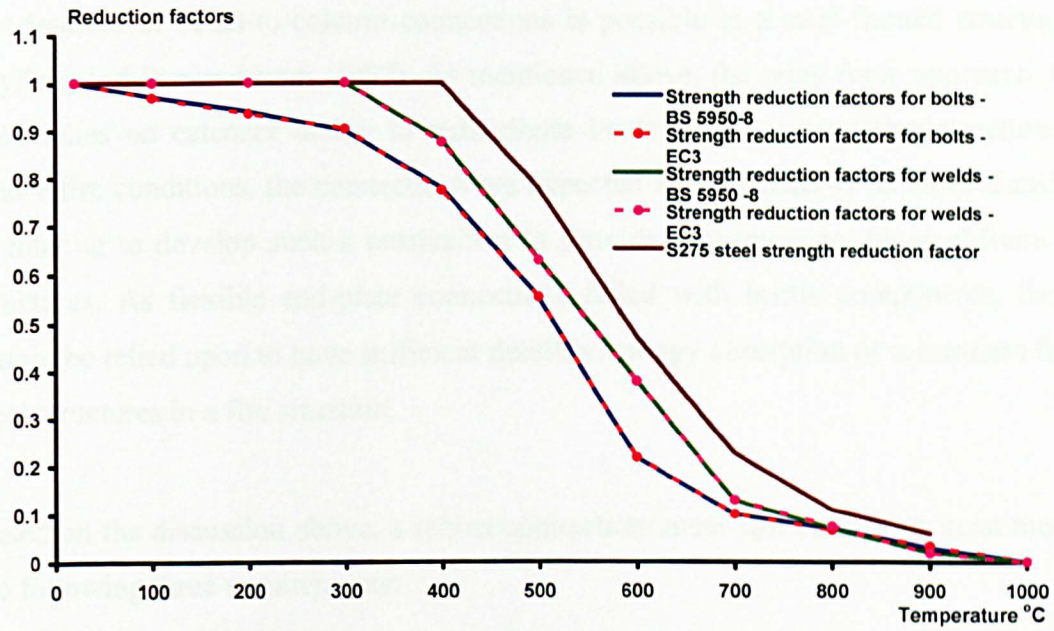

Figure 5.8: Strength reduction factors for bolts, welds and S275 steel

Based on the experimental tests, rotation capacities of these connections are obviously reduced at elevated temperatures due to rupture of the end-plates *before* the beam flange contacts with the column flange in the connection zone, whereas the end-plate connections have already been found to be more ductile at ambient temperatures owing to the rupture occurring *after* contact with the column flange. As shown in Figure 5.8, the strength reduction in welds is initially assumed to be the same as that for S275 steel (no reduction in strength below the temperature of 300°C). But note that the strength reduction of the weld material is faster than the S275 steel in the temperature range of 400°C to 700°C. The faster reduction in weld strength might cause a smaller fracture load in the weld component at high temperatures, if compared with the T-stub elements, and eventually limit the elongation for each bolt row, particularly for the ductile components. As a result of this, the rotation capacities of the connections were reduced at high temperatures. If the welds could

be made strong enough, the end-plate connection might be expected to fail in a ductile manner under fire conditions.

From the experimental results recorded, the available maximum rotation is about 4^{o} for an end-plate connection in a standard fire test. In the case study of catenary action , this value of rotation is sufficient to allow the development of catenary action, and fracture of beam-to-column connections is possible in a steel-framed structure (Byfield and Paramasivam, 2007). As mentioned above, the tying force approach as used relies on catenary action to redistribute loads to the surrounding structures. Under fire conditions, the connections are expected and required to be more ductile in rotating to develop such a mechanism to provide robustness to the steel-framed structures. As flexible end-plate connections failed with brittle components, they cannot be relied upon to have sufficient ductility, energy absorption or robustness for steel structures in a fire situation.

Based on the discussion above, a robust connection under fire conditions must meet the following three requirements:

a. avoidance of failure in brittle components
b. sufficient ductility
c. resistance to catenary actions as required by horizontal tying force rules

5.6 Conclusions

The tying force method, as recommended by UK Building Regulations, is a popular low-cost means to improve robustness of steel-framed structures to prevent progressive collapse. As mentioned above, this approach relies on the development of catenary action to bridge the damaged zone in order to redistribute the loads. Based on UK Building Regulations, the tying resistance of beam-to-column connections is generally determined in the absence of beam rotations. However, it should be recognized that the beam-to-column connections may be subjected to *inclined tying forces* owing to catenary action developed under fire conditions. Thus the tying resistance, estimated by using the approach stipulated in both EC3 and Building Regulations, are likely to overestimate the ability of a connection to resist

the tying force. The review of experimental results indicates that even the minimum tying resistance of 75 kN might not be assured for flexible end-plate connections in a fire situation. In the discussion of connection robustness, the component-based approach has been introduced in order to understand brittle failure of end-plate connections due to weld failure. These experimental tests show the ductility available from end-plate connections to be limited at elevated temperatures. If low ductility connections are used with the tying force method, it will not be possible to fully develop catenary action to prevent progressive collapse in steel-framed buildings in fire. Consequently, specifying partial depth end-plate connections with the potential for brittle failure in the welds seems inadvisable for robustness of steel structures where large connection rotations are anticipated.

CHAPTER 6

A COMPONENT-BASED MODEL FOR AN END-PLATE CONNECTION*[1]

6.1 Introduction

Conventional steel frame building design often assumes the joints between beams and columns to behave as pins with lateral stiffness provided by braced bays or shear cores. In order to realise this design assumption in the completed structure, flexible (or simple) connections are required. A popular form of such connections is a shallow plate welded to the beam web and bolted to the column, known as a partial depth end-plate, header plate or flexible end-plate. To be classified as pinned or simple, the connection should possess large rotational capacity and low stiffness so that it transfers shear but negligible moment to the column. In accidental situations, for example fire or blast, the structural behaviour of joints is critical in avoiding structural collapse. Full-scale fire tests conducted on an eight storey composite building at the Building Research Establishment's Large Building Test Facility at Cardington and the collapse of the World Trade Centre buildings demonstrated that steel joints may be particularly vulnerable during the heating and cooling phases of fire despite their somewhat lower temperatures due to the higher concentration of mass in this area (Burgess *et al.*, 2007). In fire conditions, it is generally accepted that the performance of steel beams is affected by the restraint forces due to interaction between the fire-affected members and the adjacent cold structure (Allam *et al.*, 1999). Considerable moments and axial forces are produced, even in simple steel connections, due to the large deformations of the heated beams (Block *et al.*,2004), and these can change significantly as the fire develops. At ambient temperature the connection is under moment (although this should be low in a simple connection) and shear. In the early and intermediate stages of a fire, a connection will additionally be subject to significant compression due to the restraint to thermal

[1] This chapter has been published as a journal paper (Hu, et al., 2009)

expansion of the heated beams. As the fire develops and the beam loses bending stiffness, loads are carried by catenary action and the connections will be required to carry large tensile forces and vertical shear whilst simultaneously undergoing large rotations in order to generate the deformations necessary for catenary action (Block *et al.*, 2006). Once the fire starts to decay, the effects of cooling on a steel connection can be critical for the survival of a structure; this is because large tensile forces can be induced as the highly deformed beam tries to contract. For example, if a connection is loaded to a certain level and the material softens due to increasing temperatures, the connection components will eventually become plastic and the weakest component will dominate the failure of the connection (Block, 2007). However, before approaching the failure, reduction in temperatures leads to plastic deformations of the connection components kept as constant, and only the elastic deformations recover. The complex variation of internal forces and elastic-plastic deformations presents a very difficult challenge in simulating the connection performance during the heating and cooling phases of a fire. Advanced structural analysis methods can produce excellent predictions of the overall response of a steel building in fire but the inclusion of realistic connection characteristics is problematic. The development of a practical model for a flexible end-plate, suitable for use in structural fire analysis, was the aim of the research described herein.

Al- Jabri and his co-researchers (2005) reviewed the published research work on the performance of steel beam-to-column joints in fire including developments in modelling this behaviour. Although curve-fit models adapted to account for the change of strength and stiffness at elevated temperatures (El-Rimawi, 1989) may be used to represent the moment-rotation curves of joints and are convenient for frame analysis, the presence of significant axial forces (first compressive then tensile) during the heating and cooling phases of a fire makes such an approach impractical (Burgess, 2007). In fire situations, where the effect of thermal expansion and contraction, together with temperature induced changes to material properties, must all be accounted for, the use of component-based models is attractive. Component-based models were first proposed by Tschemmernegg et al. (1987) for the ambient temperature design of steel joints and after much development have been incorporated into Eurocode EC3-1.8 (EC3, 2005). The attraction of this approach is

its relative simplicity and its ability to simulate the whole connection behaviour to an acceptable level of accuracy (Al-Jabri, 2004).

Eurocode EC3-1.8 provides guidance on the use of the component method for the prediction of the moment-rotation relationship of flush and extended end-plate beam-to-column joints. In principle the same methodology can be used for any joint configuration and loading conditions (for example moment combined with axial force), provided that the basic components are properly characterized. Fig. 6.1 illustrates the methodology (Spyrou, 2002). The end-plate joint shown is assumed to be divided into three major zones: tension, compression and shear. Within each zone, a number of individual and basic spring-like components have been specified, which contribute to the overall deformation and capacity of a steel joint. Each of these basic components possesses its own initial stiffness and load-against-displacement relationship in tension, compression or shear.

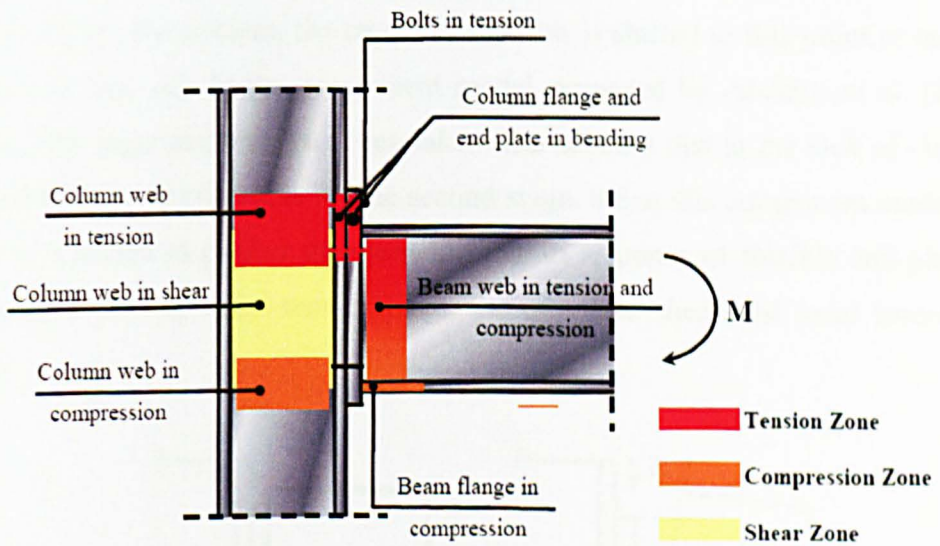

Figure 6.1: End-plate joint separated into three zones and key components (Spyrou, 2002)

The application of the component method requires the following three basic steps (Jaspart, 1999; Weynand,1995).

i) Identification of the active components in a structural joint

ii) Characterization of the nonlinear load-displacement response for each individual component

iii) Assembly of all the components and evaluation of the structural response of the whole joint

Jaspart (1998) and Simões da Silva *et al.* (2001) presented detailed explanations of the component approach, including consideration of ductility. The various components in steel joints (e.g.T-stubs, bolts, welds etc) may be classified in terms of deformation capability, namely those with (a) high ductility, (b) limited ductility or (c) brittle. A particular zone within a joint may comprise a number of active components some of which may be ductile and others brittle.

Al-Jabri *et al.*, (2005) proposed a spring-based component model for a flexible end-plate connection. The rotational response of the joint was considered to comprise two stages: unimpeded rotation of the joint followed by stiffer behaviour once the beam lower flange contacts the column. In the first stage, the joint is assumed to rotate about the lower edge of the end-plate and the lower flange of the beam is not in contact with the column flange. After sufficient rotation to cause the beam flange to bear directly on the column, the centre of rotation is shifted to this point of contact, as shown in Fig. 6.2. In the component model proposed by Al-Jabri *et al.* (2005), only the first stage response has been taken into account due to the lack of elevated temperature experimental data for the second stage. Since this component model was primarily intended to predict the moment-rotation response of flexible end-plates at both ambient and elevated temperatures, the effect of shear and axial forces was ignored.

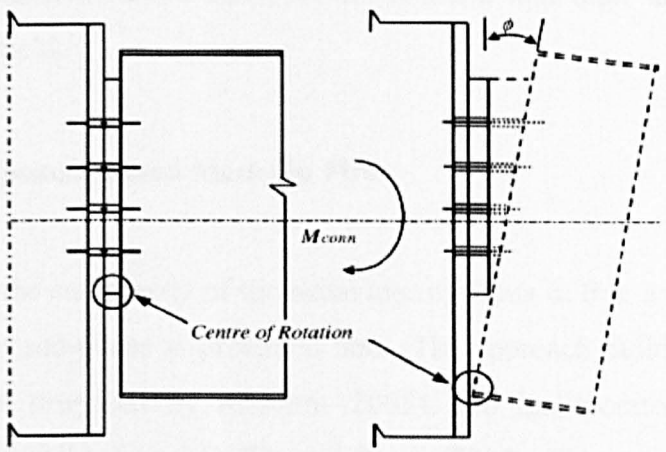

Figure 6.2: Movement of the centre of rotation for flexible end-plates (Al-Jabri, 2005)

This chapter describes a component-based model developed to simulate the behaviour of flexible end-plate steel connections at both ambient and elevated temperatures. In the model, the components of the joint are treated as sets of nonlinear springs at the level of each bolt row interconnected by a rigid bar. Each component, plate, weld or bolt, is modelled with mechanical characteristics such as stiffness, strength and ductility. By assembling the contributions of these individual components, the entire behaviour of the connection may be determined for use in structural analysis at both ambient and elevated temperatures.

6.2 Flexible End-plate Connections in Fire

In order to provide experimental data on the performance of flexible end-plates in fire, a series of high temperature connection tests was carried out at the University of Sheffield. The details of the tests and a summary of the experimental results, including testing temperatures, failure loads, maximum rotations and failure modes, have been reported in Chapter 5. In these tests, the rotational capacity of the joint was found to reduce with increasing temperature as a result of rupture of the end-plates before the beam flange came into contact with the column flange. Hence, the large rotations and increased stiffness associated with this contact were unable to develop. Experimental research by Owens and Moore (1992), conducted to examine the tensile resistance of flexible end-plate connections showed two modes of failure (i) bearing failure and (ii) fracture of the end-plates close to the toe of the weld. The latter was the dominant failure mode in the ambient and high temperature tests conducted at Sheffield.

6.3 A New Component-based Model in Fire

To accommodate the complexity of the behaviour of joints in fire, a new component model for flexible end-plates is presented here. The approach builds on the earlier mechanical model proposed by Al-Jabri (2005), and incorporates developments made by Spyrou (2004b), Sarraj (2007) and Block (2007). This new model includes all the active components of a flexible end-plate connection, which may contribute to tension, compression and shear deformation in a fire situation, as shown in Fig. 6.3.

The failure mechanism of the connection will be controlled by the weakest component in the model. From the experimental results, most of the end-plate connections failed by rupture of the end-plate close to the toe of the weld within the first bolt row. The modelling of the various components in the tension zone will be discussed first.

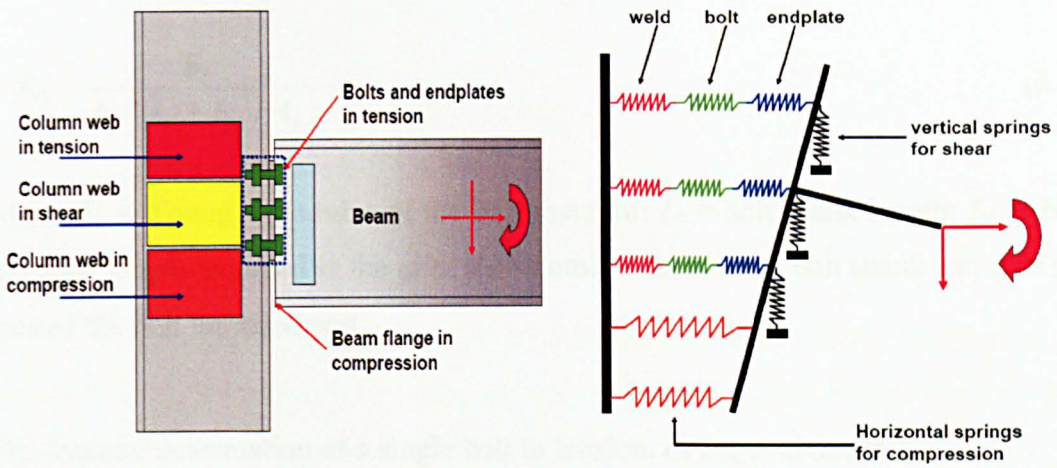

Figure 6.3: Component model for partial depth end-plate connections

6.3.1 Tension zone components

In an end-plate connection, the components in the tension zone include the column web, column flange in bending, bolts, weld, and a T-stub comprising the end-plate and beam web. Since flexible end-plate connections are designed as simple with limited stiffness in comparison with the column to which they are attached, the contribution of the column flange and column web components was ignored. The experimental results confirmed this to be a reasonable assumption as the majority of the deformation arose from bolt elongation and end-plate bending.

6.3.1.1 Bolt behaviour

In the research conducted by da Silva *et al.* (2001), bolts are classified as brittle components because of their limited deformation before failure. However, the authors have found that maximum displacement for the bolts subjected to direct

tensile forces can be 15% - 20% of the effective length (taken as the grip length) at ambient temperatures for grade 8.8 bolts (Hu *et al.*, 2007). In the present study, the bolts are simply assumed to be subjected to pure tensile forces and their mechanical response is incorporated by means of an extensional spring with an elastic-plastic force-deformation (B - δ_b) curve as shown in Fig. 6.4. As proposed by Swanson (1999), the bolt elastic stiffness, K_b, is evaluated as follows:

$$K_b = \frac{E_b}{L_s / A_b + L_{tg} / A_s} \tag{6.1}$$

where E_b = Young's modulus of the bolt material; L_s = bolt shank length; L_{tg} = bolt threaded length included in the grip; A_b = nominal area of the bolt shank and A_s = net area of the bolt threaded part.

The fracture deformation of a single bolt in tension, $\delta_{b.fract}$, is given by :

$$\delta_{b.fract} = \frac{0.9 B_u L_s}{A_b E_b} + \varepsilon_{u.b}\left(L_{tg} + \frac{2}{n_{th}}\right) \tag{6.2}$$

where n_{th} = the number of threads per unit length of the bolt and B_u = the ultimate load for the bolt. These predictions are based on the assumption that the bolt shank remains elastic and the inelastic deformation is concentrated in the threads included in the grip length (Swanson, 1999). Fully-threaded grade 8.8 bolts have been used throughout this experimental programme; hence L_s = 0. Therefore, the above equations may be simplified, as follows:

$$K_b = E_b A_s / L_{tg} \tag{6.3}$$

$$\delta_{b.fract} = \varepsilon_{u.b}\,(L_{tg} + 2 / n_{th}) \tag{6.4}$$

Applying Swanson's bolt material model to the new component model, the load-deformation curve can be simplified to a bi-linear relationship with an assumed yield force for bolts equal to 85% of the ultimate load capacity, as shown in Fig. 6.4.

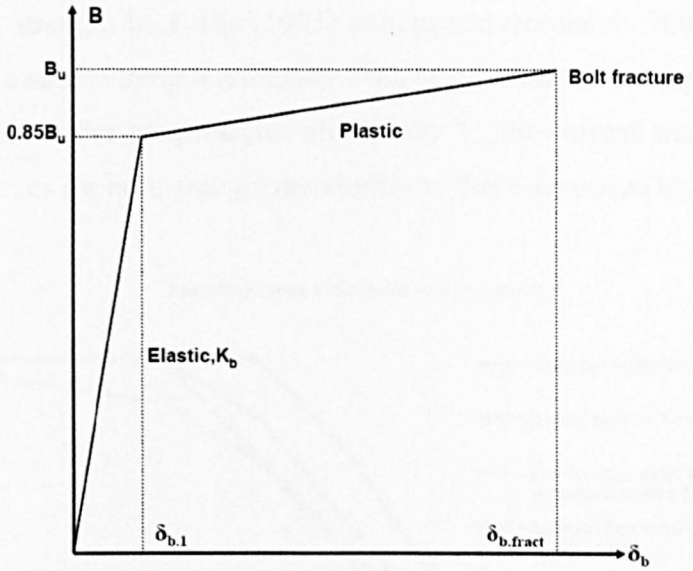

Figure 6.4: Elastic and plastic response of a bolt

Under fire conditions, failure modes for bolts may include thread stripping of the nuts and bolt breakage. These are undesirable failure mechanisms because they compromise robustness of steel connections in fire. Kirby (1995) carried out a series of high temperature tests on Grade 8.8 bolts and showed that they suffer a significant decrease in strength and Young's modulus between 300°C and 700 °C. The following strength reduction factors (SRF) were recommended:

$$\begin{aligned} SRF &= 1.0 && (T \leq 300\ ^{o}C) \\ &= 1.0 - 0.2128\,(T - 300) \times 10^{-2} && (300\ ^{o}C < T \leq 680\ ^{o}C) \\ &= 0.17 - 0.5312\,(T - 680) \times 10^{-3} && (680\ ^{o}C < T \leq 1000\ ^{o}C) \end{aligned}$$

Hu and his co-authors (2007) conducted a further series of tests for Grade 8.8 bolts, complying with recently introduced British and European standards (BS 4190: 2000, and BS EN ISO 4014, 4017 respectively). Based on these tests, alternative strength reduction factors for bolts are proposed for use in the component approach:

$$\begin{aligned} SRF &= 1.0 - (0.2275\,T - 4.55) \times 10^{-3} && (T \leq 300\ ^{o}C) \\ &= 0.9363 - 0.24\,(T - 300) \times 10^{-2} && (300\ ^{o}C < T \leq 600\ ^{o}C) \\ &= 0.5407\,(1 - T/1000) && (600\ ^{o}C < T \leq 1000\ ^{o}C) \end{aligned}$$

These two series of bolt strength reduction factors are compared with the one recommended by European codes EC3 1-2 in Fig. 6.5. Whereas no reduction was

observed in bolt strength by Kirby (1995) at temperatures below 300 °C, the current study identified a small strength reduction even at relatively low temperatures, and is consistent with EC3. For temperatures above 600 °C, the current study assumes that the reduction curves for bolt strength are similar to those proposed by Kirby.

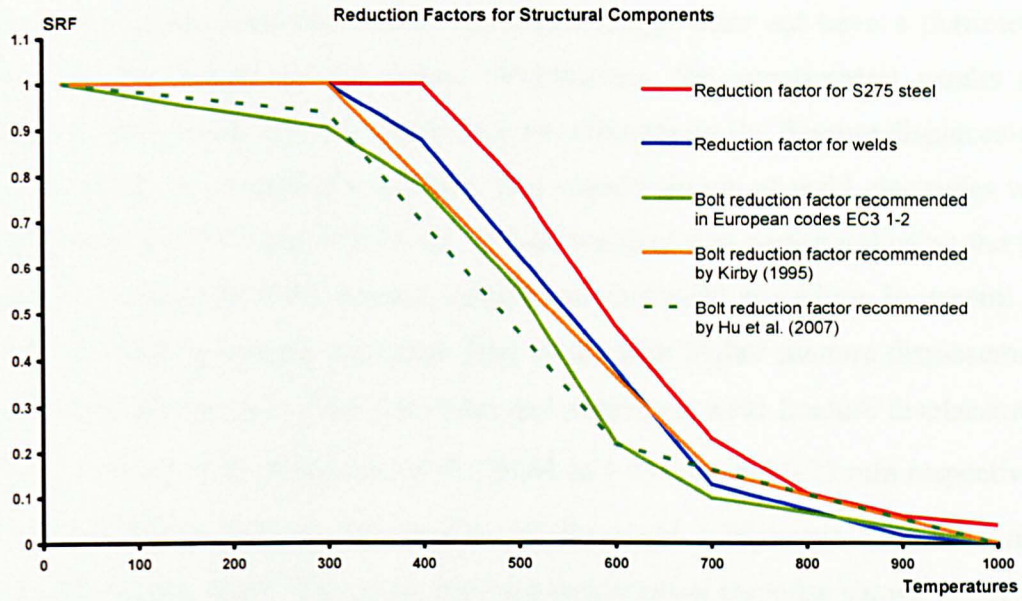

Figure 6.5: Strength reduction factors for structural components

6.3.1.2 Weld behaviour

Fillet welds have limited deformability and are classified as brittle elements in the component approach (Simoes da Silva *et al.*, 2001). The mechanical response of the fillet weld can be defined by a linear load-deformation relationship. In EC3 1-8, the stiffness of a weld is assumed to be infinite and the strength may be given by the following equation:

$$F_{w,Rd} = af_u / \sqrt{3}\beta_w \gamma_{M2} \tag{6.5}$$

where a = the effective throat thickness of a fillet weld; f_u = the nominal ultimate tensile strength of the weaker of the two parts joined; β_w = the appropriate correlation factor (taken from Table 4.1 in EC3-1.8); and γ_{M2} = a partial safety factor. In this analysis, the partial safety factor is taken as 1.0 instead of the 1.25 recommended for design, and the maximum displacement at failure of the

connections is assumed to be 20% of the effective throat thickness (about 0.85 mm). This assumption adopted for the fracture (or failure) displacements is based on the experimental work of Kanvinde et al. (2008) on fillet welds. In his cruciform weld tests, the main variables of root notch length, filler metal and weld size have been investigated throughout the programme. The important finding within these parameters is that variation of the root notch length does not have a detrimental effect on the strength of the welds. Nevertheless, the experimental results also indicate that electrode classifications have an influence on the fracture displacements of fillet welds. In Kanvinde's research, two classifications of weld electrodes were tested, namely E70T7 and E70T7-K2, and all welding was performed using the flux cored arc welding (FCAW) process, using a standard weld procedure. In general, the E70T7-K2 weld electrodes produced fillet welds with higher fracture displacements in the experimental tests. The maximum and minimum weld fracture displacements ($\Delta_{fracture}^{Test}$) are reported (Kanvinde et al., 2008) as 1.93 mm and 0.71 mm respectively. So assuming the fracture deformation of the weld component as 0.85 mm is reasonable in this study. Therefore, the load-deformation response shown in Fig. 6.6 may be used for description of the weld component:

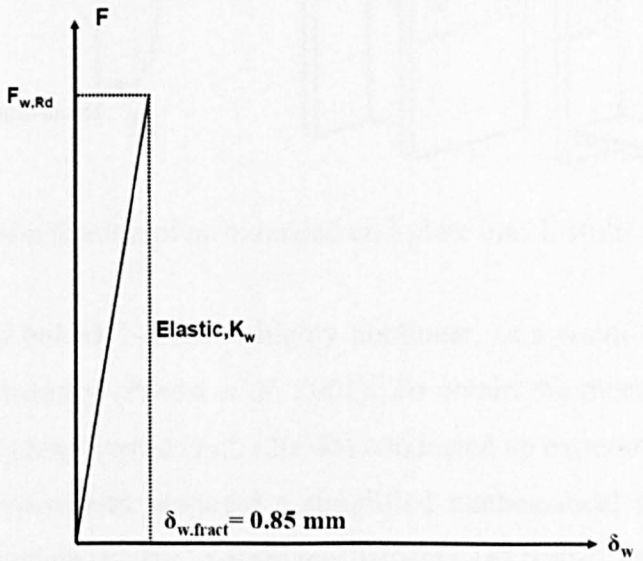

Figure 6.6: The mechanical response of a fillet weld

In addition, the failure displacement for weld components is assumed to be unaffected by increasing or decreasing temperatures, namely 20% of the effective throat thickness (about 0.85 mm). The reduction factors for carbon steel cannot be used for estimating the ultimate tensile strength of a weld in fire, as fillet welds lose

strength more rapidly than carbon steel as temperatures increase. The corresponding strength reduction factor, as recommended in EC3 1-2, is shown in Fig. 6.5.

6.3.1.3 End-plate behaviour and T-stub

When load is applied to an end-plate connection, rotation of the beam under gravity loads can cause plastic deformation at the top of the end-plate and local separation from the column face. The end-plate may be considered to act as an assembly of T-stub elements, where the flange of the T-stub represents the end-plate, and the stem simulates the beam web (Coelho *et al.*, 2004; Spyrou *et al.*, 2004b; Al-Jabri *et al.*, 2005; and Block, 2006). Fig. 6.7 shows the idealisation of the end-plate connection into T-Stubs within the tension zone for an extended end-plate connection.

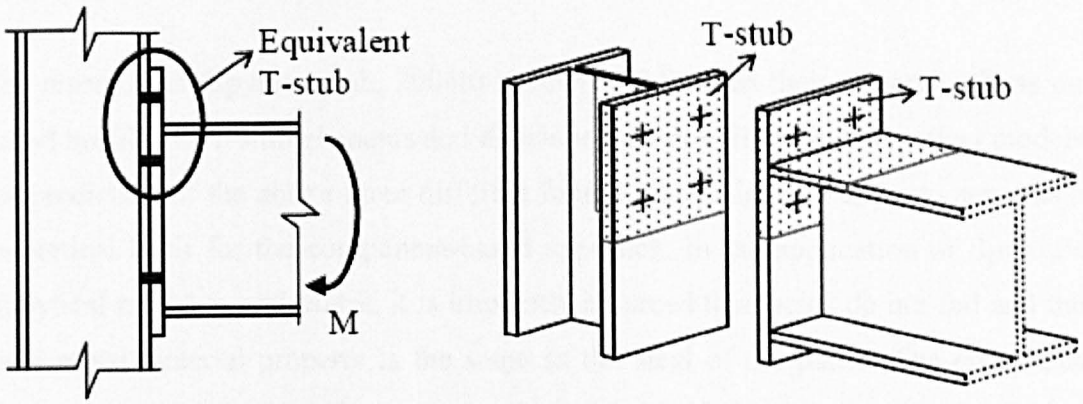

Figure 6.7: Idealisation of an extended end-plate into T-stubs (Coelho, 2004)

The behaviour of bolted T-stubs is highly nonlinear, as a result of mechanical and geometrical nonlinearity (Piluso *et al,* 2001). To obtain the mechanical response at elevated temperatures, Spyrou *et al.* (2004b) conducted an experimental investigation of T-stubs in tension, and proposed a simplified mathematical model. This model included three possible 'plastic' failure mechanisms: (a) type-1: complete yielding of the flange, with the development of four plastic hinges (double curvature bending), (b) type-2: partial yielding of the flange with bolt "plastic" failure, and the development of two plastic hinges at the toe of fillet welds (single curvature bending) and (c) type-3: bolt "plastic" failure without yielding of the flanges, shown as Fig. 6.8.

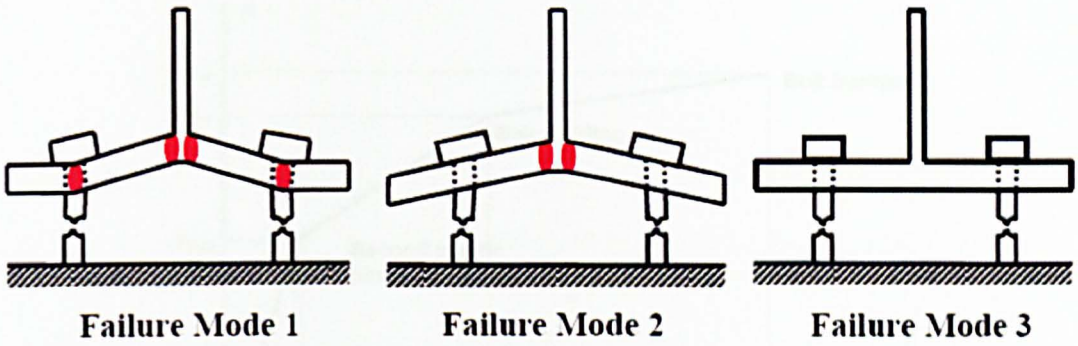

Figure 6.8: Failure mechanism of T-Stubs (Spyrou, et al., 2004b)

The experiments showed that most of the partial depth end-plates or T-stubs failed by the type-1 failure mechanism. This failure mechanism provides the end-plate connections/T-stubs with the maximum deformation under the loading conditions. It is expected for steel connections in practice to perform in this ductile failure manner, which is also what structural engineers attempt to achieve in design.

The researchers (Spyrou et al., 2004b) at Sheffield focused their research efforts on rolled profiles as T-stub elements and developed the simplified mathematical models for prediction of the above three different failure mechanisms in order to serve as a theoretical basis for the component-based approach. In the application of Spyrou's analytical model to end-plates, it is implicitly assumed that welds do not fail and the weld metal material property is the same as the steel of the plates. The end-plates (flanges in the T-stub) behave in an elastic-plastic fashion and strain hardening effects have been included (1.5% of the flange elastic Young's Modulus). The bolt behaviour has already been discussed. Therefore, the T-stub load-deformation response may be represented by a piecewise linear curve, as shown in Fig. 6.9. The first plastic hinge is commonly formed in the middle of the T-stub assembly, due to reaching the maximum bending moment first, and followed by the formation of the second plastic hinge at the bolt line. The ultimate failure of a T-stub is controlled by the yielding and fracture of bolts. Further details of the equations to evaluate the displacements and forces of T-stubs have been well documented by Spyrou *et al.* (2004b) and therefore will not be repeated here. The mathematical models for the other failure modes have also been formulated and validated in Spyrou's thesis.

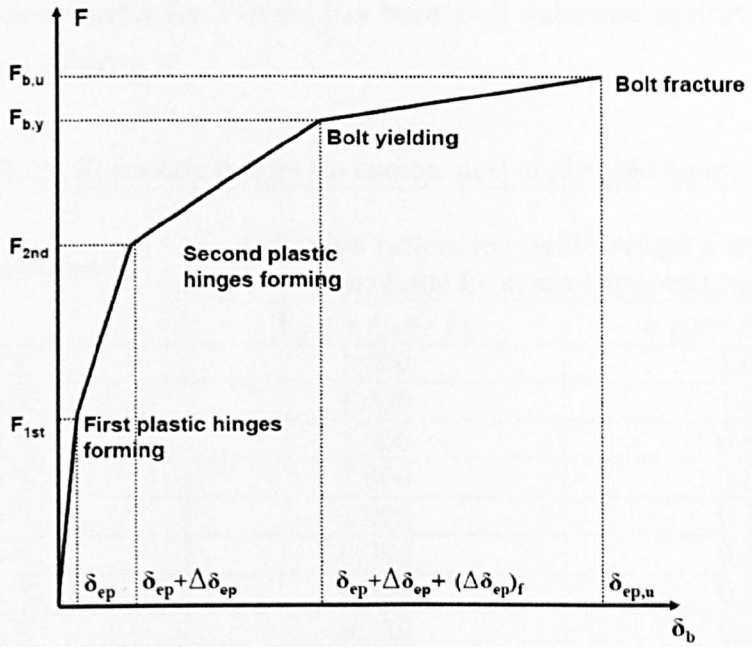

Figure 6.9: The mechanical response of a single T-stub

Spyrou applied these mathematical models into the component-based approach to explain the behaviour of steel T-Stubs at both ambient and elevated temperatures. It is well known that strength and Young's modulus of steel weakens with increasing temperatures. Therefore, in order to simulate the end-plate performance in fire using a T-stub model, the variation of yield strength and Young's modulus for bolts and structural steel needs to be taken into account. In the previous sections, the performance of structural bolts in fire and the simplified analytical model of these bolts for use in a component-based model have been discussed. Herein, the researcher only takes into account the material behaviour of structural steel in fire. According to design codes, the stress-strain relationship of structural steel may be approximated to a bi-linear relationship with a distinct yield plateau at ambient temperature. The yield strength and Young's modulus of the steel may be easily determined in this case. However, at elevated temperatures, the stress-strain curves degrade and lose the bi-linear form, making it difficult to define the exact yield point and elastic modulus (Spyrou *et al.*, 2004b). To overcome this problem, design codes adopt suitable strain limits such as 0.5%, 1.5% and 2%, with the corresponding stress representing the reduced strength. Table 6.1 shows the strength reduction factors (SRF) for carbon steel (S275) at 2% strain and the elastic modulus reduction factors, taken from EC3: Part 1-2. These SRF values are applied in the T-stub mathematical model at elevated temperatures to simulate the behaviour of the T-stub assemblies.

The mathematical model for T-stubs has been well validated against experimental results by Spyrou (2002).

Table 6.1: Reduction factors for carbon steel at elevated temperatures

Steel Temperature θa	Reduction factors for yield strength fy and Young's modulus Es at steel temperature θa	
	$k_{y,\theta}=f_{y,\theta}/f_y$	$k_{E,\theta}=E_{s,\theta}/E_s$
20 °C	1.000	1.000
100 °C	1.000	1.000
200 °C	1.000	0.900
300 °C	1.000	0.800
400 °C	1.000	0.700
500 °C	0.780	0.600
600 °C	0.470	0.310
700 °C	0.230	0.130
800 °C	0.110	0.090
900 °C	0.060	0.0675
1000 °C	0.040	0.0450
1100 °C	0.020	0.0225
1200 °C	0.000	0.000

Most of the T-stubs tested by Spyrou failed by tension fracture of the bolts after complete yielding of the T-stub flange. However, Coelho and his co-researchers (2004) carried out some experimental tests on T-stub elements made up of welded plates. They found that some of the specimens showed early damage of the plate material near the weld toe due to the effect of the welding consumable. The deformation capacity of the T-stub element, made up of welded plates, primarily depends on the plate/bolt strength ratio and the weld resistance, which is associated with the consumable electrode type and properties. When dealing with the component-based model, the welded T-stub element may be represented as three individual linear or nonlinear components: bolt component, weld component and T-stub component (without welding). Bolts and welds are classified as brittle components because of the limited deformation afforded to the deformation of a steel connection. But, as explained in Chapter 5, the ultimate capacities of these two components may have an influence on the elongation of each bolt row of the partial depth end-plate connection. The overall deformation of a connection primarily relies on the failure load of the weakest component and the maximum extension of the ductile components under this failure load. Brittle components like bolts and welds

may be the weakest components in a connection under fire conditions, and the failure of bolts and welds may affect the connection performance in fire. Therefore, it is reasonable to have these three components (bolts, welds and T-stubs) to represent the behaviour of each bolt row in a partial depth end-plate connection.

6.3.2 Compression zone components

As previously mentioned, flexible end-plate connections first rotate about the lower edge of the end-plate until the beam lower flange contacts the column face. In the first rotation stage, the column web is subjected to a direct compression force from the bottom edge of the end-plate pushing into the column face. In the further rotation stage the compressive force at the lower edge of the end-plate reduces as the contact force at the beam flange to column face increases. As the tensile forces in the T-stub are now acting at an increased lever arm, the moment resistance and rotational capacity increase.

For column sections with stocky webs, the failure of the compression zone is governed by yielding (crushing) of the web and the formation of a plastic hinge mechanism in the column flanges (Block, 2006, and Spyrou, 2002). For more slender webs, the behaviour of the compression zone is governed by plastic or inelastic buckling of the column web. For very slender webs, failure may be by elastic buckling or web crippling - a local instability phenomenon (Block,2006). For practical column sections the most likely form of failure is web crushing (Spyrou, 2002).

In order to simulate such a complicated alternation of compression forces, the authors have introduced two spring elements into the component model: one spring represents the contact of the lower edge of the end-plate and the column face, and the other simulates the contact between the beam bottom flange and the column. Block (2006) discusses in detail a number of analytical approaches for evaluating the compressive force of the compression zone. The analytical approach by Lagerqvist and Johansson (1995; 1996) has been recommended, as its mechanics are transparent and it also includes the associated plastic hinge mechanism developed in the column

flange as the web collapses. More importantly this approach can be extended to elevated-temperature conditions. The details and equations of this approach have been well documented by Block (2006).

The elastic, or initial stiffness, is required to describe a force-displacement curve for the compression zone. A comparative investigation by Aribert *et al.* (2002) of six design approaches to determine the initial stiffness suggested two alternatives:

$$k = 0.45E\sqrt{\frac{b_{fc}t_{fc}^3 t_{wc}}{d_{wc}}} \tag{6.6}$$

or

$$k = 0.95E\sqrt{\frac{b_{fc}t_{fc}^3 t_{wc}^2}{b_{eff}d_{wc}}} \tag{6.7}$$

Where b_{eff} is the effective length given by Eq. 6.8; b_{fc} is the width of the column flange; t_{fc} is the thickness of the column flange; t_{wc} is the thickness of the column web and d_{wc} is the clear depth of the column web (the distance between the root radii).

$$b_{eff} = t_{fb} + a_f\sqrt{2} + t_p + 5(t_{fc} + s) + \min(u; a_f\sqrt{2} + t_p) \tag{6.8}$$

Where t_{fb} is the thickness of the beam flange in compression; a_f is the weld thickness between the beam flange and the end-plate; u is the distance between the beam flange and the edge of the end-plate and t_p is the thickness of the end-plate.

Based on a parametric study, Block (2002 and 2004b) derived an empirical equation for the deformation capacity (ultimate displacement) of the column web, δ_u given by:

$$\delta_u = \frac{l_y t_{wc}^2}{2b_{fc}t_{fc}}\sqrt{\frac{t_{wc}d_{wc}}{t_{fc}c}}\chi \tag{6.9}$$

In the above equation, the slenderness parameter χ (Lagerqvist and Johansson, 1995 and 1996) has been introduced to increase the deformation capacity for stocky webs and reduce it for slender webs. l_y is the yielded length of the web (Lagerqvist and Johansson, 1996); c is the load width calculated by using a dispersion angle of 45° in

the end-plate; therefore, $c = t_p$ in the first load case, as shown in Fig. 6.10 (a). Once the beam flange contacts the column flange, it is assumed that half of the beam flange thickness is in contact with the column face, as shown in Fig. 6.10 (b), so $c = t_{bf}/2$. As a further simplification, it is assumed that the compressive resistance of the column web is the same for both these cases.

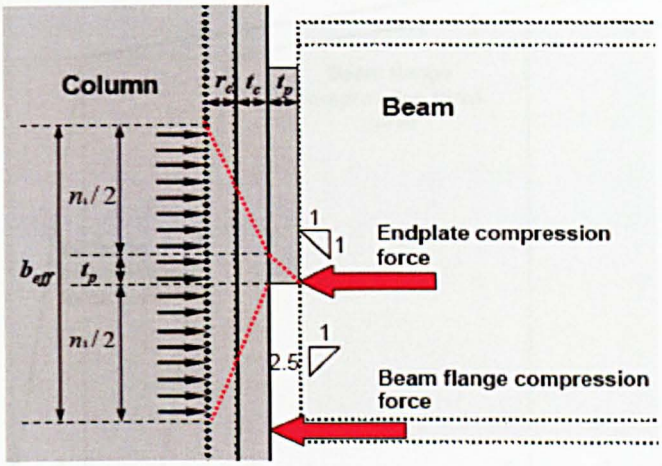

(a) End-plate compression force

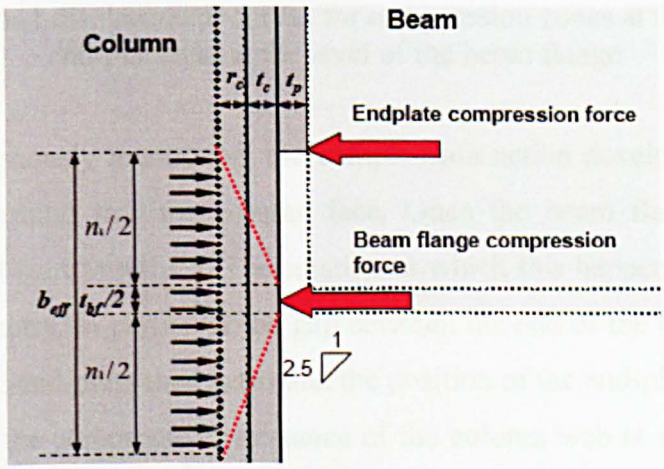

(b) Beam flange compression force

Figure 6.10: Two different loading cases for the compression zone (a) End-plate compression force (b) Beam flange compression force

As most rolled column sections have rather stocky webs, yielding of the web accompanied by formation of plastic hinges in the column flange governs the form of failure. As a consequence, the shape of the force–displacement curve is similar to the steel stress–strain curve. Block (2006) modified the force-displacement curve for the

compression zone to account for the effects of temperature by using an approach similar to that for calculating the stress-strain curve for mild steel at elevated temperatures, given in European code EC3 1-2 (EC3, 2005b). As a further simplification, a bi-linear force-displacement relationship was assumed for the compression zone at both normal and elevated temperatures, as shown in Fig. 6.11.

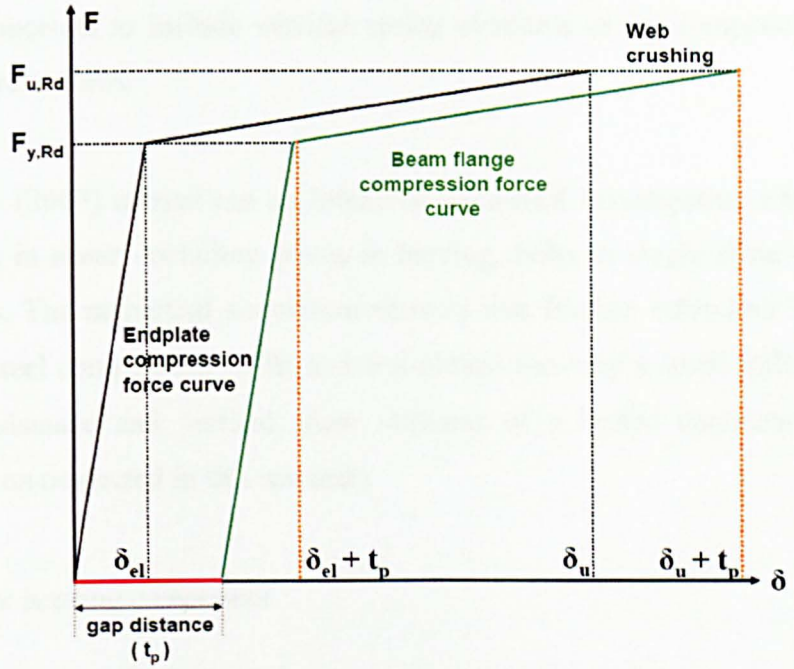

Figure 6.11: Load-displacement curves for compression zones at the bottom of the end-plate and at the level of the beam flange

However, as previously mentioned, the compression action develops as a result of the end-plate pushing into the column face. Once the beam flange contacts the column, this will start to reduce. The rotation at which this happens depends on the connection geometry, in particular the gap between the end of the beam and column face (equal to the end-plate thickness) and the position of the end-plate relative to the beam depth. As the compressive resistance of the column web is assumed to be the same in these two cases, the load–displacement curves are as illustrated in Fig. 6.11. The gap distance is nominally equal to the thickness of the end-plate, but in practice might be smaller due to imperfections. The gap distance in the specimens tested in the current study were therefore measured and found to vary between 7 mm and 8 mm. The empirical value used in the component-based model was therefore taken as 7 mm, a little smaller than the nominal gap of 8 mm. Note, the compression components in the model cannot resist the tensile forces; therefore, the tensile behaviour is assumed to be zero for these two compressive springs.

6.3.3 Vertical components for shear

Component modelling of connections has tended to concentrate on predicting the moment capacity and rotational behaviour. However, in practice simple connections are designed to resist shear forces, and may also be subjected to tensile forces. It is therefore important to include vertical spring elements in the component model in order to represent this.

Sarraj *et al.* (2007) carried out an intensive numerical investigation into the active components in shear; including plates in bearing, bolts in single shear and friction components. The numerical simulation showed that friction behaviour between the individual steel components (bolts and end-plates) has only a small influence on the ultimate resistance and vertical shear stiffness of a bolted connection, and has therefore been neglected in this research.

6.3.3.1 Plate bearing component

The plate bearing component characterizes the deformation behaviour of the holes as the bolts bear against them. Rex and Easterling (2003) carried out 48 tests on a single bolt bearing onto a single plate. They used a non-linear equation (Richard, 1991) to approximate the load-displacement behaviour for a single plate bearing against a single bolt. Sarraj (2007) further investigated the influence of different geometrical parameters, including end distance, bolt size, plate width and plate thickness, on the load-displacement characteristics and modified the equations to give:

$$\frac{F}{F_{b,Rd}} = \frac{\psi\bar{\Delta}}{(1+\sqrt{\bar{\Delta}})^2} - \Phi\bar{\Delta} \tag{6.10}$$

$$\bar{\Delta} = \Delta\beta K_i / F_{b,Rd} \tag{6.11}$$

$$F_{b,Rd} = \frac{e_2}{d_b} \times f_u \times d_b \times t \tag{6.12}$$

or

$$F_{b,Rd} = 0.92\frac{e_2}{d_b} \times f_u \times d_b \times t \tag{6.13}$$

Where Ψ and Φ are curve fitting parameters; $\bar{\Delta}$ is the normalized deformation; Δ is the hole elongation [mm]; β is a steel correction factor, for typical steels taken as unity; F is the applied force [N] and K_i is the initial stiffness [N/mm]; e_2 is the end distance (centre of the hole to the edge of the plate in the direction of loading); d_b is the nominal diameter of the bolt.

$$\frac{1}{K_i} = \frac{1}{K_{br}} + \frac{1}{K_b} + \frac{1}{K_v} \tag{6.14}$$

Bearing stiffness $$K_{br} = 120 t_p f_y (d_b/25.4)^{0.8} \tag{6.15}$$

Bending stiffness $$K_b = 32 E t_p (e_2/d_b - 0.5)^3 \tag{6.16}$$

Shearing stiffness $$K_v = 6.67 G t_p (e_2/d_b - 0.5) \tag{6.17}$$

Considering the influence of end distance (e_2), Sarraj (2007) recommended the bearing resistance ($F_{b,Rd}$) in small end distance cases ($e_2 \leq 2d_b$) should be determined from Eq. (6.11) for M20 bolts, while for large end distance cases ($e_2 \geq 3d_b$) Eq. (6.12) should be applied. In vertical shear, it may be assumed that the tensile and compressive load-displacement characteristics are the same as the end distance (ie along the column length) is very large in both cases.

6.3.3.2 Bolt in single shear

Sarraj (2007) evaluated the load-displacement relationship for a bolt in single shear and presented a modified Ramberg – Osgood expression for describing the single shear behaviour of bolts.

$$\Delta = \frac{F}{K_{v,b}} + \Omega \left[\frac{F}{F_{v,Rd}}\right]^n \tag{6.18}$$

where

Δ is relative bolt deflection [mm];

F is the corresponding level of shear force [N]

$K_{v,b}$ is the bolt shearing stiffness [N/mm]

$F_{v,Rd}$ is the bolt shearing strength (Equ. 6.18) [N]

Where Ψ and Φ are curve fitting parameters; $\overline{\Delta}$ is the normalized deformation; Δ is the hole elongation [mm]; β is a steel correction factor, for typical steels taken as unity; $\boldsymbol{F}$ is the applied force [N] and $\boldsymbol{K_i}$ is the initial stiffness [N/mm]; e_2 is the end distance (centre of the hole to the edge of the plate in the direction of loading); d_b is the nominal diameter of the bolt.

$$\frac{1}{K_i} = \frac{1}{K_{br}} + \frac{1}{K_b} + \frac{1}{K_v} \tag{6.14}$$

Bearing stiffness $$K_{br} = 120 t_p f_y (d_b / 25.4)^{0.8} \tag{6.15}$$

Bending stiffness $$K_b = 32 E t_p (e_2 / d_b - 0.5)^3 \tag{6.16}$$

Shearing stiffness $$K_V = 6.67 G t_p (e_2 / d_b - 0.5) \tag{6.17}$$

Considering the influence of end distance (e_2), Sarraj (2007) recommended the bearing resistance ($F_{b,Rd}$) in small end distance cases ($e_2 \leq 2d_b$) should be determined from Eq. (6.11) for M20 bolts, while for large end distance cases ($e_2 \geq 3d_b$) Eq. (6.12) should be applied. In vertical shear, it may be assumed that the tensile and compressive load-displacement characteristics are the same as the end distance (ie along the column length) is very large in both cases.

6.3.3.2 Bolt in single shear

Sarraj (2007) evaluated the load-displacement relationship for a bolt in single shear and presented a modified Ramberg – Osgood expression for describing the single shear behaviour of bolts.

$$\Delta = \frac{F}{K_{v,b}} + \Omega \left[\frac{F}{F_{v,Rd}} \right]^n \tag{6.18}$$

where

Δ is relative bolt deflection [mm];

F is the corresponding level of shear force [N]

$K_{v,b}$ is the bolt shearing stiffness [N/mm]

$F_{v,Rd}$ is the bolt shearing strength (Equ. 6.18) [N]

$$F_{v.Rd} = R_{f,v,b} \times f_{u,b} \times A \quad (6.19)$$

$R_{f,v,b}$ is the strength reduction factor for bolt in shear (20°C, $R_{f,v,b} = 0.58$)

n is a parameter defining the curve sharpness for curve fitting

Ω is a curve fitting parameter

Regarding the bolt shear stiffness, it can be described by the following expression:

$$K_{v,b} = \frac{kAE_b}{2(1+v)d_b} \quad (6.20)$$

E_b is the elastic modulus

k is a shear correction factor for consideration of the error in shear strain energy caused by assuming a constant shear strain through the bolt section, as opposed to the classical parabolic distribution. The shear correction factor depends on the cross-sectional shape and material properties, and it has been found that k = 0.15 is a suitable value (Hayes, 2003; Madabhusi-Raman and Davalos, 1996; Sarraj, 2007).

To include the influence of temperature into these two mathematical models, Sarraj *et al.* (2007) carried out a series of numerical studies to determine appropriate curve fitting parameters for both ambient and elevated temperatures.

6.4 Component-based Model Assembly

The component-based model for the end-plate connection may be constructed as an assembly of spring elements in the tension, compression and shear zones, as shown in Fig. 6.3. There are a number of fundamental assumptions implicit in this new model. The first is that the behaviour of each spring element is assumed to be multi-linearly elastic throughout the analysis. Secondly, the considerable compressive axial forces which develop in connections in a real steel frame during the heating phase, are ignored, as is the thermal expansion of the connection components. Finally, as mentioned previously, it is assumed that the compressive resistance is the same for the two different compression loading cases (end-plate in contact with column face and beam bottom flange contacting with column face, as shown in Fig. 6.10).

6.5 Validation of a Component-based Model

The component-based model has been verified against experimental data at ambient and elevated temperatures using the results of the connection tests carried out in Chapter 5 and published by Yu et al. (2009a) to determine the resistance and rotational capacities of flexible end-plates. In the experimental programme, twelve tests have been conducted for flexible end-plate connections, including three tests at ambient temperatures and the rest of the tests at high temperatures. The rotation of the connection was recorded by inclinometers (angular transducers) for the first three tests at ambient temperatures, and the applied external loads were captured directly by strain gauges on the loading system, shown in the previous chapter. At elevated temperatures, using an image-acquisition system (Spyrou and Davison, 2001), the rotation of the connections was recorded through a small rectangular glass viewing panel in the door using a digital camera. The external load applied to the connection was measured via strain gauged loading bars.

As noted earlier, the failure mode was fracture of the end-plates close to the toe of the weld. To capture this brittle failure behaviour, a weld spring element, with an assumed maximum failure displacement equal to about 20% of the effective throat thickness (0.85 mm), was introduced into the component-based model. This was then used to compare with the experimental results, as shown in Figs. 6.12 and 6.13. Considering the maximum resistance of the three components (welds, bolts and end-plates) in the tension zone (Table 6.2), the weld component clearly provides the smallest tensile resistance, both at ambient and elevated temperatures, indicating that it is this component which is likely to govern the ultimate ductility and resistance of steel connections.

Table 6.2: Comparison of maximum resistance of three components in the tension zone

Temperature	Components in the tension zone (kN)		
	Welds	Bolts	End-plates
20 °C	183.567	352.8	281.053
450 °C	137.951	233.73	160.957
550 °C	92.243	135.828	109.331
650 °C	46.626	56.448	63.872

For the three tests conducted at room temperature, the load was applied at angles of 35°, 45° and 55° to induce different combinations of vertical shear, axial tension and moment. The output of the component model was compared with the experimental results with very good agreement between the two for all stages of behaviour, as shown in Fig. 6.12. The transition in behaviour when the beam flange contacts the column is clearly seen in the change in force-rotation relationship, and this is modelled very well by the component method.

A similar comparison was made for the elevated temperature tests (Fig. 6.13). In contrast to the experimental evidence at ambient temperature, the rotational capacity was limited by the rupture of the end-plates before the beam flange contacted with the column. The transition in behaviour from elastic to plastic is therefore simpler, with no intermediate increase in rotational stiffness associated with the contact. This is evident in the experimental results and the component model also predicts such behaviour.

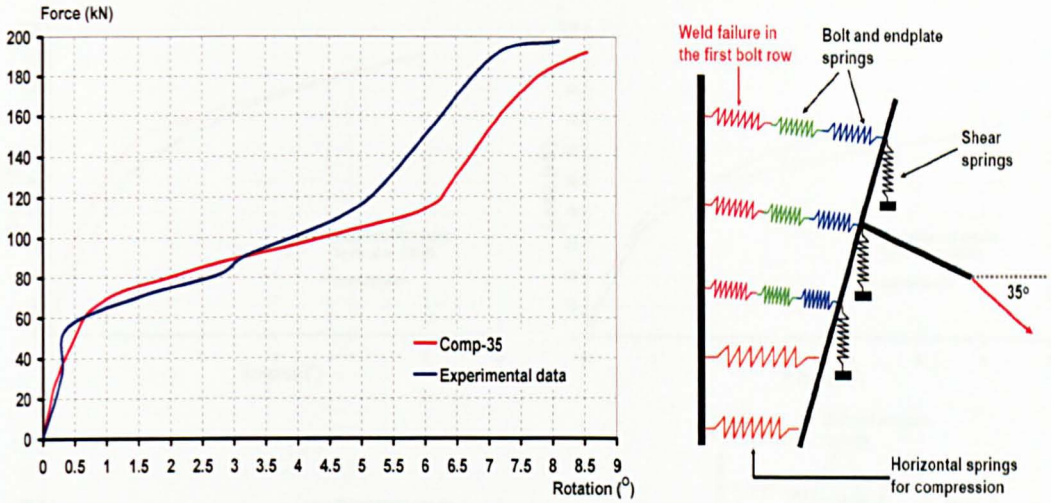

(a) 35°

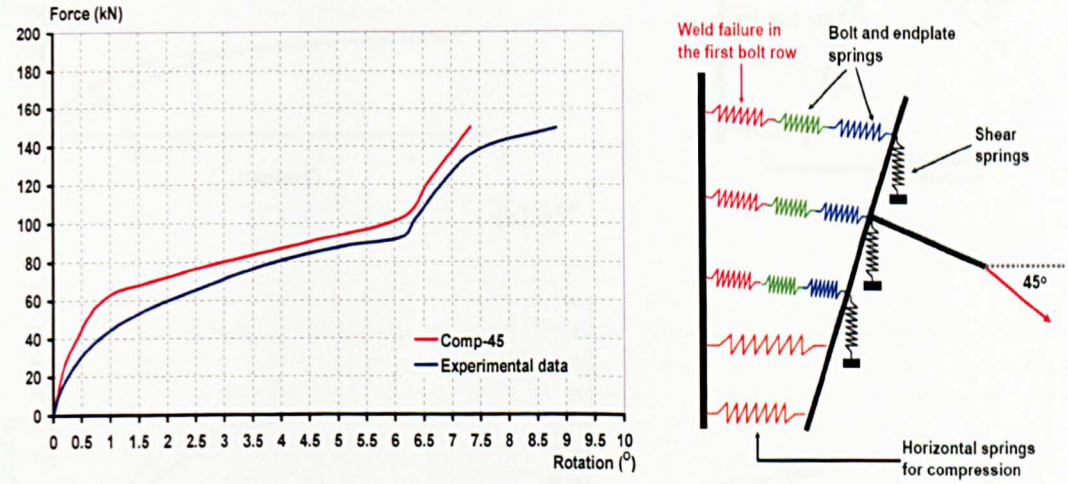

(b) 45°

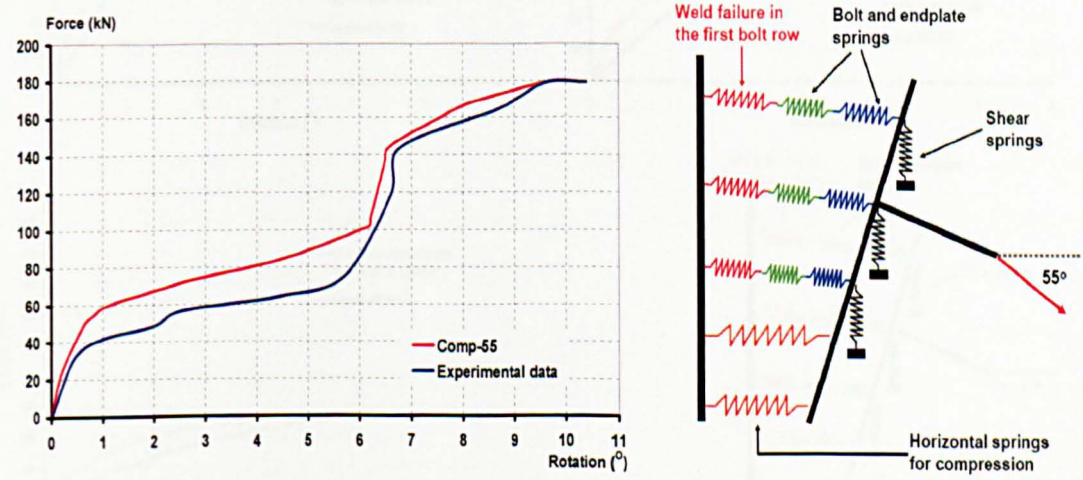

(c) 55°

Figure 6.12: Validation of the component models against experimental test results (a) 35° (b) 45° (c) 55°

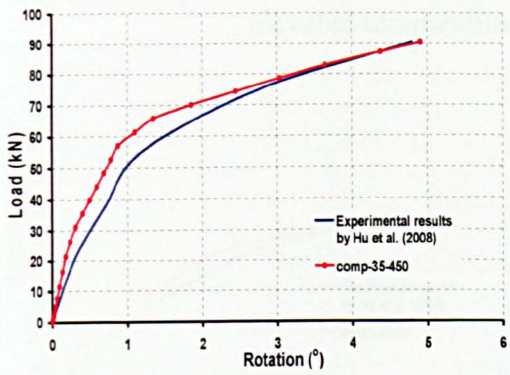
Load (kN)
Rotation (°)
Experimental results by Hu et al. (2008)
comp-35-450

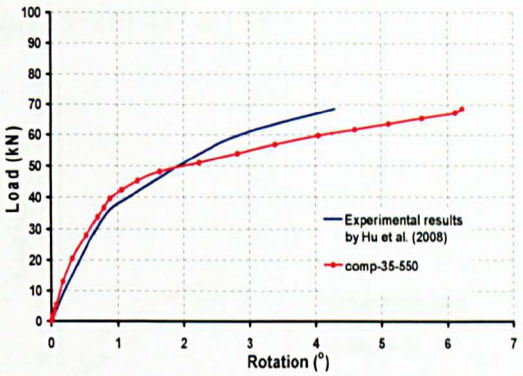
Load (kN)
Rotation (°)
Experimental results by Hu et al. (2008)
comp-35-550

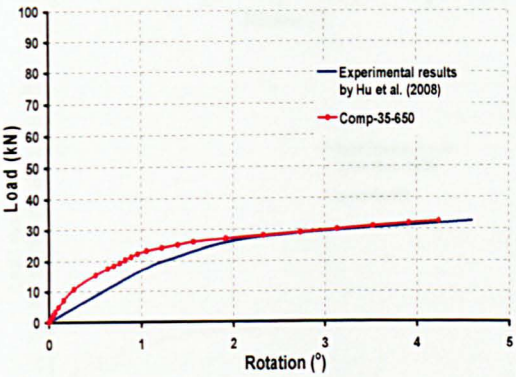
Load (kN)
Rotation (°)
Experimental results by Hu et al. (2008)
Comp-35-650

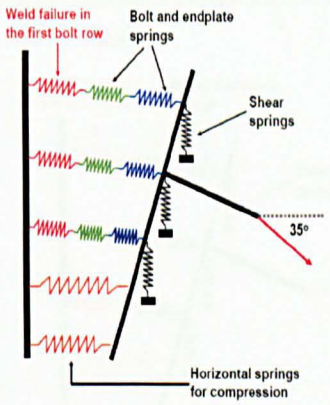
Weld failure in the first bolt row
Bolt and endplate springs
Shear springs
35°
Horizontal springs for compression

(a) 35°

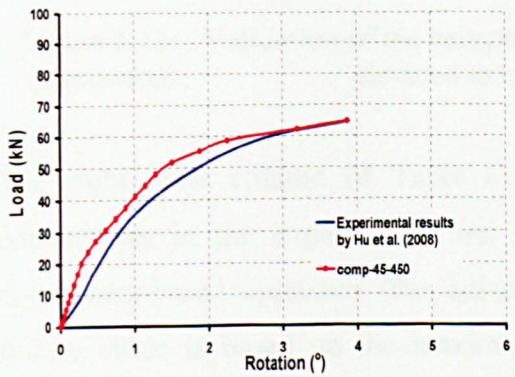
Load (kN)
Rotation (°)
Experimental results by Hu et al. (2008)
comp-45-450

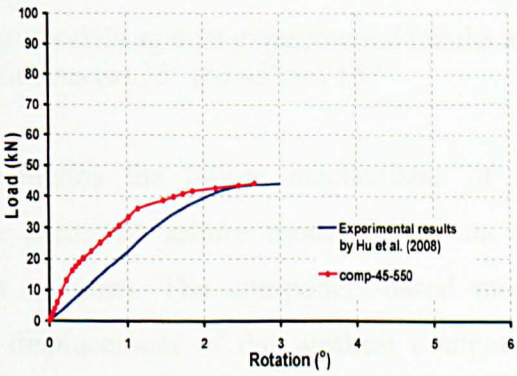
Load (kN)
Rotation (°)
Experimental results by Hu et al. (2008)
comp-45-550

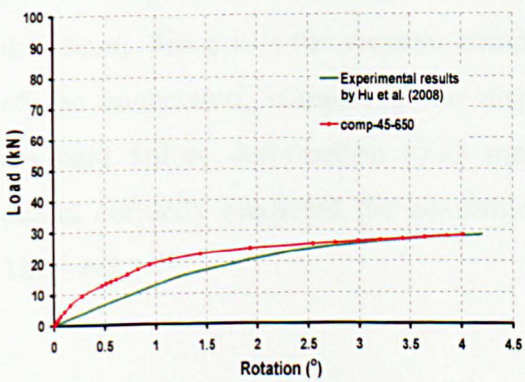
Load (kN)
Rotation (°)
Experimental results by Hu et al. (2008)
comp-45-650

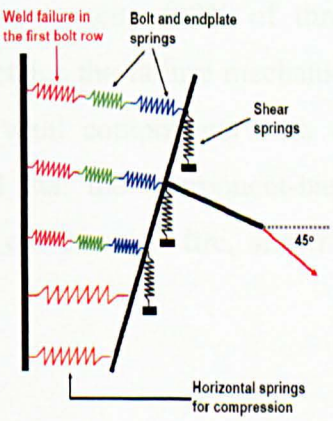
Weld failure in the first bolt row
Bolt and endplate springs
Shear springs
45°
Horizontal springs for compression

(b) 45°

Figure 6.13: Validation of the component models against experimental results at elevated temperatures (a) 35° (b) 45° (c) 55 °

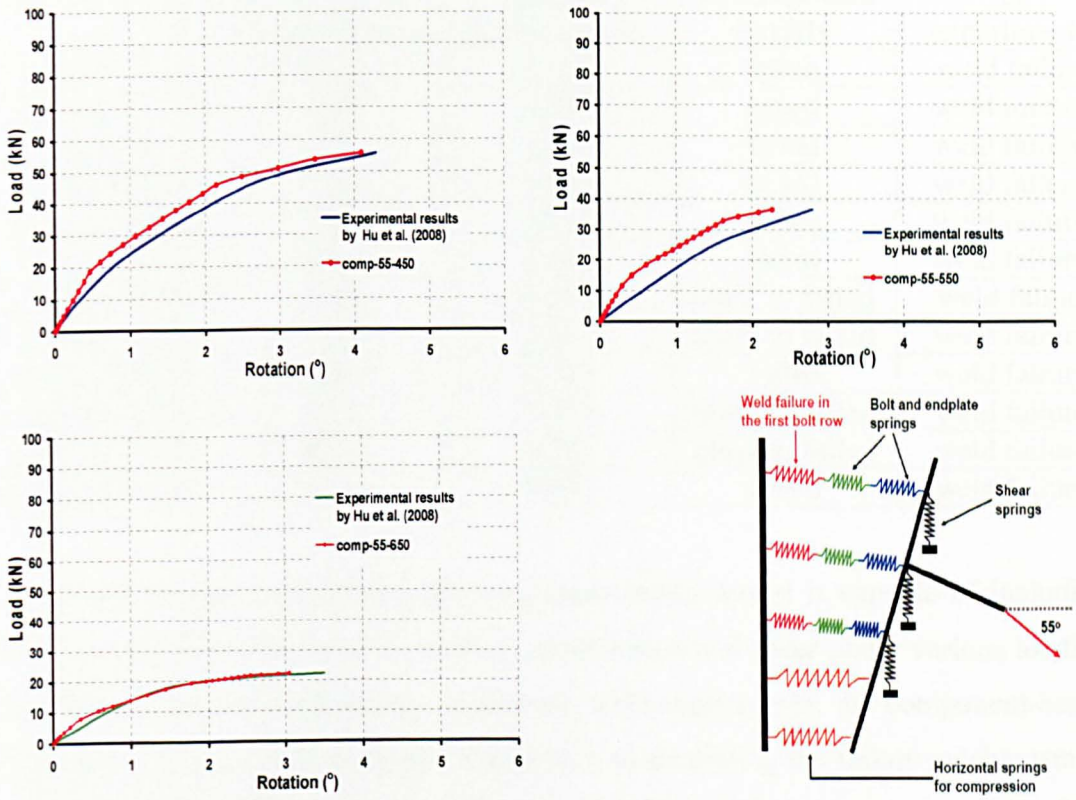

(c) 55°

Figure 6.13: (continued) Validation of the component models against experimental results at elevated temperatures (a) 35° (b) 45° (c) 55 °

The right hand column of Table 6.3 contains the failure mechanisms of the connections in the experiments and the predicted failure modes based on the component-based approach (the adjacent column). The component-based model failure mode is based on the maximum displacement of the weakest component (weld component) exceeding the assumed deformation capacity (20% of throat thickness). Since it is the weakest component which dictates the failure mechanism of the connection, comparing the displacements for weld components with the assumed failure deformation (0.85 mm) demonstrated that the component-based model correctly predicted the connection performance of failure in fire, shown in Table 6.3.

Table 6.3: Maximum displacements of the weld component

Specimen No	Weld components (mm)		Failure mechanism	
	Assumed max displacements	Maximum displacements	for component models	for experiments
Comp-35	0.85	1.196	failed	weld failure
Comp-45	0.85	0.954	failed	weld failure
Comp-55	0.85	3.970	failed	weld failure
Comp-35-450	0.85	0.875	failed	weld failure
Comp-35-550	0.85	0.958	failed	weld failure
Comp-35-650	0.85	0.952	failed	weld failure
Comp-45-450	0.85	0.793	close to failed	weld failure
Comp-45-550	0.85	0.815	close to failed	weld failure
Comp-45-650	0.85	0.945	failed	weld failure
Comp-55-450	0.85	0.773	close to failed	weld failure
Comp-55-550	0.85	0.796	close to failed	weld failure
Comp-55-650	0.85	0.880	failed	weld failure

From the previous validation, the component-based model is capable of including the connection performance in tension, compression and shear under various loading conditions. Also looking at the comparison with experiments, the component-based simulation already demonstrated the potential of predicting the failure mechanism of steel connections under fire conditions, provided that all the active components of the connection had already been assembled in the model. In this series of tests, the connection failure is governed by the rupture of end-plates around the welds. The question which may concern engineers is whether such a connection type is able to be more ductile under fire conditions.

The component based approach provides useful insight into how to design more robust steel connections. As the failure of the component model is dominated by the weakest element, the basic design philosophy is to set the brittle elements to be the strongest in the model and the connection failure will then be controlled by the ductile elements in the simulation. For example, in the flexible end-plate connections, the typical failure mode is the rupture of the end-plates close to the toe of the welds and the component-based model also proved that the weld component is the weakest element in the connection. In the Green Book (SCI, 2002), the assumed failure mode for end-plate connections is formation of four plastic hinges in the bending plates. At ambient temperatures, this form of failure has already been proved in the experimental tests by Owen and Moore (1992). However, since the reduction

of weld strength is faster than the strength reduction of carbon steel in fire, shown in Fig. 6.5, most header plate connections failed with lack of deformation of the plates at high temperatures, which was found in the experimental tests. If engineers increased the strength and size of the welds in practice, the failure form of these connections might therefore be dominated by plastic deformation of end-plates under fire conditions. To design a more ductile or robust connection type at elevated temperatures, engineers should retain the mode of failure governed by the ductile connection components in the detailed design of steel connections. As stated earlier, the component-based approach is a good basis for engineering design, as it can help engineers to recognize the weakest components and the possible dominant failure mechanism in the initial design stage.

6.6 Conclusions and Recommendations

This chapter has presented a new component-based model for flexible end-plate connections at both ambient and elevated temperatures. The model comprises all the active components in the tension zone, in the compression zone and in the vertical shear direction, and is able to simulate the complex behaviour (shear, tension and rotation) of simple steel connections under various loading conditions. Validation of the model shows a very good correlation with experimental results at ambient and elevated temperatures. This approach is a much simpler alternative to finite element analysis, but provides a sufficiently accurate simulation, making it a good basis for a design tool.

Since all the research work discussed herein is based on the isolated connection tests under fire and the steady-state analysis, the component-based model presented in this paper is just workable under various loading conditions, lack of considering the heating and cooling issues. However, if looking at the connections in a steel frame, large compressive or tensile axial forces are commonly produced within the steel beams during the heating and cooling phases of a fire. This is caused by the restraint to thermal expansion of steel beams by the surrounding cold structure and in the later stage, as the temperatures become very high the beams sag and generate tensile force due to formation of catenary actions. Therefore, to progress the research, it is

recommended to programme this component-based connection model into a connection element, which may be incorporated into a finite element frame analysis programme.

CHAPTER 7

FINITE ELEMENT SIMULATION OF THE BEHAVIOUR OF SIMPLE END-PLATE CONNECTIONS IN FIRE*[2]

7.1 Introduction

Conducting fire tests on structures or isolated structural members is time-consuming, expensive, and poses the additional difficulties of recording movement and strain within a furnace. So the development of accurate predictive methods to simulate the behaviour of steel structures in fire has long been regarded as desirable (Wang, 2002). The ABAQUS program has been used to study the behaviour of steel and composite framed structures in fire by Corus Research (O'Callaghan and O'Connor, 2000; O'Connor and Martin, 1998) and Edinburgh University (Gillie, 1999; Gillie *et al.*, 2000). This finite element program shows the ability to simulate complex structural behaviour under fire conditions as comparisons with test results from the Cardington fire tests demonstrated. This commercial programme has a large library of finite elements to enable efficient and detailed modelling of many of the special features of structural behaviour in fire. The complex real phenomena such as local/distortional buckling, lateral torsional buckling, detailed connection modelling and membrane actions can be accounted for in a numerical fashion. Therefore, detailed finite element modelling of connections in fire provides a good opportunity for wider parametric investigations and eliminates the limitations associated with experiments (Sarraj, 2007), provided that the numerical models have been adequately validated against experimental data.

Initial attempts to simulate steel connections started with two dimensional models, owing to the limitations in computational resources both in terms of software and

[2] This chapter has been published as a conference paper (Hu, et al., 2008)

hardware. In a 2D model, each component of a connection can be represented by using shell or truss elements, and the interactions between these components are numerically simplified to avoid convergence difficulties in the numerical computation. Because of the rapid improvement in hardware and software, computers are now able to perform more detailed simulations for connections in 3D models. Krishnamurthy *et al.* (1976) and Kukreti *et al.* (1987) compared numerical results produced by two-dimensional and three-dimensional simulations, and found the three-dimensional numerical model to be more ductile than the two-dimensional counterpart, resulting in larger displacements and stresses. Vegte *et al.* (2002) believe that, since bolted steel connections are three-dimensional in nature, two-dimensional numerical models are therefore unable to represent the three-dimensional behaviour satisfactorily. Hence, a three-dimensional non-linear finite element analysis approach has been developed as an alternative method for the investigation of connection robustness in fire.

7.2 The Finite Element Model Description

Sherbourne and Bahaari (1994, 1997) developed a three-dimensional finite element model for simulating end-plate connections by using brick elements. The model was assumed to have a continuous connection between the nodes of the bolt head and nut, and the nodes of end-plates, and as a consequence, the relative motions between bolt, column flange and end-plates were numerically simplified. The bolt shank behaviour was represented using truss elements instead of brick elements which prevents the numerical model reproducing properly the bearing action between bolts and bolt holes, because the interface between the bolt shank and the hole boundary was neglected. Bursi and Jaspart (1997) presented a more realistic finite element model for T-stub connections. This numerical model is capable of simulating the complex interactions such as contact, friction, stick and slip conditions, stress concentrations and prying actions in a real connection. Bolts and end-plates in the simulation are represented as individual components using brick elements, and are no longer connected through common nodes, enabling relative movement between these components (Vegte, 2008). Although this numerical approach results in finite element simulations which are much more complicated and computationally

expensive in terms of time, it has nevertheless been adopted by many researchers owing to the improvement in numerical accuracy.

A three dimensional numerical model was created for a flexible end-plate connection, using the ABAQUS finite element code, in order to investigate its resistance and ductility at ambient and elevated temperatures. This model started with the creation of individual components such as bolts, end-plates, beams and columns, and then assembled these components into a connection, as shown in Fig. 7.1.

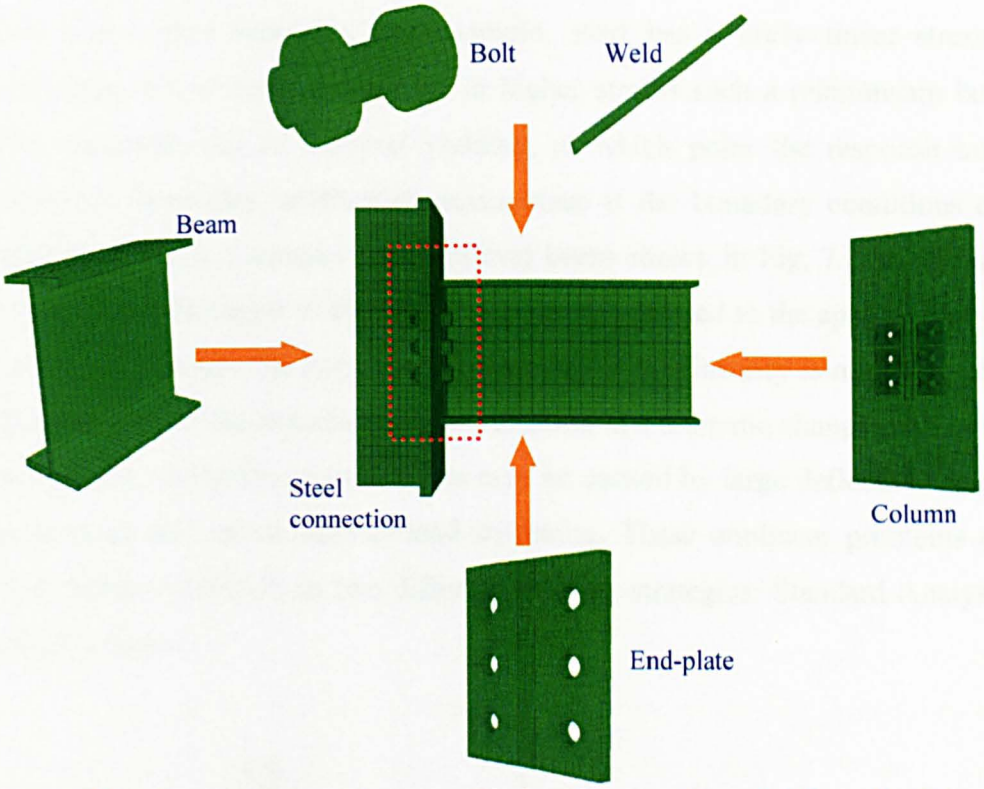

Figure 7.1: Components to be assembled to form a FE model for a flexible end-plate connection

All these components were modelled using eight-node continuum hexahedral brick elements. A small number of cohesive elements were used in the heat affected zone (HAZ) where the failure of end-plates was seen to occur. The brick element has the capability of representing large deformation, and geometric and material nonlinearity, whilst the traction separation law of cohesive elements is able to demonstrate the rupture of end-plates in a real connection. The contacts between bolts, end-plates and column flanges were simulated by surface-to-surface

formulations. In order to simulate this nonlinear performance, an intensive mapped mesh was made within the bolts and the vicinity of the bolt holes, shown in Fig. 7.1. The following discusses the details of how to create a FE model for a flexible end-plate connection.

7.2.1 Solution strategies in solving nonlinearity

In most nonlinear problems, there are three sources of nonlinearity in structural mechanics simulations: material nonlinearity, boundary nonlinearity and geometric nonlinearity (Abaqus, 2006). Material nonlinearity is commonly observable in most metals and rubber materials. For example, steel has a fairly linear stress/strain relationship at low strain values; but at higher strains such a relationship becomes highly nonlinear due to material yielding, at which point the response becomes irreversible. Boundary nonlinearity takes place if the boundary conditions change during the analysis. Consider the cantilever beam shown in Fig. 7.2 as an example, the vertical displacement of the beam tip is linearly related to the applied load before the beam tip contacts the stop. The third source of nonlinearity is related to changes in the geometry of the numerical model resulting in a dramatic change in the stiffness of this model during the analysis. This may be caused by large deflections/rotations, snap through and initial stresses/load stiffening. These nonlinear problems can be treated within ABAQUS in two different solution strategies: Standard Analysis and Explicit Solution.

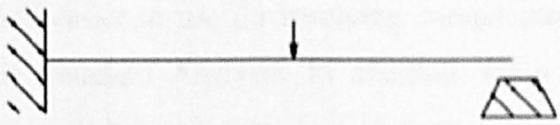

Figure 7.2: Cantilever beam hitting a stop (Abaqus, 2006)

The Standard Analysis in ABAQUS is implicitly based on static equilibrium (internal forces $\boldsymbol{I}$ and external forces $\boldsymbol{P}$ must balance each other), characterized by an assembly of a global stiffness matrix and the simultaneous solution of a set of linear or nonlinear equations (Vegte, 2008). The Newton-Raphson method is used to converge the solution at each time step along the force deflection curve. By default, this method adjusts the size of the time increments automatically during the analysis

(automatic incrementation control), and only the size of the first increment in each step needs to be specified for solving nonlinear problems. This default function is suitable for most nonlinear static analyses. However, the nonlinear static problems can be unstable, i.e. the tangent stiffness of a numerical model is close to zero or negative during the analysis. Such instabilities may be caused by local/global buckling or material softening under fire conditions. If the tangent stiffness is zero or negative the classical Newton-Raphson method is unable to achieve the convergence, so the standard analysis presents an automatic stabilization mechanism for unstable quasi-static problems through automatic addition of volume-proportional damping to the numerical model. The damping factors applied can be constant within a step or can vary over the course of a step, which is typically preferred for the adaptive approach. In addition, to avoid these unstable problems, the Riks method (Arc-Length algorithm) can be used to allow the load and displacement to vary throughout the time step (Abaqus, 2006). Nevertheless, for a numerical model with complicated contact interactions, these two solution algorithms are unlikely to produce an easy and smooth solution in the computation.

For complex contact problems and highly nonlinear quasi-static problems, the Explicit Solution is very efficient in solving certain classes of unstable static analyses. The Explicit Solution approach is a dynamic-based numerical procedure, originally developed to simulate high-speed impact events in which inertia plays a dominant role in the analysis. Achieving convergence is not needed in the simulation. This approach has proven to be valuable in dealing with unstable static problems and is much easier to use for resolving complicated contact problems in comparison with the Standard Analysis. In addition, for a very large numerical model, the explicit procedure requires less system resources than the implicit procedure (Abaqus, 2006). However, to achieve a realistic simulation for a static problem, the minimum stable time increment is usually quite small and hence most problems require a large number of increments.

Since a quasi-static event needs a long-time process, it is often computationally impractical to have the simulation in its natural time scale, which would require an excessive number of small time increments (Abaqus, 2006). Therefore, some special

considerations need to be taken in applying the explicit dynamic procedure to solve quasi-static problems. To achieve an economical solution, such an event must be accelerated in some way in the simulation; however, the arising problem is that inertial forces (dynamic effects) become more dominant as the event is accelerated and the issue of static equilibrium evolves into an issue of dynamic equilibrium. So the crucial point for a quasi-static simulation is to model the event in the shortest time period in which inertial forces remain insignificant. In order to achieve this, Vegte (2008) recommends researchers to monitor the various components of the energy balance throughout the loading process. The total energy in the system (E_{total}) remains constant during the explicit solution procedure. If a simulation is quasi-static, the work applied by the external forces (E_W) is nearly equal to the internal energy of the system (E_I), as shown in Fig.7.3. The viscously dissipated energy is generally small and the inertial forces are negligible in a quasi-static analysis due to the small velocity of the material in the model. As a general rule, the kinetic energy (E_{KE}) of the deforming material should not exceed a small fraction (typically 5% to 10%) of its internal energy throughout most of the process (Abaqus, 2006). In order to reduce the solution time in simulations, *mass scaling* (artificially increasing the mass to reduce inertial effects) is an alternative option to researchers, which enables an analysis to be performed economically without increasing the loading rate (Abaqus, 2006). This option is also used to deal with simulations involving a rate-dependent material or rate-dependent damping. In these simulations, increasing loading rate is not allowed in the analysis because material strain rate increases by the same factor as the loading rate. Therefore, mass scaling is the only option to achieve a quasi-static solution.

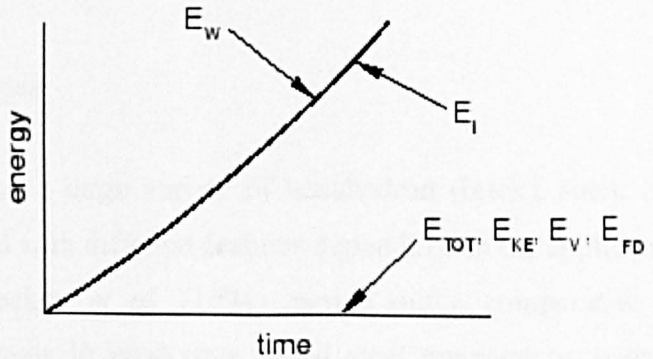

Figure 7.3: Energy balance in a quasi-static analysis (Abaqus, 2006)

For the Explicit Solution, the crucial consideration is the stability limit, which determines the maximum time increment used in a quasi-static analysis. The stability limit has a great effect on reliability and accuracy during the analysis. If the time increment is larger than this maximum amount of time, the increment is said to have exceeded the *stability limit*. A possible side effect of exceeding this limit is numerical instability, which may lead to a diverged solution. For computational efficiency, the explicit approach adopts time increments as close as possible to the stability limit without exceeding it. Furthermore, a simple and efficient estimate can be made for determining the stability limit, based on formulation 7.1 and 7.2, although it is not computationally feasible to calculate the exact value of the stability limit in a system (Abaqus, 2006).

$$\Delta t_{stable} = \frac{L^e}{c_d} \tag{7.1}$$

Where L^e is the element length and c_d is the wave speed of the material, which can be determined by:

$$c_d = \sqrt{\frac{E}{\rho}} \tag{7.2}$$

Where E is the Young's modulus and ρ is the mass density. The stiffer the material, the higher the wave speed, resulting in a smaller stability limit; the higher the density, the lower the wave speed, resulting in a larger stability limit. For more details of the stability limit, readers are referred to the Abaqus Help Documentation 6.7 (Abaqus, 2006), which explains an analytical approach for the calculation of the exact stability limit, based on the highest frequency and critical damping in a system.

7.2.2 Element types

ABAQUS contains a large variety of hexahedron (brick), shell, contact and beam elements endowed with different features depending on the application. Kukreti *et al.* (1987) and Gebbeken *et al.* (1994) carried out a comparative investigation on numerical techniques in analyzing bolted steel connections with the intention of reproducing the experimental results in a finite element approach. They set up a two-

dimensional finite element model (using shell elements) and a three-dimensional finite element model (using brick elements) within ABAQUS. The comparison between numerical results and experimental data illustrated that the two-dimensional model was too stiff for the representation of the real deformations (Gebbeken *et al.*, 1994), and the hexahedron (brick) element was much more suitable to model the continuum behaviour of bolted connections compared to standard shell elements.

The current ABAQUS element library offers engineers and numerical analysts a number of hexahedron elements in finite element simulations. For hyperbolic problems (plasticity-type problems), Bursi and Jaspart (1998) suggest that the first order elements are likely to be the most successful in reproducing yield lines and strain field discontinuity. This is because some components of the displacement solution can be discontinuous at element edges. Simulations performed by Bursi and Jaspart (1998) compared three eight-node brick elements: (1) The C3D8 element with full integration (8 Gauss points). This element is accurate in the constitutive law integration but the shear locking phenomenon is commonly associated with it when simulating bending-dominated structures (Abaqus, 2006). (2) The C3D8R element with reduced integration (1 Gauss point). This element supplies a remedy for the shear locking problem caused by using C3D8, but the rank-deficiency of the stiffness matrix may produce spurious singular (hourglassing) modes (Abaqus, 2006), which can often make the elements unusable. In order to control the hourglass modes in elements, Flanagan and Belytschko (1981) proposed the artificial stiffness method and the artificial damping method in the ABAQUS code; although the artificial damping approach is available only for the solid and membrane elements in ABAQUS Explicit. (3) The C3D8I element with full integration (8 Gauss points) and incompatible modes. This element has 13 additional degrees of freedom and the primary effect of these degrees of freedom is to eliminate the so-called parasitic shear stresses that are observed in regular displacement elements in analyzing bending-dominated problems (Abaqus, 2006). In addition, these degrees of freedom are also able to eliminate artificial stiffening due to Poisson's effect in bending.

Through comparative modelling with the aforementioned three brick elements, the C3D8I elements were found to perform particularly well both in the elastic and

inelastic regimes, and are suitable for representing the bending-dominated behaviour of a structure (Bursi and Jaspart, 1997). As expected from the theoretical formulation, C3D8R elements underestimate the strength value and the plastic failure load in the finite element modelling. From calibration tests, Bursi and Jaspart (1997) also state that C3D8 elements appear to be unsatisfactory, owing to the overestimation of the plastic failure load and the shear locking phenomenon. Therefore, in order to predict the behaviour in a conservative fashion, the element selected for bolted steel connections is the reduced integration brick element C3D8R. In order to control the hourglass modes, a very dense mesh finite element model has been set up.

7.2.3 Contact modelling within ABAQUS

In numerical simulations, obtaining realistic representation of connection performance depends upon handling the difficult issues of modelling the contact interaction between various joint components. Within ABAQUS, the contact behaviour can be simply reproduced by using so-called "gap elements", which require the user to define pairs of nodes and specify the value of a clearance gap. These elements allow for two nodes to be in contact (gap closed) or separated (gap open) under large displacements (Bursi and Jaspart, 1997). The limitation of this sort of element is the friction between two contacted components being ignored in the simulation. Furthermore, simulation using these elements is a tedious and time-consuming task (Vegte, 2008).

In order to overcome these problems, a "surface-to-surface" contact interaction was developed for the numerical model. The simulation requires the researcher to first determine the slave and master surfaces for two deformable bodies and then define the interaction behaviour between these two surfaces. In the standard analysis, ABAQUS provides two formulations, small-sliding formulation and finite-sliding formulation, for modelling the interaction between two discrete deformable bodies. In the explicit analysis, the interactions between surfaces are modelled by a different contact formulation, which includes the constraint enforcement method, the contact surface weighting, the tracking approach and the sliding formulation. In the explicit analysis, the friction conditions (sliding and sticking) between the master and slave

surfaces may be represented by the classical isotropic Coulomb friction model, which has proved to be suitable for steel elements (Charlier and Habraken, 1990). However, it is of great importance to be careful with the assignment of the slave and master surfaces (Sarraj, 2007). It is generally accepted that the surfaces working as master surfaces should belong to the bodies with the stronger material or a finer mesh. So the contact surfaces of the bolt shank, bolt head and bolt nut are always modelled as master surfaces in this research, as highlighted in red in Fig.7.4. In the contact action between the column and the end-plate, the column face is always the master surface in the numerical model because these columns are likely to be of a higher grade steel (S355) compared with the plates which are most often S275. In simulating bolted steel connections, experience shows that heat generation caused by frictional sliding is not significant in experimental tests and therefore may be ignored in the finite element modelling. A friction coefficient μ of 0.25 has been accepted for all contact surfaces during the analysis and pretension was not applied to the bolts, in line with structural steelwork construction practice.

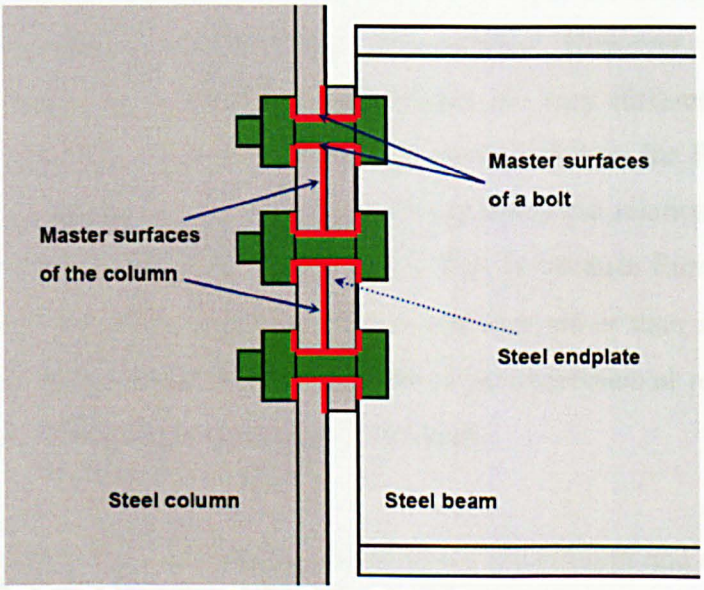

Figure 7.4: Master surfaces for a finite element connection model

7.2.4 Mesh convergence

As far as the stability limit is concerned, it is advantageous to keep the element size as large as possible during the analysis. However, coarse meshes in a model can produce inaccurate numerical results. Moreover, the numerical solution for a model is required to create a unique value as the mesh density increases during the solution

procedure (Abaqus, 2006). So the mesh of a numerical model is said to be converged, when further mesh refinement yields a negligible change in the analysis. For the brick elements, Sarraj (2007) created a number of finite element models with different mesh sizes for a mesh convergence check. The deflections and stresses of these models were plotted against the number of mesh elements. The numerical results show the deflections and stresses started to converge in a numerical model with approximately 1500 elements. So the mesh pattern used in his research has been adopted in the finite element analyses in the current research work.

7.2.5 Material properties for a finite element model

For realistic simulations, Bursi and Jaspart (1998) note that proper material properties are required to be adopted in the solution procedure. The material properties for the various components of steel connections may be determined from the engineering stress-strain relationship using nonlinear material curves recommended in Eurocode 3. They may also be defined according to stress-strain relationships obtained in standard tensile tests of steel. However, the stress-strain relationships determined by these two approaches are very different in the plastic region, as shown in Fig. 7.5 (the dashed blue curve indicates the Eurocodes-based stress-strain relationship and the solid red curve presents the relationship of stresses and strains produced in the steel tensile tests). This is because Eurocode 3 stresses are intended to give a safe margin for design purposes rather than simulation. As a result of this, the stress-strain relationships based on experimental results have been applied to the numerical model throughout this study.

In these connection tests, a 254UC89 was used for the column and a 305x165UB40 for the beam. The thickness of the end-plate was 10 mm. The steel used was S275 for end-plates and UB sections; and S355 was used for UC sections. All the bolts were M20 grade 8.8 used in 2 mm clearance holes. The nominal material properties of these structural components are summarised in Table 7. 1.

Table 7.1: Material properties of steel and bolt steel

Material type	Yield stress [N/mm^2]	Ultimate stress [N/mm^2]	Density [kg / m^3]	Young's modulus [kN/mm^2]	Poisson's ratio
S275	275	450	7850	205	0.3
S355	355	550	7850	205	0.3
8.8 bolt	640	800	7850	205	0.3

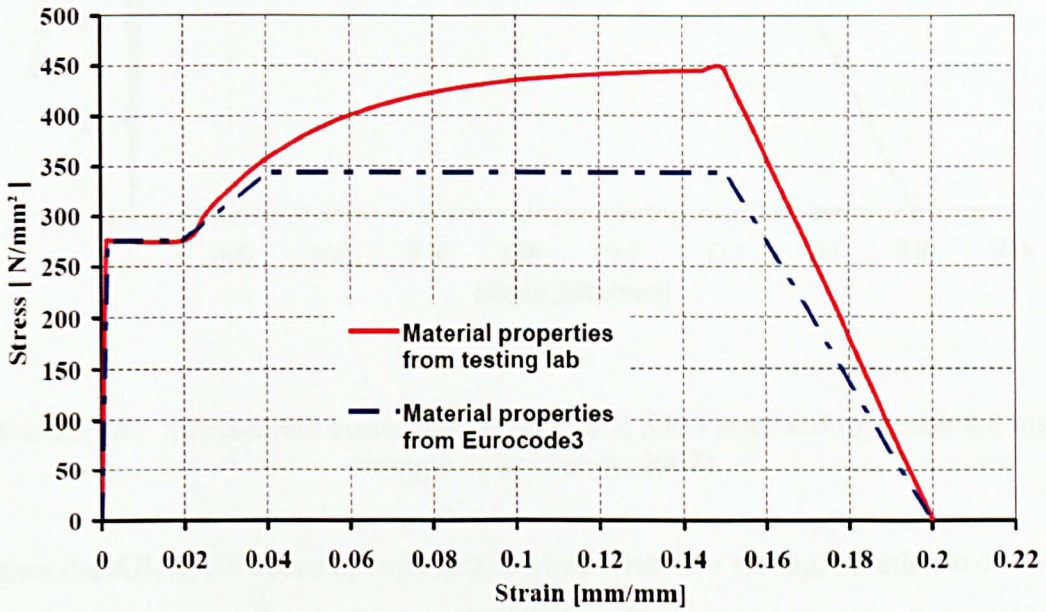

Figure 7.5: Material properties for steel

The stress-strain relationships for the structural steel and 8.8 bolts are illustrated in Fig. 7.6, and are the same as those used by Sarraj (2007).

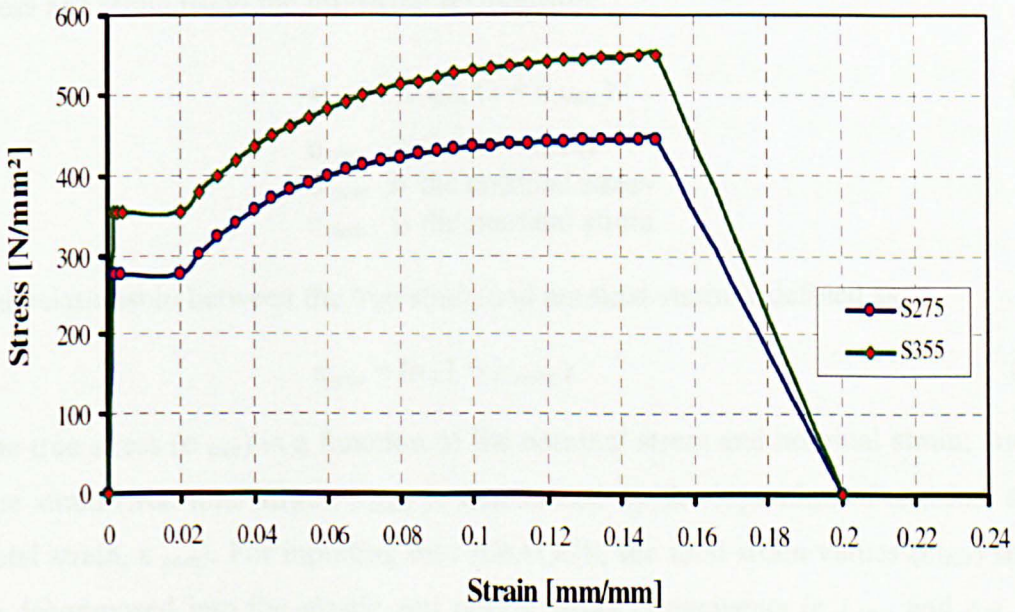

(a)

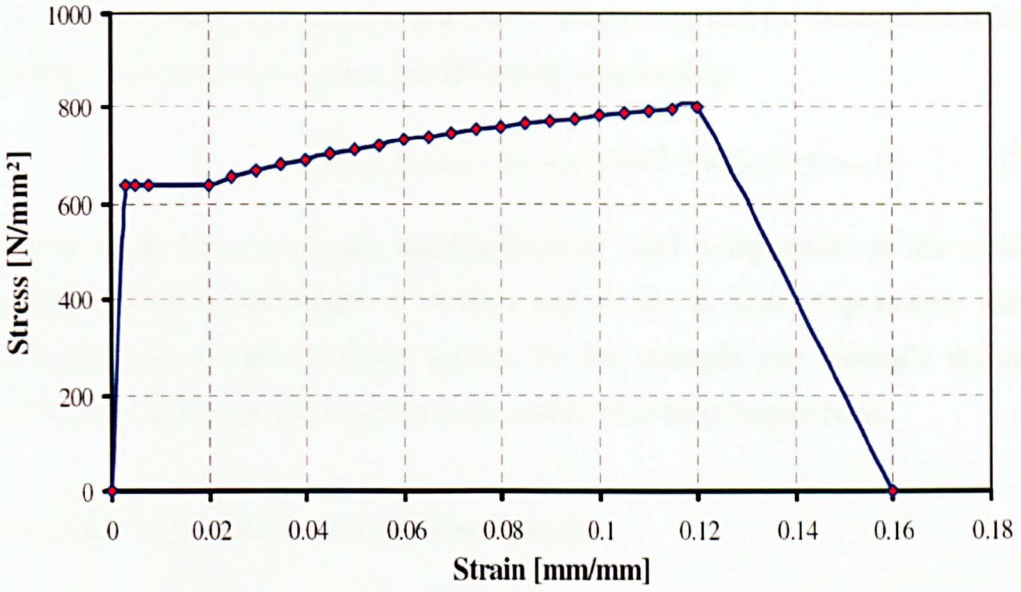

(b)

Figure 7.6: Stress-strain curves for (a) S275 and S355 steel and (b) grade 8.8 high strength bolts (Sarraj, 2007)

Since the ABAQUS codes operate in a large deformation setting, in order to consider the deformed area the nonlinear relationship of *true stress* versus *true strain* is required to be defined for steel components. However, most material test data are supplied with engineering stresses and strains (nominal stresses and nominal strains) according to the uniaxial material testing response (Bathe, 1982). In such situations, it is necessary to convert material data from engineering stress and strain to true stress and strain using the following relationship:

$$\sigma_{true} = \sigma_{nom} (1 + \varepsilon_{nom}) \tag{7.3}$$

σ_{true} is the true stress
σ_{nom} is the nominal stress
ε_{nom} is the nominal strain

The relationship between the true strain and nominal strain is defined as:

$$\varepsilon_{true} = \ln (1 + \varepsilon_{nom}) \tag{7.4}$$

The true stress (σ_{true}) is a function of the nominal stress and nominal strain; and the true strain (true total strain, ε_{true}) is determined by the logarithm of nominal strain (total strain, ε_{nom}). For inputting into ABAQUS, the total strain values (ε_{true}) should be decomposed into the elastic and plastic strain components ($\varepsilon_{el, true}$ and $\varepsilon_{pl, true}$). The true elastic strain ($\varepsilon_{el, true}$) can be captured by the true stress (σ_{true}) divided by

the Young's modulus (E); and the true plastic strain, required for the explicit solution procedure, can be obtained using the following relationship:

$$\varepsilon_{pl,\,true} = \varepsilon_{true} - \varepsilon_{el,\,true} = \ln(1 + \varepsilon_{nom}) - \sigma_{true}/E \qquad (7.5)$$

Once we have the stress-strain relationships of steel components at the ambient temperatures, the relationships of stresses and strains at high temperatures can be produced based on the reduction factors for the strength and Young's modulus, which has already been documented in an earlier chapter (Chapter two).

7.2.6 Modelling rupture with cohesive elements

To simulate the rupture process of a connection, the classical failure criterion adopted is to assume that the steel material starts softening at 15% strain and the strength drops to zero at 20% strain. But the performance of fillet welds and the material around these welds appear to be very brittle in the experimental tests. So Kanvinde et al. (2009) carried out some detailed research on fillet welds. Fracture of fillet welds in connections has been found to be a typical failure mechanism and the fracture displacements of these fillet welds are commonly in the range of 0.71 mm and 1.93 mm. Moreover, the experimental results in Chapter 5 showed that the rupture of end-plates always took place around the heat affected zone (HAZ) in a partial depth end-plate connection. So a small number of cohesive elements have been embedded into the heat affected zone in the numerical model to capture this failure behaviour. Cohesive elements represent a fracture of a material as a separation across a surface and the constitutive response of these elements is determined by the relationship of traction versus separation (*traction separation law*), as shown in Fig. 7.7. When these cohesive elements and their neighbouring components have matched meshes, it is straightforward to connect cohesive elements to other elements in a model simply by sharing nodes. If the neighbouring elements do not have matched meshes, ABAQUS enables the cohesive elements to be connected to other components by using surface-based tie constraints (Abaqus, 2006).

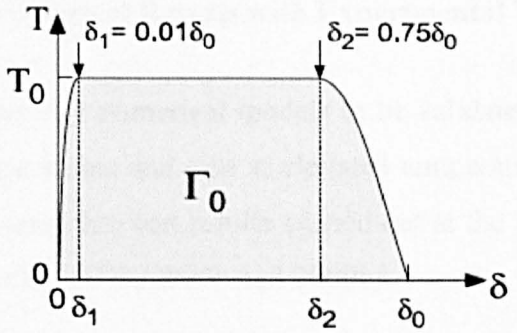

Figure 7.7: Traction-separation law for fracture (Cornec et al., 2003)

The available traction-separation model in ABAQUS assumes initially linear elastic behaviour followed by the initiation and evolution of damage. To determine this constitutive response, a number of parameters, such as critical separation (δ_0), cohesive energy (Γ_o) and cohesive strength (T_0), are required for the explicit solution procedure, as displayed in Fig. 7.7. Cornec et al. (2003) recommend that the cohesive strength (T_0) may be taken as the maximum stress at fracture in a round notched tensile bar. But Scheider et al. (2006) add that this procedure might not be applicable to thin specimens, as round notched bars can not be machined from sheet metal and the individual failure mode (normal fracture) would be different from that in the flat specimen (slant fracture). As an estimation for the simulation, Scheider et al. (2006) recommend that the nominal stress of the flat tensile specimen at fracture (load divided by the area of the normal projection of its inclined fracture surface, $F_{frac}/A_{frac} \approx 470.5$ MPa) may be used as T_0 . To simulate the progressive damage in the cohesive zone, it is of great importance to determine the critical separation (δ_0) and cohesive energy (Γ_0). The determination of δ_0 heavily relies on experience in numerical simulation and experimental tests, and three times the separation value at damage initiation (δ_1, shown in Fig. 7.7) or over has been adopted for the explicit solution procedure. Thus the cohesive energy (Γ_0) may be estimated by using one of the following relationships (Cornec et al., 2003):

$$\Gamma_o = 0.87\, T_0\, \delta_0 \quad \text{.....(7.6)}$$

or

$$\Gamma_o = T_0\, \delta_0 \quad \text{.....(7.7)}$$

7.3 Comparison of Numerical Results with Experimental Tests

It is a standard procedure for numerical models to be validated against experimental results at ambient temperatures and also at elevated temperatures. The experimental data was taken from connection test results carried out at the University of Sheffield (Hu et al., 2008; Yu et al., 2009a, 2009b and 2009c).

7.3.1 Comparison of Flexible End-plate Model at Ambient Temperatures

The author investigated the resistance and rotation capacity (ductility) of one typical simple connection type (partial depth end-plate) subjected to inclined tying forces at both ambient and elevated temperatures (Hu et al., 2008). In this programme, twelve connection tests have been performed for end-plate connections, including three tests at ambient temperatures and nine tests for high temperatures. The deformation (rotation) in the connection zone was recorded by inclinometers (angular transducers) for the first three tests at ambient temperatures, and the applied external force was captured by strain gauges on the loading system.

The numerical model was developed for flexible end-plates using the ABAQUS commercial software package (as outlined in 7.2), and the geometrical details of the numerical model are shown in Fig. 7.8 and material properties used in Table 7.1. Dimensions in Fig. 7.8 are shown in mm.

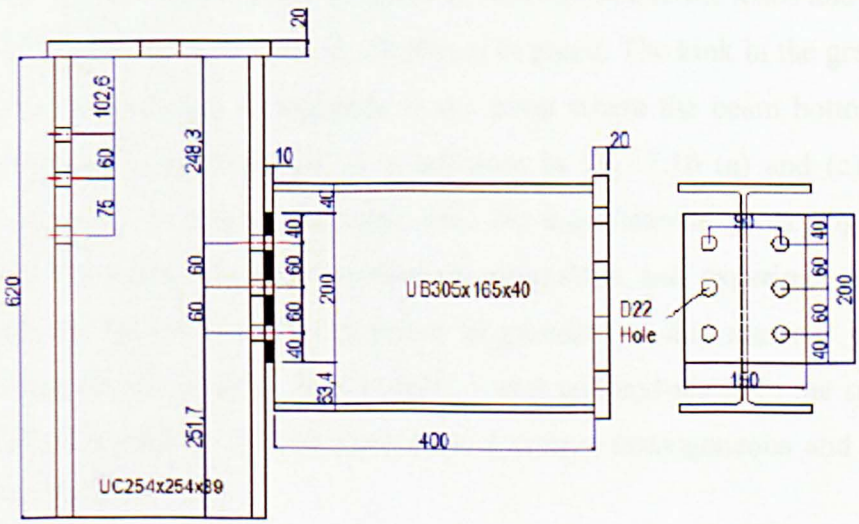

Figure 7.8: Geometrical details of the flexible end-plate connection (mm)

The deformed and undeformed shapes of the numerical model are displayed for flexible end-plates in Fig.7.9, including the contour plots for the components as well, such as bolts and end-plates. The FE analysis clearly demonstrates that the rotation capacity of these connections is mainly produced by deformation in the end-plates, welds and bolts, and the deformation of the column flange and beam web may be neglected in the analysis. The ductile failure mechanism of partial depth end-plates has been represented in the simulation.

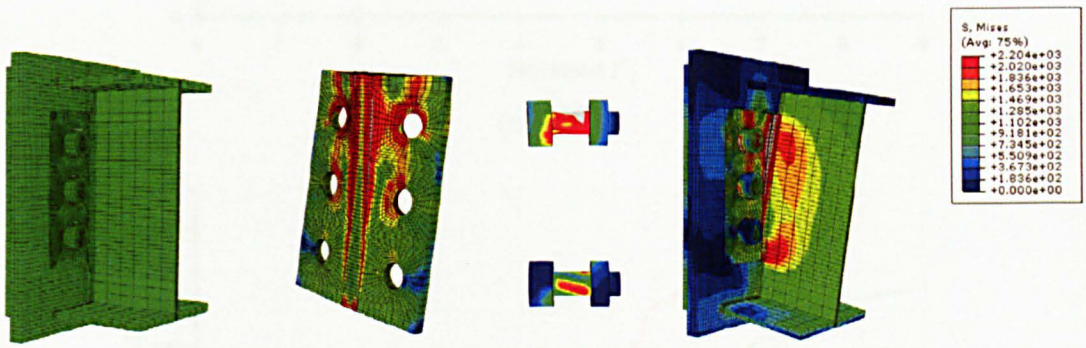

Figure 7.9: FE model of flexible end-plate connection: deformed and un-deformed shapes

For simple steel connections, the relationships of moments and rotations are not of great importance in the sense of structural design (they are assumed to be pinned). Of greater concern is the response of these connections to the inclined tying forces and their ductility under fire conditions. So the relationships of loads and rotations of the numerical model have been compared with experimental data of three connection tests at ambient temperatures, as shown in Fig. 7.10. The red curves in Fig. 7.10 (a), (b) and (c) are the numerical plots produced in ABAQUS; and the loads and rotations recorded in the experimental tests are displayed in green. The kink in the green curve is at about 6^{o} rotation and corresponds to the point where the beam bottom flange contacted with the column flange. It is apparent in Fig. 7.10 (a) and (c) that the numerical plots are in good agreement with the experimental plots. Fig.7.10 (b) shows some discrepancy between numerical simulation and experimental results, which might be caused by slight variation in geometrical and material properties between structural components such as bolts, welds and end-plates in the specimens tested, which is unable to be represented by a unique homogeneous and isotropic finite element model.

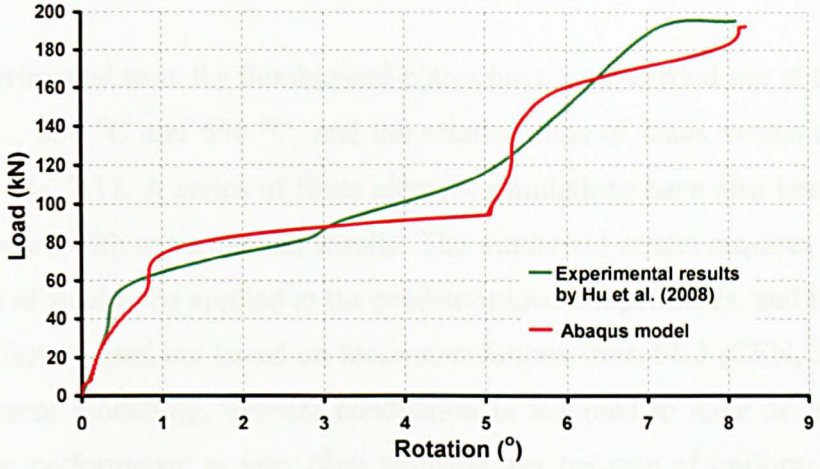

(a) 35°

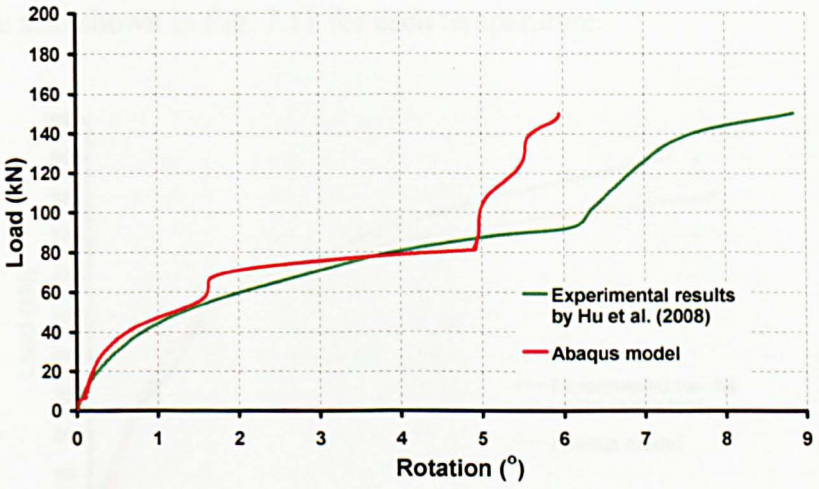

(b) 45°

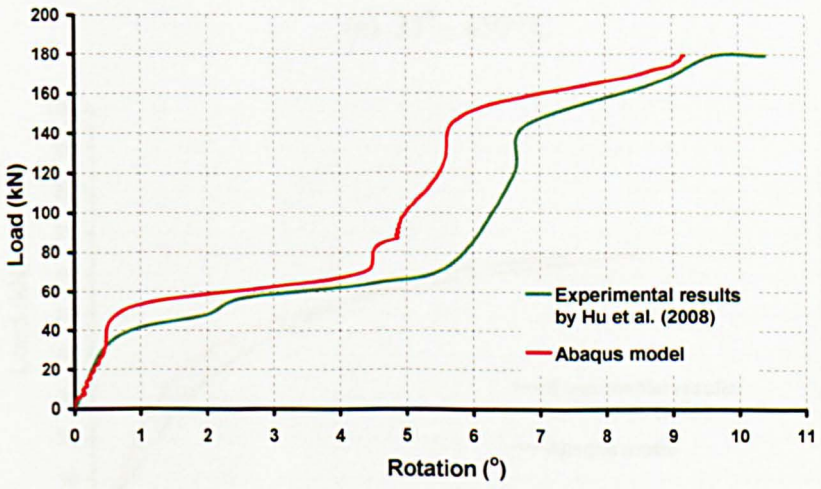

(c) 55°

Figure 7.10: Load-Rotation comparisons between FE model and experimental results for flexible end-plate connections (a) 35° (b) 45° (c) 55°

7.3.2 Comparison of Flexible End-plate Model at Elevated Temperatures

Nine experimental tests for flexible end-plates have been carried out at temperatures of 450 °C , 550 °C and 650 °C, and the relationships of loads versus rotations are plotted in Fig. 7.11. A series of finite element simulations have also been conducted and compared with experimental results. The numerical model requires the material properties of steel to be applied at the predetermined temperatures, and the reduction retention factors used are based on recommendations from EC3 (CEN, 2005). In the finite element modelling, thermal conduction is assumed to have no effect on the connection performance at very high temperatures because of uniform temperature distribution in the specimens. The deformed shapes of connections and finite element models are also shown in Fig. 7.11 for each temperature.

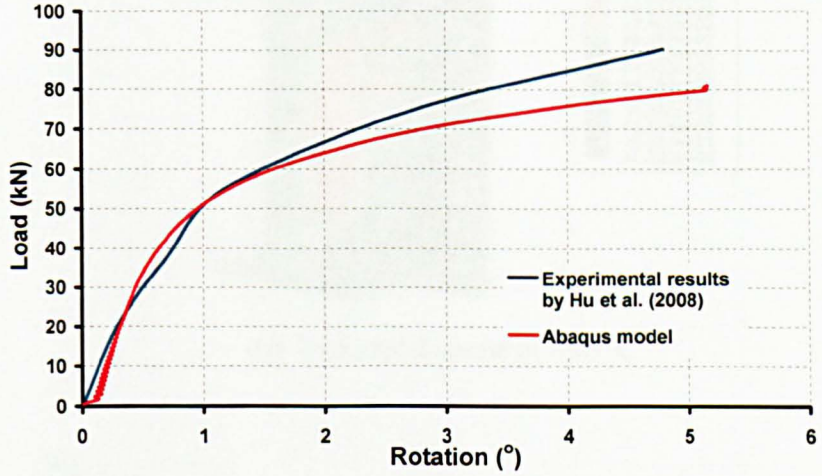

(a) 35° - 450 °C

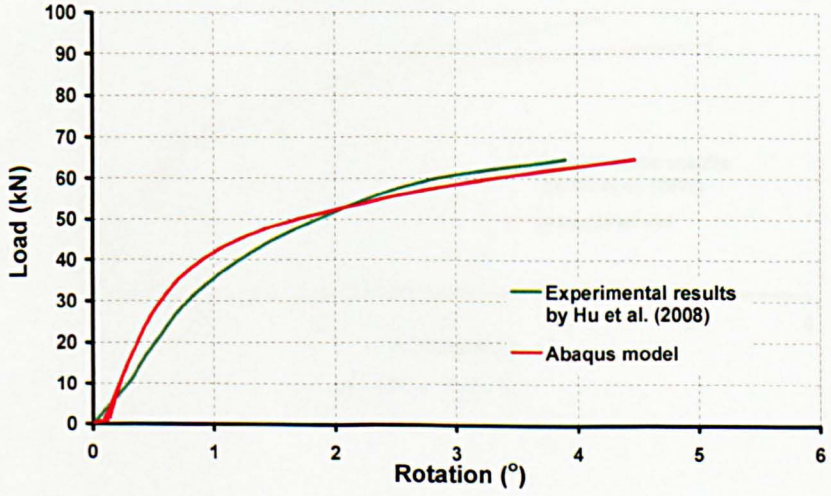

(b) 45° - 450 °C

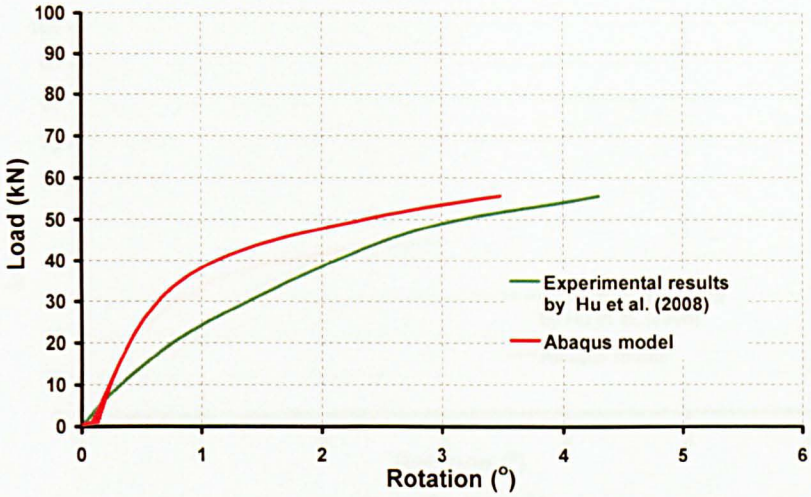

(c) 55° - 450 °C

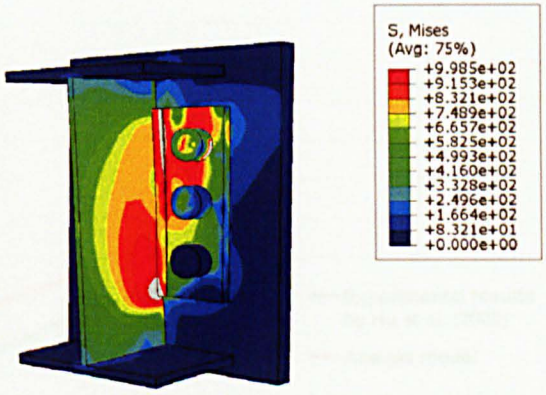

(d) Deformed shape at 450 °C

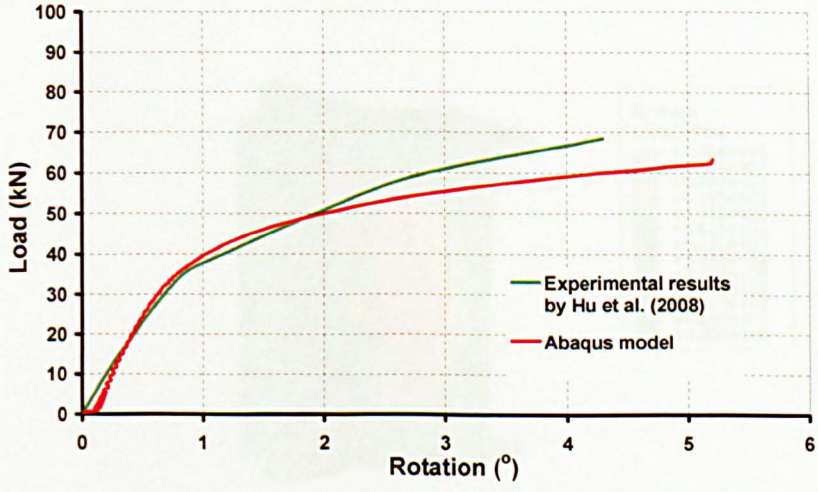

(e) 35° - 550 °C

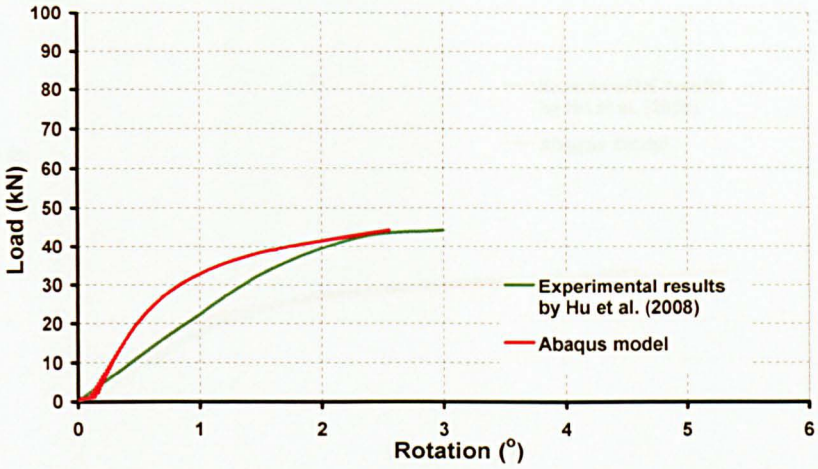

(f) 45° - 550 °C

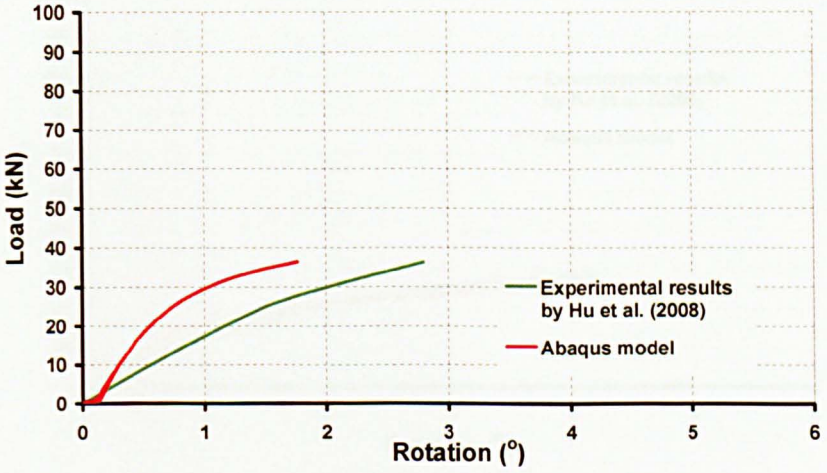

(g) 55° - 550 °C

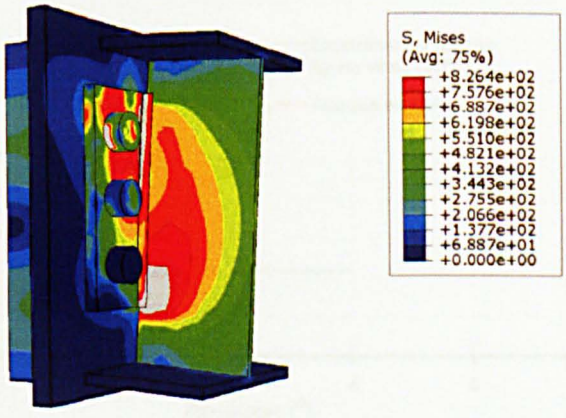

(h) Deformed shape at 550 °C

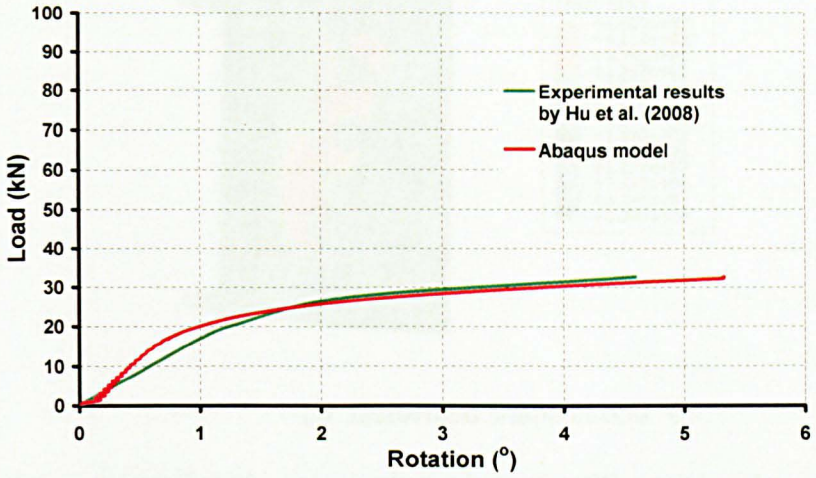

(i) 35° - 650 °C

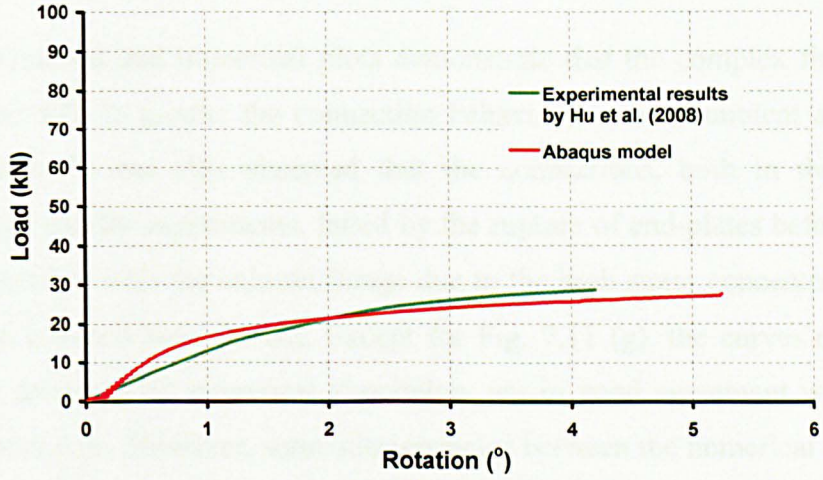

(j) 45° - 650 °C

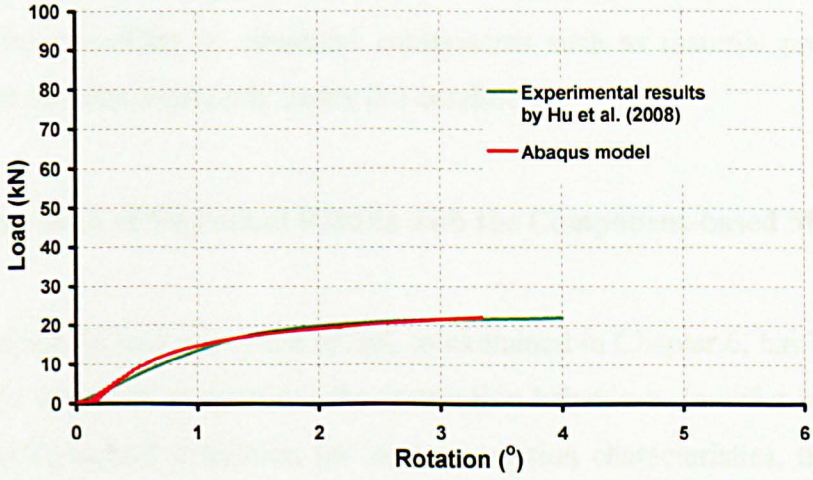

(k) 55° - 650 °C

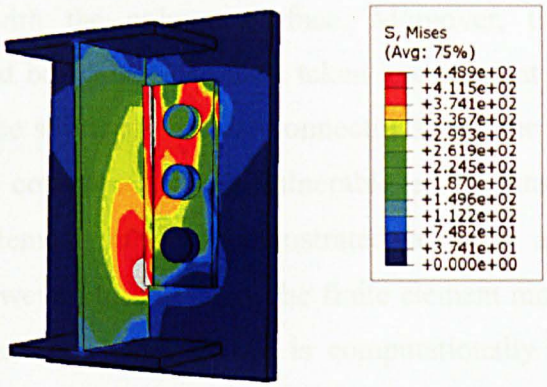

(l) Deformed shape at 650 °C

Figure 7.11: Load-Rotation comparisons between FE model and experimental results for flexible end-plate connections

The experimental and numerical plots demonstrate that the complex finite element models are able to predict the connection behaviour at both ambient and elevated temperatures. It was also observed that the connections, both in the numerical simulations and the experiments, failed by the rupture of end-plates before the beam flange contacted with the column flange due to the high stress concentration around the heated affected zone (HAZ). Except for Fig. 7.11 (g), the curves of loads and rotations, produced by numerical simulation, are in good agreement with recorded experimental data. However, some discrepancies between the numerical analysis and experimental data should be accepted in the finite element simulation, which is because the unique homogeneous and isotropic finite element model are unable to represent the variability in structural components such as material properties and geometrical features, especially under fire conditions.

7.4 Comparison of Numerical Results with the Component-based Model

The component-based connection model, as explained in Chapter 6, has been used as a simplified approach to represent the connection behaviour. In order to provide an accurate and practical prediction for steel connection characteristics, this approach has been extended to include the shear components in the vertical direction instead of assuming infinite vertical stiffness. The second stage behaviour of partial depth end-plate connections has been simulated with two spring-like components in the compression zone, which enable this model to capture the connection response after

the beam contacts with the column surface. Moreover, the effect of brittle components (welds and bolts) has also been taken into account instead of assuming these components as the strongest in these connections; and the experimental results also proved that these components were vulnerable in fire attacks. In the previous section, the finite element model demonstrated a good agreement with the experimental tests. However, utilization of the finite element model (brick elements) to investigate the connection performance is computationally time-consuming for engineering design. Compared to complex finite element analysis, the analytical component-based model is a more simplified and economical approach for design. It is therefore worth conducting a comparison between the numerical analyses and the analytical component-based models, see Fig.7.12.

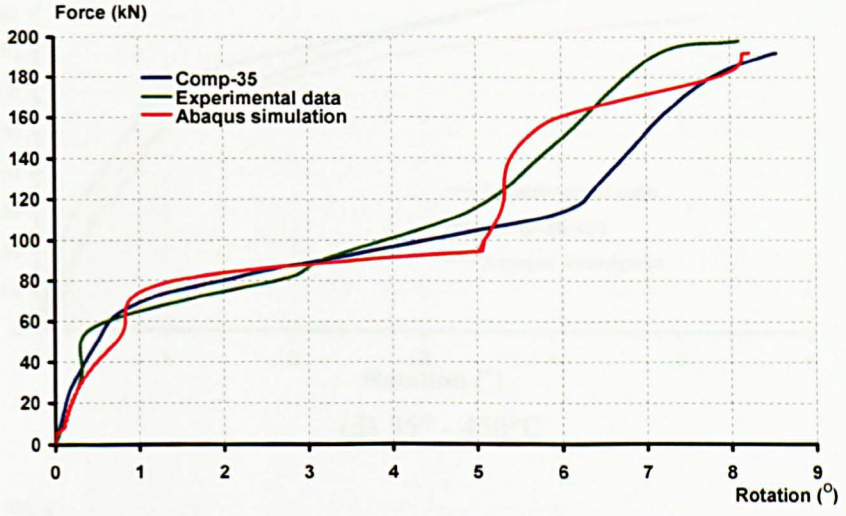

(a) 35°

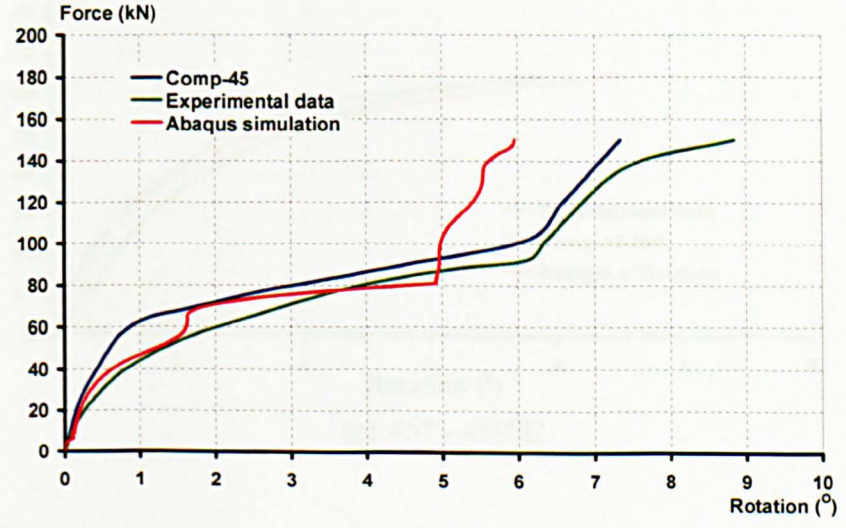

(b) 45°

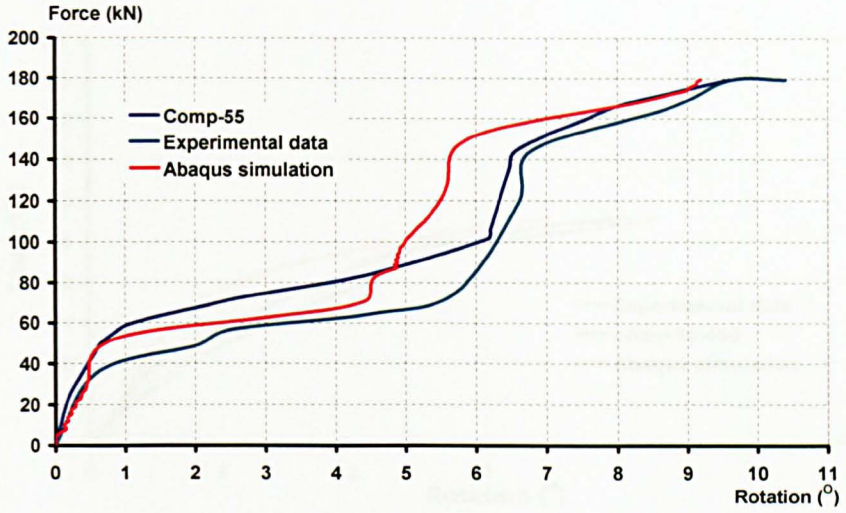

(c) 55°

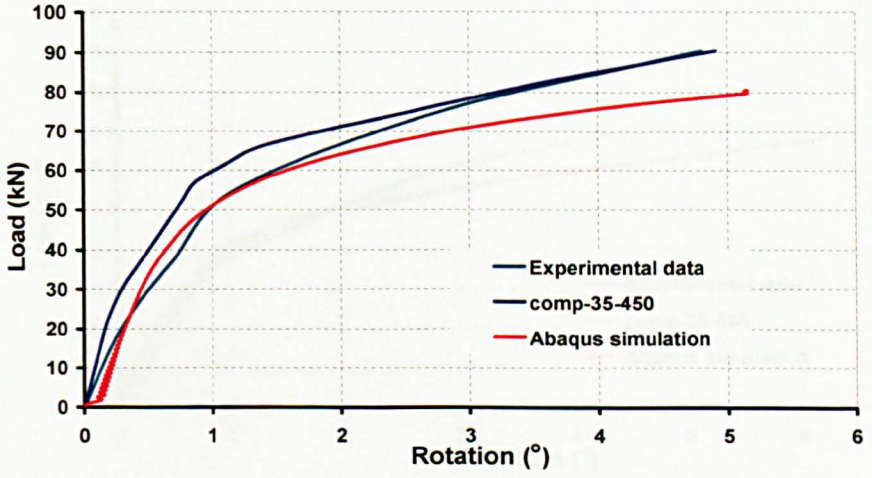

(d) 35° - 450°C

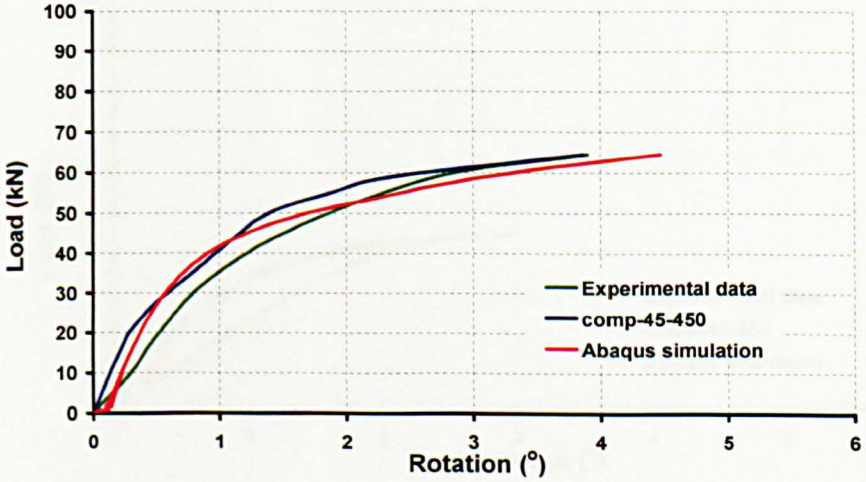

(e) 45° - 450°C

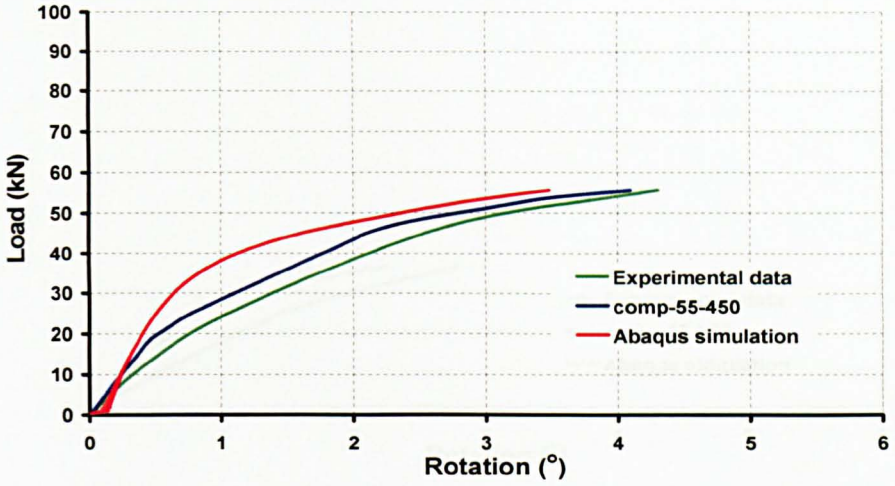

(f) 55° - 450°C

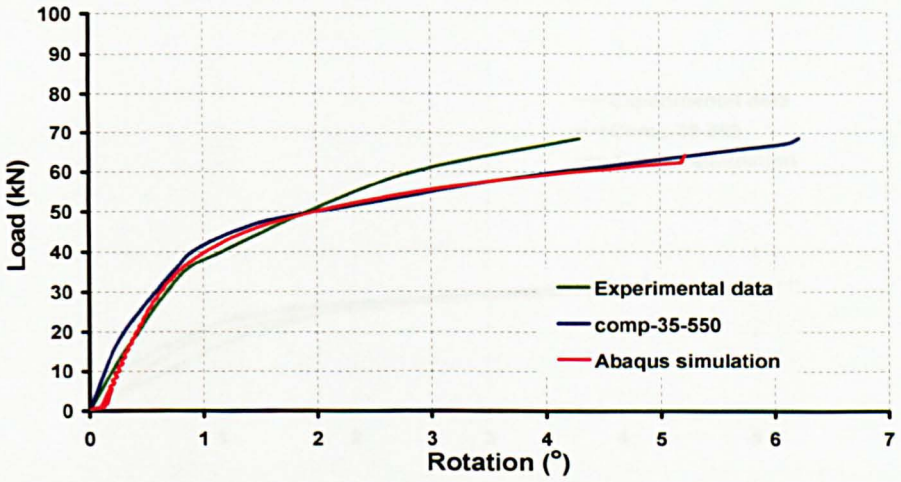

(g) 35° - 550°C

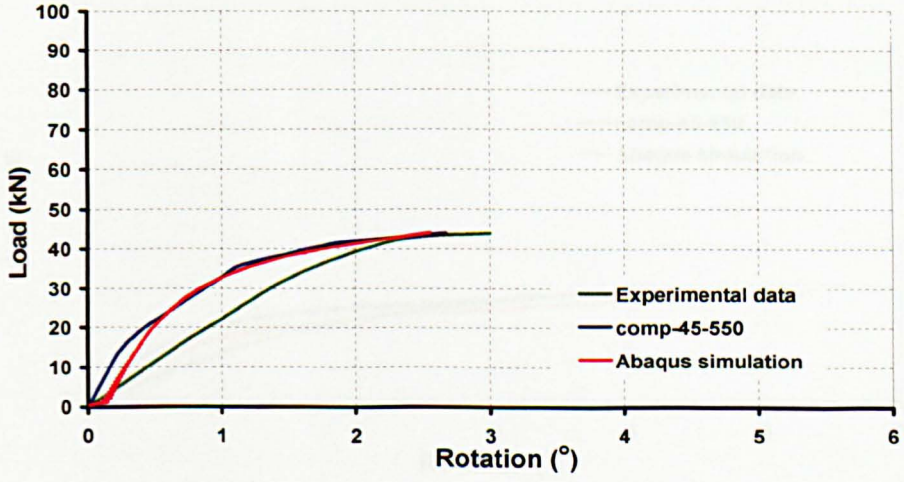

(h) 45° - 550°C

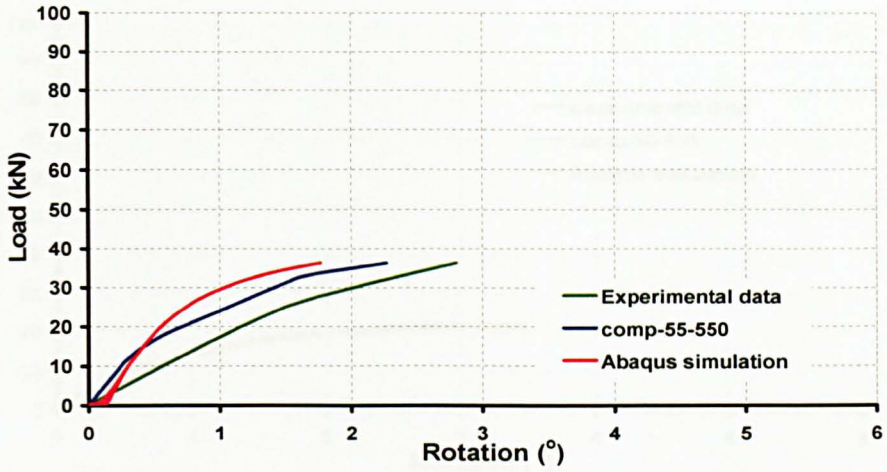

(i) 55° - 550°C

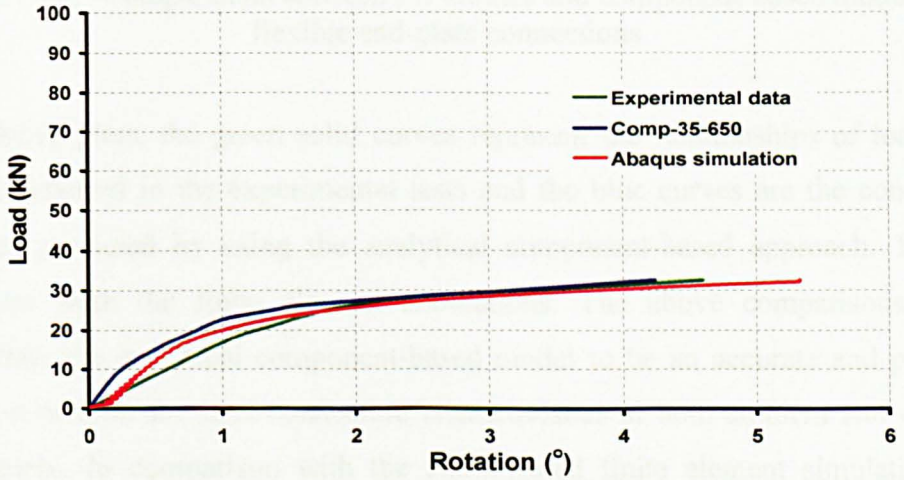

(j) 35° - 650°C

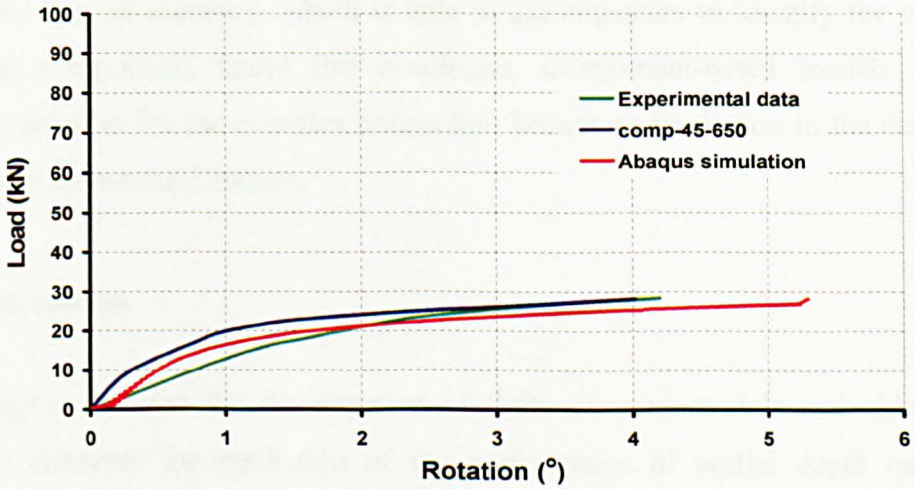

(k) 45° - 650°C

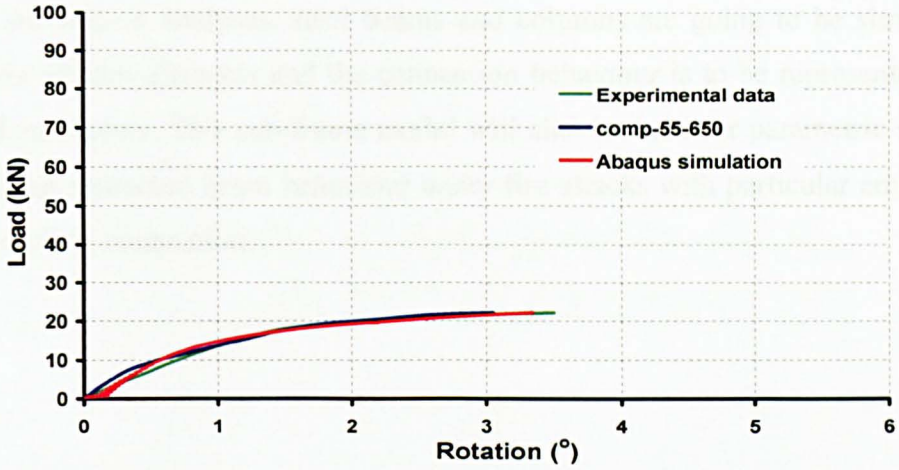

(l) 55° - 650°C

Figure 7.12: Comparisons between FE models and component-based models for flexible end-plate connections

In the above plots, the green solid curves represent the relationships of loads and rotations reported in the experimental tests and the blue curves are the connection responses predicted by using the analytical component-based approach. The red curves are from the finite element simulations. The above comparisons above demonstrate the analytical component-based model to be an accurate and practical prediction method for steel connection characteristics at both ambient and element temperatures. In comparison with the complicated finite element simulation, the component-based model is a more simplified and economical approach without significant loss of accuracy, which is able to aid engineers to identify the weakest structural components under fire conditions. Component-based models are an effective solution for the complex connection behaviour prediction in the design of steel or composite-steel frames.

7.5 Conclusions

This chapter reported the development of finite element models embedded with cohesive elements for prediction of the performance of partial depth end-plate connections under fire conditions. Comparisons between the finite element simulation and the component-based modelling were presented, which demonstrated the simplified connection model to be capable of representing the complex behaviour of steel joints. This new simplified method will be used to analyze the performance

of a Rugby-post sub-frame under fire conditions in the following chapter (Chapter 8). In the subsequent analyses, steel beams and columns are going to be simulated as finite shell/beam elements and the connection behaviour is to be represented by the simplified models. This sub-frame model will also be used for parametric studies to investigate restrained beam behaviour under fire attacks with particular emphasis on the role of the connections.

CHAPTER 8

PARAMETRIC STUDIES OF SUB-FRAME TESTS IN MANCHESTER

8.1 Introduction

In the previous chapters, the component-based analytical approach and the finite element simulation have been compared and discussed for the analysis of the connection-related problems under fire conditions. Although the simplified model (component-based model) has been shown to be capable of representing the connection behaviour realistically in a fire situation, the previous study was based on the isolated connection tests, which did not take the connection performance in a steel frame or sub-frame into account. As identified by Wang (2002), the main difference between an isolated connection and a connection in a frame is the presence of an axial load in the frame connection. Such an axial load could be compressive at the early stage of fire exposure, and then change to a tensile force during the later stage of a fire. This tensile force could be high enough to fracture the connection, and the constraints of a steel beam at both ends, furnished by the connections, will be destroyed during this process. This is one possible failure mechanism in a steel-framed structure, which was not expected for performance-based fire protection design under fire conditions.

Currently, fire resistant design of a steel beam is based on bending moment resistance of the beam (BSI, 1990 and CEN, 2005b). This resistance is limited to the reduced plastic bending moment capacity or lateral torsional buckling capacity of the beam at small deflection (Yin, et al. , 2004). According to this design philosophy, the steel beams would require expensive fire protection to achieve the design moment resistance, owing to the relatively low survival temperatures of steel in fire. So

alternative design approaches have been developed to eliminate or reduce fire protection for example by using tensile membrane action (SCI, 2000) and catenary action (Wang, 2002). In tensile membrane action, the reinforcement in the slab is in tension and the slab resists the applied vertical loading by stretching of the reinforcement mesh under deflection. The tensile membrane action can only occur when the slab undergoes very large deflections, and failure of the slab is usually indicated by fracture of the reinforcement (Wang, 2002). Under fire conditions, catenary action is a structural mechanism developed in steel beams at large deflections as the behaviour of a steel beam changes from flexural bending to a cable-like action. In this mechanism, the axial force of a steel beam, as mentioned already, will experience compression and then tension. The steel beam acts as a cable hanging from the adjacent structure, and plastic hinges usually form at both ends of the steel beam. Unlike tensile membrane action that can develop in a self-contained manner in two-way slabs without the need for in-plane restraint around the edges, catenary forces in a steel beam must be anchored by the adjacent structure in catenary action, which is why the failure of connections under fire conditions is important. As a consequence, Yin (2004) and Wang (2002) recommend the design methods that make use of catenary action in steel beams should consider the effect of catenary forces on the adjacent structure, including the connections as well. This implies that it is of great importance for the catenary forces to be precisely estimated and it might also be valuable for the beam deflections to be accurately quantified.

This chapter presents numerical results, using the ABAQUS (2001) finite element program, of the large deflection behaviour and axial forces of restrained steel beams at elevated temperatures. In a sub-frame model, the connection is represented by using the component-based approach and conventional pin and rigid connection assumptions have also been adopted in this analysis. After validating the capability of the numerical model against experimental results, a series of parametric studies have been carried out. The parameters involved in the parametric studies include beam span, different load ratios, uniform and non-uniform temperature distributions, different types of loads and different connection temperatures. The present study is to achieve a general understanding of connection performance and the variation of axial forces in the catenary action.

8.2 Numerical Validations of Manchester Tests

The numerical simulations of the performance of the Manchester sub-frame tests at elevated temperatures were carried out by using the finite element software ABAQUS. This study adopted the same numerical modelling strategies used in the research work of Yin et al. (2004). According to the experimental tests, non-uniform temperature distribution has been taken into account, and shell elements of type S4R and beam elements of B31 have been used for modelling of steel beams and columns respectively. The component-based connection model has been represented by using nonlinear spring elements in ABAQUS. The finite element simulation for high temperature analysis was divided into two steps, in which the structural loading was applied first, and then the thermal loading (temperatures) of steel sections were increased. As previously discussed in Chapter Seven, the numerical solution process could become unstable in the elevated temperature analysis. In order to achieve a stable solution, a pseudo-dynamic modelling procedure, recommended by Yin (2004), has been adopted with a dissipated energy fraction of 1E-10. The energy fraction was chosen by trial and error to be small enough, so the artificial damping added to the sub-frame model is able to stabilize the numerical simulation process with no effect on the deflection behaviour of the beams.

In the experimental tests of Manchester, one of their responsibilities was to provide experimental data for validation of the sub-frame numerical models. In these tests, 178x102UB19 was used for the beam sections and the steel used was nominally S275 for universal beams. In order to investigate the effect of different levels of restraint on the steel beams, universal columns of 254UC73 and 152UC23, classified as S355 and S275 respectively, were used as the column sections throughout testing. In order to capture the temperature distribution in the sub-frame tests, numerous thermocouples were placed into the beams, columns and connection components. To account for the lateral restraints provided by the concrete slabs in reality, a specially designed truss system was bolted onto the beam top flange for each sub-frame test, and 15 mm thick fire protection (ceramic fibre blanket) was also applied to the beam top flange and the truss system, to represent the heat sink effect produced by concrete slabs. The secondary objective of the Manchester project was to check the different modes of failure for the connection configurations involved in this robustness project

and their effects on the structural fire performance of the steel beam in the sub-frame. So the ten completed fire tests on sub-frames contained five different connection types, which were fin plates, partial depth end-plates, web cleats, flush and extended end-plates. The load ratio for each sub-frame test was assumed to be 0.5 during the testing. However, this chapter concentrates on the sub-frame tests for the connection type of partial depth end-plates.

8.2.1 Manchester Test Two

(a)

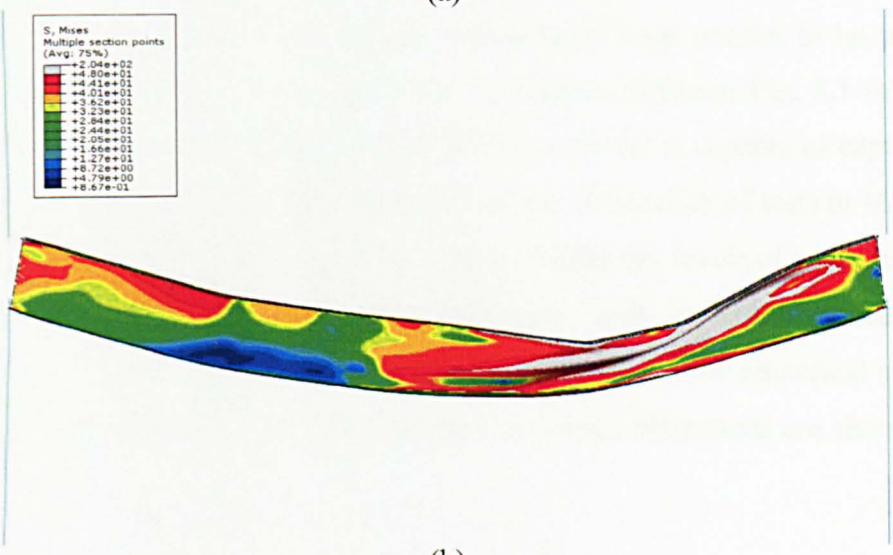

(b)

Figure 8.1: Manchester Test 2 (a) The deformed shape in testing (b) The numerical simulation

The previous section briefly introduced background information for the tests by the fire research group at Manchester. In the second test at Manchester, the universal beam (178x102UB19) and the larger column section (254UC73) were used in the

sub-frame structure, and two 40kN concentrated loads were applied onto the top flange of the steel beam by using two hydraulic jacks. According to the experimental data, as shown in Fig. 8.1(a), the steel beam experienced asymmetrical deformation in the furnace and plastic buckling took place on the right hand side of the specimen. This was because the steel beam experienced an inconsistent temperature distribution along its longitude direction when applying the thermal loading. The recorded temperatures in the connection zone at the right of this specimen were about 100°C to 150°C higher than those at its left hand side. Therefore, the failure mechanism of the specimen was due to facture of the specimen close to the connection welds on the right.

To replicate the performance of this specimen in fire, the component-based sub-frame numerical model, shown in Fig. 8.1 (b), was created, and needs to account for the non-uniform temperature distribution along the longitude direction of the specimen and the thermal gradient in a cross section as well. During the testing, the two hydraulic loading jacks could not maintain a constant load level in fire due to the asymmetrical deformation and non-uniform temperature distribution existing in the steel beam. So variation of the applied concentrated loads needed to be taken into account in the numerical simulation. The comparison between Fig. 8.1 (a) and (b) demonstrates that the component-based numerical model is capable of capturing the deformed shape of the specimen during the testing. This series of tests in Manchester had a third objective: to investigate the effects of different levels of axial restraint on the fire performance of structural components such as columns, beams and connections. Therefore, comparison of axial forces between the numerical model and this test is displayed in Fig. 8.2 (a) and their mid-span deflections are shown in Fig. 8.2 (b).

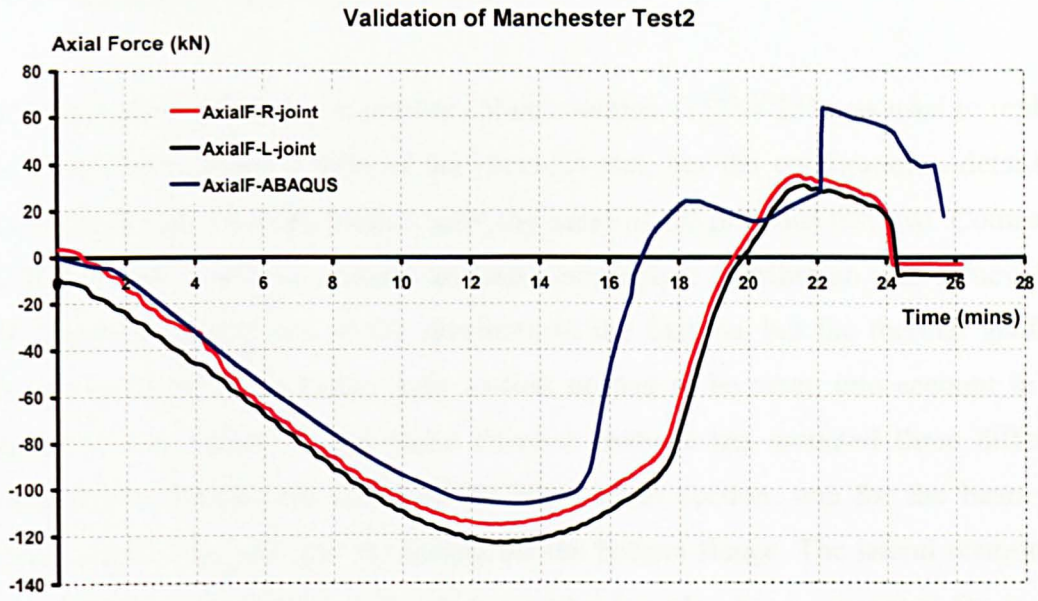

(a)

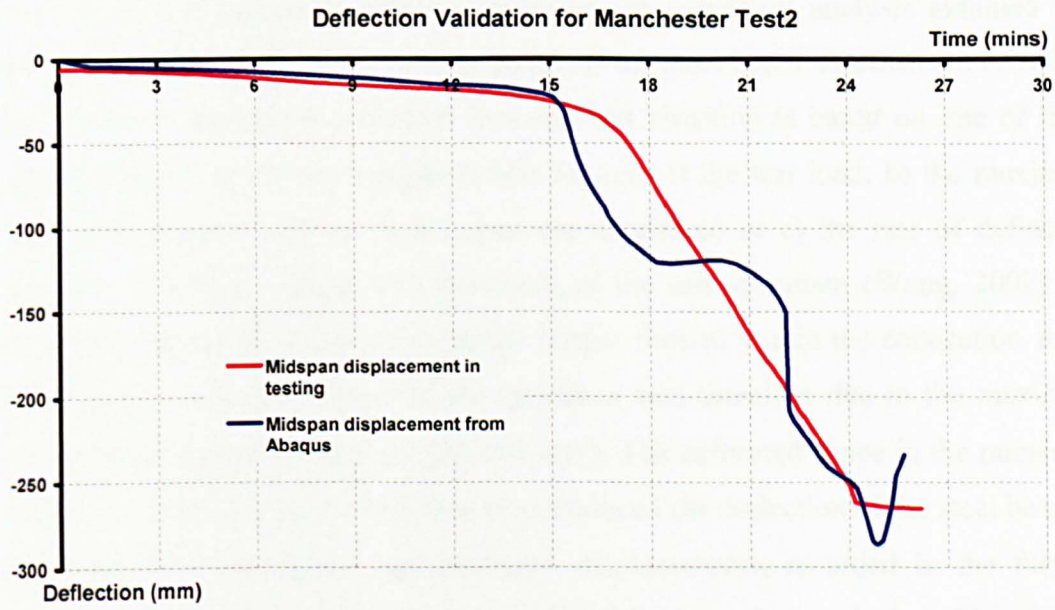

(b)

Figure 8.2: Validation of Manchester Test 2 (a) Axial Force (b) Midspan Deformation

As demonstrated in the above figures, the component-based numerical model has proved its capability of replicating the axial force variation and the deflections of a sub-frame structure under fire conditions. In order to gain adequate confidence to believe the numerical model, one more component-based numerical model was set up for Manchester Test Seven.

8.2.2 Manchester Test Seven

In Manchester Test Seven, a smaller column section (152UC23) was used to replace the 254UC73 column section of the previous test, but the configuration details of connections and the beam section were the same as the previous test two. Compared to Manchester Test Two, a more uniform temperature distribution was achieved in the longitudinal direction of the specimen in the furnace, but the thermal gradient across the depth of the beam cross section needed to be taken into account in the numerical simulation. So the finite element analysis has assumed three different temperatures through the depth of the beam cross section, one for the beam top flange, one for the web and the hottest for the bottom flange. The lateral restraint to the steel beam, provided by the truss system, has also been accounted for in this numerical model. In this experiment, the applied loads were maintained at a constant level of 40 kN during the heating stage, so the numerical analysis assumed two invariable loads applied onto the top flange of the steel beam. Assessment of failure for a steel or composite specimen in a fire test situation is based on one of three failure criteria: a) the test specimen fails to support the test load, b) the maximum deflection exceeds $L/20$ (L is the span the specimen) or c) the rate of deflection exceeds $L^2/(9000d)$, where d is the depth of the test specimen (Wang, 2002). As demonstrated in Fig. 8.3 (a), two plastic hinges formed within the connection zones at the beam ends, and failure of the specimen was therefore due to the maximum deflection recorded exceeding $L/20$ (100 mm). The deformed shape in the numerical model, as shown in Fig. 8.3 (b), almost reproduced the deflection of the steel beam in this test. The axial forces and mid-span displacements, recorded in the furnace testing, have been compared with the results of the numerical analysis in Figs. 8.4 (a) and (b), which demonstrate good agreement between the numerical model and the experimental test.

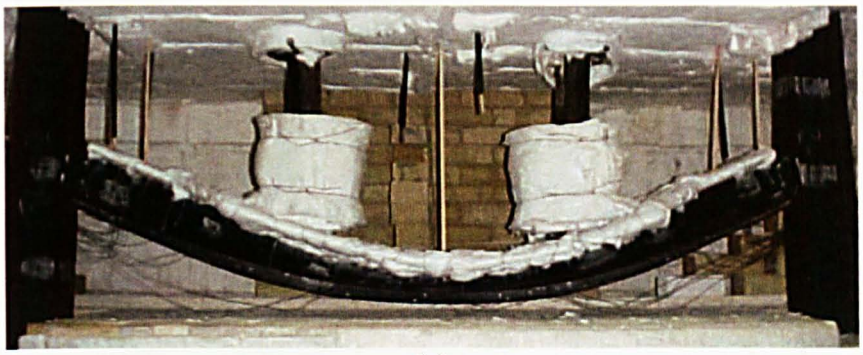

(a)

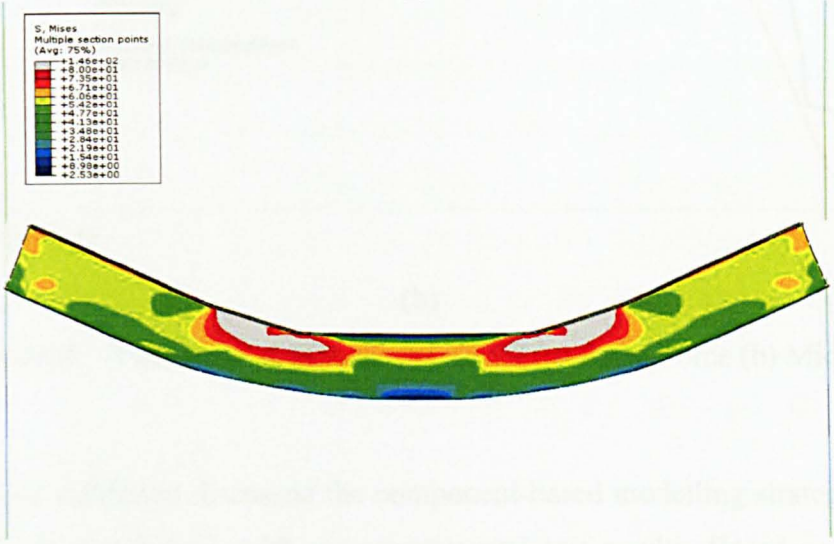

(b)

Figure 8.3: Manchester Test 7 (a) The deformed shape in testing (b) The numerical simulation

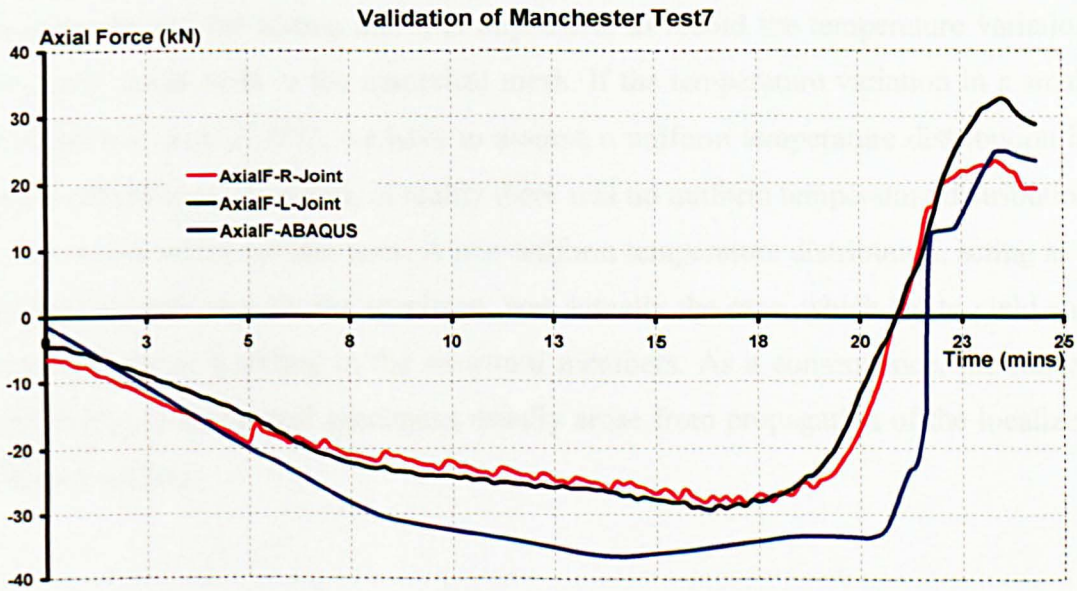

(a)

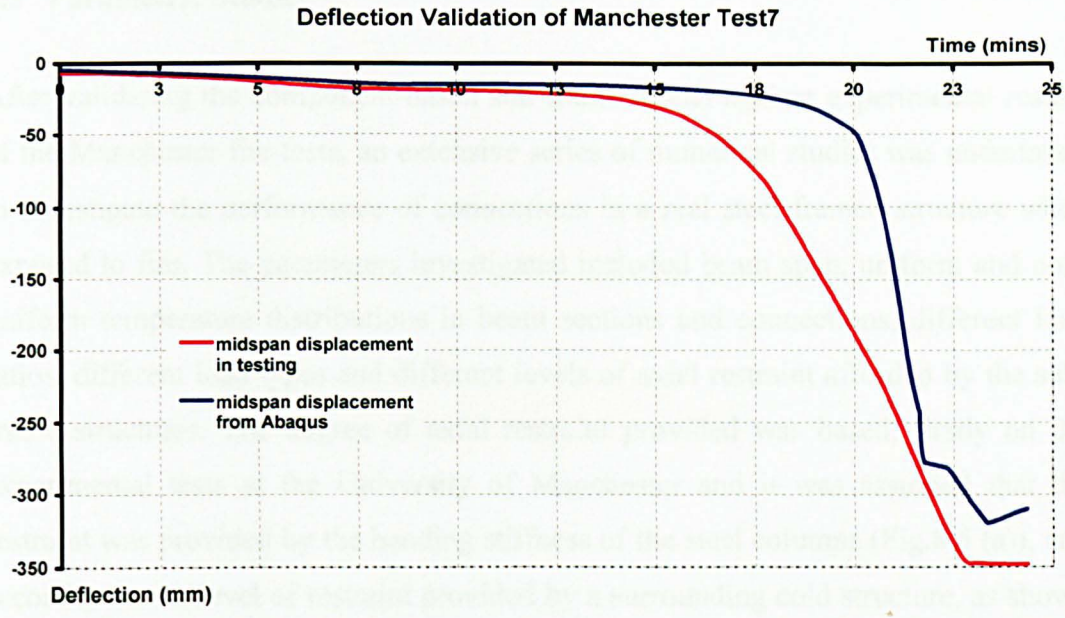

(b)

Figure 8.4: Validation of Manchester Test 7 (a) Axial Force (b) Midspan Deformation

The previous validation discussed the component-based modelling strategies for the sub-frames, in comparison with the experimental test results. Based on the above evidence, there is no doubt of the capability of the numerical model to replicate the fire performance of the sub-frame structure under fire conditions. However, some small discrepancies between the numerical results and experimental tests, as shown in Fig. 8.2 and 8.4, are inevitable. This was because some thermal couples were damaged during the testing and it is impossible to record the temperature variation for every single node in the numerical mesh. If the temperature variation in a small area did not exceed 50°C, we have to assume a uniform temperature distribution in this localized area. However, in reality there was no uniform temperature distribution in the two standard furnace tests. A non-uniform temperature distribution, acting as a thermal imperfection for the specimen, was actually the case, which led to yield and localized plastic buckling in the structural members. As a consequence, the failure mechanism of these steel specimens usually arose from propagation of the localized plastic buckling.

8.3 Parametric Studies

After validating the component-based sub-frame model against experimental results of the Manchester fire tests, an extensive series of numerical studies was undertaken to investigate the performance of connections in a real steel-framed structure when exposed to fire. The parameters investigated included beam span, uniform and non-uniform temperature distributions in beam sections and connections, different load ratios, different load types and different levels of axial restraint afforded by the sub-frame structures. The degree of axial restraint provided was based, firstly on the experimental tests at the University of Manchester and it was assumed that the restraint was provided by the bending stiffness of the steel columns (Fig.8.5 (a)), and secondly on the level of restraint provided by a surrounding cold structure, as shown in Fig. 8.5 (b), which gives stiffer restraints to the sub-frame structure in the horizontal direction. Rotational restraints to the steel beam are maintained by the end-plate connections, and if the connections in both cases are the same, the rotational restraints should be identical.

With respect to the applied load ratios (load ratio is defined as the ratio of the maximum bending moment applied at elevated temperatures to the beam's plastic bending moment capacity as a simply supported beam at ambient temperature), this parametric study adopts two different load levels, load ratios of 0.4 or 0.7, which were utilized in the research work of Yin (2004). Different load types, uniformly distributed load and concentrated load cases, have been taken into account in this analysis, to investigate the effects of different load distributions on the connection performance in a steel frame under fire conditions.

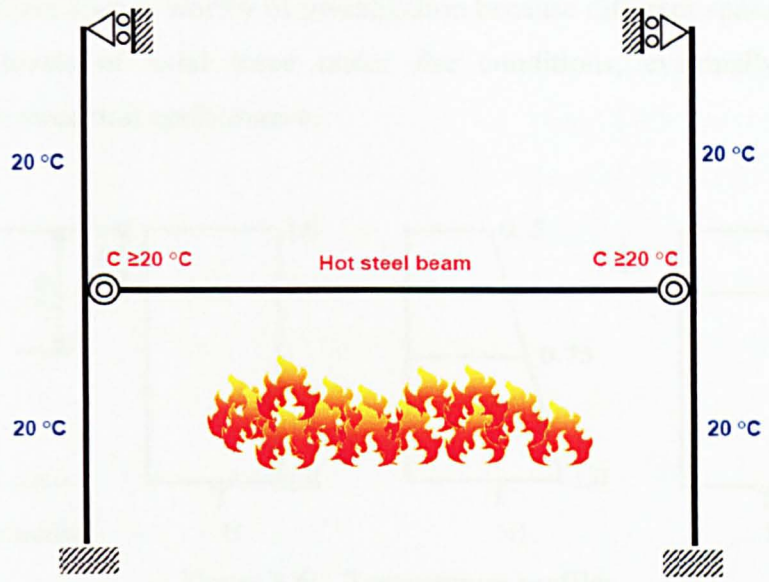

(a)

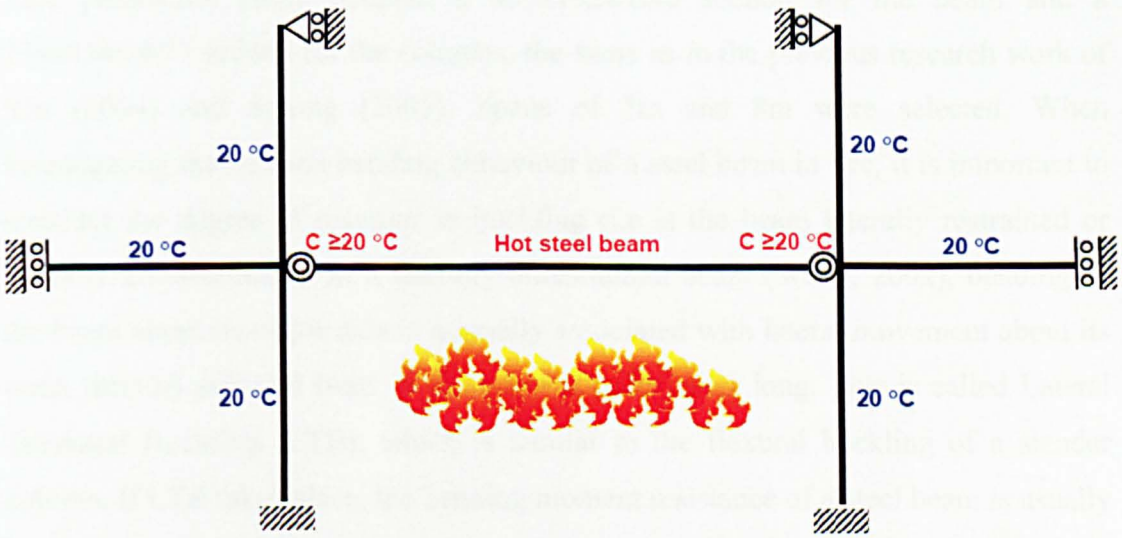

(b)

Figure 8.5: Sub-frame structures for different levels of lateral restraints (a) without lateral beams (b) with lateral beams

Uniform and non-uniform temperature distributions across a beam section were investigated by Yin (2004), and this study assumes similar temperature profiles, as shown in Fig. 8.6. The work of Yin was chosen as a basis because it assumed the connection response as independent lateral and/or rotational springs, whereas the present study represents the connection response by a component-based model capable of modelling the interaction of axial and rotational stiffness. In a real fire situation, the temperature distributions in connection zones are usually non-uniform and the connection response may be affected by these non-uniform temperatures.

Finally, the beam span is worthy of investigation because different spans might result in varying levels of axial force under fire conditions, eventually leading to differences in structural performance.

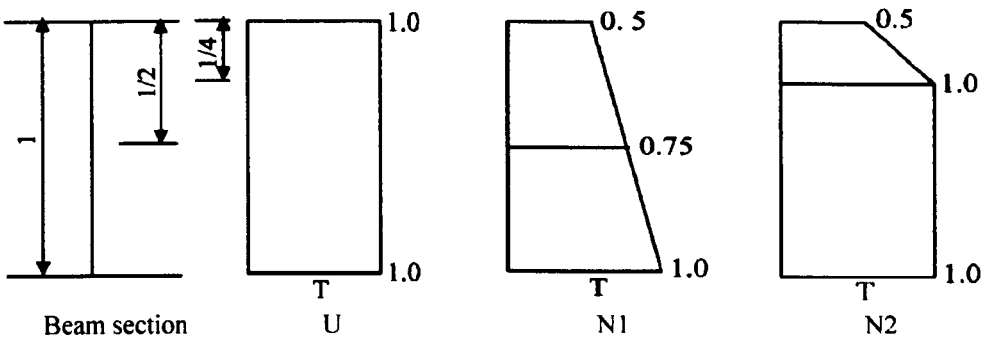

Figure 8.6: Temperature profiles

This parametric study adopted a 457x152UB60 section for the beam and a 254x254UB73 section for the columns, the same as in the previous research work of Yin (2004) and Sulong (2005). Spans of 5m and 8m were selected. When investigating the flexural bending behaviour of a steel beam in fire, it is important to consider the degree of restraint to buckling (i.e is the beam laterally restrained or laterally unrestrained?). In a laterally unrestrained beam (Wang, 2002), bending of the beam about its major axis is normally associated with lateral movement about its weak (minor) axis and twist, if the beam is sufficiently long. This is called Lateral Torsional Buckling (LTB), which is similar to the flexural buckling of a slender column. If LTB takes place, the bending moment resistance of a steel beam is usually much lower than the plastic bending moment capacity of the beam cross section. This is because the beam's slenderness has an effect on its resistance to flexural bending.

However, in a realistic construction, most beams are laterally restrained. In steel composite structures, for example, a simply supported steel beam is laterally restrained by the concrete slabs it supports. If local buckling does not occur, the plastic bending moment capacity of the composite beam cross-section can be reached. In this series of parametric studies, the behaviour of a laterally restrained beam (although not a composite one) and a laterally unrestrained beam under fire conditions will be considered individually, as recommended by Wang (2002).

Before discussing the results of the numerical analysis, it will be helpful to recap on the failure criteria for a steel beam under fire conditions. In Chapter three, the failure criteria for horizontal specimens, recommended by Wang (2002), were referred to. However these criteria of failure are intended for standard fire resistance tests of isolated bending elements. In structures where catenary action can develop, the contribution of bending resistance is usually small and different failure criteria should be used (Wang, 2002). Failure of a restrained steel beam in catenary action may be deemed to occur when any of the following takes place:

- The beam deflection is high enough to cause integrity failure of the building's FR compartmentation
- The steel beam fractures
- The adjacent structure, including connections, cannot resist the catenary force of the steel beam.

The above failure criteria relate to a restrained steel beam in catenary action in a fire situation. However, based on the experimental work in Chapter 5, failure of flexible end-plate connections at elevated temperatures was due to the rupture of the end-plates close to the welds (in the heat affected zone), which took place before the bottom beam flange was in contact with the column flange. The ductility of these connections is reduced in fire. In the analytical research on connections in Chapter 6, the author applied the component-based connection model to explain the connection performance in Chapter 5 and found the failure of end-plate connections was due to the brittle failure of fillet welds. Furthermore, in the experimental research work of Kanvinde et al. (2009) on fillet welds, the fracture displacements of the fillet welds in tests were found to be in the range 0.71 mm to 1.93 mm. The weld component in the component-based connection model has also been found to be the weakest element in the analysis. If extension of weld components exceeds this limited range (0.71mm – 1.93mm), the weld components are assumed to be 'fractured' and the connection model starts the failure propagation to form plastic hinges in the analysis.

8.3.1 Load types and span length

As mentioned already, uniformly distributed and concentrated load cases have been considered in this numerical analysis. Since the applied load ratios (0.4 and 0.7) have been defined as the ratio of the maximum bending moment of a simply supported beam to the plastic bending moment capacity of the beam at ambient temperature, the plastic moments at mid-span should be the same for these two loading cases. Apart from the applied load ratios and load types, this section has one more parameter involved in the investigation, which is the beam span. The connections for both loading cases are represented by component based models and the lateral restraints are provided by the bending stiffness of the steel columns, as shown in Fig 8.5 (a). Connection type is not a variable in this investigation.

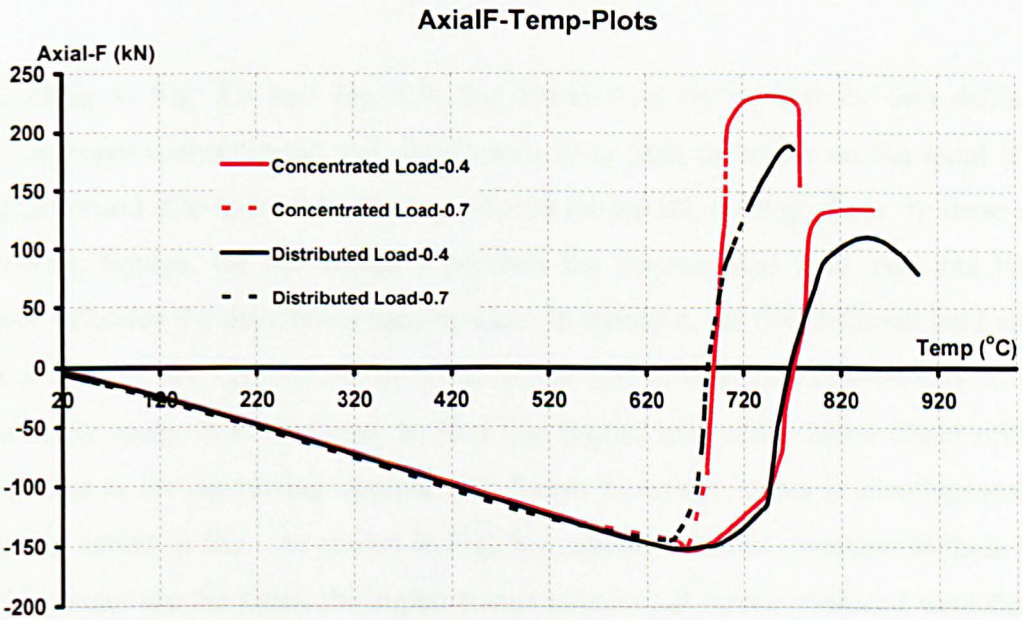

(a) Span = 5 m

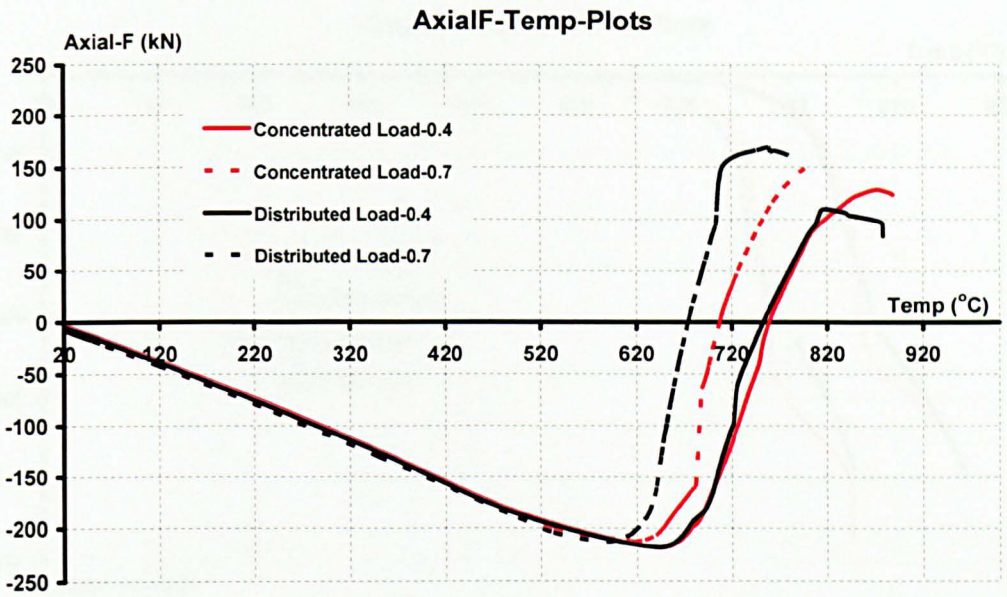

(b) Span = 8 m

Figure 8.7: The axial force variation in two different spans for two load types

According to Fig. 8.6 and Fig. 8.7, the observation shows that the two different loading types (concentrated and distributed) have little influence on the axial force variations and mid-span deflections produced during the heating phase. In these and following figures, the red colour represents the concentrated load case and black colour indicates the distributed loading case. In addition, the two different load ratios of 0.4 and 0.7 are symbolized by solid curves and dotted lines respectively in this parametric study. It is also easy to find that higher load ratios cause lower critical temperatures for converting compressive forces to tensile forces in development of catenary action in fire. As shown in Fig. 8.6, since the lateral restraints in these two loading cases are the same, the higher compressive axial forces produced were due to thermal expansion of the longer span beam (8m).

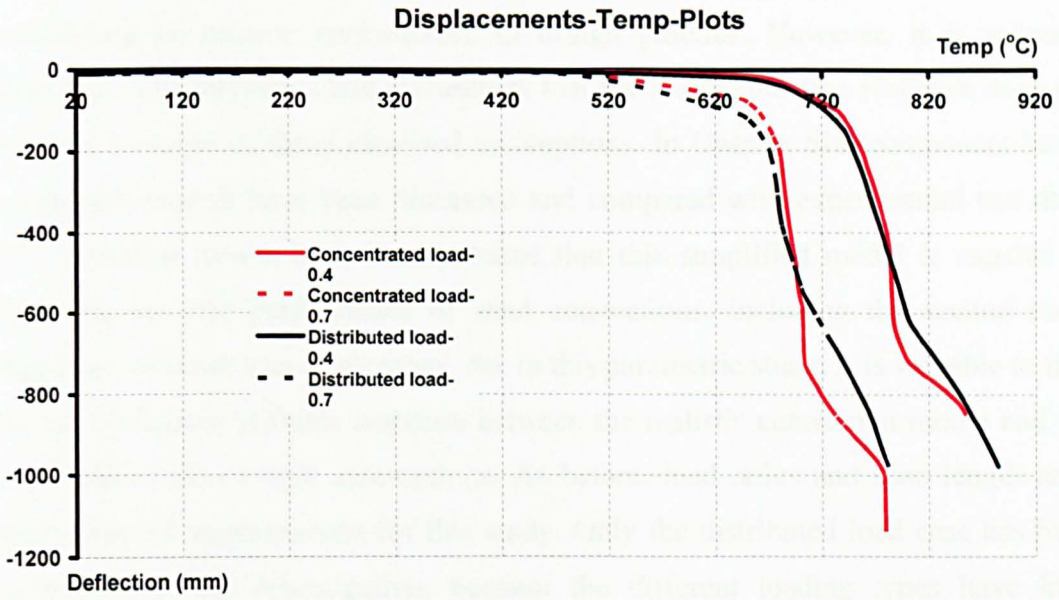

(a) Span = 5 m

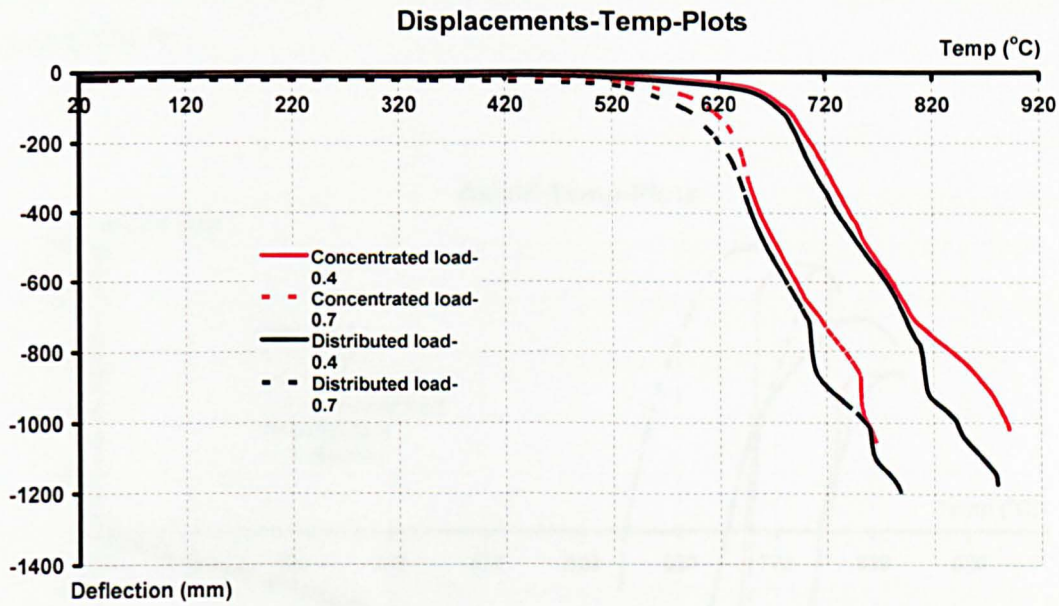

(b) Span = 8 m

Figure 8.8: Central deflections in two different spans for two load types

8.3.2 Pin, rigid connection assumptions and component-based connections

As indicated in Chapter 2, steel connections are usually assumed as pinned or rigid in design practice. The 'pin' assumption defines the connection as capable of resisting shear forces only, with no moment resistance. For 'rigid' (or continuous) construction, the connections have the capability of transmitting moment, shear and

axial forces. These assumptions are made to permit a simplified procedure for considering connection performance in design practice. However, it is acknowledged by both engineers and researchers that the real connection response does not conform to either of these idealised assumptions. In Chapter Six, component-based connection models have been discussed and compared with experimental test data. The analytical results have demonstrated that this simplified model is capable of capturing the real performance of steel connections, including the second stage behaviour, without loss of accuracy. So, in this parametric study, it is valuable to find out the difference in frame response between the realistic connection model and the conventional pin-or-rigid assumptions. As before, load ratios and span length have been accepted as parameters for this study. Only the distributed load case has been considered in this investigation, because the different loading types have little influence on the structural performance under fire conditions. The connections have been assumed to be fully protected in fire, so their maximum temperatures cannot exceed 400 °C.

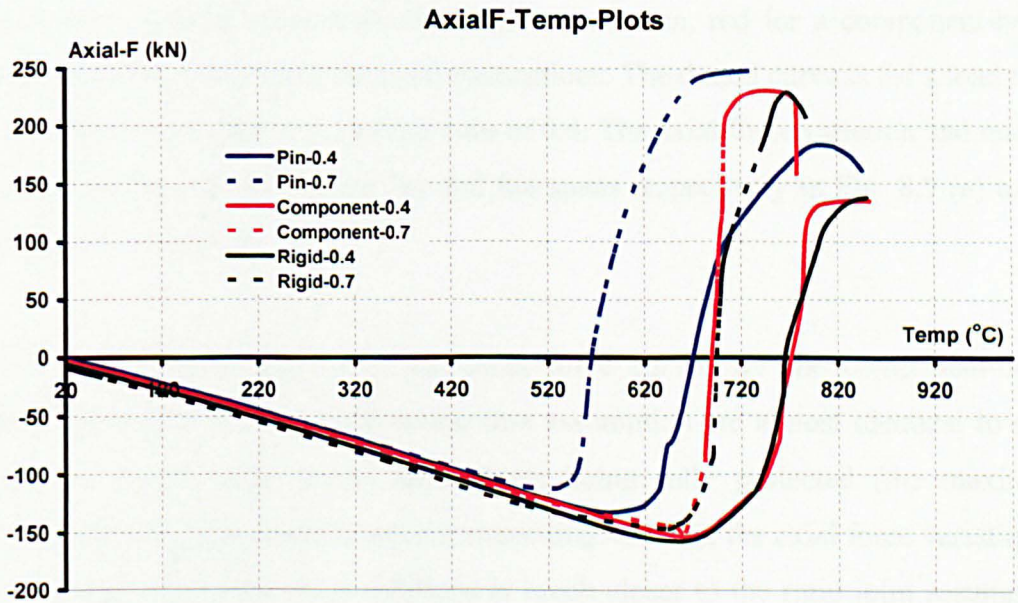

(a) Span = 5 m

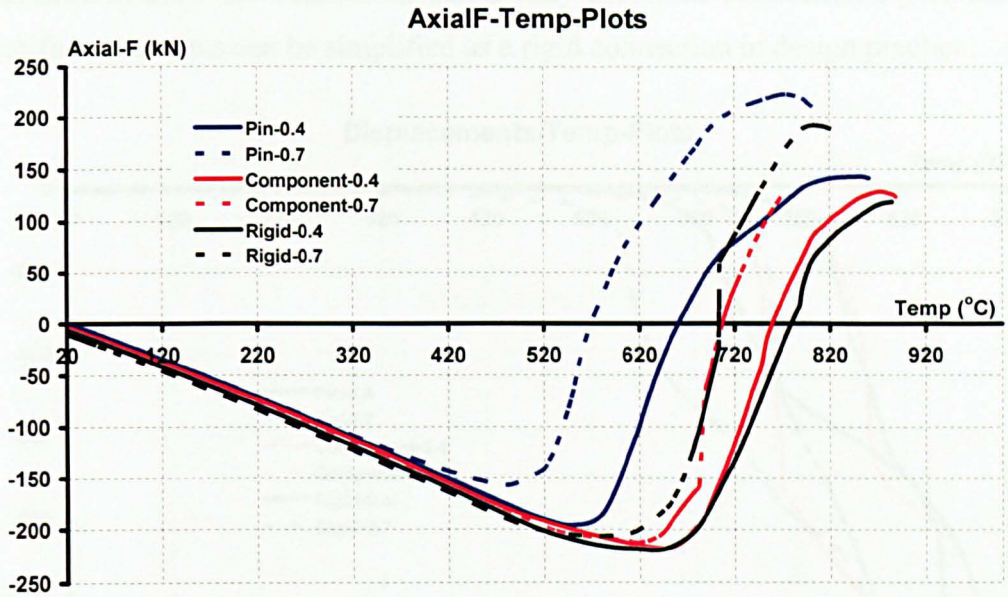

(b) Span = 8 m

Figure 8.9: Axial force variation in two different spans for different connection assumptions

In the figures (Fig. 8.9 and Fig. 8.10), the colours represent different connection assumptions: blue is associated with a pin connection, red for a component-based connection model and black for rigid connections. The dotted curve is for a load ratio of 0.7 and the solid line is for a load ratio of 0.4. The axial force variation and middle span deflections are plotted for 5m and 8m spans respectively in Fig. 8.9 (a) to (b) and Fig. 8.10 (a) to (b).

In the above figure (Fig. 8.9), the axial force curves for the component-based connection model and the rigid connection assumption are almost identical to each other. So, in the case of the connections being fully protected (the maximum temperatures of these connections not exceeding 400 °C), the axial force variation of a real connection under fire conditions is much closer to the rigid joint assumption used in design practice.

However, to have more confidence in this finding, it is valuable to check with the mid-span deflections of steel beams under fire conditions. As displayed in Fig. 8.10, the mid-span deflections for the component-based connection model have been found to be in agreement with the rigid connection assumption. Hence it appears

reasonable to draw the conclusion that a fully protected connection's performance under fire conditions can be simplified as a rigid connection in design practice.

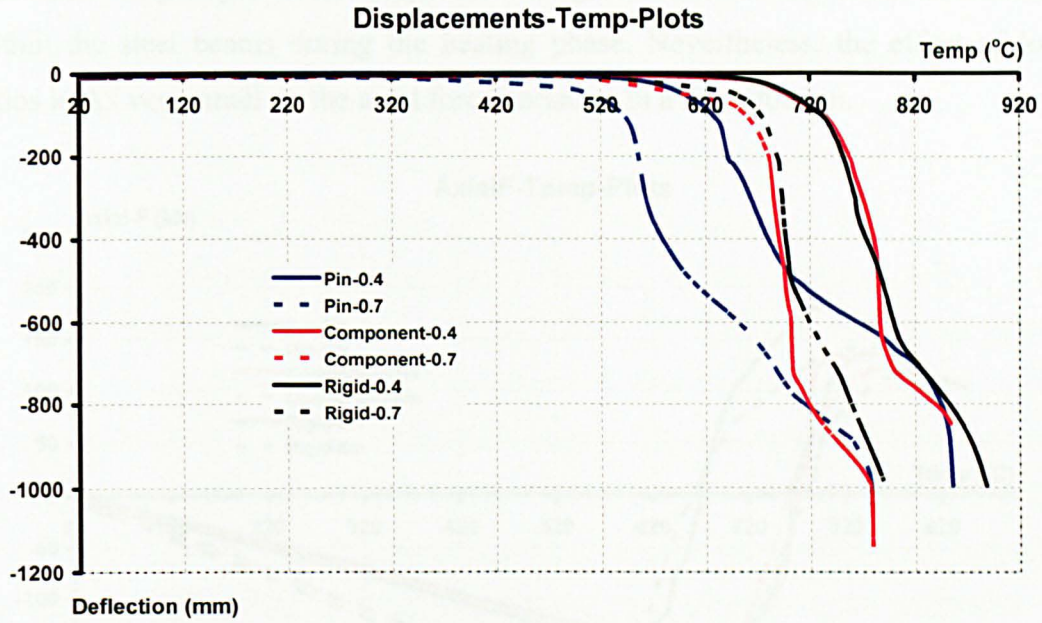

(a) Span = 5 m

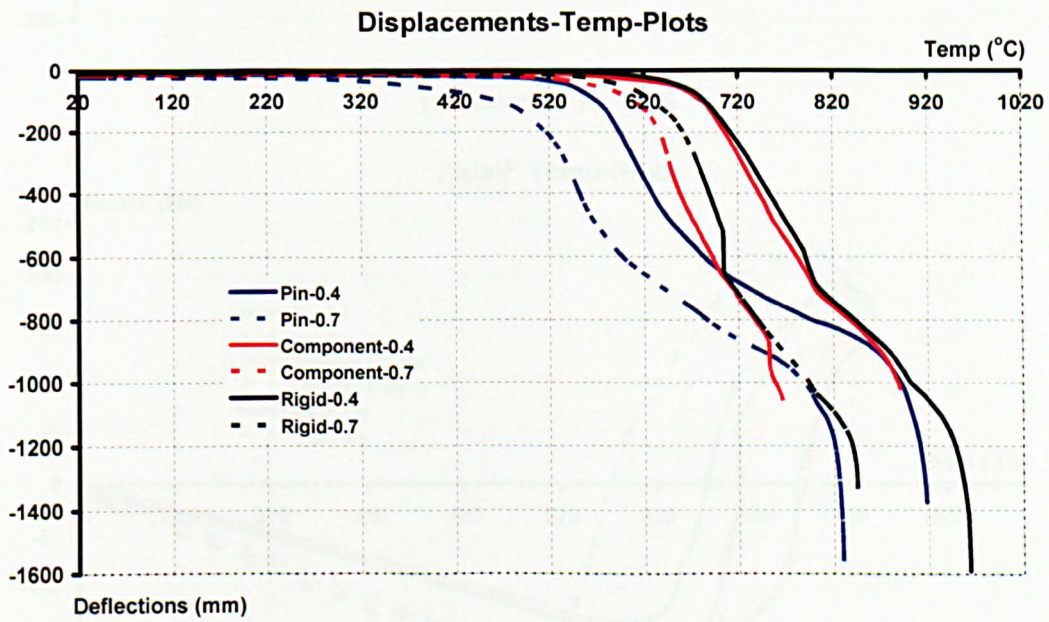

(b) Span = 8 m

Figure 8.10: Central deflections in two different spans for different connection assumptions

Fig. 8.11 is a rearrangement of Fig. 8.9 to discover the effects of beam span length on the axial compressive forces due to the restraint of thermal expansion of steel beams. As before, the colours still represent the different connection assumptions.

The dotted curve is for the structural response of an 8m span, and the solid curve shows the performance under fire conditions for the shorter span. As demonstrated below, the longer span is able to produce a higher level of compressive axial forces within the steel beams during the heating phase. Nevertheless, the effect of load ratios looks very small on the axial force variation in a fire situation.

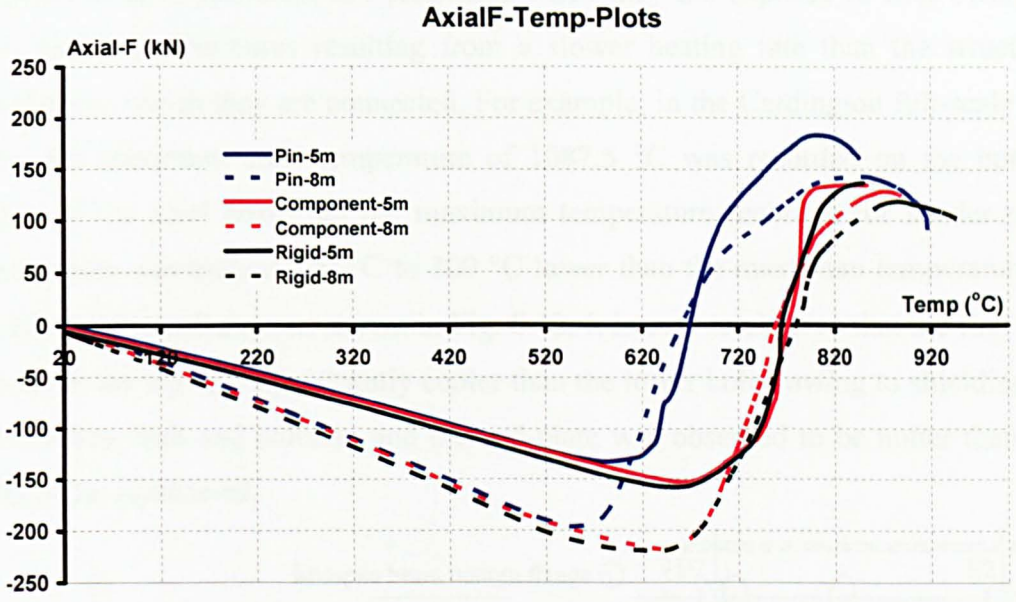

(a) Load ratio = 0.4

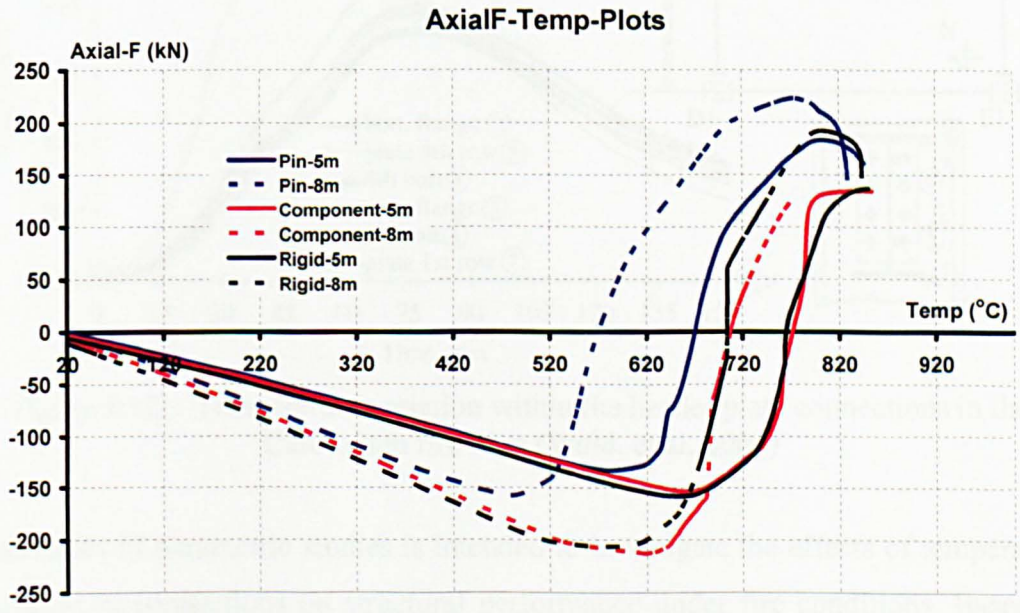

(b) Load ratio = 0.7

Figure 8.11: Axial force variation with two different load ratios for different connection assumptions

8.3.3 Connection temperatures

The previous discussion is based on steel connections which have been fully protected under fire conditions. However, many steel beam-to-column connections in design practice are left without fire protection. This is because these connections are assumed to have sufficient fire resistance when they are exposed to fire, owing to their cooler temperatures resulting from a slower heating rate than the structural members to which they are connected. For example, in the Cardington full-scale fire tests, the maximum steel temperature of 1087.5 °C was recorded on the bottom flange of the steel beam but the maximum temperature recorded for header plate connections was around 200 °C to 300 °C lower than the maximum temperature of the beam bottom flange, as shown in Fig. 8.12. It is easy to observe that the first bolt row from the top was significantly cooler than the lower bolts, owing to shielding by the concrete slab and column, and the end-plate was observed to be hotter than the bolts at the same level.

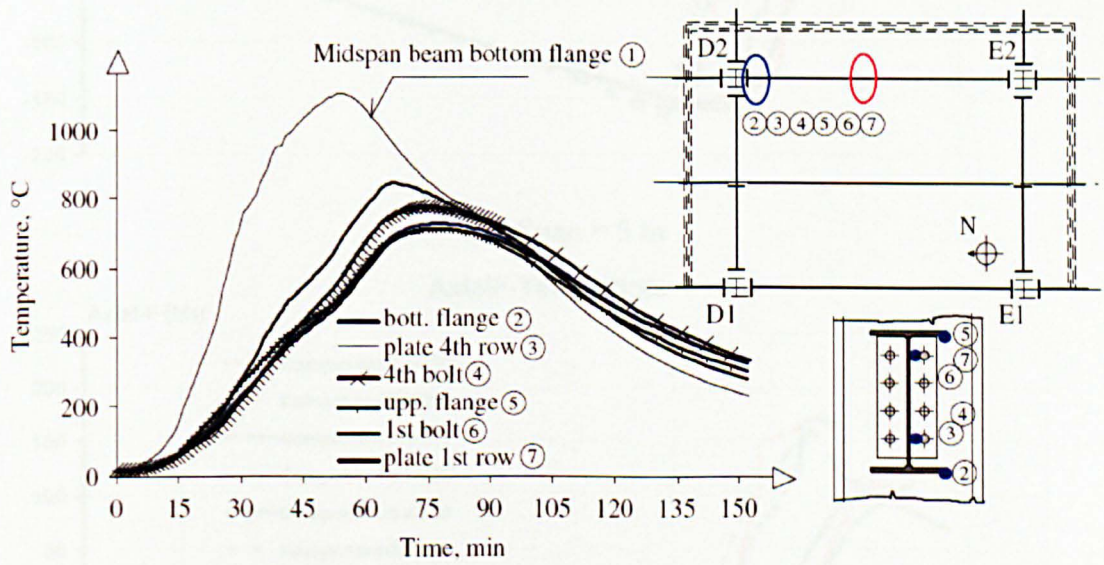

Figure 8.12: Temperature variation within the header plate connections in the Cardington fire tests (Wald, et al. 2006)

This series of parametric studies is intended to investigate the effects of temperature variation in connections on structural performance under fire conditions. Based on the temperatures reported in the Cardington fire tests, the connection temperature was focused on the temperature range of 600 °C to 800 °C, and was assumed to be uniformly distributed in the numerical analysis. So three connection temperatures (600 °C, 700 °C and 800 °C) have been taken into account and the beam temperature

has been assumed to reach 1000 °C within one hour in the finite element analysis. To observe the connection failure mechanism, the failure criteria for the connections need to be repeated here. In previous experimental results (Kanvinde et al., 2009), the fracture displacements of fillet welds were found to be in the range of 0.71 mm to 1.93 mm. So, if the weld component in the numerical analysis exceeds this failure displacement range, the connection has been assumed to start the failure propagation, and finally two plastic hinges have been formed within the connection zones.

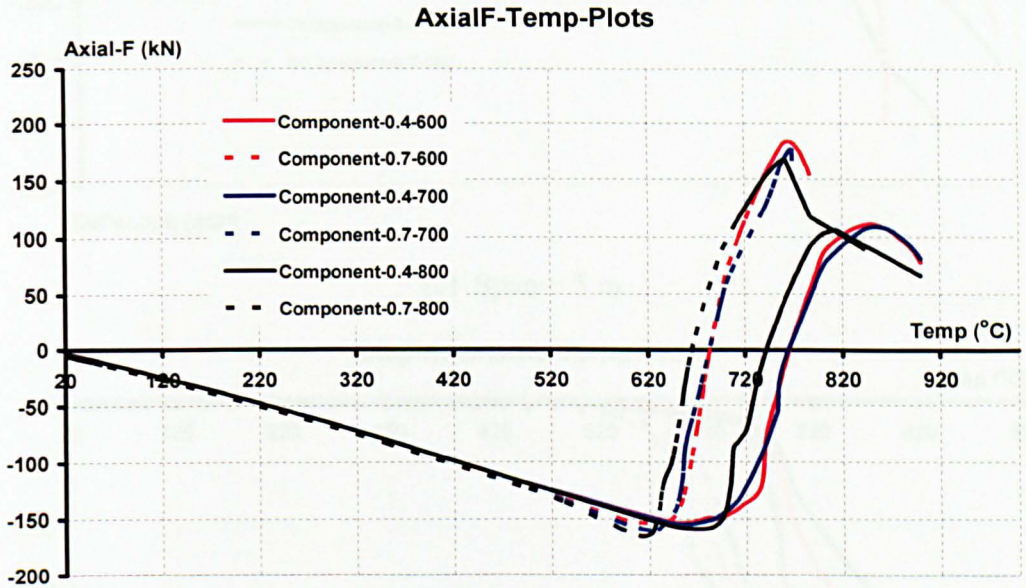

(a) Span = 5 m

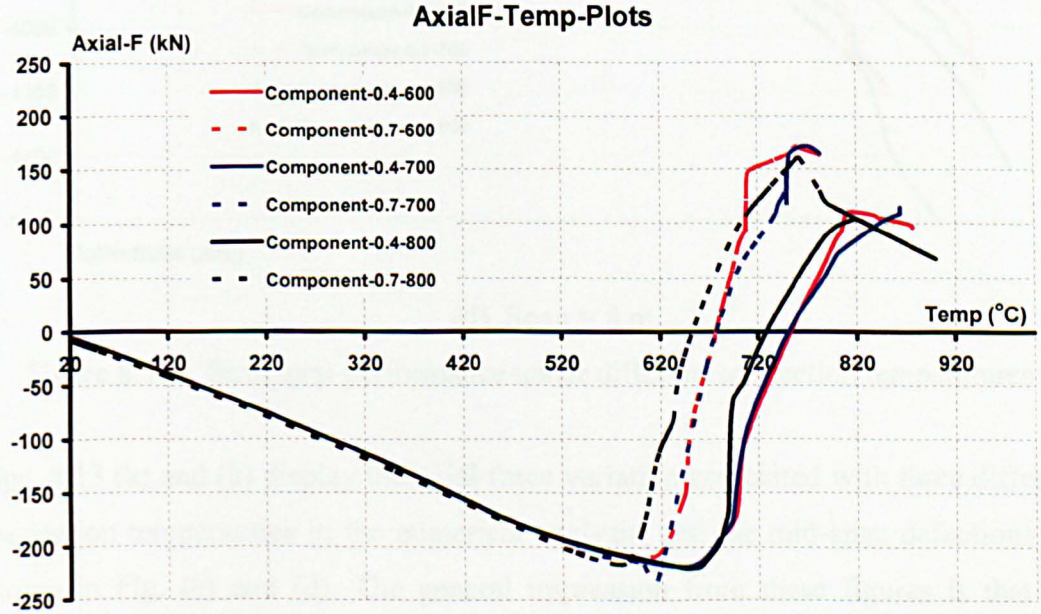

(b) Span =8 m

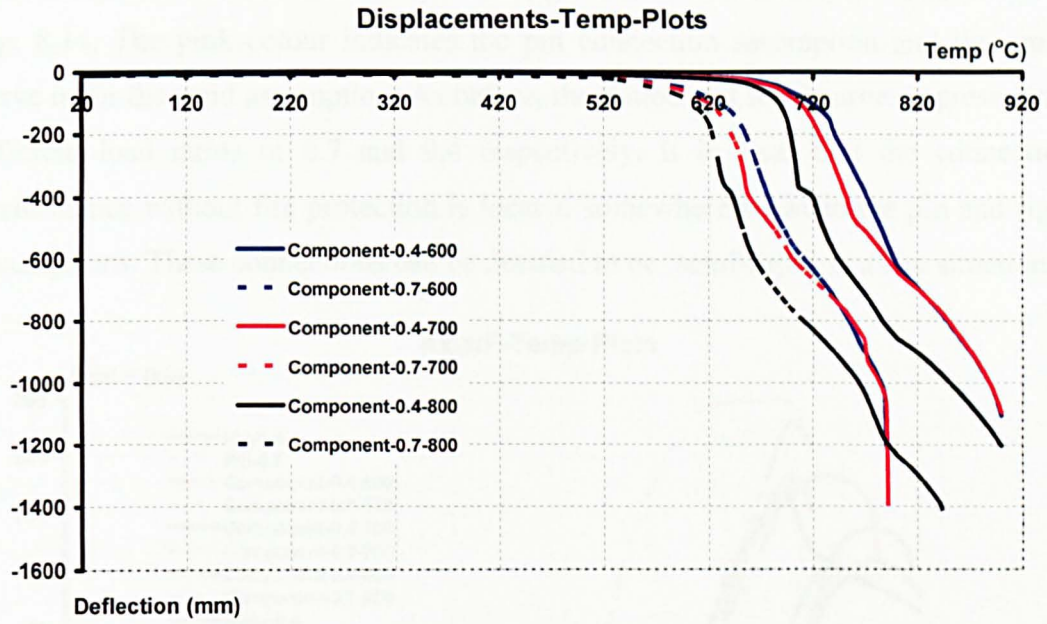

(c) Span = 5 m

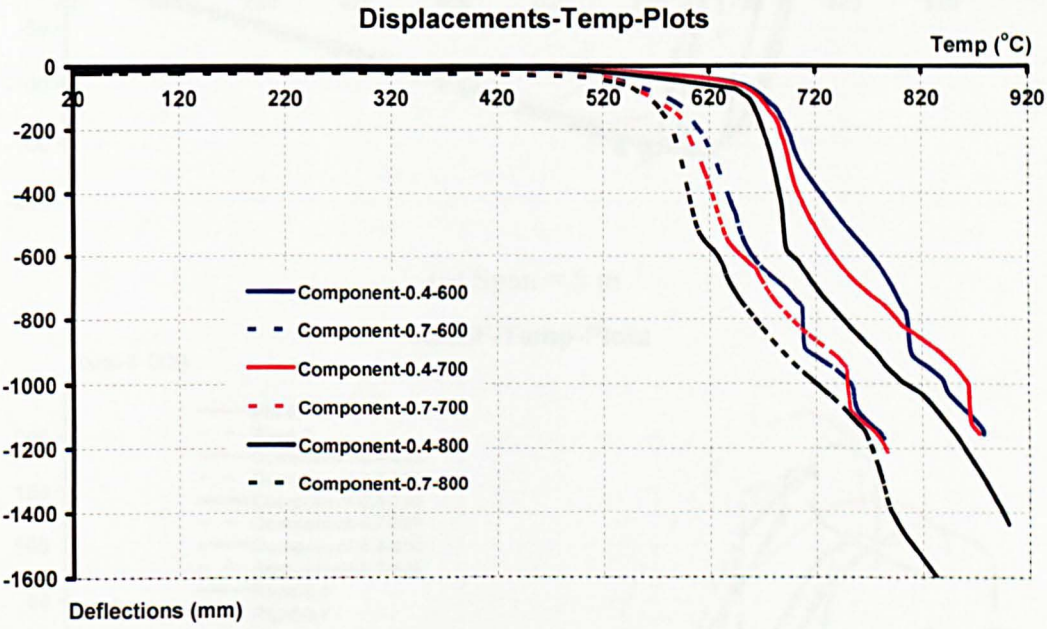

(d) Span = 8 m

Figure 8.13: Structural performance under different connection temperatures

Figs. 8.13 (a) and (b) display the axial force variation associated with three different connection temperatures in the numerical analysis, and the mid-span defections are shown in Fig. (c) and (d). The general impression from these figures is that the connection temperature variation has little influence on the axial force and mid-span deflections in a fire situation, although the load ratios have a high influence. In addition, the connection performance associated with very high temperatures has

been compared with that from the pin and rigid connection assumptions, as shown in Fig. 8.14. The pink colour indicates the pin connection assumption and the green curve is for the rigid assumption. As before, the dotted and solid curves represent the different load ratios of 0.7 and 0.4 respectively. It is clear that the connection performance without fire protection is located somewhere between the pin and rigid assumptions. These connections can be deemed to be 'semi-rigid' in a fire situation.

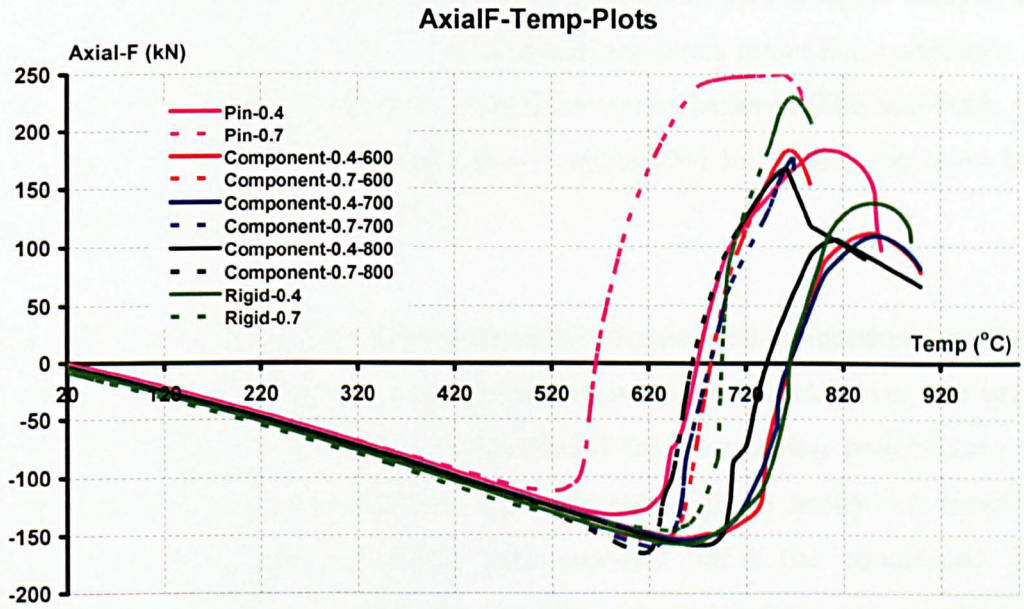

(a) Span = 5 m

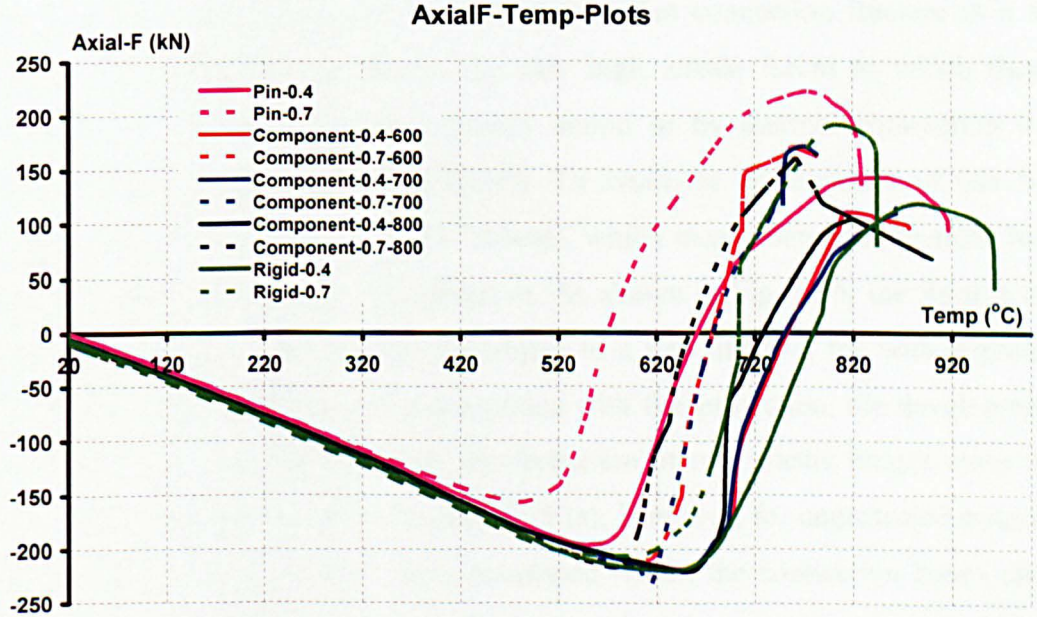

(a) Span = 8 m

Figure 8.14: Comparison of axial force variation between unprotected connections and nominal pin & rigid assumptions

The previous discussion has already demonstrated the nature of the semi-rigidity of end-plate connections under fire conditions in a sub-frame structure. As a substantial parameter, the ratio of connection temperature to beam (bottom flange) temperature ($R_{T.cb}$) should be stressed in the discussion of the connection failure mechanism. According to the Cardington fire tests, the ratio of connection temperature to beam temperature is in the range of 0.65 to 0.85 (Wald, et al., 2006), and the research work completed by Sulong (2005) adopted the value of 0.7 in his numerical analysis as the temperature ratio between these two structural members under fire conditions. The above numerical studies assumed temperature ratios between 0.66 and 0.88, which indicates that the connection temperature is about 75% lower than the beam bottom flange temperature in a fire situation.

As mentioned in Chapter 2, in design practice simple steel connections are assumed to behave as pin connections between beams and columns. However, the previous component-based modelling has demonstrated that connection performance under fire conditions is neither pinned nor rigid, but semi-rigid in reality (i.e. simple steel connections are capable of taking some moment under fire conditions). In the discussion of structural performance in fire, catenary action was expected to be developed in fire, creating a catenary force in the beam to help with structural survival under fire conditions. It was believed that connection fracture in a steel-framed structure could be due to the very high tensile forces to which they are subjected in fire, produced by catenary action or by thermal contraction in the cooling process of very hot steel beams. To avoid the development of this failure mechanism connections need to be 'robust', which means these connections require flexibility and strength in a fire situation. As shown in Fig. 8.15, the finite element analysis covers catenary actions developed in a fire situation for both unprotected and protected connections. For connections with fire protection, the development of catenary action was dependent on the formation of two plastic hinges close to the ends of the steel beams, shown in Fig. 8.15 (a). However, for unprotected connection cases, the two plastic hinges were developed within the connection zones on both sides, as shown in Fig. 8.15 (b), illustrating that the unprotected connection was much more flexible under fire conditions than the connection with fire protection.

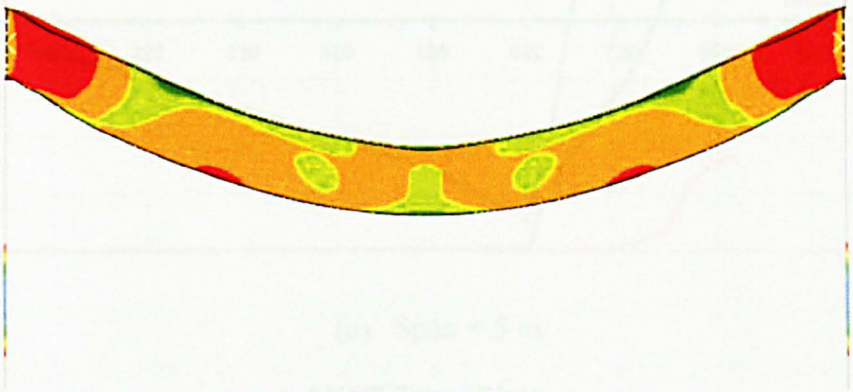

(a) Connections with fire protections

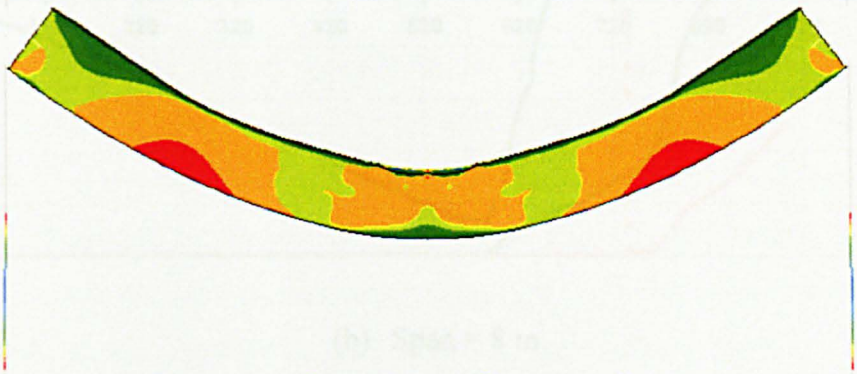

(b) Connections without fire protections

Figure 8.15: Typical deformed shape of sub-frame (a) with fire protection (b) without fire protection to connections

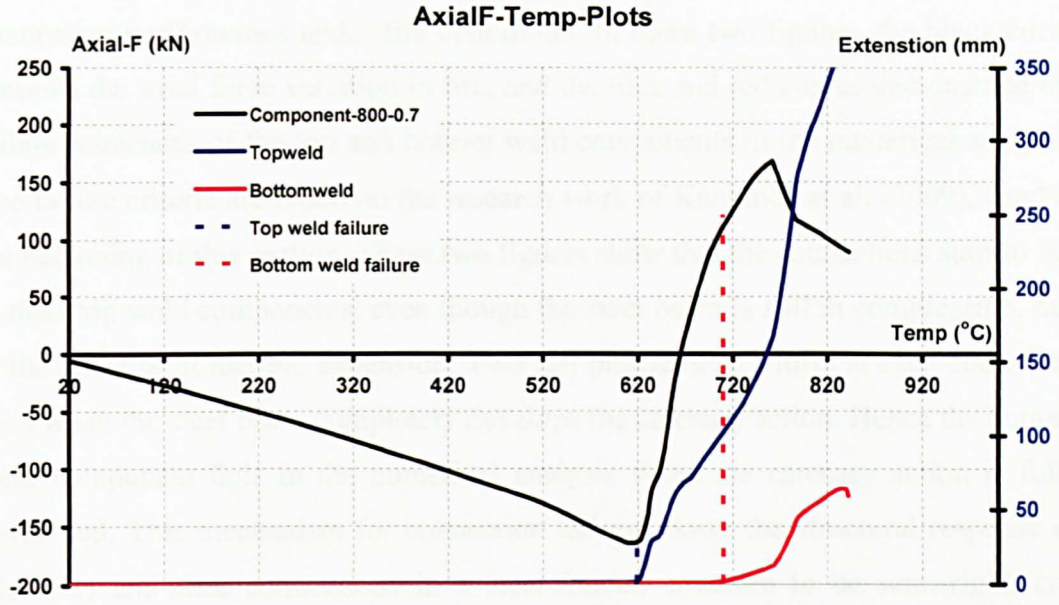

(a) Span = 5 m

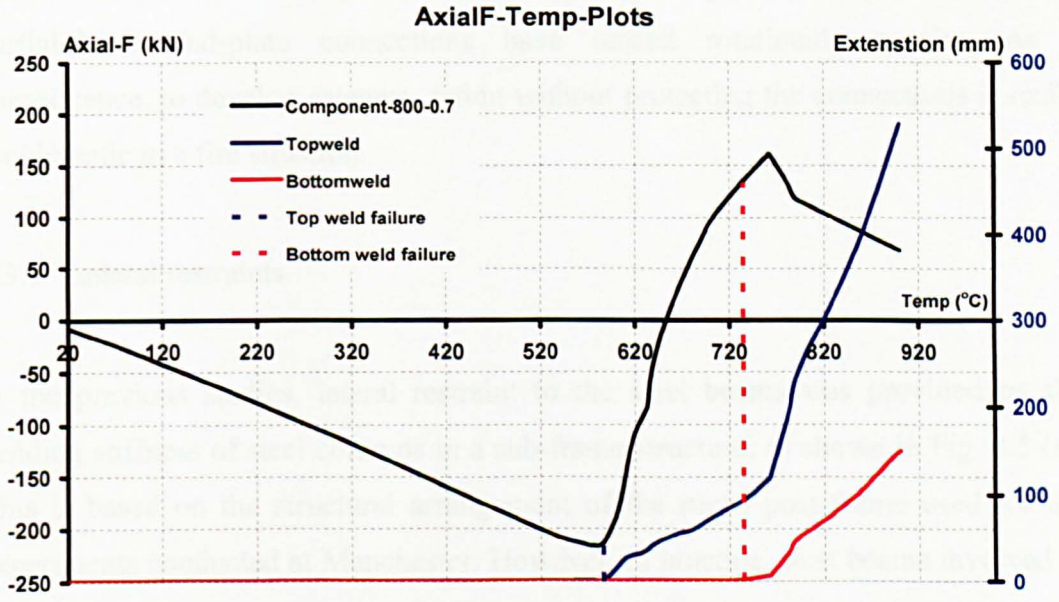

(b) Span = 8 m

Figure 8.16: Relationships between axial force variation and connection failure propagation

According to Fig. 8.15 (a), the connections with fire protection are capable of providing a very strong tie between columns and beams in a fire situation. However, for the unprotected connection cases, especially when fillet welds were the weakest components in a connection, the flexibility (ductility) of unprotected connections is more likely to be a concern under fire conditions. Figs. 8.16 (a) and (b) present the

relationships between the axial force variation within a steel beam and the connection performance under fire conditions. In these two figures, the black curve presents the axial force variation in fire, and the blue and red curves demonstrate the failure sequences of the top and bottom weld components in the numerical analysis. The failure criteria are based on the research work of Kanvinde et al. (2009), cited at the beginning of this section. These two figures show that the connections start to fail in their top weld components, even though the steel beam is still in compression, due to the restraint of thermal expansion. Two full plastic hinges form at each end of the span when the steel beam completely develops the catenary action. Hence the bottom weld component fails in the numerical analysis when the catenary action is fully developed. This mechanism for connection failure shows the structural response of (flexible) end-plate connections in a steel-framed structure to be semi-rigid, and therefore the connection failure might be caused by a lack of rotational capacity in a fire situation rather than by lack of strength. In the previous experimental tests, partial-depth end-plate connections have lacked rotational capacity. As a consequence, to develop catenary action without protecting the connections is really problematic in a fire situation.

8.3.4 Lateral restraints

In the previous studies, lateral restraint to the steel beams was provided by the bending stiffness of steel columns in a sub-frame structure, as shown in Fig. 8.5 (a). This is based on the structural arrangement of the rugby-post frame used for the experiments conducted at Manchester. However, in practice, steel beams involved in a compartment fire are not only restrained by the steel columns on both sides, but are also restrained by the surrounding cold structure, especially by the beam system in the adjacent compartment, as shown in Fig. 8.5 (b). This part of the research concentrates on two different levels of lateral restraint in fire, as already shown in Fig. 8.5. The connection temperature has been assumed to approach the maximum temperature of 800 °C within 60 minutes, and steel beams are expected to reach much higher temperature in the same fire scenario. The beams outside the fire affected area have been assumed to remain cold.

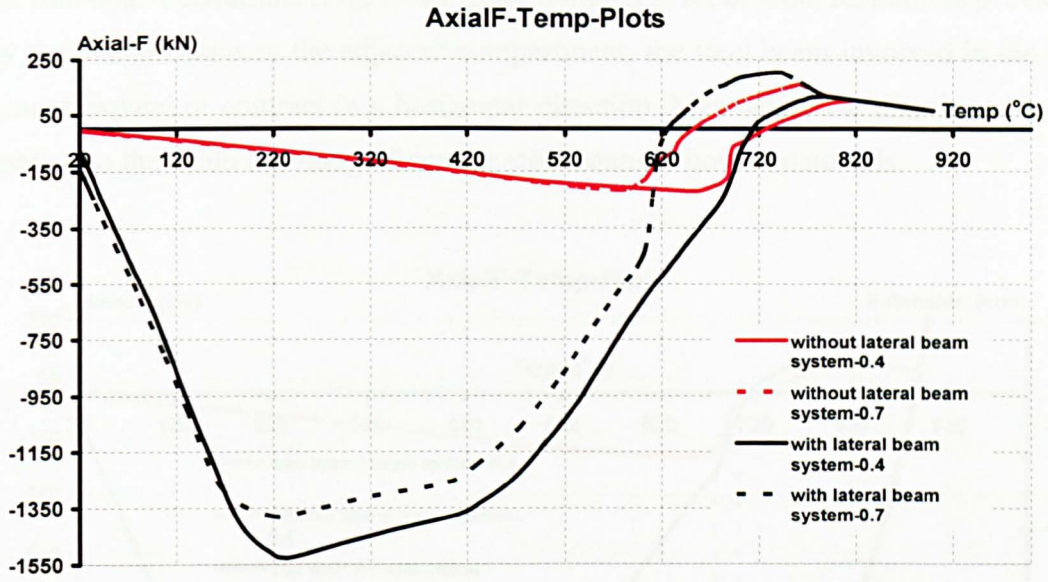

Figure 8.17: Axial force variations for different levels of lateral restraints

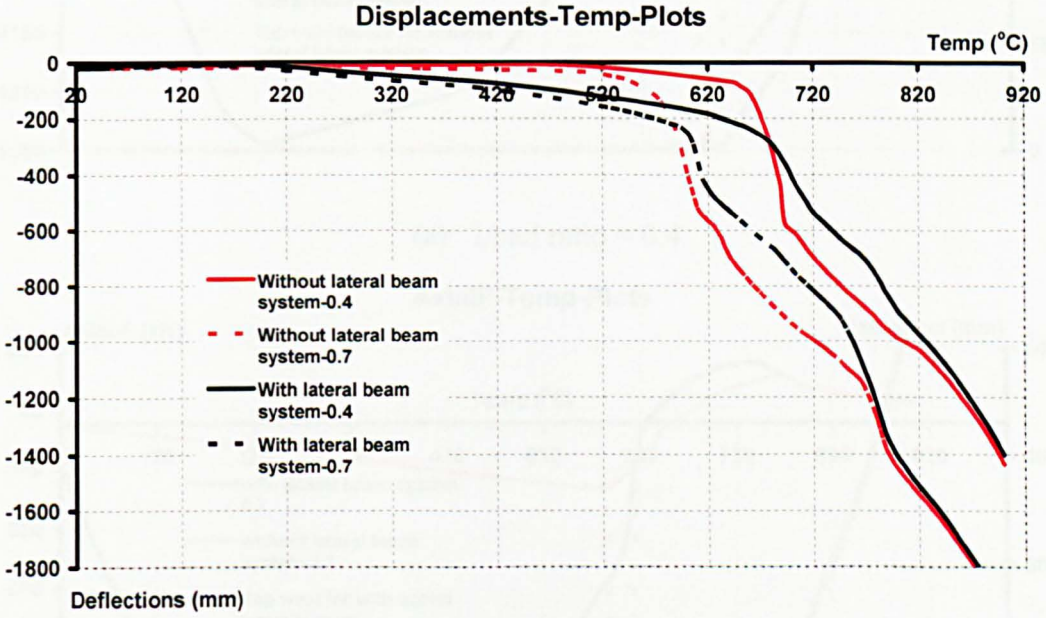

Figure 8.18: Deflections in mid-span for different levels of lateral restraints

As displayed in Fig. 8.17, two different levels of lateral restraint have been examined for two different load ratios. Note that the structural arrangement with the lateral beam system (Fig. 8.5 (b)) applies a higher level of axial restraint to the steel beams in a fire situation, so the magnitude of axial force variation in this structural arrangement is dramatically larger than that in the structural arrangement shown in Fig. 8.5 (a). It is also observed that the effect of load ratio is very small on the maximum compressive axial forces in the same structural arrangement. In the figure

for mid-span deflections (Fig. 8.18), since a higher level of axial restraint is provided by the lateral beams in the adjacent compartment, the steel beam involved in the fire cannot expand or contract in a horizontal direction. Meanwhile the distributed loads applied to the beam top flange force the steel beam to bow downwards.

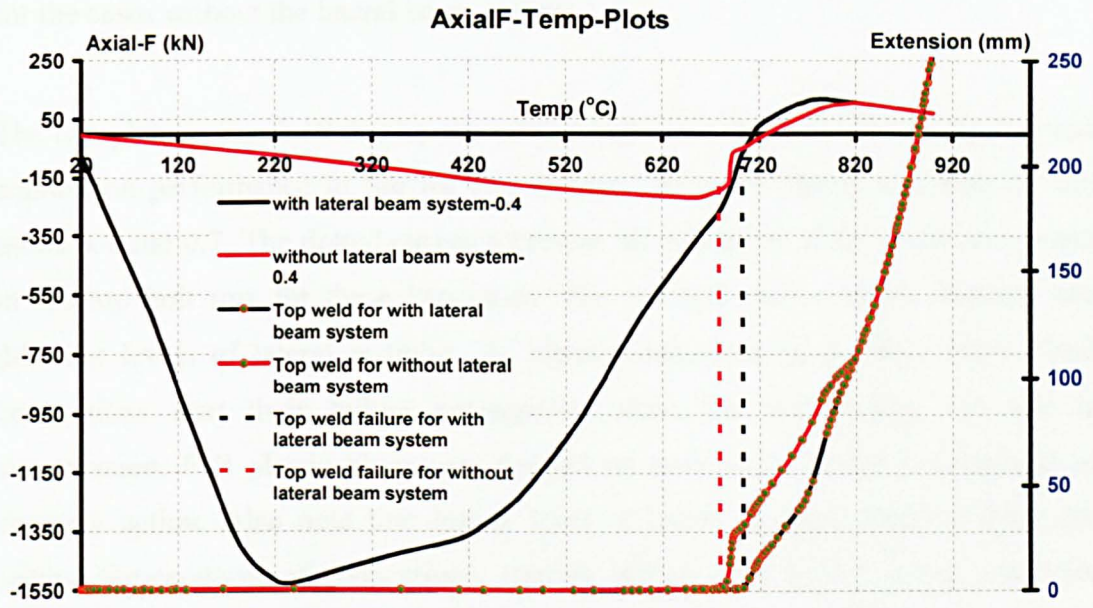

(a) Load ratio = 0.4

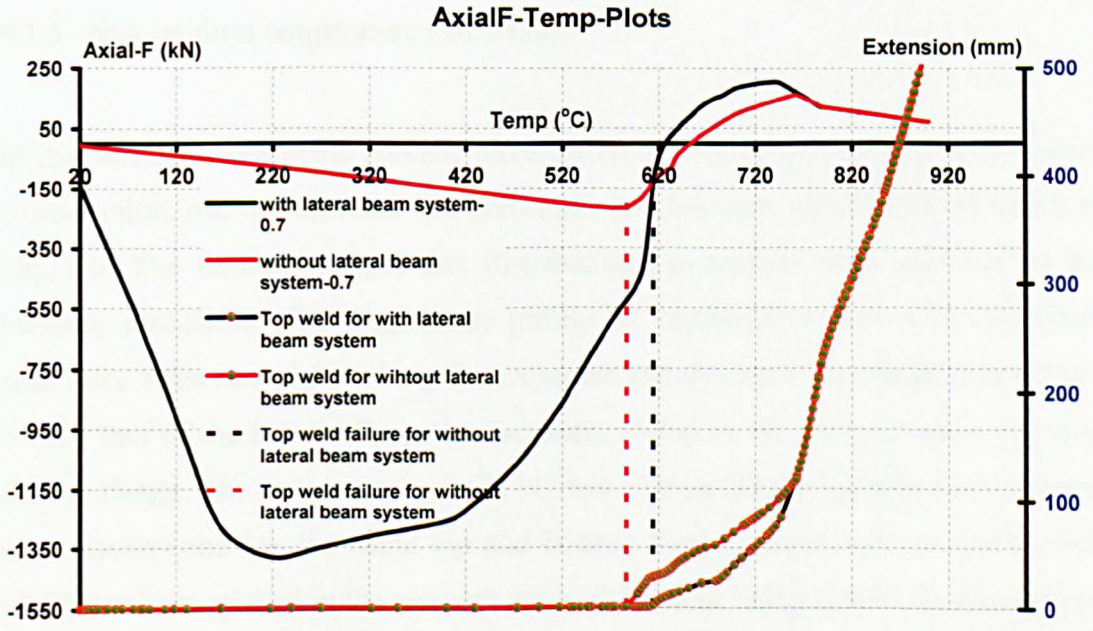

(b) Load ratio = 0.7

Figure 8.19: Relationships between axial force variation and connection failure propagation for 8 m span

For the mid-span deflections, the structural arrangement without the lateral beam system (shown as red curves in Fig. 8.18) has been compared with the case with a much higher level of lateral restraint (shown as black curves in Fig. 8.18). Note that the mid-span deflections for the latter cases are much easier to be observed in the numerical simulation and their maximum deflections are obviously higher than those for the cases without the lateral beam system.

The two plots in Fig. 8.19 display the relationships between axial force variation and connection performance in fire for two different levels of lateral restraints at load ratios 0.4 and 0.7. The dotted curves represent the extension of the weld component in the top bolt row for these two cases. The red and black colours indicate two different levels of lateral restraint. As already demonstrated in these plots, these connections start their failure propagation when the steel beams are still in compression. Full plastic hinges are formed on both sides in the development of catenary action. Also note that higher level of lateral restraint tends to raise the critical temperatures of connections, starting failure a bit higher in the same fire scenario.

8.3.5 Non-uniform temperature distribution

In this series of parametric studies, three different temperature profiles in the beam cross-section, one uniform and two non-uniform, have been considered, as shown in Fig. 8.6. The uniform temperature distribution has already been analysed in the previous discussion. The temperature profile N2 represents a case of a steel beam with three sides heated for a long fire exposure and the top beam flange temperature is only half of the bottom flange temperature, owing to the concrete slabs covering the top flange. The temperature profile N1 has a linear thermal gradient in the beam cross section and has the same top and bottom flange temperatures as profile N2, which has been studied in the research work of Yin and Wang (2003). In the study of non-uniform temperature profiles, connection temperatures were assumed to approach 800 °C within 60 minutes, and the beam bottom flange temperatures reached over 900 °C. Only the structural arrangement shown in Fig. 8.5 (b) has been taken into account for the 8 m span beam with a load ratio of 0.7.

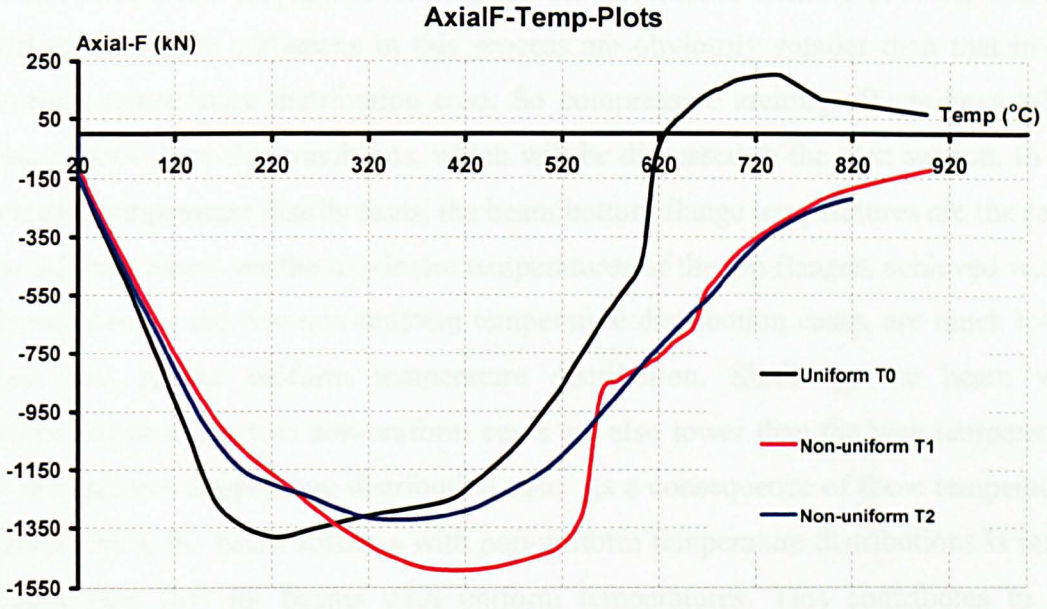

(a) Axial force variation

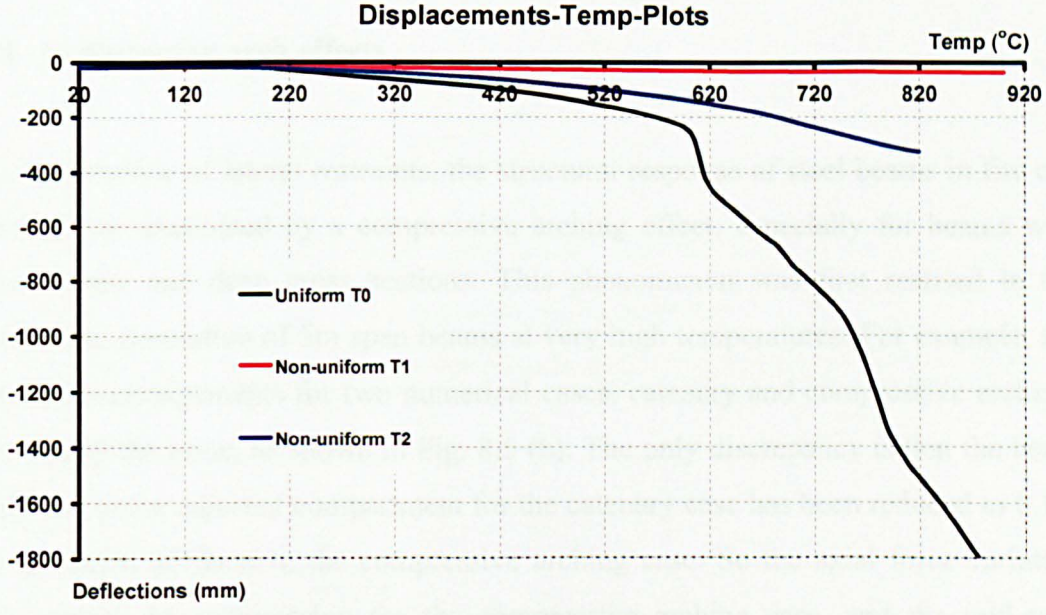

(b) Mid-span deflections

Figure 8.20: Comparison of different temperature profiles in beam cross sections (a) Axial force variation (b) Mid-span deflections

The plots shown in Fig. 8.20 display the structural responses of a sub-frame under different temperature distributions, including two non-uniform temperature profiles and one for uniform temperature distribution. As shown in this figure, catenary action has been developed only for a beam cross-section with uniform temperature profiles. For the two non-uniform temperature distribution cases, compressive axial

forces have been propagated throughout the continuous heating process, and the deflections at the mid-spans in this process are obviously smaller than that in the uniform temperature distribution case. So compressive arching effects have taken place under these fire conditions, which will be discussed in the next section. In the selected temperature distributions, the beam bottom flange temperatures are the same for all three cases, yet the maximum temperatures of the top flanges, achieved within 60 minutes for the two non-uniform temperature distribution cases, are much lower than that in the uniform temperature distribution. Similarly, the beam web temperatures in the two non-uniform cases are also lower than the web temperature in the uniform temperature distribution case. As a consequence of these temperature distributions, the beam stiffness with non-uniform temperature distributions is much higher than that for beams with uniform temperatures. This contributes to the development of compressive arching effects in this numerical analysis.

8.4 Compressive arch effects

In the presence of lateral restraints, the structural response of steel beams in fire can initially be dominated by a compressive arching effect, especially for beams with short spans and deep cross sections. This phenomenon was first realised in the numerical simulation of 5m span beams at very high temperatures. For example, the structural arrangements for two numerical cases, catenary and compressive arching, are nearly the same, as shown in Fig. 8.5 (b). The only discrepancy is that the beam stiffness in the adjacent compartment for the catenary case has been reduced to 0.1% of the beam stiffness in the compressive arching case. So the axial force variation was always in compression for the compressive arching case, and the mid-span deflections were obviously smaller than those in the catenary case, as shown in Fig. 8.21. These results gave a numerical illustration of how compressive arching can affect the structural performance in fire. As with compressive membrane actions (Wang, 2002), a compressive arching effect is a viable load carrying mechanism and the beam section is very deep. Local buckling and distortional buckling within steel beams should not occur as these would prevent the development of compressive arching effects in fire. In order to utilise compressive arching effects at very high temperatures, strong external supports should be available to support the compressive

forces produced within the steel beams. However, it should also be recognised that compressive arching effects are at best a transitional phenomenon for the beam behaviour in most cases under fire conditions, and is highly dependent on parameters such as the beam sections, applied loads, beam spans and strong external supports. If compressive arching effects are developed within steel beams in fire, the performance of the steel connections should be safe under these conditions.

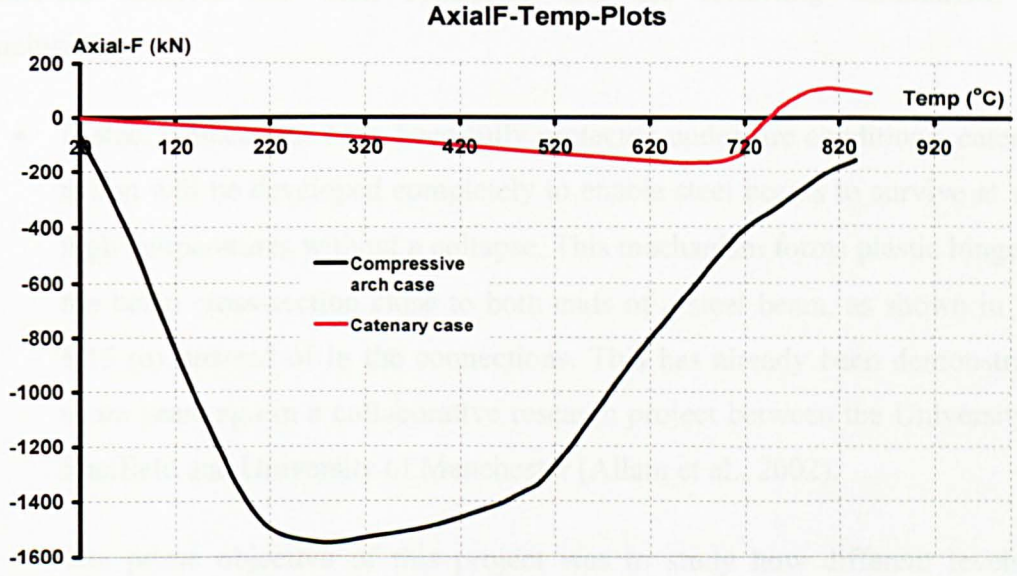

(a) Comparison of axial force variation

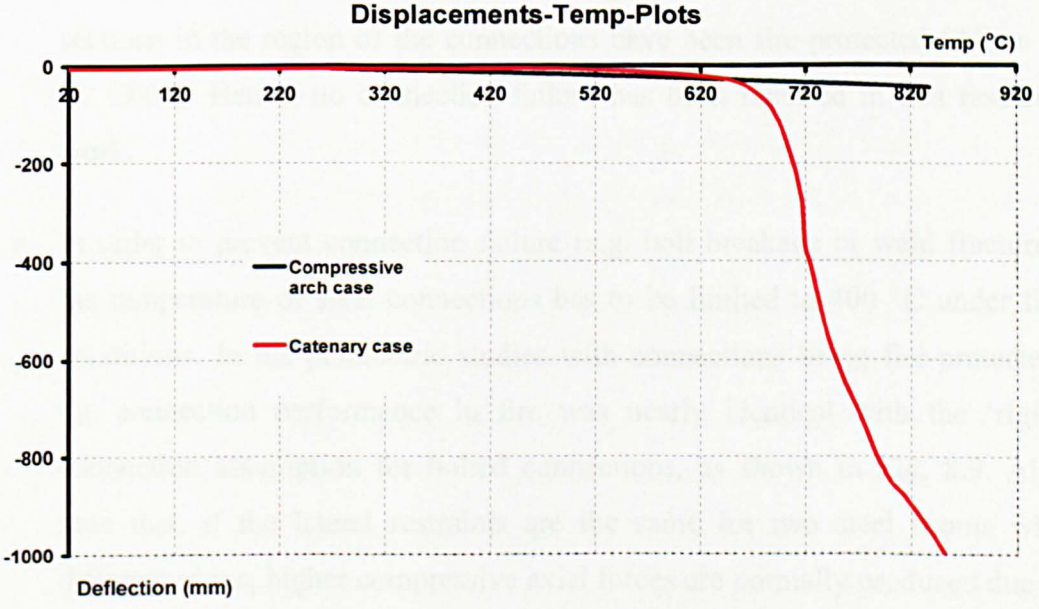

(b) Comparison of middle span deflections

Figure 8.21: Compressive arching effects under fire conditions

8.5 Conclusions and recommendations

This chapter has presented the results of a series of parametric studies using Abaqus, to analyse the large deflection behaviour of steel beams at elevated temperatures with proper consideration of connection performance in fire. After validating the numerical model against the experimental results of fire tests at Manchester, the numerical analysis has been conducted and the following summarises the conclusions:

- If steel connections have been fully protected under fire conditions, catenary action will be developed completely to enable steel beams to survive at very high temperatures without a collapse. This mechanism forms plastic hinges in the beam cross-section close to both ends of a steel beam, as shown in Fig. 8.15 (a), instead of in the connections. This has already been demonstrated some years ago in a collaborative research project between the University of Sheffield and University of Manchester (Allam et al., 2002).

- The prime objective of this project was to study how different levels of restraint from surrounding structure affects the survival of steel framed structures in fire. In order to prevent integrity failure, the beam and column sections in the region of the connections have been fire-protected (Allam et al., 2002). Hence, no connection failure has been reported in this research work.

- In order to prevent connection failure (e.g. bolt breakage or weld fracture), the temperature of steel connections has to be limited to 400 °C under fire conditions. In the parametric studies with connections being fire-protected, the connection performance in fire was nearly identical with the 'rigid' connection assumption for bolted connections, as shown in Fig. 8.9. Also note that, if the lateral restraints are the same for two steel beams with different spans, higher compressive axial forces are normally produced due to restrained thermal expansion of the longer span beam. In the numerical analysis, if the bending moments in the middle of the spans are consistent for different load cases, the types of loading (distributed or concentrated) have little influence on the performance of steel beams under fire conditions.

- If steel connections are not fire-protected, these connections can experience very high temperatures (600 °C to 800 °C) in a fire compartment. The connection performance at elevated temperatures is no longer consistent with the 'rigid' connection assumption, as displayed in Fig. 8.14. Catenary action has also been developed and this enables steel beams to survive at very high temperatures. However, the mechanism of developing catenary actions in fire is distinguished from the cases of fire-protected steel connections. As demonstrated in Fig. 8.15 (b), the plastic hinges in the structural arrangement are formed in the connection zones owing to connection rotation. This demands more ductility and strength from these connections in forming the plastic hinges. So the rotational capacity of connections is more likely to be of concern to structural engineers under fire conditions. After studying the relationship between axial force variation and connection failure, it is recognised that the connections can fail due to fracture of weld components when steel beams are experiencing thermal expansion in compression. This failure process starts in the compression stage and is complete when the bottom weld component extends beyond the failure elongation assumption. As a conclusion, end-plate connections can fracture (fail) in fire due to a lack of rotational capacity, after thermal bowling of steel beams has taken place.

This study has investigated parameters such as beam span, load type, load ratio, connection temperature, uniform and non-uniform temperature profiles in beam cross-sections. Because of the limitation of time, this study could not be extended to include more parameters in the numerical analysis. A subsequent study might focus on different beam cross sections, non-uniform temperature profiles in beam cross sections and steel connections, and investigate how they affect the axial force variation at high temperatures. In the Cardington full scale fire tests, local and distortional buckling of steel beams was observed. These types of failure have not been taken into account in this numerical analysis. So researchers or engineers in structural fire engineering could also concentrate their research efforts on these two buckling phenomena in fire to understand how they affect the structural performance at very high temperatures.

CHAPTER 9

DESIGN RECOMMENDATIONS FOR IMPROVED ROBUSTNESS OF STEEL CONNECTIONS IN FIRE

9.1 Introduction

The full-scale fire tests at Cardington (British Steel, 1999) demonstrated the performance of beam to floor slab connections (via shear connectors) and beam to column connections at very high temperatures. Beam-to-column connections usually have the greater influence on the structural behaviour than beam to beam connections. Overall behaviour is dependent upon the type of connection adopted in a structure. In considering steel beams in a structure under fire attacks, axial restraints are supplied to the end of these beams as well as rotational restraints. Due to thermal expansion of steel beams, an axial load is produced in a frame connection, which is a key difference between connections in isolated testing and a steel frame.

Structural design even under exceptional conditions (e.g. fire or explosion) is intended to prevent progressive collapse of a structure. The possibility of structural collapse due to fire is a lesson engineers learned in studies of the failure of WTC 7 (NIST, 2008). Under fire conditions, structural integrity may be assured by the robustness of individual structural elements such as connections, columns and beams, which must possess sufficient strength and ductility to resist the changes in forces and deformations arising from exceptional loading. This research work has investigated the behaviour of partial depth end-plates in detail, both experimentally and through numerical modelling, and will now discuss the issues of robustness associated with steel connections and their critical components (bolts and welds).

9.2 Brittle Components in Connections

9.2.1 High strength structural fasteners

In the collapse of the WTC towers, many high strength bolts failed in bolted end-plate (column) connections. These bolts were observed to exhibit classical tensile fracture in the threaded area and also large bending of the bolt shank took place before failure of the bolts (Fisher, 2009). In the full-scale fire tests at Cardington, the bolts in fin plate connections were sheared due to thermal contraction of the steel beam during the cooling stage of the fire. In experimental research work on high strength bolts with property class 8.8 (Hu et al., 2007 and Kirby, 1995), the available deformation in both tension and shear has been found to be rather limited. The maximum elongation of structural bolts in testing was in the range of 10mm to 30 mm from room temperature (20 °C) to high temperatures (600 °C). For structural bolts at high temperatures, reduction in bolt steel strength is usually faster than structural steel (S275), as shown in Fig. 4.9 of Chapter 4. Failure modes in experimental tests were found to be bolt breakage or thread stripping. The latter failure mechanism suggests a weakness in the threads of the (bright finish) nuts and usually resulted in a 5%-20% reduction in ultimate capacities of bolt assemblies (Hu et al., 2007). In considering robustness of steel connections, this failure should be prevented under accidental fire conditions. Kirby (1995) indicated that the cause for bright finished nuts and bolts failing by the threads being stripped was not solely dependent on any one of these components, but the overall interaction between these two components. Clearly a more closely fitting nut and bolt provides a greater surface contact area between their threads, thereby spreading the load and effectively reducing the stresses (Kirby, 1995). So in order to avoid nut threads being stripped, bolts and nuts with a closer fit should be adopted (the dimensional tolerance class should be in line with BS EN ISO 4014/4017 and ISO 4032) and also higher strength grade nuts (class 10) are preferred combined with property class 8.8 bolts for use under fire conditions (Hu et al., 2007).

Presently, high strength bolts and nuts are ordered to either British Standard (BS 4190) or European Standards (BS EN ISO 4014 /4017 and BS 4032), but these standards will be superseded when all parts of BS EN 15048 are published, as clearly

noted in the National Structural Steel Work Specification for Building Construction 5 edition (BCSA, 2007). The research on bolts presented in Chapter 4 was completed about three years before, and was based on current bolt standards and established the understanding of fire performance of structural bolts. As a result of this, future research is required to understand the difference between the current bolt standards and the new bolt standards which will soon supersede them.

The manufacturing process of fasteners (bolts and nuts) is of great importance because how they are made can affect the strength, reliability, cost, and serviceability of an entire structure (Phebus and Kasper, 1998). There is a vast variety of materials, processes, and surface coatings in fastener manufacturing processes. In general, there are two stages in fastener manufacturing methods: forming and threading. The primary forming methods include cold/warm heading, hot/cold forging (or forming), and turning or screw machining. Normally nuts and bolts are made from steel wire rods, from which rust particles have already been removed before lubricating and straightening. Bolts are produced by a cold forging method at room temperatures: cutting and shaping the steel into many small pieces slightly longer than bolt length, then forcing them through a series of dies to shape one end into a hexagon bolt head at very high pressure; the opposite end is used for creating threads by high pressure rollers, which is again a cold forging process. Manufacturing nuts employs hot forging: steel bars are cut into small pieces and then heated up to 1200 °C, and hydraulic hammers punch these pieces into small hexagons and a drilling machine (called tapper) cuts threads. The primary threading method is roll threading. Apart from this method, threads may also be created by cut threading and ground threading. Cut threading is one of the oldest methods used to produce a thread, but is the least desirable from the point of view of thread finish quality and thread strength (Phebus and Kasper, 1998). Many small fasteners have cut threads. The ground threading method results in a high quality thread against dimensional control, thread strength and surface finish. Unfortunately this method is more costly than thread rolling and cut threading.

Fastener coating such as blackening, zinc plating and galvanizing is the final process for production of bolts and nuts, and is intended to create an anti-corrosive layer to

prevent oxidation of these products under atmospheric and marine conditions. There are more than 20 metals and alloys used for coatings of bolts and nuts with various coating thicknesses and coating processes. All fastener coatings affect the performance of bolts and nuts in a steel connection in some respect, although some effects may arise not from the physical presence of the coatings but from the method of applying coatings (Laurilliard, 1998). Most structural 8.8 bolts and nuts are supplied with a zinc electroplating finish. This process is capable of depositing a thin, adherent uniform metallic layer on the material surfaces of bolts and nuts. However, there are two issues associated with thread performance in this coating method: hydrogen embrittlement and diametral overtap. Hydrogen embrittlement is a delayed brittle failure mechanism during static loading at stress levels well below the tensile strength of the material due to the presence of absorbed hydrogen (Laurilliard, 1998). The process of hydrogen embrittlement and the role of contributing factors are very complex. The degree of embrittlement is highly dependent on the amount of hydrogen absorbed and retained in the basic metal during the manufacturing and coating processes, and the major factors affecting the degree of hydrogen embrittlement in high strength bolts and nuts have been summarized in the research work of Lauriliard (1998). In order to reduce the rate of hydrogen absorption and retainment in the basis metal, it demands solution control, process control and post-plate inspection for the entire manufacturing process of structural fasteners.

In order to accommodate extra coatings, internal threads of nuts are commonly over-tapped by 0.2-0.4 mm, called 'diametral over-tap'. Bolt threads are never made undersized and all space for the coating is gathered from the nuts (Wallace, 2009a and 2009b). If it is assumed that the coating thickness is 40 microns, the coating space required for fasteners (nuts) is eight times the coating thickness (about 0.32 mm). This process suggests a weakness on the threads of nuts, possibly resulting in the premature failure (thread stripping) observed in the previous tests of structural bolts and connections in fire. To prevent premature failure, Xylan coating has been recommended to be employed during the manufacturing process (which usually gives a black appearance to structural bolts) because it requires the least coating thickness (about 14 microns) of bolts and nuts. So the 'over-tap' thickness taken from nuts only needs to be about 0.1 mm - 0.2 mm, which is able to create a closer fit

between the bolts and nuts. Unfortunately, Xylan coating is far more expensive than zinc coating or Dacromet coating (a typical coating process used for structural fasteners in USA).

9.2.2 Fillet welds

Fillet welds have a triangular cross section and they are commonly used to make T-joints, corner joints and lap joints, as shown in Fig. 9.1. Weld fracture has been observed both in the isolated connection tests (Chapter 5) and the full scale fire tests at Cardington. This failure mechanism is not desirable under accidental fire conditions, because it may reduce the deformation capability of end-plate connections. Possible factors causing brittle failure of fillet welds are 1) hydrogen generated by the welding process 2) residual stresses acting on the welds and 3) the relative stiffness/strength between fillet welds and their connected elements. In a connection, the welds must be designed according to the rules specified in 4.5 of EC3 Part 1.8, and application of the rules in 4.5.3.2 may lead to rather thin welds in the case of relatively small loads in relation to the capacity of the web (Jaspart and Demonceau, 2008). If the rupture strength of these thin welds is lower than the yield strength of the weakest of the connected metal elements, the connection is unable to possess sufficient deformation capacity to accommodate imposed effects due to applied loads. To prevent this failure, the fillet welds may be designed as 'full strength': the rupture strength of welds is greater than the rupture strength of the adjacent metals (Jaspart and Demonceau, 2008). So the welds are designed at 70% - 80% of the full strength, as adopted in the Dutch standard NEN 6770 (1990). This design strategy may ensure the plastic failure (yielding) of the connected parts before the rupture of welds in the case of overloading, and helps with achieving a ductile failure mechanism of end-plate connections under normal and elevated environmental conditions. As demonstrated in Chapters 5 and 6, the component-based approach can be applied to ensure a ductile failure of end-plate connections under these conditions. The only rule that needs to be satisfied is

$$F_{weld,\theta} \geq F_{rest,\theta}$$

$F_{weld,\theta}$ is the resistance of a weld component at temperature θ and $F_{rest,\theta}$ is the resistances of other components such as bolts and T-stubs at different temperatures. This approach can be employed in the design of ductile steel connections in practice and can also be used in the analysis of structural performance of these connections to help with the determination of the connection deformation capacities.

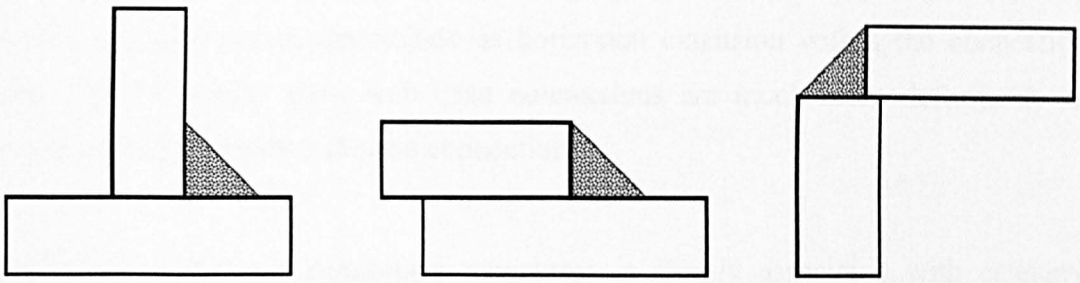

(a) (b) (c)

Figure 9.1: Fillet weld configurations (a) T-joints, (b) lap joints, (c) corner joints

9.3 Connection Typology, Tying Resistance and Ductility

Robustness is the ability of a structure to withstand events like fire, explosions, impact or the consequences of human errors, without being damaged to an extent disproportionate to the original cause (CEN, 2006), which has also been rephrased in the research work of Starossek and Wolff (2008) as structural insensitivity to local failure. Robustness of simple steel connections is closely associated with two aspects: tying force (resistance) and ductility. The concept of tying force appeared in regulations from the partial collapse of Ronan Point, which was caused by a gas explosion resulting in a domino style (progressive) collapse of wall and floor sections from the top of the building to the ground. This failure mechanism resulted from a lack of positive attachment between principal structural elements in this structure using the Larsen-Nielsen design approach. In order to prevent progressive collapse and achieve at least a minimum structural robustness against exceptional loading, one approach is tying all the principal elements of a structure together, which means beam-to-column connections of a structure must be capable of transferring a horizontal tying force (in a steel structure they must also be designed to transmit the vertical shear forces as well) to maintain the structural integrity (BSI,

2000). Owens and Moore (1992) carried out a series of experimental tests on simple steel connections (flexible end-plates and web cleats) to examine their resistances to horizontal tying forces. The test results demonstrated these connections to be capable of providing resistance against progressive collapse by tying the principal structural components together. These connections have at least 75 kN horizontal tying resistance, (required by BS 5950: Part 1) and inherent structural robustness has been achieved. In this series of tests (Owens and Moore, 1992), the deformation capacity of these connections is determined as horizontal extension within the connection zone and the results show web cleat connections are much more deformable in general, compared with end-plate connections.

Under fire conditions, connection robustness is closely associated with catenary actions and tensile membrane actions (Wang, 2002). These actions demand that the connections retain their strength and ductility when exposed to fire. In catenary actions, the steel beam, as shown in Fig. 5.1 in Chapter 5, acts as a cable hanging from the surrounding cold structure, and the *tying force* is the action which is generated within steel beams and passed on to steel connections (Hu et al., 2008). But this *tying force* is inclined to the horizontal direction (*inclined tying force*) and is representative of the forces arising due to catenary actions, differentiated from the previous situation. In the isolated fire tests, most connections were unable to supply the minimum tying resistance (75 kN) to a structure due to the first rupture of welds in a connection. Robust fillet welds are therefore required in the design of steel connections in fire. Robustness in fire also demands more deformable steel connections for two primary reasons, in comparison with the connections at normal temperature environmental conditions: a) forming plastic hinges to develop catenary actions, b) dissipating energy. So the provision of adequate ductility should ensure that the plastically deformed connections absorb energy without fracture, which precludes the failure of brittle components like bolts and welds in a fire situation. Unfortunately, the ductility (rotational capacities) of end-plate connections has been found to be limited at ambient temperatures and reduced at high temperatures, due to the brittle failure of fillet welds (Hu et al., 2008). The component-based approach may be used to avoid the failure of fillet welds in a connection. Structural bolts, as

brittle components in a connection, can be treated by using the same approach, as follows:

$$F_{bolt,\theta} \geq F_{rest,\theta}$$

$F_{bolt,\theta}$ is the total resistance of bolt components at different temperatures and $F_{rest,\theta}$ denotes the resistances of other components at different temperatures such as T-stubs (but except welds). Bolts should not be the weakest component in each row within the connections.

Apart from the testing on flexible end-plate connections, which is the focus of this thesis, other experimental tests have been executed in this robustness project on simple connections such as fin plates, web cleats and flush end-plate connections. Burgess (2009) summarized and examined the detailed responses of these connections at very high temperatures. Note that all fin plate connections tested failed by shear fracture of their bolts and rotational capacities of these connections was reported to be slightly better than that of flexible end-plates. It is very obvious that the failure mechanism of fin plates and flexible end-plate connections is dominated by the strength and ductility of brittle components, which is a fundamental reason for these connections being limited to small rotational capacities under fire conditions. As has been reported in the research paper of Yu et al. (2009a), the failure mechanism of fin connections may be altered from bolt shear failure to block-shear fracture of the beam webs by replacing structural 8.8 bolts with Grade 10.9 bolts, and rotational capacities have therefore been increased at elevated temperatures.

Web cleat connections are found to be the most ductile connection configuration in all the connection tests. At 450 °C and 550 °C, these connections failed due to fracture of the angle close to heel; the connection failure mechanism is transformed to shear fracture of bolts at 650 °C. To explain these different failure mechanisms, the strength reduction factors documented in Chapter 4, should be considered for bolts and S275 steel. In general, the strength reduction factors for bolts change faster than those for S275 steel, as shown in Fig. 4.9. Over 600 °C, the strength retained by bolts is lower than 20% of the bolt strength at normal temperatures, but the S275

steel strength still possesses 45 % of its original strength, which is the cause of the change in failure modes from fracture of angles to bolt shear failure.

Flush end-plate connections are able to carry more moment actions, but their ductility is very limited at both ambient and elevated temperatures. Structural engineers can employ this type of connection to develop the catenary actions in fire, but they must ensure the moment capacity of these connections at high temperatures is higher than the moment capacity of the steel beam to which it is connected.

9.4 Conclusions

This chapter summarized and refined the robustness ideas based on the previous investigation on structural bolts and welds, steel connections and parametric studies of sub-frame structures in fire. The following statements summarise recommendations to improve the robustness of steel connections in fire:

a) Brittle failure (fracture) of fillet welds should be prevented in end-plate connections, as this failure mechanism reduces the ductility of these connections at elevated temperatures.

b) Premature failure of structural bolts (thread stripping) should be avoided in end-plate connections, which will diminish the capacities of these bolts in fire, and result in reduction of the connection resistance.

c) The rotational capacity of a bolted connection is mainly determined by the deformational ductility of its components, and their ductility can be affected by temperatures (Burgess, 2009). In simple steel connections, brittle failure mechanisms such as weld fracture and bolt shear failure should be avoided in fire conditions. This is because structural components such as bolts and welds are identified as non-ductile components with less deformation capability in a bolted connection. If the brittle failure of a connection component is present under fire conditions, the ductile components (e.g. T-stubs) cannot be fully elongated and the connection ductility has therefore been decreased in fire. Connection design in fire should ensure that the

resistance of these (brittle) components is not less than that of other components at both ambient and elevated temperatures. As a consequence, the connection failure mechanism may be dominated by the components with more ductility in fire.

d) This robustness project investigated four different types of connections in fire: fin plates, partial depth end-plates, web cleats and flush end-plates, for their performance (Yu et al., 2009a, 2009b, 2009c and Hu et al., 2008). The experimental results demonstrated that web cleats were the most ductile connection type under fire conditions. For all the connections, ductility may be enhanced if the bolt rows are placed as close to the lower flange of the beam as possible, however this also causes a significant sacrifice of moment capacity (Burgess, 2009). Nevertheless, these connections are commonly in use for bare steel frames and they may also be employed in composite steel structures. If this is a case in practice, the influence of concrete slabs in the connection zone may need to be investigated further.

e) Bolted connections are intended to allow a steel structure to achieve basic fire resistance requirements through developing catenary actions in fire. If these bolted connections have been fully protected, catenary actions are developed due to material softening at high temperatures or distortional buckling of steel beams, and plastic hinges then form close to the two ends of a steel beam. The fundamental concept of this approach is to strengthen the stiffness and strength of the bolted connections (using fire protection or specifying high connection resistance) to achieve catenary action under fire conditions. The alternative approach is to make use of ductile bolted connections such as web cleats (these connections may not be fire protected) and the plastic hinges are therefore contained within these connections for the development of catenary actions in fire.

CHAPTER 10

CONCLUSIONS AND RECOMMENDATIONS

The research work presented in this thesis, involving experimental tests, development of simplified component-based connection models and finite element simulation, aims to answer questions closely associated with performance-based design in fire, as follows:

a) What are the basic requirements for a robust connection under fire conditions?

b) How do the brittle components affect the performance of a bolted connection at elevated temperatures?

c) How do flexible end-plate connections perform in a steel-framed structure and what factors differentiate the connection performance in a structure and the behaviour of isolated connections in fire?

In the research on structural 8.8 bolts, the importance of the manufacturing process of the bolts and nuts was highlighted. If bolts and nuts are required to have resistance to corrosion, threads of nuts are usually over-tapped to accommodate the protective coating layer (normally zinc). However, this mechanical/chemical process produces a weakness of the threads of nuts and thread stripping is a common failure mechanism between bolts and nuts in fire. To prevent this premature failure (thread stripping), black (self-finished or Xylan coated) and higher grade nuts (grade 10) may be recommended for grade 8.8 bolts and the tolerance class between the threads of bolts and nuts should be in line with BS EN ISO 4017/4032 (2001). This research also revealed the strength reduction of bolts between 20 °C and 300 °C and some

adjustments have been made to the reduction factors suggested by Kirby (1995). In the review of reduction factors for bolts and welds, the strength reduction of these components is faster than that of structural steel (S275) in a fire situation (over 300 °C), as shown in Fig. 10.1. This strength reduction may cause different resistances for the connection components (bolts, welds and T-stubs) at high temperatures and failure mechanisms of a bolted connection may therefore alter due to temperature variation. Further research associated with a steel connection should focus efforts on the shear behaviour of bolts, which occurs in some connections (fin plates and web cleats) as a critical failure mode.

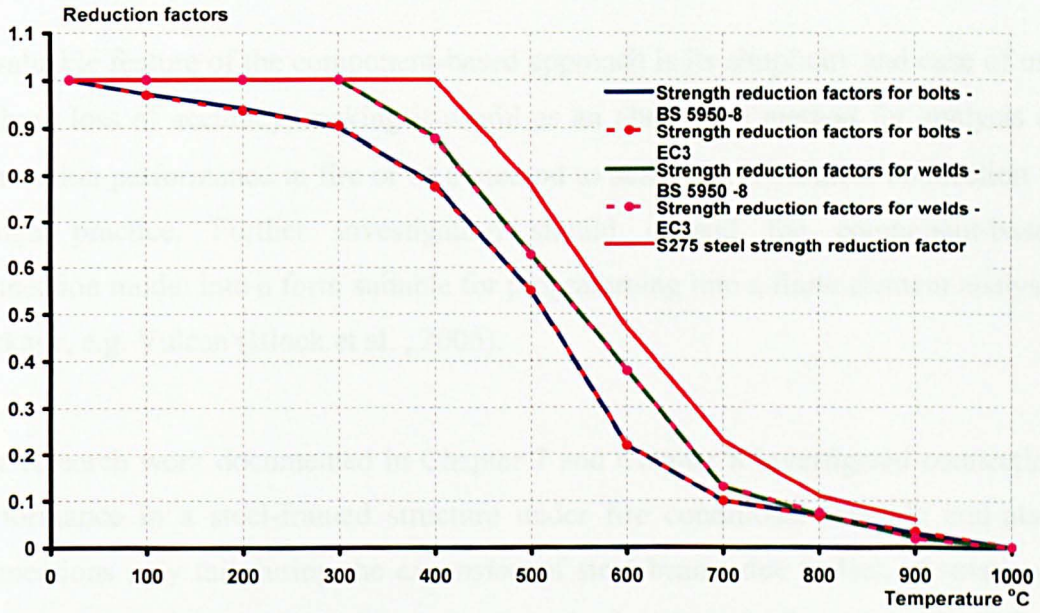

Figure 10.1: Reduction factors for brittle components and structural steel

Investigation of flexible end-plate connections in Chapter 5 shows that these connections failed by the rupture of the end-plates in the vicinity of the welds and their rotational capacities (ductility) decreased under fire conditions. This is because the strength reduction of welds is faster than that of structural steel (S275) in a fire situation (shown in Fig. 10.1). In addition, the ultimate strength of structural steel as supplied is usually higher than its nominal strength. As a consequence, the failure modes of these end-plate connections are transformed from a ductile mode at room temperature to a less ductile fashion in fire. These non-ductile failure modes may prevent the development of catenary actions in a compartment fire, and are likely to occur unless the connections are fully fire-protected.

As a further extension of Chapter 5, the component-based approach in Chapter 6 has been utilized to explain the failure mechanism of these connections in detail and show how to achieve ductile behaviour in fire. The connection failure mechanism is highly dependent on the weakest component in a connection (especially for welds and bolts) in a fire situation and the ductility of these connections is closely associated with the resistance of the weakest component and the elongations of ductile connection components. Hence, for a bolted end-plate connection in fire, non-ductile components (welds and bolts) should be prevented from being the weakest links in a connection and ductility of the connection can therefore be developed by the ductile component (end-plate bending) under fire conditions.

A valuable feature of the component-based approach is its simplicity and ease of use without loss of accuracy, making it useful as an alternative method for analysis of connection performance in fire or as a method to achieve a robustness connection in design practice. Further investigation should expand the component-based connection model into a form suitable for programming into a finite element analysis package, e.g. Vulcan (Block et al. , 2006).

The research work documented in Chapter 7 and Chapter 8 investigated connection performance in a steel-framed structure under fire conditions. Flexible end-plate connections may fail during the *expansion* of steel beams due to lack of rotational capacity, caused by rupture of the end-plates in the vicinity of welds in fire before the beam bottom flange contacts with the column face. The research in Chapter 8 also considered the effects of different parameters, such as beam spans, connection temperatures, load ratios and different levels of lateral restraints, on the performance of a sub-frame structure. In this series of parametric studies, the influence of connection temperatures was highlighted. For fire- protected connections (connection temperatures under 400 °C), the performance of end-plate connections was nearly identical to that of a 'rigid' connection assumption and plastic hinges were formed at both ends of a steel beam for development of catenary action in fire. For end-plate connections without fire protection (connection temperatures over 500 °C), the performance of the connections was more likely to be semi-rigid and catenary action

may only be developed due to plastic hinges formed within these end-plate connections if they are ductile enough in a fire situation.

Recommendations to improve the robustness of steel connections were presented in Chapter 9. Connections should be designed to avoid brittle failure models at elevated temperatures. Increasing weld sizes and careful specification of structural bolts can ensure connections exhibit good ductility in fire.

REFERENCES

BSI (1990). "*BS5950-8:1990 Structural use of steelwork in building – Part8: Code of practice for fire resistant design*," British Standards Institution, London

BSI (2000). "*BS5950-1:2000 Structural use of steelwork in building - Part1: Code of practice for design – Rolled and welded sections*," British Standards Institution, London

BSI (2001). " BS *3692:2001 ISO metric precision hexagon bolts, screws and nuts – Specification*," British Standards Institution, London

BSI (2001). " *BS 4190:2001 ISO metric black hexagon bolts, screws and nuts – Specification*, " British Standards Institution, London

BSI (2005). "*BS 5950-8:2005 Structural Use of Steelwork in Building - Part 8: Code of Practice for Fire Resistance Design*," British Standard Institution, London

CEN(1999). " *BS EN ISO 898-1: 1999 Mechanical properties of fasteners made of carbon steel and alloy steel – Part 1: Bolts, screws and studs*, " European Committee for Standardisation, Brussels

CEN(2001). " *BS EN ISO 4014: 2001 Hexagon head bolts – Products grades A and B*," European Committee for Standardisation, Brussels

CEN(2001). " *BS EN ISO 4017: 2001 Hexagon head screws – Products grades A and B*," European Committee for Standardisation, Brussels

CEN(2001). " *BS EN ISO 4032: 2001 Hexagon nuts, style 1 – Products grades A and B* ," European Committee for Standardisation, Brussels

CEN(2002). "*BS EN 1991-1-2:2002 Eurocode 1: Actions on structures – Part 1-2: General actions – Actions on structures exposed to fire*," European Committee Standardization, Brussels

CEN(2005). "*BS EN 1993-1-8:2005 Eurocode 3: Design of steel structures - Part 1.8: Design of joints*," European Committee for Standardisation, Brussels

CEN(2005b). "*BS EN 1993-1-2:2005 Eurocode 3: design of steel structures - Part 1.2: General rules- structural fire design*," European Committee for Standardisation, Brussels

CEN(2006). "*BS EN 1991-1-7:2006 Eurocode 1: Actions on structures – Part 1-7: General actions – Accidental actions*," European Committee for Standardisation, Brussels

NEN 6770 (1990). Nederlands Normalisatie Instituut, NEN 6770 Staalconstructies TGB, basiseisen

ABAQUS (2001). Standard user's manual. Hibbitt, Karlsson and Sorensen, Inc.

ABAQUS (2006). Standard user's manual. Hibbitt, Karlsson and Sorensen, Inc

Al-Jabri, K.S. , Burgess, I. W. and Plank, R. J. (1997). '*Behaviour of steel and composite beam-to-column connections in fire. Volume 2: Appendices*' , Research Report DCSE/97, The University of Sheffield

Al-Jabri, K. S. (1999) *The behaviour of Steel and Composite Beam-to-Column Connections in Fire*, PhD Thesis, Department of Civil and Structural Engineering, University of Sheffield

Al-Jabri,K.S., Burgess, I.W. and Plank, R.J. (2005). "Spring-stiffness model for flexible end-plate bare-steel joints in fire", *Journal of Constructional Steel Research*, Vol. 61, pp. 1672-1691

Allam, A.M. , Burgess, I.W. and Plank, R. J. (2002). "*Performance-Based Simplified Model for a Steel Beam at Large Deflection in Fire*," Proceedings of 4th International Conference on Performance-Based Codes and Fire Safety Design Methods, Melbourne, Australia

Ana Margarida Girao Coelho (2004) *Characterisation of the Ductility of Bolted End Plate Beam-to-column Steel Connections*, PhD Thesis, University of Coimbra, Portugal

Ana M. Girao Coelho, Frans S. K. Bijlaard, Nol Gresnigt and Lius Simoes da Silva (2004). "Experimental assessment of the behaviour of bolted T-stub connections made up of welded plates," *Journal of Constructional Steel Research*, Vol.60, pp. 269-311

Ang K.M. and Morris, G.A. (1984). "Analysis of 3-Dimensional Frames with Flexible Beam-Column Connections", *Canadian Journal of Civil Engineering*, Vol. 11 , pp. 245-254

Aribert, J. M., Younes, I. and Lachal, A. (2002). " *Low-cycle fatigue of steel connections subjected to a transverse concentrated load: experimental investigation and practical formulation*", Eurosteel 2002 – 3rd European Conference on Steel Structures, Coimbra, Portugal, Editor: Antonio Lamas and Luis Simões da Silva, Volumne 2, pp 1067-1078

Astaneh, A. (1989). " Demand and Supply of Ductility in Steel Shear Connections," *Journal of Constructional Steel Research*, Vol.14, pp. 1-19

Astaneh-Asl, A. McMullin, K. M. and Call, S. M. (1993). " Behaviour and Design of steel Single Plate Shear Connections," *Journal of Structural Engineering*, Vol. 119. No. 8, pp. 2421-2440

Bailey, C. (2006). One Stop Shop in Structure Fire Engineering @ http://www.mace.manchester. ac.uk/project/research/structures/strucfire/default.htm

Barber, H. (2003). Chapter 23 Bolts, In Davison, J. B. and Owens, G.W.(Eds), *Steel Designers' Manual* : 671-684, London and Cambridge: Blackwell Science.

Bathe, K. J. , (1982). "*Finite Element Procedures*", Prentice Hall, Englewood Cliffs, New Jersey

BCSA (2007). *National Structural Steelwork Specification for Building Construction 5th Edition*, The British Constructional Steelwork Association Ltd., Whitehall Court, Westminster, London.

Beg, D. , Zupancic, E. and Vayas, I. (2004). "On the rotation capacity of moment connections", *Journal of Constructional Steel Research*, Vol. 60, No. 3-5, pp.601-620

Block, F.M. (2002). *"Numerical and Analytical Studies of Unstiffened Column Webs at Elevated Temperatures"*, Internal Report, Department of Civil and Structural Engineering, University of Sheffield

Block, F.M., Burgess, I.W. and Davison, J.B. (2004). *"Numerical and Analytical Studies of Joint Component Behaviour in Fire"*, SIF04 - Third International Workshop on Structures in Fire, Ottawa, Canada, pp383-395

Block, F.M., Burgess, I. W., Davison, J.B. and Plank, R.J. (2004b). *"A Component approach to modelling steelwork connections in fire: behaviour of column webs in compression"*, Proceedings of ASCE Structures Congress 2004, Nashville, Tennessee

Block, F. , Burgess, I. , Davison, J. B. and Plank, R. (2006). " *The Development of A Component-based Connection Element for Endplate Connections in Fire,*" Proceedings of the Four International Workshop: Structures in Fire, Aveiro, Portugal

Block, F.M. (2006). *"Development of a Component-Based Finite Element for Steel Beam-to-Column Connections at Elevated Temperatures"*, PhD thesis, University of Sheffield

Block, F.M., Burgess, I. W., Davison, J.B. and Plank, R.J. (2007) "The Development of A Component-Based Connection Element for End-plate Connections in Fire", *Fire Safety Journal*, Vol.42, pp 498-506

British Steel (1999). *The Behaviour of Multi-storey Steel Framed Buildings in Fire*, Swinden Technology Centre, Moorgate, Rotherham, South Yorkshire, UK

Buchanan, A.H. (2001). *Structural design for fire safety*, Chrichester: John Wiley & Sons, Ltd.

Burgess, I. W. (2007). *Connection Modelling in Fire*, Proceeding of COST C26 Workshop "Urban Habitat Constructions under Catastrophic Events", Prague, pp. 25-34

Burgess, I. W. (2009). "*The Robustness of Steel Connections in Fire,*" Proceedings of 9th International Conference on Steel Concrete Composite and Hybrid Structures, Leeds, United Kingdom

Bursi, O.S. and Jaspart, J.P. (1997). "Benchmarks for finite element modelling of bolted steel connections", *Journal of Constructional Steel Research*, Vol. 43, No. 1-3, pp. 17-42

Bursi, O.S. and Jaspart, J.P. (1998). "Basic issues in the finite element simulation of extended end plate connections", *Computers and Structures*, Vol. 69, pp. 361-382

Byfield M. and Paramasivam S. (2007). 'Catenary action in steel-framed buildings', *Structures & Buildings*, volume 160, Issue 5, 247 -257

Charlier, R. and Habraken A.M. (1990). "Numerical metallisation of contact phenomena by finite element method" , *Comput. Geotech.*, Vol.9, pp. 59-72

Cornec, A. , Scheider, I. and Schwalbe, K. H. (2003). "On the practical application of the cohesive model", *Engineering Fracture Mechanics*, Vol. 70, pp.1963-1987

El-Rimawi, J.A. (1989). *"The Behaviour of Flexural Members Under Fire Conditions"*, PhD Thesis, Department of Civil Engineering, University of Sheffield, 1989

FEMA (2002). *World Trade Centre Building Performance Study*, Federal Emergency Management Agency, Washington DC and New York, USA

FEMA (2002b). *World Trade Center, Building Performance Study: Data Collection, Preliminary Observations, and Recommendations.* Federal Emergency Management Agency, Washington, DC and New York, USA

Fisher, J. (2009). *Structural Steel and Steel Connections*, @ http://www.fema.gov/pdf/library/fema403_apb.pdf

Flanagan, D.P. and Belytschko, T.A. (1981). "A uniform strain hexahedron and quadrilateral with orthogonal hourglass control", *International Journal for Numerical Methods in Engineering*, Vol. 17, No.5, pp. 679-706

Gebbeken, N. , Rothert, H. and Binder, B. (1994). "On the numerical analysis of end plate connections", *Journal of Constructional Steel Research*, Vol. 30, pp. 177-196

Gehri, E. (1985). "The Fire Resistance of Steel Structures," *Fire Technology*, Vol.21, No.1, pp. 22-33

Gillie, M. (1999). " Development of generalized stress strain relationships for the concrete slab in shell models," PIT Project research Report SS1, The University of Edinburgh

Gillie, M. , Usmani, A. and Rotter, M. (2000). "Modelling of heated composite floor slabs with reference to the Cardington experiments," University of Edinburgh

Girão Coelho, A. M. (2004). *"Characterization of the ductility of bolted end-plate beam-to-column steel connections"*, PhD thesis, Universidade de Coimbra

Girão Coelho, A. M., Simões da Silva, L. and Bijlaard, F.S.K (2004). "*Ductility analysis of end-plate beam-to-column joints*", Eurosteel 2005 – 4th International

Conference on Steel and Composite Structures, Maastricht, The Netherlands, Editor: B. Hoffmeister and O. Hechler, Volume C, pp 123 - 130

Godley, M. H. R. and Needham, F. H. (1983), "Comparative tests on 8.8 and HSFG bolts in tension and shear", *The Structural Engineer*, Vol.60, No.3, pp. 21-26

Gomes, F. C. T., Kuhlmann, U., De Matteis, G. and Mandara, A. (1998). *Recent Development on Classification of Joints*, Proceedings of the international conference: Control of the semi-rigid behaviour of civil engineering structural connections, COST C1, Liege, Belgium

Hayes, M.D. (2003). *"Structural analysis of a pultruded composite beam: shear stiffness determination and strength and fatigue life predictions"*, PhD thesis in Engineering Mechanics, Faculty of the Virginia Polytechnic Institute and State University

Hu, Y., Davison, J. B. , Burgess, I. W. and Plank, R. J. (2007). "Comparative study of the behaviour of BS 4190 and BS EN ISO 4014 bolts in Fire," Proceedings of the 3rd international conference on steel and composite structures, Manchester, UK

Hu, Y., Davison, J. B., Burgess, I. W. and Plank, R.J. (2008). "*Experimental Study on Flexible End Plate Connections in Fire*," Proceedings of 5th European Conference on Steel Structures, Graz, Austria, pp. 1007-1012

Hu, Y., Burgess, I. W. , Davison, J.B. and Plank, R. J. (2008). "*Modelling of Flexible End Plate Connections in Fire Using Cohesive Elements*," Proceedings of Structures in Fire Workshop, Singapore, pp. 127-138

Hu, Y., Davison, J.B., Burgess, I.W. and Plank, R. J. (2009). "Component Modelling of Flexible End-plate Connections in Fire," *International Journal of Steel Structures*, Vol.9, pp.1-15

IStructE (2002). *Safety in tall buildings and other buildings with large occupancy*, The Institution of Structural Engineers, London, United Kingdom

Izzuddin, B.A. , and Moore, D. B. (2002). "*Lessons from a full-scale fire test*," Proceedings of the Institution of Civil Engineers: Structures and Buildings, pp. 319-329

Izzuddin, B.A. , Vlassis, A. G. , Elghazouli, A.Y. and Nethercot, D.A. (2008). " Progressive collapse of multi-storey buildings due to sudden column loss – Part I: Simplified assessment framework," *Engineering Structures*, Vol.30, No.5, pp. 1424-1438

Jaspart, J. P. (1996). "Plastic hinge idealisation of structural joints. EC3 philosophy" , Document COST C1/WD2/96-02, Aachen.

Jaspart, J.P. (1997). Drafts of chapters 1, 2, and 3 of the COST C1 WG2 Publication in preparation, Document COST C1/WD2/97-21, Innsbruck.

Jaspart (1998). *Contributions to recent advances in the field of steel joints: Column bases and further configurations for beam-to-column joints and beam splices*, Professorship Thesis, Université de Liège, Belgium

Jaspart (1999). *"Semi-Rigidity in Connections of Structural Steelworks: Theory, Analysis and Design"*, Lecture notes for Advance Professional Training, Italy

Jaspart, J. P. and Demonceau, J. F. (2008). "European design recommendations for simple joints in steel structures, " *Journal of Constructional Steel Research*, Vol. 64, pp. 822-832

Johansson, B. and Lagerqvist, O. (1995). "Resistance of Plate Edges to Concentrated Loads", *Journal of Constructional Steel Research*, Vol. 32, pp 69-105

Kanvinde, A.M., Gomez, I.R. Roberts, M. , Fell, B.V. and Grondin, G.Y. (2009). " Strength and ductility of fillet welds with transverse root notch," *Journal of Ccontructional Steel Research*, Vol.65, pp. 948-958

Kirby, B.R. and Preston, R. R. (1988). " High temperature properties of hot-rolled structural steels for use in fire engineering design studies," *Fire Safety Journal*, Vol. 13, pp.27-37

Kirby, B.R. (1995), "The Behaviour of High-strength Grade 8.8 Bolts in Fire," *Journal of Constructional Steel Research*, Vol.33, No.1, pp. 3-38.

Krishnamurthy, N. and Graddy, D.E. (1976). "Correlation between 2- and 3-Dimensional Finite Element Analysis of Steel Bolted End-Plate Connections", *Computers and Structures*, Vol. 6, pp. 381-389

Kruppa, J. (1976). *"Resistance on feu des assemblage par boulous"*, Centre Technique Industrial de la Construction Metallique, St. Remy Chevzuese, France, CTICM Report, Document No. 1013-1, English translation available entitled *"Fire Resistance of Joints with High Strength Bolts"*.

Kuhlmann, U., Davison, J. D. and Kattner, M. (1998). *Structural Systems and Rotation Capacity*, Proceedings of the international conference: Control of the semi-rigid behaviour of civil engineering structural connections, COST C1, Liege, Belgium

Kukreti, A. R. , Murray, T.M. and Abolmaali, A. (1987). "End plate connection moment-rotation relationship", *Journal of Constructional Steel Research*, Vol. 8, pp. 137-157

Lagerqvist, O. and Johansson, B. (1996). "Resistance of I – girders to Concentrated Loads", *Journal of Constructional Steel Research*, Vol. 39, No. 2, pp 87-119

Laurilliard, J. (1998). Fastener Coatings, In Bickford, J. H. and Nassar, S. (Eds), *Handbook of Bolts and Bolted Joints*: 75-106, New York: Marcel Dekker, INC.

Lawson R.M. (1990) "Behaviour of Steel beam-to-column connections in fire", *The Structural Engineer*, Vol. 68, No.14, pp. 263-271

Lawson R. M. and Newman, G. M. (1996). *Structural Fire Design to EC3 and EC4, and Comparison with BS 5950*, Technical Report SCI publication 159, The Steel Construction Institute, Silwood Park, Ascot, Berkshire, United Kingdom

Leston-Jones, L.C. (1997). *The Influence of Semi-Rigid Connections on the Performance of Steel Framed Structures in Fire*, PhD Thesis, Department of Civil and Structural Engineering, University of Sheffield

Leston-Jones, L. C. , Burgess, I. W. , Lennon, T. and Plank, R. J. (1997). "*Elevated-temperature moment-rotation tests on steelwork connections,*" Proceedings of the Institution of Civil Engineers: Structures and buildings, pp. 410-419

Liu, T.C.H. , Fahad, M.K. and Davies, J. M. (2002). "Experimental Investigation of Behaviour of Axially Restrained Steel Beams in Fire," *Journal of Constructional Steel Research*, Vol. 58, pp. 1211-1230

L. Simões de Silva, Aldina Santiago and Paulo Vila Real (2001). "A component model for the behaviour of steel joints at elevated temperatures," *Journal of Constructional Steel Research*, Vol. 57, pp 1169-1195

Madabhusi-Raman, P. and Davalos, J.F. (1996). "Static shear correction factor for laminated rectangular beams," *Composites Part B : Engineering*, Vol. 27, No. 3-4, pp 285-293

Madas, J.P. (1993). "*Advanced Modelling of Composite Frames Subjected to Earthquake Loading*, " Imperial College Science, Technology and Medicine, University of London

Mouritz, A.P. (1994), "Failure Mechanisms of Mild Steel Bolts under Different Tensile Loading Rates", *International Journal of Impact Engineering*, Vol.15, No.3, pp. 311-324.

NIST (2008). *Federal Building and Fire Safety Investigation of the World Trade Center Disaster: Final Report on the Collapse of World Trade Center Building 7*, National Institute of Standards and Technology, NIST NCSTAR 1A, Gaithersburg, MD, USA

Nethercot, D. A. (2000). " Frame structures: global performance, static and stability behaviour: General Report," *Journal of Constructional Steel Research*, Vol.55, pp. 109-124

Nethercot, D. A. (2007). *Withstanding natural and man made hazards: increasing the robustness of steel structures,* Pacific Structural Steel Conference 2007: Steel Structures in Natural Hazards, 13-16 March, Wairakei, New Zealand

Newman, G.M. , Robinson, J. T. and Bailey, C.G. (2004). *Fire Safety Design: A New Approach to Multi-Storey Steel-Framed Buildings*, The Steel Construction Institute

O'Callaghan, D.J. and O'Connor, M. A.(2000). " *Comparison of finite element models of composite steel framed buildings behaviour in fire,*" Proceedings of the First International Workshop on Structures in Fire, Copenhagen, Denmark, June

O'Connor, M. A. and Martin, D.M. (1998). " Behaviour of a multi-storey steel framed building subjected to fire attack, " *Journal of Constructional Steel Research*, Vol. 46, No. 1/3, pp. 295

Owens, G.W. and Moore, D.B. (1992). "Steelwork connections: The robustness of simple connections," *The Structural Engineer*, Vol. 70, No.3/4, pp. 37-46

Phebus, J.A. and Kasper, P. F. (1998). Fastener Manufacturing, In Bickford, J. H. and Nassar, S. (Eds), *Handbook of Bolts and Bolted Joints*: 69-104, New York: Marcel Dekker, INC.

Piluso, V. , Faella, C. and Rizzano, G. (2001). "Ultimate Behaviour of Bolted T-Stubs. Two: Model Validation", *Journal of Structural Engineering*, ASCE, Vol. 127, No. 6, pp 694-704

Pucinotti, R. (2001). " Top and Seat and Web Angle Connections: Prediction Via Mechanical Method," *Journal of Constructional Steel Research*, Vol. 57, pp. 661-694

Purkiss, J.A. (2007). *Fire Safety Engineering Design of Structures*, London: Butterworth-Heinemann

Ramberg, W. and Osgood, W.R. (1943). "*Description of Stress – Strain Curves by Three Parameters*", National Advisory Committee for Aeronautics, Technical Report 902

Rex, C.O. and Easterling, S. W. (2003). "Behaviour and modelling of a bolt bearing on a single plate", *Journal of Structural Engineering*, ASCE, Vol. 129, No. 6, pp 792-800

Richard, R. M. and Elsalti, M.K. (1991). " *PRCONN, Moment-Rotation Curves for Partially Restrained Connections*", Users manual for program developed at The University of Arizona, Department of Civil Engineering and Engineering Mechanics, Tucson, Ariz

Robinson, J.T. and Latham, D. J. (1986). " Fire resistant steel design – the future challenge," in R. D. Anchor, H. J. Malhotra and J. A. Purkiss (eds), *Design of Structures Against Fire*, pp. 225-236

Sanad, A.M., Rotter, J.M., Usmani, A.S. and O'Connor, M.A. (2000). "Composite beams in large buildings under fire – numerical modelling and structural behaviour," *Fire Safety Journal*, Vol. 35, No. 3, pp. 165-188

Sarraj, M. (2007). "*The Behaviour of Steel Fin Plate Connections in Fire*", PhD thesis, Department of Civil and Structural Engineering, University of Sheffield

Scheider, I. , Schödel, M. , Brocks, W. and Schönfeld, W. (2006). "Crack propagation analyses with CTOA and cohesive model: Comparison and experimental validation", *Engineering Fracture Mechanics*, Vol. 73, pp. 252-263

SCI (1991). *Investigation of Broadgate Phase 8 Fire*, The Steel Construction Institute, Silwood Park, Ascot, Berkshire, United Kingdom

SCI (1995). *Joints in Steel Construction: Moment Connections*, The Steel Construction Institute, Silwood Park, Ascot, Berkshire, United Kingdom

SCI (2000). *Fire Safe Design: A New Approach to Multi-storey Steel-Framed Building* , The Steel Construction Institute, Silwood Park, Ascot, Berkshire, United Kingdom

SCI (2002). *Joints in Steel Construction: Simple Connections*, The Steel Construction Institute, Silwood Park, Ascot, Berkshire, United Kingdom

Sherbourne, A.N. and Bahaari, M.R. (1994). "3D Simulation of End-Plate Bolted Connections", *Journal of Structural Engineering*, Vol. 120, No. 11, pp. 3122-3136

Sherbourne, A.N. and Bahaari, M.R. (1997). "Finite Element Prediction of End-Plate Bolted Connections Behaviour. I : Parametric Study", *Journal of Structural Engineering*, Vol. 123, No. 2, pp. 157-164

Shi, Y. J., Chan, S. L. and Wong, Y. L. (1996). "Modelling for Moment-Rotation Characteristics for End-Plate Connections," *Journal of Structural Engineering, ASCE*, Vol. 122, No. 11, pp. 1300-1306

Simoes da Silva, L. and Coelho, Ana Margarida Girao (2001) "A ductility model for steel connections", *Journal of Constructional Steel Research*, Vol.57, No.1, pp. 45-70

L. Simoes da Silva, Aldina Santiago and Paulo Vila Real (2001) "A component model for the behaviour of steel joints at elevated temperatures", *Journal of Constructional Steel Research*, Vol. 57, No.11, pp. 1169-1195

Spyrou, S. (2002). *Development of A Component-based Model of Steel Beam-to-column Joints at Elevated Temperatures*, PhD Thesis, Department of Civil and Structural Engineering, University of Sheffield

Sprou, S. and Davison, J.B. (2001). " Displacement measurement in studies of steel T-stub connections," *Journal of Constructional Steel Research*, Vol. 57, pp. 647-659

Spyrou, S. , Davison, J. B. Burgess, I. W. and Plank, R. J. (2004a). " Experimental and Analytical Investigation of the 'Compression Zone' Component within a Steel Joint at Elevated Temperatures," *Journal of Constructional Steel Research*, Vol. 60, No. 6, pp. 841-865

Spyrou, S. , Davison, J. B. Burgess, I. W. and Plank, R. J. (2004b). " Experimental and Analytical Investigation of the 'Tension Zone' Component within a Steel Joint at Elevated Temperatures," *Journal of Constructional Steel Research*, Vol. 60, No. 6, pp. 867-896

Starossek, U. and Wolff, M. (2005a). "Progressive collapse: Design Strategies," Report, IABSE Symposium 'Structures and Extreme Events,' Lisbon, Portugal

Starossek, U. and Wolff, M. (2005b). "Design of collapse-resistant structures," Workshop paper, JCSS and IABSE Workshop on Robustness of Structures, Building Research Establishment, Garston, Watford, UK

Starossek, U. (2006). " Progressive collapse of structures: Nomenclature and procedures," IABSE, *Structural Engineering International*, Vol.16, No. 2, pp.113-117

Starossek, U. (2007). "Typology of progressive collapse", *Engineering Structures*, Vol. 29, No.9, pp. 2302-2307

Starossek, U. (2008). " Avoiding Disproportionate Collapse of Tall Buildings," @ www.sh.tu-harburg.de/starossek/index.htm

Starossek, U. and Haberland, M. (2008). "*Measures of structural robustness – Requirements & Applications*", Proceedings, ASCE SEI 2008 Structures Congress – Crossing Borders, Vancouver, Canada

Sulong, N. H. R. (2005). *Behaviour of Steel Connections Under Fire Conditions*, PhD Thesis, Department of Civil and Environmental Engineering, Imperial College London

Swanson, J. A. (1999). *"Characterization of the strength, stiffness and ductility behaviour of T-Stub connections,"* PhD dissertation, Georgia Institute of Technology, Atlanta, USA

Swanson, J. A. and Leon, R. T. (2001). "Stiffness Modelling of Bolted T-Stub Connection Components", *Journal of Structural Engineering*, Vol. 127, No. 5, pp 498-505

Tschemmernegg, F. and Humer, C. (1988). " The Design of Structural Steel Frames Under Consideration of the Non-Linear Behaviour of Joints," *Journal of Constructional Steel Research*, Vol.11, pp. 73-103

Tschemmernegg, F. ; Tautschnig, A. ; Klein, H. ; Braun, Ch. And Humer, Ch. (1987) "*Zur Nachgiebigkeit von Rahmenknoten – Teil 1"* (Semi-rigid joints of frame structures Vol. 1 - in German), Stahlbau 56, Heft 10, S. 299-306

Vegte, G.J. van der, Makino, Y. and Sakimoto, T. (2002). "Numerical Research on Single-Bolted Connections Using Implicit and Explicit Solution Techniques", Memoirs of the Faculty of Engineering, Kumamoto University, Vol. 47, No.1

Vegte, G.J. van der, (2008). "Numerical Simulations of Bolted Connections: The Implicit Versus The Explicit Approach", *@http://www.bouwenmetstaal.nl/ congres_eccs_04/Vegte_Makino_bolted.pdf*

Wald, F. , Simoes da Silva, L. , Moore, D.B. , Lennon, T. , Chladna, M. , Santiago, A. , Benes, M. and Borges, L. (2006). "Experimental behaviour of a steel structure under natural fire," *Fire Safety Journal*, Vol. 41, pp. 509-522

Wales, M. W. and Rossow, E. C. (1983). " Coupled Moment-Axial Force Behaviour in Bolted Joints," *Journal of Structural Engineering*, Vol. 109, No. 5, pp. 1250-1266

Wald, F. , Simoes da Silva, L. , Moore, D.B. , Lennon, T. , Chladna, M. , Santiago, A. , Benes, M. and Borges, L. (2006). "Experimental behaviour of a steel structure under natural fire," *Fire Safety Journal*, Vol. 41, pp. 509-522

Wallace, W. (2009a). *Bolt Coating Thickness & Nut Overtapping – A Lesson in Practical Necessity @http://www.appliedbolting.com/pdf/Coated_Bolts_and _Overtapping.pdf*

Wallace, W. (2009b). *Coated Bolts Can Improve Constructability @ http://www.appliedbolting.com/pdf/Coated_Bolts_Constructability.pdf*

Wang, Y.C. (2002). *Steel and Composite Structures: Behaviour and Design for Fire Safety*, London and New York: Spon Press

Wang, Y.C. , Dai, X. H. and Bailey, C.G. (2009). "An Experimental study of structure fire behaviour and robustness of different types of steel joints in restrained steel frames," submitted for publication

Weynand, K. , Jaspart, J.P. and Steenhuis, M. (1995). "*The Stiffness Model of Revised Annex J of Eurocode 3*," Proceedings of the Third International Workshop: Connections in Steel Structures: Behaviour, Strength and Design, Trento, Italy, pp. 441-452

Yin, Y.Z. and Wang, Y.C. (2003). " Numerical simulations of the effects of non-uniform temperature distributions on lateral torsional buckling resistance of steel I-beams, " *Journal of Constructional Steel Research*, Vol. 59, pp. 1009 -1033

Yin, Y.Z. (2004). Advanced Behaviour of Steel Beams under Fire Conditions, PhD Thesis, faculty of science and engineering, University of Manchester

Yin, Y.Z. and Wang, Y.C. (2004). " A numerical study of large deflection behaviour of restrained steel beams at elevated temperatures, " *Journal of Constructional Steel Research*, Vol. 60, pp. 1029 -1047

Yu, H.X. , Davison, J. B., Burgess, I. W. and Plank, R. J. (2007). "Experimental Investigation of the Robustness of Fin Plate Connections in Fire", Proc. ICASS 2007, Singapore, pp. 722-727

Yu, H.X. , Burgess, I.W. and Davison, J. B. and Plank, R.J. (2009a). " Experimental Investigation of the Behaviour of Fin Plate Connections in Fire," *Journal of Constructional Steel Research*, Vol.65, pp.723-736

Yu, H.X., Burgess, I.W. and Davison, J. B. and Plank, R.J. (2009b). "Tying Capacity of Web Cleat Connections in Fire – Part 1: Test and Finite Element Simulation," *Engineering Structures*, Vol.31. , No.3, pp.723-736

Yu, H.X., Burgess, I.W. and Davison, J. B. and Plank, R.J. (2009c). "Experimental Investigation of the Behaviour of Flush Endplate Connections in Fire," submitted for publication

Zoetemeijer, P. (1974). "A Design Method for the Tension Side of Statically Loaded, Bolted Beam-to-Column Connections," *HERON*, Vol. 20, No. 1, pp. 1-60